

博士論文

Development of Late Transition Metal-Catalyzed  
Novel Aerobic Oxidative Cross-Dehydrogenative  
Coupling Reactions

(後期遷移金属触媒による酸素を酸化剤とした新規脱水素型  
クロスカップリング反応の開発)

金 雄杰

Xiongjie Jin

Department of Applied Chemistry, School of Engineering  
The University of Tokyo

東京大学大学院工学系研究科応用化学専攻

2015



# **Contents**

<b>Chapter 1 General Introduction</b>	<b>1</b>
1.1. Preliminary	2
1.2. Background	3
1.2.1. Green Chemistry	3
1.2.2. Catalyst and Catalysis	7
1.2.2.1. Definition	7
1.2.2.2. Classification	7
1.2.3. Cross-Coupling Reactions	9
1.2.3.1. General	9
1.2.3.2. Classification of Cross-Couplings	10
1.2.3.3. Cross-Dehydrogenative Coupling Reactions	18
1.2.3.4. Copper-Catalyzed Aerobic Cross-Dehydrogenative Coupling Reactions	24
1.2.4. Gold Nanoparticles for Aerobic Oxidative Bond-Forming Reactions	35
1.3. Overview of This Thesis	39
1.4. References	44
<b>Chapter 2 Cu(OH)<sub>2</sub>-Catalyzed Aerobic Cross-Dehydrogenative Coupling of Terminal Alkynes and Amides</b>	<b>55</b>
<i>2-1 Cu(OH)<sub>2</sub>-Catalyzed Selective Aerobic Cross-Dehydrogenative Coupling of Terminal Alkynes and Amides to Ynamides</i>	56
2-1.1. Introduction	56
2-1.2. Experimental Section	62
2-1.2.1. General	62

2-1.2.2. General Procedure for the Cross-Coupling of Terminal Alkynes and Amides	63
2-1.2.3. Spectral Data of Ynamides	64
2-1.3. Results and Discussion	71
2-1.3.1. Characterization of Cu(OH) <sub>2</sub>	71
2-1.3.2. Optimization of the Reaction Conditions	72
2-1.3.3. Substrate Scope	77
2-1.3.4. Reaction Mechanism	80
2-1.4. Conclusion	84
2-1.5. References	85
<i>2-2 One-pot Synthesis of Imides by the Oxidative Cross-Coupling to Ynamides Followed by Their Successive Hydration</i>	87
2-2.1. Introduction	87
2-2.2. Experimental Section	90
2-2.2.1. General	90
2-2.2.2. General Procedure for the Preparation of the Sn–W Mixed Oxides	91
2-2.2.3. General Procedure for the Catalytic Alkyne Hydration	91
2-2.2.4. General Procedure for the Synthesis of Imides	93
2-2.2.5. Spectral Data of Imides	93
2-2.3. Results and Discussion	99
2-2.3.1. Optimization of the Reaction Conditions	99
2-2.3.2. Substrate Scope	104
2-2.3.3. Sn–W Mixed Oxide-Catalyzed Rupe and Meyer–Schuster	

Rearrangements	106
2-2.3.4. Recyclability and Heterogeneous Catalysis of the Sn–W Mixed Oxide Catalyst	106
2-2.3.5. Reaction Mechanism	108
2-2.3.6. New Green Synthetic Procedure for Imides	110
2-2.4. Conclusion	113
2-2.5. References	114

## **Chapter 3 Cu(OAc)<sub>2</sub>-Catalyzed Aerobic Cross-Dehydrogenative Coupling of *H*-Phosphonates and Amides** **117**

3.1. Introduction	118
3.2. Experimental Section	121
3.2.1. General	121
3.2.2. General Procedure for the Cross-Coupling of <i>H</i> -Phosphonates and Amides	121
3.2.3. Spectral Data of <i>N</i> -Acylphosphoramidates	122
3.3. Results and Discussion	131
3.3.1. Optimization of the Reaction Conditions	131
3.3.2. Substrate Scope	136
3.3.3. Reaction mechanism	139
3.4. Conclusion	140
3.5. References	141

## **Chapter 4 Supported Gold Nanoparticle-Catalyzed Aerobic**

<b>Dehydrogenative Amination of <math>\alpha,\beta</math>-Unsaturated Aldehydes</b>	<b>145</b>
4.1. Introduction	146
4.2. Experimental Section	150
4.2.1. General	150
4.2.2. Preparation of Supported Gold Nanoparticle Catalysts	151
4.2.3. Typical Procedure for the Dehydrogenative Amination	152
4.2.4. Spectral Data of Enaminals and Enaminones	153
4.3. Results and Discussion	168
4.3.1. Characterization of Au/OMS-2 Catalyst	168
4.3.2. Optimization of the Reaction Conditions	169
4.3.3. Substrate Scope	174
4.3.4. Recyclability and Heterogeneous Catalysis of Au/OMS-2	178
4.3.5. Reaction Mechanism	181
4.4. Conclusion	186
4.5. References	186
<b>Chapter 5 Zn<sup>2+</sup> and OMS-2 Co-catalyzed Aerobic Cross-Dehydrogenative Coupling of Terminal Alkynes and Tertiary Amines</b>	<b>191</b>
5.1. Introduction	192
5.2. Experimental Section	195
5.2.1. General	195
5.2.2. Typical Procedure for the Cross-Coupling of Terminal Alkynes and Tertiary Amines	195

5.2.3. Reuse Experiment of OMS-2	196
5.2.4. Spectral Data of Propargylamines	196
5.3. Results and Discussion	204
5.3.1. Optimization of the Reaction Conditions	204
5.3.2. Substrate Scope	208
5.3.3. Recyclability of OMS-2	211
5.3.4. Reaction Mechanism	212
5.4. Conclusion	213
5.5. References	213
<b>Chapter 6 General Conclusions</b>	<b>217</b>
<b>List of Publications</b>	<b>223</b>
<b>Acknowledgement</b>	<b>227</b>



# **Chapter 1**

## **General Introduction**

## 1.1. Preliminary

The quality of our lives has been greatly benefitted from the evolutionary development of chemical industries. Meanwhile, the growing demand for a large variety of chemicals has also caused the damage to the environment and the crisis of the resource depletion. Thus, the development of new manufacturing processes for chemical products to achieve higher atom efficiency as well as minimization (or elimination) of waste generation and energy consumption is now our urgent task. Catalysts play a central role in the development of environmentally benign chemical processes. Efficient, selective organic reactions can be carried out in the presence of proper catalysts, thus avoiding the use of hazardous reagents and drastically reducing organic and/or inorganic wastes.<sup>[1]</sup> Therefore, the progress in catalysis science will directly contribute to our ultimate goal of realization of green and sustainable society.

The rapid evolution of catalyst research can dramatically simplify synthetic procedures and improve synthetic efficiency, which allows more cost-effective and energy-saving chemical industries. This thesis mainly focuses on “aerobic cross-dehydrogenative coupling” to realize step-economical green synthetic procedures for several important organic compounds which otherwise are synthesized by traditional multi-step or stoichiometric reactions with low efficiencies. According to target reactions, either heterogeneous or homogeneous catalyst systems are designed to fully explore the potential and advantages of these systems.

This chapter is composed of the following several sections. Firstly, the concept and importance of green chemistry are described followed by a brief introduction to homogeneous and heterogeneous catalysts. Then, historical background and recent progresses of cross-coupling reactions are discussed. Copper-based catalysts for the

aerobic cross-dehydrogenative coupling reactions and supported gold nanoparticle-catalyzed aerobic oxidative functional group transformations are also presented. Finally, the purpose and outline of this study are described.

## 1.2. Background

### 1.2.1. Green Chemistry

Chemical industries play key roles in modern society. Without the revolutionary development in chemical technologies, it is hard to imagine how our society likely to be now. However, as everything has its two sides, chemical industries also have some negative effects on our planet, such as environmental pollution and generation of a large quantity of waste from chemical factories.

Green chemistry focuses on preventing pollution and minimizing waste generation to replace end-of-the-pipe control technology and has drawn much attention in the past several decades. The term “green chemistry” is generally defined as “*the invention, design, and application of chemical products and processes to reduce or eliminate substances hazardous to human health and the environment*”, which can be explained by the 12 principles proposed by Anatas (Table 1-1).<sup>[2,3]</sup> Green chemistry deals with the issues of the environmental impact of both chemical products and processes.<sup>[4]</sup> The concept of green chemistry is relevant to high selectivity and the atom efficiency, simple synthetic procedures, and drastic reduction or elimination of wastes, and eventually to change the way of the use and manufacture of chemicals by introducing revolutionary new technologies. The ultimate goal of green chemistry is the realization of sustainable society that is defined as “*meeting the needs of the present generation without compromising the ability of future generations to meet their own needs*”.<sup>[4c,d]</sup>

**Table 1-1.** The 12 principles of green chemistry.<sup>[3]</sup>

---

1. It is better to prevent waste than to treat or clean up waste after it is formed.
  2. Synthetic methods should be designed to maximize the incorporation of all materials used in the process into the final product.
  3. Wherever practicable, synthetic methodologies should be designed to use and generate substances that possess little or no toxicity to human health and the environment.
  4. Chemical products should be designed to preserve efficacy of function while reducing toxicity.
  5. The use of auxiliary substances (e.g., solvents, separation agents, and so forth) should be made unnecessary wherever possible and innocuous when used.
  6. Energy requirements should be recognized for their environmental and economic impacts and should be minimized. Synthetic methods should be conducted at ambient temperature and pressure.
  7. A raw material or feedstock should be renewable rather than depending wherever technically and economically practicable.
  8. Unnecessary derivatization (blocking group, protection/deprotection, temporary modification of physical/chemical processes) should be avoided whenever possible.
  9. Catalytic reagents (as selective as possible) are superior to stoichiometric reagents.
  10. Chemical products should be designed so that at the end of their function they do not persist in the environment and break down into innocuous degradation products.
  11. Analytical methodologies need to be developed further to allow for real-time in-process monitoring and control before the formation of hazardous substances.
  12. Substances and the form of a substance used in a chemical process should be chosen so as to minimize the potential for chemical accidents, including releases, explosions, and fires.
-

The general methods for the evaluation of the potential environmental acceptability of chemical processes are the E-factor and the atom efficiency.<sup>[4,5]</sup>

$$\text{E-factor} = \frac{\text{total mass of byproducts (wastes)}}{\text{mass of desired product}} \quad (1)$$

$$\text{Atom efficiency (\%)} = \frac{\text{molecular weight of desired product}}{\text{sum of molecular weight of reactants}} \times 100 \quad (2)$$

The E-factor first proposed by Sheldon<sup>[4]</sup> is derived by dividing the total mass of wastes by the mass of product [Eq. (1)], which is used to quantify the amount of wastes being generated by various segments of the chemical industry (Table 1-2).<sup>[5a]</sup> These wastes are defined as everything produced in a chemical process except the desired product. The higher E-factor indicates the more waste generation in a chemical process. As shown in Table 1-2, the E-factor generally increases from bulk to fine chemical industry, and is dramatically higher for the production of pharmaceuticals partly because of the multi-step synthetic procedures and the use of stoichiometric reagents rather than catalytic methods.<sup>[5b]</sup>

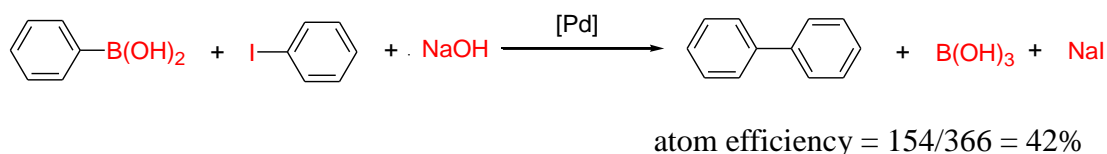
**Table 1-2.** E-factors for various sectors of chemical industry.<sup>[5b]</sup>

Industry	Product tons per year	Waste/product ratio by weight
Oil refining	10 <sup>6</sup> –10 <sup>8</sup>	~0.1
Bulk chemicals	10 <sup>4</sup> –10 <sup>6</sup>	<1–5
Fine chemicals	10 <sup>2</sup> –10 <sup>4</sup>	5–50
Pharmaceuticals	10 <sup>0</sup> –10 <sup>3</sup>	25–>100

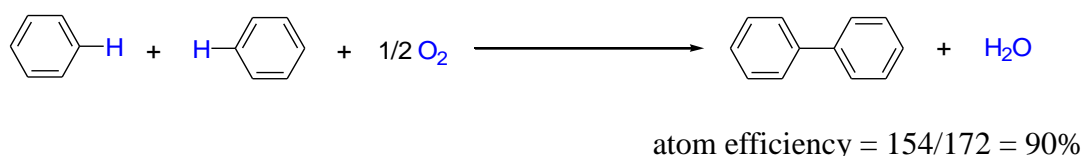
The atom efficiency (or atom economy) first introduced by Trost<sup>[6]</sup> is calculated by dividing the molecular weight of the desired product by the summed molecular weights of all of the reactants [Eq. (2)], which can be used to rapidly evaluate the amount of

wastes being generated in a chemical process. A good example to demonstrate the atom efficiency is the comparison between traditional cross-coupling and aerobic cross-dehydrogenative coupling reactions, as shown in Figure 1-1. The cross-coupling of aryl boronic acids and aryl halides, namely Suzuki–Miyaura reaction, is one of the most efficient synthetic procedures for biaryls.<sup>[6]</sup> Because of the utilization of the pre-functionalized starting materials and a stoichiometric amount of a base such as NaOH, large amounts of wastes are often generated in the cross-coupling as well as the pre-functionalization steps. In contrast, biaryl synthesis by the direct aerobic cross-dehydrogenative coupling of two arenes, which avoids the pre-functionalization steps as well as bases, can drastically reduce the amount of wastes. Consequently, the atom efficiency for the aerobic cross-dehydrogenative coupling is higher than the traditional cross-coupling. In addition, the aerobic cross-dehydrogenative coupling uses molecular oxygen as the terminal oxidant and produces water as the sole by-product, consequently greatly reduces the environmental impact.

**Traditional cross-coupling (Suzuki–Miyaura cross-coupling):**



**Aerobic cross-dehydrogenative coupling:**



**Figure 1-1.** Atom efficiencies of the traditional cross-coupling and the aerobic cross-dehydrogenative coupling reactions.

## 1.2.2. Catalyst and Catalysis

### 1.2.2.1. Definition

In 1836, Berzelius defined the term “catalyst” as “*a compound, which increases the rate of a chemical reaction, but which is not consumed during the reaction*”.<sup>[8a]</sup> In 1895, Ostwald amended Berzelius's definition of the catalyst, considering the possibility of catalyst deactivation during the reaction, as “*a substance that increases the rate of approach to equilibrium of a chemical reaction **without being substantially consumed in the reaction***”.<sup>[8a]</sup> More recently, the IUPAC (International Union of Pure and Applied Chemistry) defined the catalyst as “*a substance that increases the rate of a reaction without modifying the overall standard Gibbs energy change in the reaction*”; and “*the process is called catalysis*”.<sup>[8b]</sup>

For a catalytic process, a substoichiometric amount of the catalyst is sufficient to promote the reaction, due to the regeneration of the catalyst after a series of sequential unit reactions. Therefore, chemical reactions promoted by the catalysts rather than stoichiometric reagents can be regarded as environmentally friendly procedures due to reduced generation or even elimination of wastes. Also, the replacement of traditional stoichiometric procedures with their catalytic versions can greatly improve the atom efficiency. Hence, the development of novel catalytic processes plays a fatal role for the achievement of green and sustainable chemical industries.

### 1.2.2.2. Classification<sup>[9]</sup>

Catalysts are generally classified into two groups, that is, homogeneous and heterogeneous catalysts. For homogeneous catalyst systems, the catalysts and the reactants reside in the same phase (usually liquid phase). By contrast, the catalysts

usually exist in the different phase from the reactants for heterogeneous systems. Homogeneous catalysts are soluble, discrete, molecular species; heterogeneous catalysts are typically insoluble solid, and the reactants are often in the gas or liquid phase.

Homogeneous and heterogeneous catalysts have their own advantages and disadvantages. Homogeneous catalysts often show high catalytic activity under milder conditions due to the easy accessibility of reactants to active sites. In addition, fine-tuning of the steric and electronic properties of ligands allows these catalysts often more selective than heterogeneous catalysts. In particular, homogeneous catalysts play an irreplaceable role for the highly regio-, stereo-, and enantioselective synthesis of fine chemicals, especially natural products and pharmaceuticals. However, separation of the catalysts from reaction solutions is often very difficult, and thus the reuse of the catalysts is problematic in homogeneous systems. Furthermore, because of the difficulties in the catalyst separation, the contamination of the products by the catalysts is often problematic for the synthesis of pharmaceuticals.

Heterogeneous catalysts are often superior to their homogeneous counterparts in terms of high thermostability, simple separation of the catalysts from the products, and easy recovery and reuse of expensive catalysts. In addition, ligands that are often the most expensive part of homogeneous catalysts are not needed for heterogeneous catalysts. However, the fine-control of catalytically active sites is a very difficult task for heterogeneous catalysts. Elucidation of the reaction mechanism in a heterogeneous system is also extremely challenging largely because of the complicated structure of the active sites. In this context, remarkable progress has been made in the last several decades,<sup>[10a,b]</sup> as highlighted by the 2007 Nobel Prize in Chemistry awarded to Gerhard Ertl for his studies of fundamental chemical processes on the surface of heterogeneous



catalysts (especially, the studies of the Haber-Bosch process for the synthesis of ammonia, and the oxidation of CO on platinum).<sup>[10c]</sup> Chemical industries strongly rely on heterogeneous catalysts, especially in the field of the production of large scale commodity chemicals such as methanol, ammonia, and high octane gasoline from petroleum.<sup>[9c]</sup>

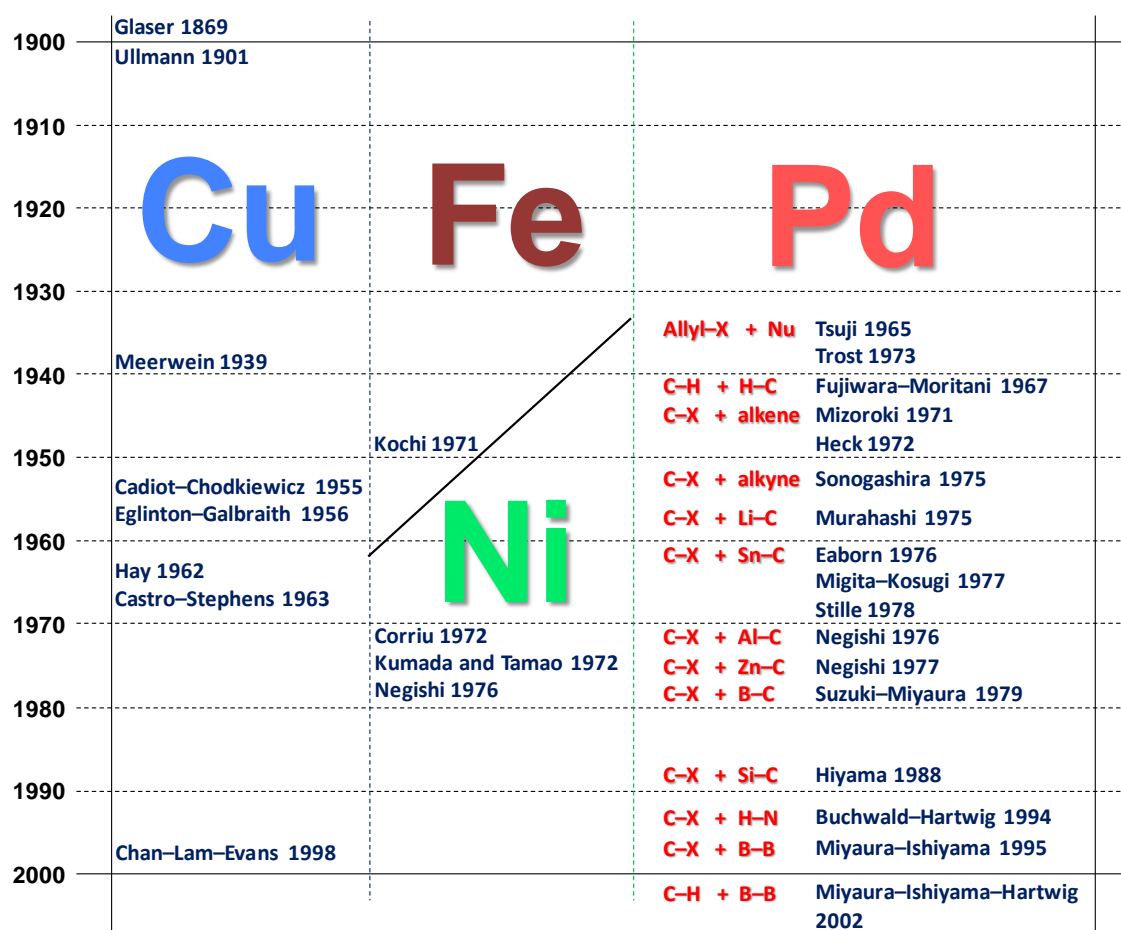
### 1.2.3. Cross-Coupling Reactions

#### 1.2.3.1. General

Since the initial development of the copper-catalyzed Glaser and Ullmann coupling reactions,<sup>[11]</sup> transition metal-catalyzed cross-coupling reactions have emerged as one of the most effective methods for the construction of various C–C and C–X (X = heteroatom) bonds.<sup>[12,13]</sup> In particular, developed in the last century, palladium-catalyzed cross-couplings between two arene rings (or between an arene ring and an alkene) to biaryls (or substituted alkenes), such as Kumada, Suzuki, Negishi, Heck, Stille, and Hiyama reactions, have a tremendous impact on the synthesis of natural products, medicines, and organic materials, largely because of their high efficiency and reliability (Figure 1-2).<sup>[12–17]</sup> The great success of these cross-coupling reactions is well showcased by the 2010 Nobel Prize in Chemistry for “palladium-catalyzed cross-couplings in organic synthesis”.<sup>[17]</sup>

The revolutionary development and great success of the palladium-catalyzed cross-coupling reactions in synthetic organic chemistry have stimulated the discovery of various types of cross-coupling reactions, for example, C–X bond coupling, direct coupling via C–H activation, and decarboxylative coupling.<sup>[13]</sup> In addition to palladium, other late-transition metals (e.g., Fe, Co, Cu, Ni, Ru, and Rh) have also proved to be

versatile for cross-coupling reactions in the last several decades.<sup>[12b]</sup> Because of the high efficiencies of cross-coupling reactions for the rapid construction of complex molecules, this type of reactions are still a main topic in synthetic organic chemistry. This highly important research area is now directing toward the replacement of the traditional cross-couplings with their novel versions having higher synthetic efficiency and more environmentally friendly nature.



**Figure 1-2.** Historical development of the metal-catalyzed cross-coupling reactions.<sup>[12-17]</sup> Nu = nucleophile.

### 1.2.3.2. Classification of Cross-Couplings

Cross-couplings can generally be classified into the following three types,

according to the substrates (electrophiles or nucleophiles) involved in the reactions; (1) cross-coupling of a nucleophile with an electrophile, (2) reductive cross-coupling between two electrophiles, and (3) oxidative cross-coupling between two nucleophiles (Figure 1-3).

**(a) Traditional Cross-Coupling**



Nu = organometallics, amines, alcohols, thiols, hydrocarbons, etc.

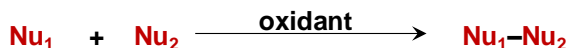
E = halides (pseudohalides)

**(b) Reductive Cross-Coupling**



E = halides (pseudohalides)

**(c) Oxidative Cross-Coupling**



Nu = organometallics, amines, alcohols, thiols, hydrocarbons, etc.

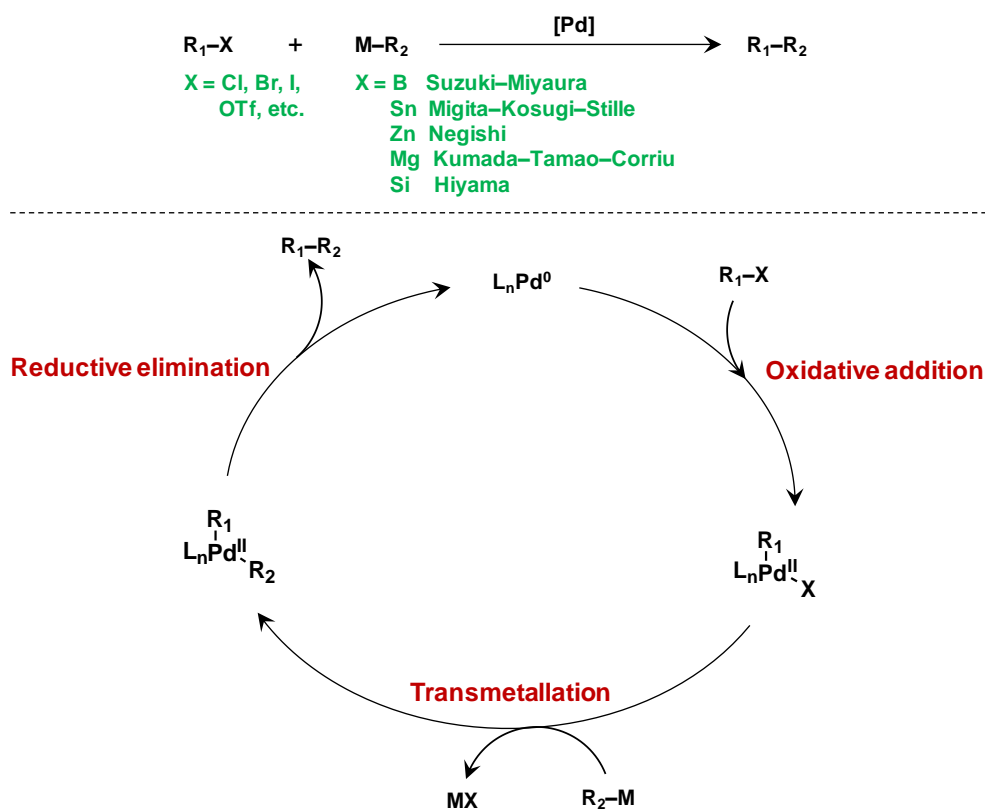
**Figure 1-3.** Classification of cross-couplings. Nu = nucleophile; E = electrophile.

### ■ Cross-Coupling of a Nucleophile with an Electrophile

The traditional cross-couplings between organometallic compounds and organohalides (or pseudohalides) are the typical reactions which can be regarded as the cross-coupling of a nucleophile and an electrophile. The last several decades have evidenced the great success of these reactions that have mostly utilized palladium-based catalysts, and many excellent name reactions exist in this field.<sup>[12-17]</sup> Because of the advantages (easily-handled, thermally stable, and water and oxygen tolerable) of using organoboronic acids instead of other organometallic compounds, one of the most successful reactions in both laboratories and industries is the Suzuki–Miyaura cross-coupling which employs organoboronic acids and organohalides as the coupling

partners.<sup>[7]</sup>

The catalytic cycles for the palladium-catalyzed cross-couplings of various organometallic compounds (organozinc, boron, tin, silicon, etc.) and organohalides share common fundamental sequential unit reactions, involving (1) oxidative addition of an organohalide to a Pd(0) species, (2) transmetalation of an organometallic compound with the oxidative addition intermediate, and (3) reductive elimination to form the final product (e.g., biaryls) and to regenerate the Pd(0) species (Scheme 1-1).<sup>[12b]</sup>



**Scheme 1-1.** Traditional palladium-catalyzed cross-couplings.<sup>[12b]</sup>

Another important reaction is the palladium-catalyzed cross-coupling of amines with arylhalides, known as the Buchwald–Hartwig amination, which has become one of

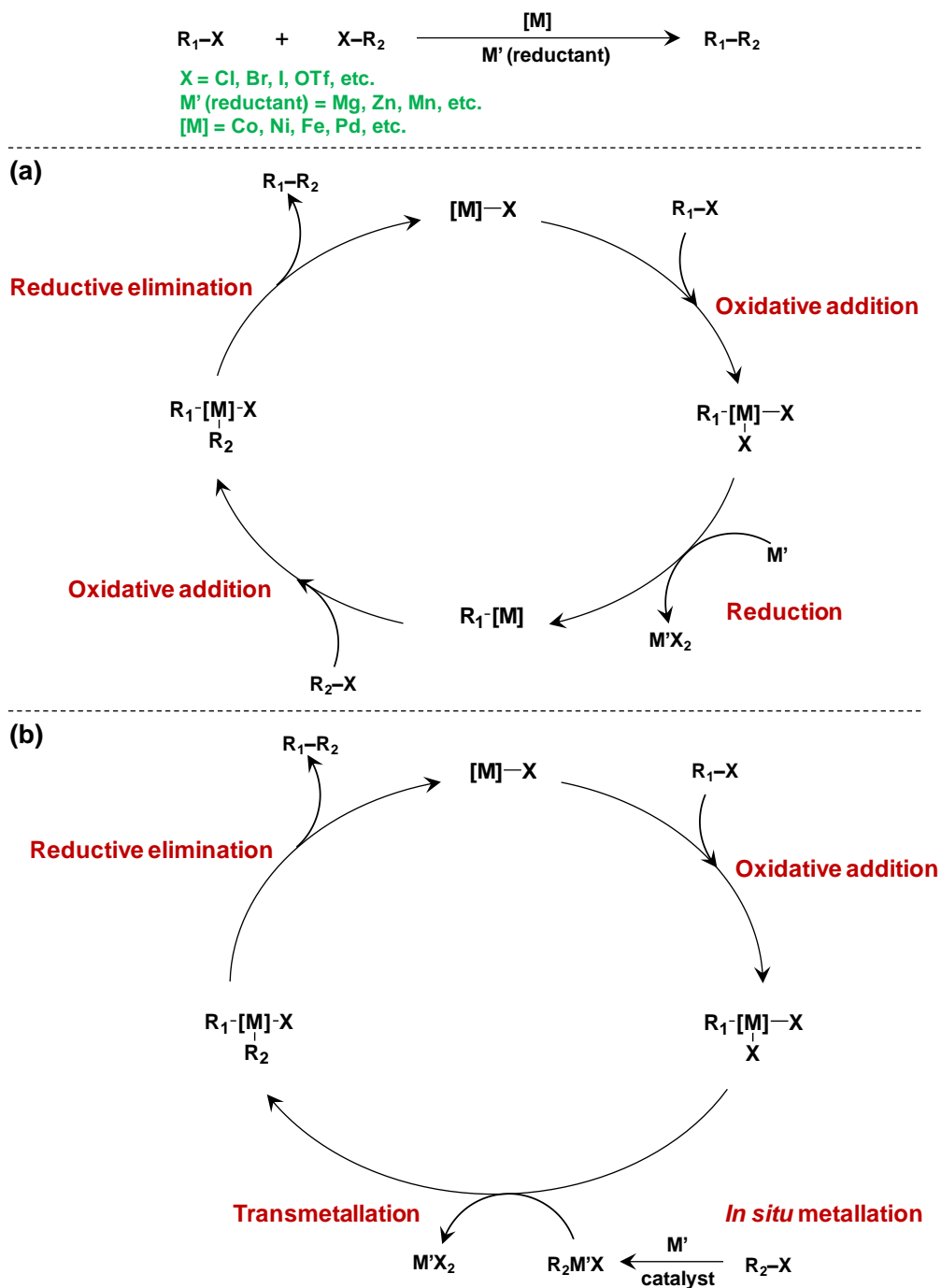
the most important methods for the synthesis of arylamines.<sup>[12]</sup> The amination proceeds through a catalytic cycle similar to that of the cross-coupling of organometallics and organohalides, except that the coordination of an amine to the palladium center occurs after the oxidative addition of an aryl halide.<sup>[12]</sup>

### ■ Reductive Cross-Coupling between Two Electrophiles

During the past decade, chemists have aspired to develop more efficient cross-coupling reactions that avoid using air and moisture sensitive organometallic reagents. Reductive cross-coupling of two electrophiles (organohalides or pseudohalides) in the presence of appropriate reductants, such as metallic Zn, Mg, and Mn, has been emerging as a versatile and simple synthetic method for selective C–C bond formations, because of easy availability of a large variety of electrophiles which are more stable and easily handled than their organometallic counterparts.<sup>[18,19]</sup> Most importantly, this kind of reactions can avoid utilizing organometallic compounds which are often prepared by metallation of organohalides or pseudohalides, therefore, the high overall synthetic efficiency can eventually be achieved.

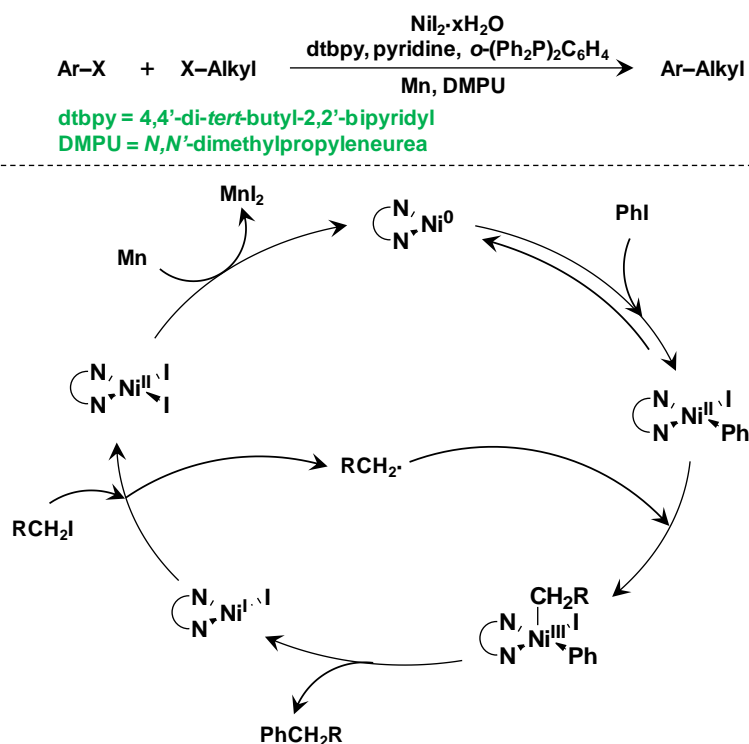
Several late-transition metals such as Co,<sup>[20]</sup> Ni,<sup>[21]</sup> Fe,<sup>[22]</sup> and Pd<sup>[23]</sup> have been known to promote reductive cross-coupling reactions. Two possible catalytic cycles for these reactions have been proposed (Scheme 1-2). One of the reaction paths consists of (1) oxidative addition of an electrophile to a lower valence metal center, (2) reduction of the oxidized metal center by external reductants such as metallic Mg, Zn, and Mn, (3) oxidative addition of a second electrophile to the metal center, and (4) reductive elimination to give the final product and to regenerate the catalyst (Scheme 1-2, a). The other is *in situ* generation of an organometallic compound from the reductant and one of

the electrophiles followed by the cross-coupling of the organometallic compound with another electrophile through the reaction path being similar to that of the traditional cross-couplings (Scheme 1-2, b).<sup>[18,19]</sup>



Scheme 1-2. Reductive cross-couplings.<sup>[18,19]</sup>

Different from the traditional palladium-catalyzed cross-couplings, reductive cross-couplings can proceed through a one-electron transfer process, which is likely the reason why the first-row transition metals are widely applied to reductive cross-couplings. For example, Weix and co-workers have reported a nickel-catalyzed reductive cross-coupling of arylhalides and alkylhalides.<sup>[21i]</sup> The mechanistic studies showed that no organomanganese species was formed, and the reaction was supposed to proceed through the Ni<sup>0</sup>, Ni<sup>I</sup>, Ni<sup>II</sup>, and Ni<sup>III</sup> intermediates formed via a single electron transfer process (Scheme 1-3).<sup>[21i]</sup>



**Scheme 1-3.** Nickel-catalyzed reductive cross-coupling of aryl halides and alkyl halides.<sup>[21i]</sup>

The central issue in reductive cross-coupling reactions is how to control the selectivity toward the desired cross-coupling product, and to avoid the formation of the

homo-coupling side products. Generally, the high selectivity was achieved by (1) the appropriate combination of two electrophiles with different electronic or steric properties, (2) the use of excess amounts of one of the coupling partners, (3) fine-tuning of the catalyst/reductant combinations, and (4) the design of ligands with suitable electronic and steric properties.<sup>[18,19]</sup> However, no universal methodology exists for the achievement of the high selectivity.

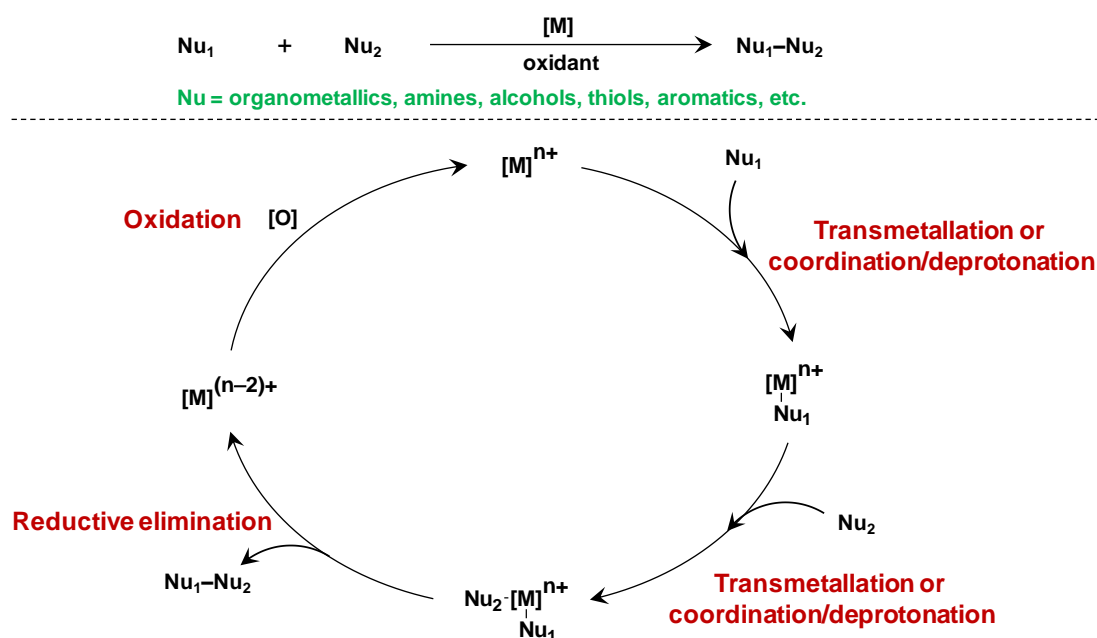
### ■ Oxidative Cross-Coupling between Two Nucleophiles

With the evolutionary development of cross-coupling chemistry, synthetic chemists are seeking more efficient and environmentally benign procedures to meet the needs of sustainable development of every aspect of chemical industries. Over the last several decades, oxidative cross-coupling between two nucleophiles has become one of the most powerful methods for synthesis of a large variety of valuable chemicals, which is now one of the most emergently developing fields in synthetic organic chemistry.<sup>[24]</sup> Directly using readily available nucleophiles as starting materials, such as aromatics, alcohols, and amines, can avoid the pre-activation step(s) to prepare electrophiles or organometallic compounds. Therefore, the overall synthetic efficiency should be generally higher than the above-mentioned nucleophile–electrophile and electrophile–electrophile cross-coupling reactions.

Traditionally, a nucleophile is considered to only react with an electrophile. Bond formation between two nucleophiles has been realized with the aid of transition metal catalysts.<sup>[24]</sup> In this case, external oxidants are needed to accept two electrons from two nucleophilic coupling partners.<sup>[24]</sup> A typical catalytic cycle for this type of reaction is shown in Scheme 1-4, which includes (1) transmetalation (in the case of organometallic



compounds) or coordination/deprotonation (or nucleophilic substitution) of one nucleophile (in the case of aromatics or other nucleophiles such as alcohols, amines, etc.) to the metal center, (2) transmetallation or coordination/deprotonation (or nucleophilic substitution) of the other nucleophile to the same metal center, (3) reductive elimination to give the final product, and (4) reoxidation of the reduced metal center by the external oxidants, for example, metal salts, organic oxidants, hydrogen peroxide, and molecular oxygen.<sup>[24,25]</sup>



**Scheme 1-4.** Oxidative cross-coupling between two nucleophiles.<sup>[24]</sup>

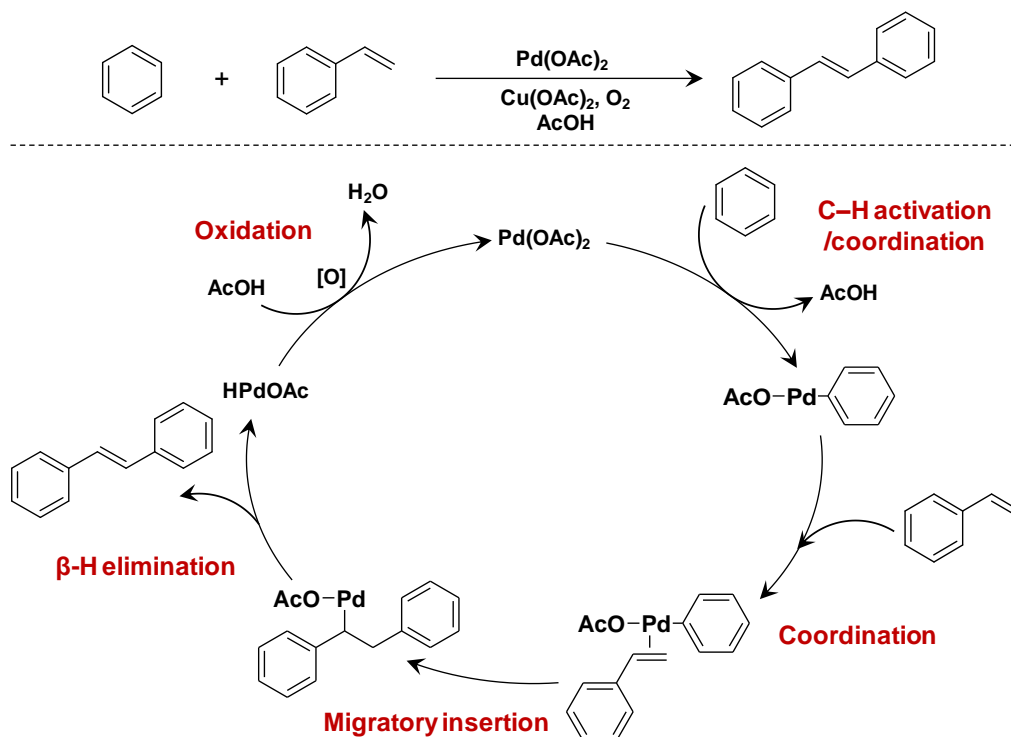
Similar to the previously described reductive cross-couplings, the selectivity problem is also the central issue in oxidative cross-couplings because of the essential side reactions such as homo-coupling of nucleophiles and oxidation of the nucleophiles by the external oxidants. Nonetheless, many reports have shown that the high selectivity can be achieved by choosing appropriate oxidants and/or fine-tuning of the oxidant/catalyst/ligand combinations.<sup>[24,25]</sup>

### 1.2.3.3. Cross-Dehydrogenative Coupling Reactions

The need for the realization of the green and sustainable society is one of the inherent driving forces for entire chemical society evolving toward the development of more step- and cost-economical synthetic methodologies. In this context, direct cross-dehydrogenative couplings of C–H or X–H bonds have several advantages, such as use of readily available starting materials, no need of pre-functionalization step(s), simple procedures, and drastic reduction of wastes, over either the traditional nucleophile–electrophile or electrophile–electrophile cross-couplings. Although such reactions have been termed as cross-dehydrogenative coupling reactions by Li in 2004, the generation of hydrogen gas is thermodynamically unfavorable, and thus appropriate external oxidants are needed.<sup>[25,26]</sup> Despite the complexities and challenges for such transformations, especially the selectivity problems as described in the previous section, great progress has been made in recent years. Palladium-based catalysts have mainly been utilized for the cross-dehydrogenative coupling reactions among various transition metal catalysts such as Cu, Rh, Ru, Pd, etc., especially for cross-dehydrogenative C–C bond forming reactions.<sup>[25,26]</sup>

The early development of cross-dehydrogenative coupling reactions can date back to late 1960s, even before the development of the traditional palladium-catalyzed cross-couplings, when Fujiwara and co-workers developed the oxidative cross-coupling of unfunctionalized aromatics and alkenes in the presence of Pd(OAc)<sub>2</sub> (OAc = acetate) using Cu(OAc)<sub>2</sub> as the co-oxidant and O<sub>2</sub> as the terminal oxidant (the Fujiwara–Moritani reaction, Scheme 1-5).<sup>[16c,27]</sup> Taking the reaction of benzene and styrene to *trans*-stilbene as an example, the reaction proceeds through (1) deprotonative palladation of benzene, (2) coordination of styrene to Pd, (3) migratory insertion of

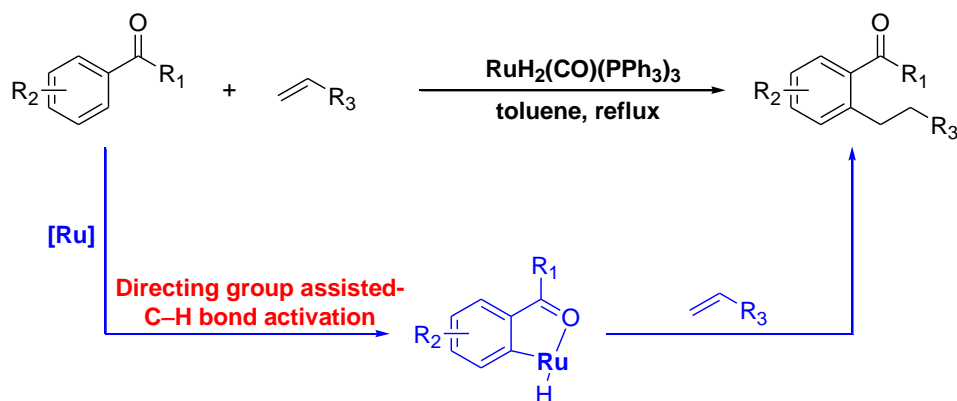
styrene to the Pd–aryl bond, (4)  $\beta$ -hydride elimination to afford stilbene, and (5) reoxidation of the reduced Pd to close the catalytic cycle.<sup>[16c,27]</sup>



**Scheme 1-5.** The Fujiwara-Moritani reaction.<sup>[16c,27]</sup>

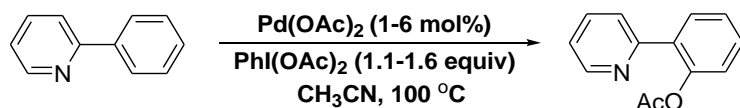
The pioneering work by Murai and co-workers on ruthenium-catalyzed *ortho*-alkylation of aromatic ketones (Scheme 1-6) has made the directing group assisted-C–H bond activation strategy become one of the most popular research areas during the last two decades (selected examples mainly by palladium based-catalysts are shown in Schemes 1-7 and 1-8).<sup>[28–31]</sup> To date, a large number of cross-dehydrogenative coupling reactions have successfully been developed based on the directing group assisted strategy (Scheme 1-8). For these reactions, the directing groups coordinate to the active metal centers to facilitate the activation of the inert C–H bonds (Scheme 1-6). Although the great success of the directing-group assisted cross-dehydrogenative

coupling strategy, there is a limitation of the need for the additional installation/uninstallation steps of the directing groups.

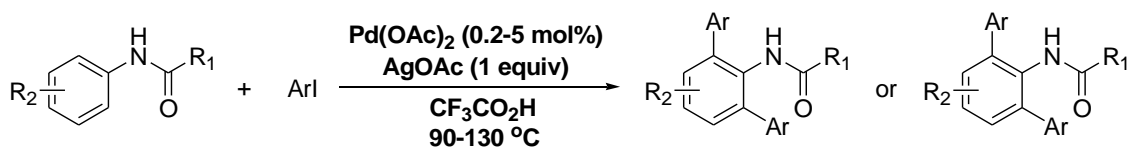


**Scheme 1-6.** Murai's work on the direct *ortho*-alkylation of aromatic ketones.<sup>[28]</sup>

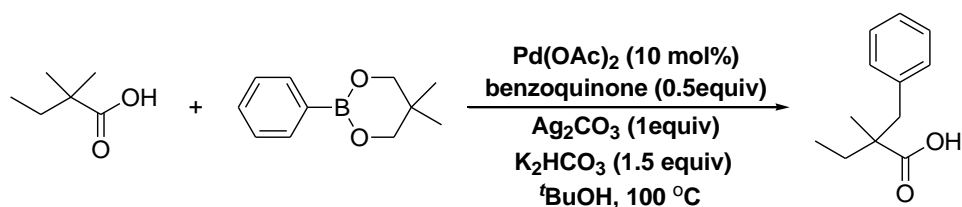
**Sanford et al. (2004)**<sup>[29]</sup>



**Daugulis et al. (2005)**<sup>[30]</sup>

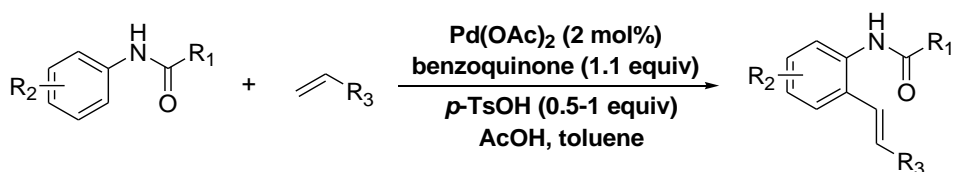


**Yu et al. (2007)**<sup>[31]</sup>

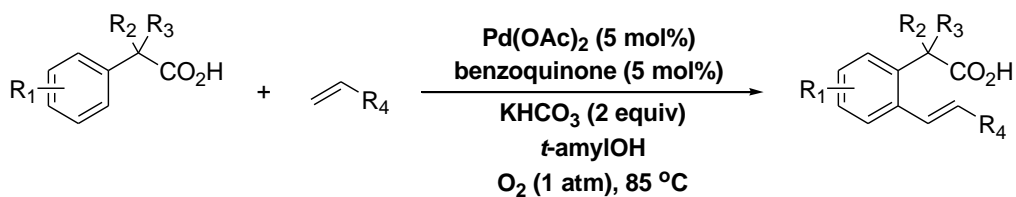


**Scheme 1-7.** Selected examples of directing group assisted-cross-coupling reactions of various C-H bonds.

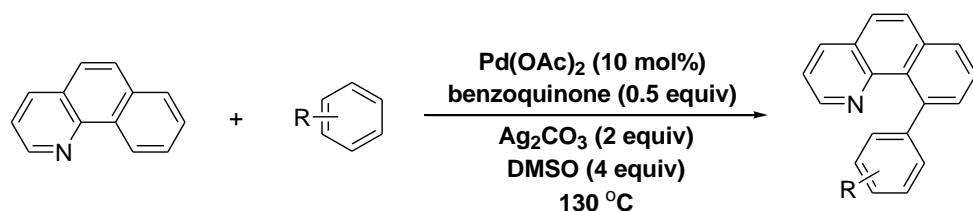
van Leeuwen et al. (2002)<sup>[32]</sup>



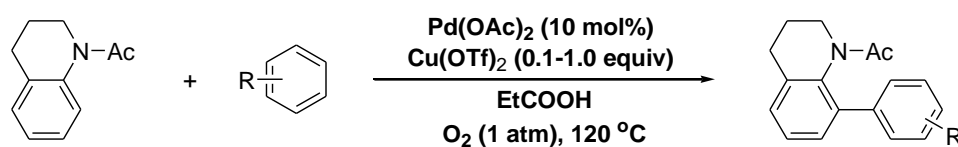
Yu et al. (2010)<sup>[33]</sup>



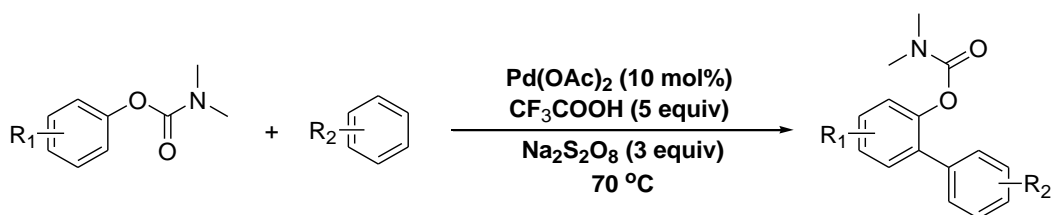
Sanford et al. (2007)<sup>[34]</sup>



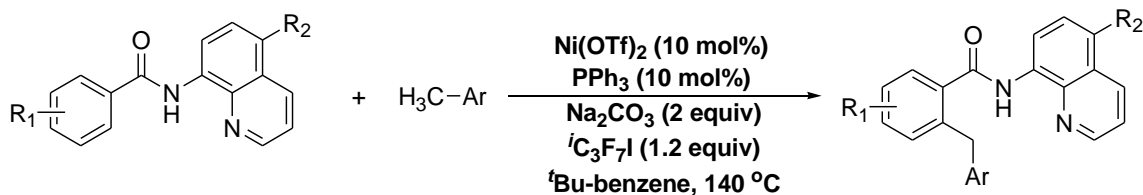
Shi et al. (2008)<sup>[35]</sup>



Dong et al. (2010)<sup>[36]</sup>



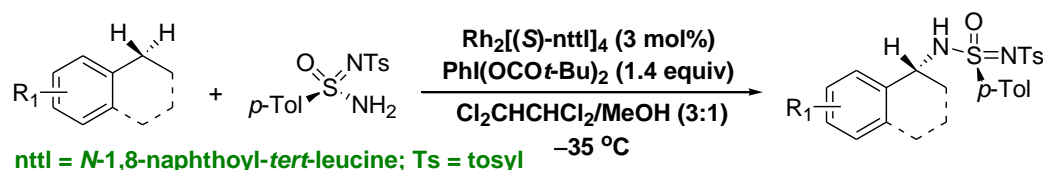
Chatani et al. (2014)<sup>[37]</sup>



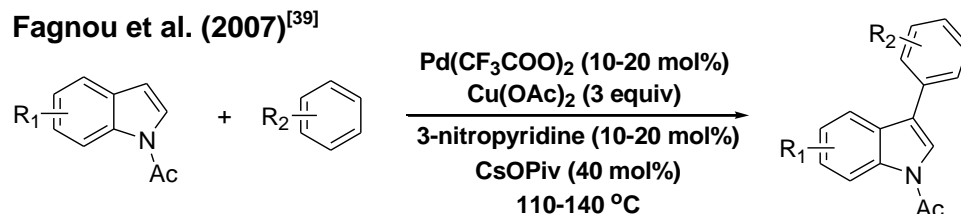
**Scheme 1-8.** Selected examples of directing group assisted-cross-dehydrogenative coupling reactions.

More recently, directing-group free cross-dehydrogenative coupling reactions have also been developed (Scheme 1-9). These reactions can be regarded as the ultimate dream for synthetic chemists due to the abundance of C–H or X–H bonds. Thus, selective activation of C–H or X–H bonds to construct new C–C, C–X, or X–X bonds can revolutionize the way by which complex molecules are synthesized from readily available starting materials. Because these reactions can be regarded as the oxidative cross-coupling of two nucleophiles, the selectivity of such reactions is also mainly controlled by employing sterically or electronically different substrates as the coupling partners and/or by fine-tuning of the catalyst/oxidant/substrate combinations.<sup>[24,25]</sup>

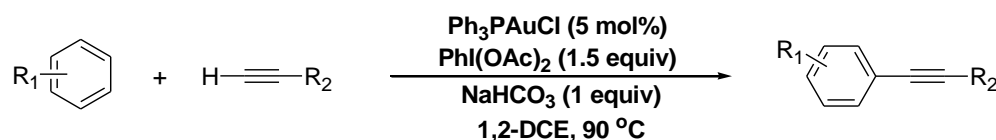
**Müller, Dodd, and Dauban et al. (2006)<sup>[38]</sup>**



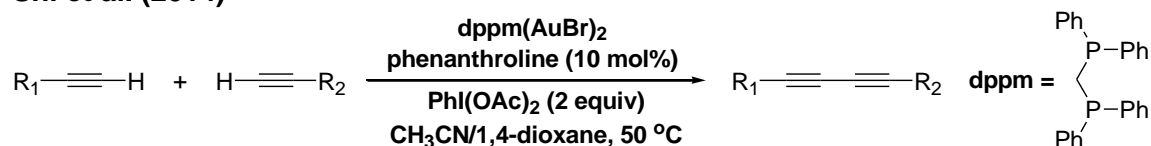
**Fagnou et al. (2007)<sup>[39]</sup>**



**Nevado et al. (2010)<sup>[40]</sup>**



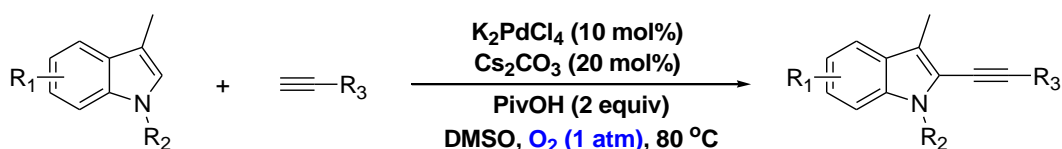
**Shi et al. (2014)<sup>[41]</sup>**



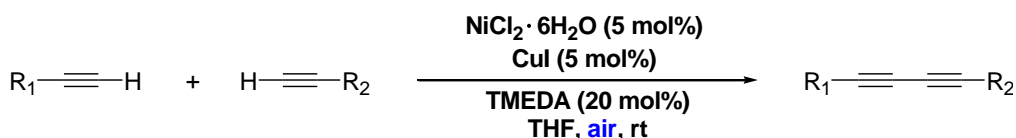
**Scheme 1-9.** Selected examples of directing group-free cross-dehydrogenative coupling reactions.

For most of the palladium-catalyzed reactions, catalytic or stoichiometric amounts of inorganic or organic oxidants are needed to reoxidize the reduced active metal center.<sup>[24,25]</sup> In recent years, aerobic cross-dehydrogenative coupling reactions using molecular oxygen as the terminal oxidant have successfully been developed (Scheme 1-10).<sup>[24,25,42–45]</sup> These reactions are more environmentally benign compared to the previously described cross-couplings, because they use molecular oxygen as the terminal oxidant and produce water as the sole byproduct. The catalytic cycle for aerobic cross-dehydrogenative coupling reactions often resembles that for oxidative cross-couplings between two nucleophiles described in section 1.2.3.2, in which the oxidant for the reduced metal center is molecular oxygen (Scheme 1-4).

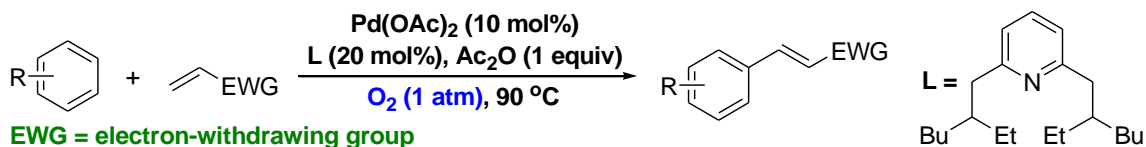
**Li et al. (2010)<sup>[42]</sup>**



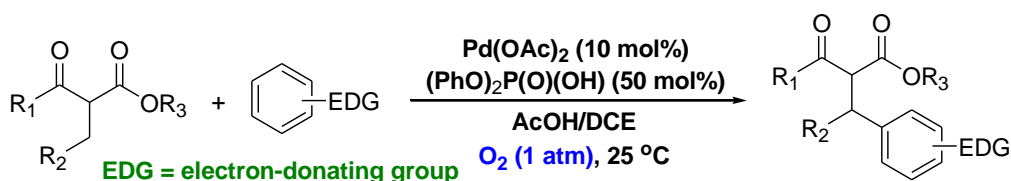
**Lei et al. (2009)<sup>[43]</sup>**



**Yu et al. (2009)<sup>[44]</sup>**



**Pihko et al. (2012)<sup>[45]</sup>**



**Scheme 1-10.** Selected examples of aerobic cross-dehydrogenative coupling reactions.

#### 1.2.3.4. Copper-Catalyzed Aerobic Cross-Dehydrogenative Coupling Reactions

In recent years, copper-catalyzed cross-coupling reactions have drawn much attention because of the natural abundance and low cost of copper.<sup>[46,47]</sup> Copper-based catalysts have shown unique activities and efficiencies for various cross-coupling reactions, especially for aerobic cross-dehydrogenative coupling reactions, because (1) they are easily accessible to Cu<sup>0</sup>, Cu<sup>I</sup>, Cu<sup>II</sup>, and Cu<sup>III</sup> oxidation states via one or two-electron transfer processes, which allows both radical and palladium-like two-electron pathways, (2) various functional groups can readily coordinate to them via Lewis acidic interactions or  $\pi$ -coordination, and (3) their lower valence states can easily be reoxidized by molecular oxygen.<sup>[46]</sup> These properties of copper catalysts allow their chemistry in cross-dehydrogenative coupling reactions extremely rich when using abundant and environmentally benign molecular oxygen as the terminal oxidant, in contrast to the palladium catalysis for which reoxidation of lower valence palladium species by molecular oxygen is relatively difficult.

In the context of copper-mediated cross-coupling reactions, an appropriate choice of copper sources, bases, ligands, and other additives is very important for the improvement of the efficiency of the catalyst system.<sup>[9a,46,47]</sup> The ligands suitable for the generation of active copper catalysts are much different from those for palladium catalysts. Because copper is a first-row transition metal, it is harder than the second-row palladium, and thus it is more liable to form complexes with nitrogen and oxygen ligands than palladium.<sup>[9a]</sup> Therefore, most of the ligands involved in the copper-catalyzed cross-coupling reactions are nitrogen or oxygen containing ones.<sup>[9a,46,47]</sup> At present, there is a lack of mechanistic foundations for the explanation of the relative reactivities of copper catalysts containing different ligands. Much of the



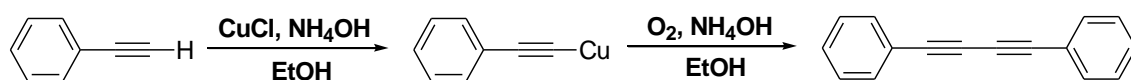
development of this field has based on empirical evaluation of copper catalysts with various ligands.

Nevertheless, copper catalysts have turned out to be especially effective for the aerobic cross-dehydrogenative coupling of two different nucleophiles having acidic C–H or X–H bonds. The Glaser–Hay and Chan–Lam–Evans reactions set the basis for today's achievement in this rapidly developing field.

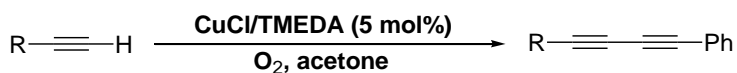
### ■ Glaser–Hay Alkyne Homo-coupling

The copper-catalyzed dimerization of alkynes, known as the Glaser–Hay reaction, originated from the stoichiometric  $\text{Cu}^{\text{I}}$ -mediated homo-coupling of phenylacetylene in the presence of ammonia under an air atmosphere in 1869 (Scheme 1-11).<sup>[11a]</sup> The catalytic version of this reaction was developed by Hay in 1962.<sup>[14d]</sup> To date, a number of homogeneous as well as heterogeneous catalyst systems for the Glaser–Hay reaction have been developed. Copper salts in combination with nitrogen-based mono- or bi-dentate ligands such as pyridine, triethylamine, TMEDA (tetramethylethylenediamine) are particularly effective.<sup>[46]</sup>

#### Glaser (1869)<sup>[11a]</sup>



#### Hay (1962)<sup>[14d]</sup>



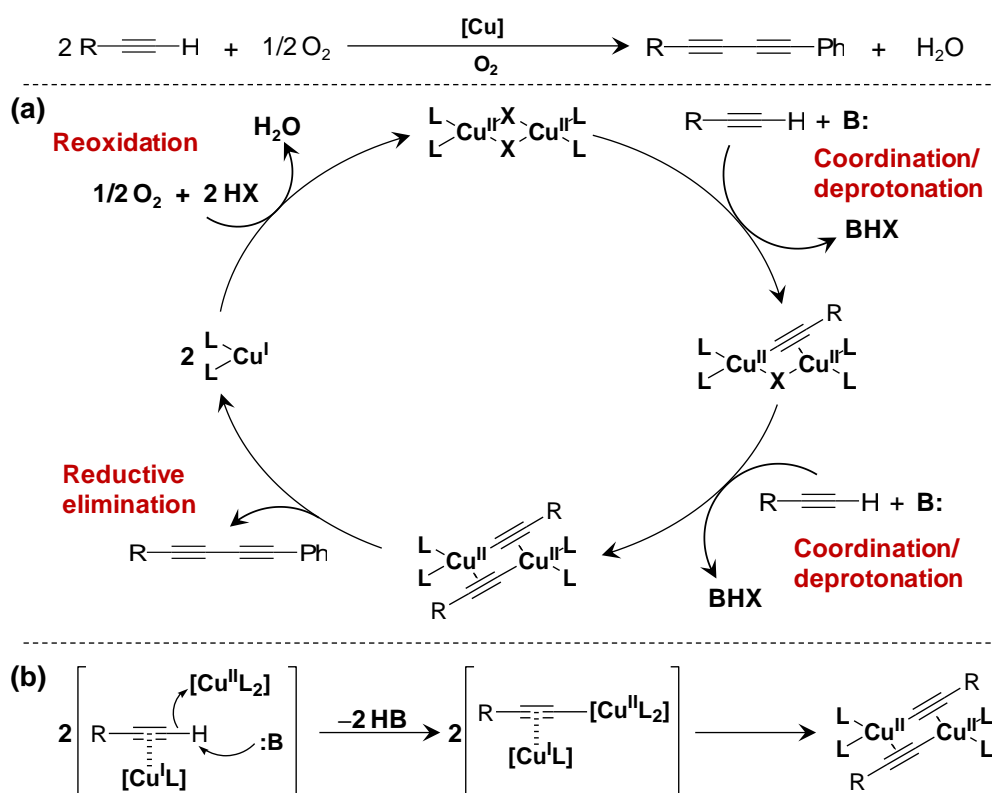
TMEDA = tetramethylethylenediamine

**Scheme 1-11.** The Glaser–Hay alkyne homo-coupling.

In spite of the great progress in the development of various copper-catalyzed systems for the Glaser–Hay reaction, the mechanism for the reaction is still under dispute. Several hypotheses exist regarding the oxidation state and the structure of active copper species during the reaction. A dimeric copper acetylide intermediate-involved catalytic cycle has been proposed based on kinetic data and density functional theory (DFT) calculation, in which  $\text{Cu}^{\text{II}}$  acts as a one-electron oxidant (Scheme 1-12).<sup>[46,48]</sup> The reaction was proposed to proceed through successive deprotonative coordination of alkynes to the dimeric copper centers, followed by reductive elimination to give the diyne products and reoxidation of the reduced copper centers by molecular oxygen to regenerate the catalyst.<sup>[46,48]</sup> Under an  $\text{O}_2$  atmosphere, reoxidation of  $\text{Cu}^{\text{I}}$  species by molecular oxygen was turned out to be a relatively fast step in the homogeneous system.<sup>[46-48]</sup> However, in a heterogeneous  $\text{Cu}(\text{OH})_x/\text{TiO}_2$ -catalyzed system, kinetic studies showed that the reoxidation of  $\text{Cu}^{\text{I}}$  species was involved in the rate-determining step.<sup>[49a]</sup> In addition, the UV/Vis spectrum of  $\text{Cu}(\text{OH})_x/\text{TiO}_2$  treated with phenylacetylene under an Ar atmosphere suggested the reduction of  $\text{Cu}^{\text{II}}$  to  $\text{Cu}^{\text{I}}$  by phenylacetylene due to the disappearance of the absorption band assignable to the d–d transition of the  $\text{Cu}^{\text{II}}$  species.<sup>[49b]</sup>

Lei and co-workers have also provided the direct spectroscopic evidences for the reduction of  $\text{Cu}^{\text{II}}$  to  $\text{Cu}^{\text{I}}$  by terminal alkynes, based on *in situ* analysis of the commonly utilized  $\text{Cu}^{\text{II}}$ /alkyne/TMEDA system by X-ray absorption spectroscopy (XAS) and electron paramagnetic resonance (EPR) under an  $\text{N}_2$  atmosphere.<sup>[49c]</sup> Both TMEDA and terminal alkynes were essential components for the reduction.<sup>[49c]</sup> TMEDA was turned out to function as both the ligand and the base, and other O and P ligands were not effective for the reaction.<sup>[49c]</sup> In a separate study, kinetic studies on the

CuCl<sub>2</sub>(TMEDA)/phenylacetylene/diisopropylamine system by *in situ* Raman spectroscopy under an N<sub>2</sub> atmosphere showed that an induction period was observed, and upon addition of a Cu<sup>I</sup> source, [CuCl(TMEDA)]<sub>2</sub>, the induction period disappeared.<sup>[49d]</sup> Kinetic studies also showed that the rate-determining step involved the reaction of phenylacetylene with [CuCl(TMEDA)]<sub>2</sub> but not with CuCl<sub>2</sub>(TMEDA).<sup>[49d]</sup> Although the reaction starting from phenylacetylene was completely suppressed at -20 °C, the reaction using lithium phenylacetylide smoothly proceeded even at -70 °C, suggesting that the reductive elimination was a relatively fast step compared to the copper acetylide formation.<sup>[49d]</sup> Based on the above experimental evidences, a Cu<sup>II</sup>-Cu<sup>I</sup> cooperated activation mode of terminal alkynes has been proposed (Scheme 1-12, b).<sup>[49d]</sup>

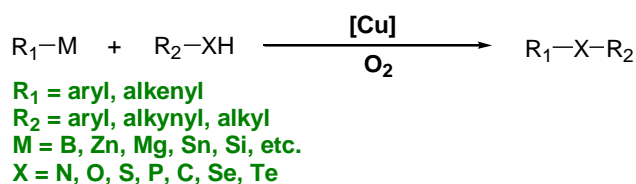


**Scheme 1-12.** The proposed mechanism for the Glaser-Hay alkyne homo-coupling. B: = base.<sup>[46,48,49d]</sup>

Although the above experimental evidences strongly support the dimeric copper-involved mechanism, an alternative monomeric copper species-involved palladium-like two electron transfer process, for example, reductive elimination from a monomeric Cu<sup>III</sup> acetylide species, can not be completely excluded at this point.

### ■ Chan–Lam–Evans Reaction

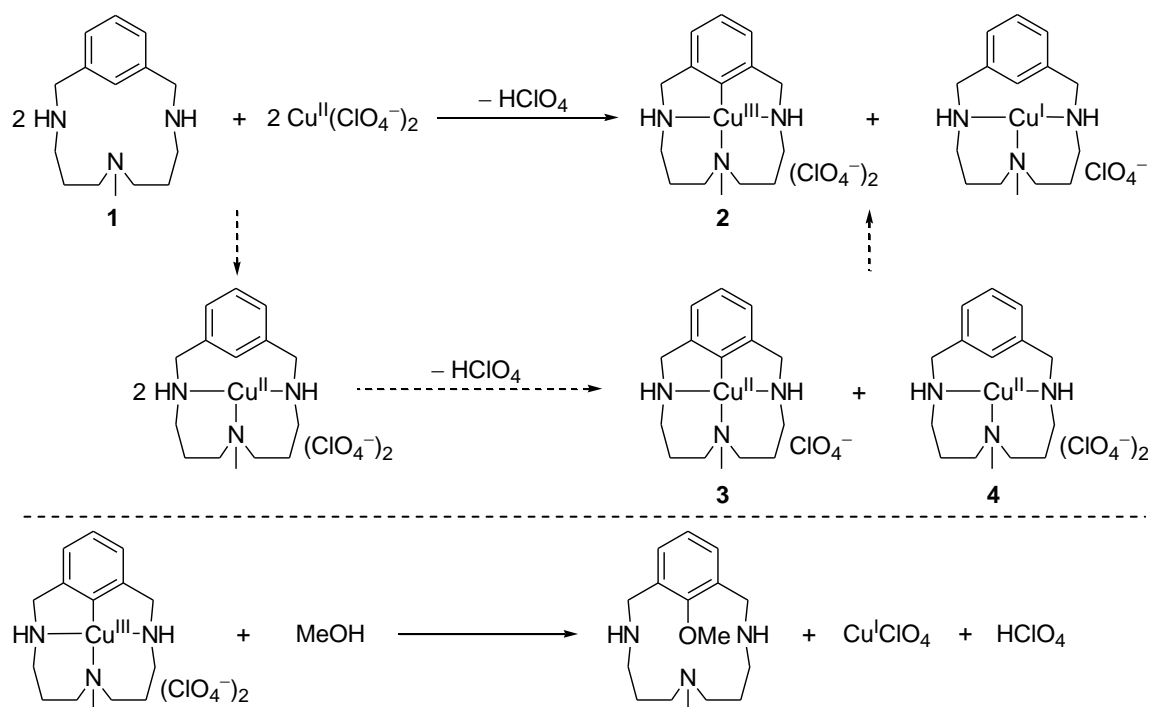
Developed independently by Chan, Lam, and Evans, the aerobic oxidative cross-coupling of aromatic or alkenyl organometallic compounds with various nucleophiles in the presence of copper-based catalysts, known as Chan–Lam–Evans reaction, has become a valuable method for the construction of C(sp<sup>2</sup>)-heteroatom bonds.<sup>[14f-h,50]</sup> Initial development of such reactions mainly focused on the cross-coupling of aryl boronic acids with alcohols, amines, and thiols. Developed to date, the cross-coupling has successfully been applied to C–N, C–O, C–S, C–P, C–C, C–Se, C–Te, C–Cl, C–Br, and C–I bond forming reactions (Scheme 1-13).<sup>[50]</sup> Among these reactions, the Chan–Lam–Evans C–N coupling reaction has become a valuable complementary to the well known Buchwald-Hartwig amination.<sup>[12]</sup> The Chan–Lam–Evans reaction often proceeds in the presence of appropriate copper-based catalysts in combination with amine bases or pyridines using molecular oxygen as the terminal oxidant.<sup>[50]</sup>



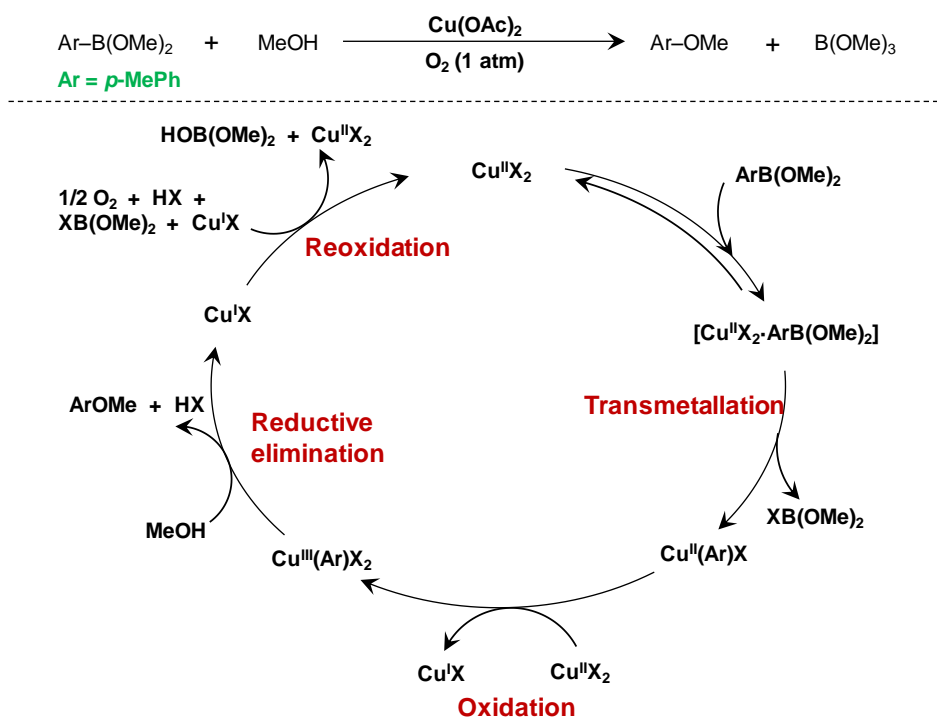
**Scheme 1-13.** The Chan–Lam–Evans reaction.<sup>[50]</sup>

Similar to the Glaser–Hay alkyne homo-coupling, the mechanism for the Chan–Lam–Evans reaction is also a disputable topic among the synthetic organic community. However, some mechanistic insights based on experimental results have been reported.<sup>[50b]</sup> Generally, the reaction does not likely proceed through radical intermediates, because the presence of a radical scavenger such as 1,1-diphenylethylene does not affect the reaction outcome.<sup>[50b]</sup>

Systematic studies on the reaction mechanism for the cross-coupling of phenylboronic esters and alcohols/amines have been carried out by Stahl and co-workers.<sup>[51]</sup> The stoichiometries of O<sub>2</sub>/product and Cu<sup>II</sup>/product were 1:2 and 2:1, respectively, which suggest that O<sub>2</sub> is a four-electron oxidant and Cu<sup>II</sup> is a one-electron oxidant. Kinetic studies showed the first-order dependence on Cu<sup>II</sup>, the saturation dependence on ArB(OMe)<sub>2</sub>, and the zero-order dependence on O<sub>2</sub>, suggesting the fast reoxidation of Cu<sup>I</sup> by O<sub>2</sub> and the rate-determining step of transmetallation of the aryl group to the copper center. The EPR spectroscopic analysis of the reaction mixture showed that the catalyst resting state consists of Cu<sup>II</sup> species lack of aryl group, also indicating the transmetallation step is the rate-determining step. Additional mechanistic studies were carried out using a cyclic Cu<sup>III</sup> model substrate (**2**) first reported by Ribas, Hedman, Hodgson, Llobet, and Stack, as shown in Scheme 1-14.<sup>[52]</sup> The Cu<sup>III</sup> complex **2** was obtained by the C–H activation of a cyclic amine (**1**) with a Cu<sup>II</sup> salt, which resulted in the formation of equimolar amount of **2** and a Cu<sup>I</sup> complex (Scheme 1-14). Compound **2** was proposed to be formed by oxidation of a Cu<sup>II</sup>-cyclic amine complex **3** by another Cu<sup>II</sup> complex **4**. In a separate experiment, **2** was found to readily react with methanol to form C–O bonds (Scheme 1-14).<sup>[53]</sup> These results strongly support the involvement of a Cu<sup>III</sup> species in the Chan–Lam–Evans cross-coupling.



**Scheme 1-14.** Synthesis and reaction of the  $\text{Cu}^{\text{III}}$  species.<sup>[51–53]</sup>



**Scheme 1-15.** Proposed mechanism for the oxidative cross-coupling of an arylboronic ester and methanol.<sup>[51]</sup>

Based on the above mechanistic studies, Stahl and co-workers proposed a plausible reaction mechanism for the Chan–Lam–Evans cross-coupling (Scheme 1-15).<sup>[51]</sup> The catalytic cycle was proposed to include the following several key steps; (1) rate-determining transmetallation from an arylboronic ester to the Cu<sup>II</sup> center, (2) oxidation of Cu<sup>II</sup> to Cu<sup>III</sup>, (3) nucleophilic substitution of the Cu<sup>III</sup> species with methanol followed by reductive elimination to afford an aryl ether, and (4) reoxidation of Cu<sup>I</sup> to Cu<sup>II</sup> species to close the catalytic cycle. Because both one- and two-electron transfer processes are included in the catalytic cycle (the Cu<sup>II</sup>–Cu<sup>III</sup>–Cu<sup>I</sup>–Cu<sup>II</sup> cycle), the copper-catalyzed Chan–Lam–Evans reaction is distinct from the traditional palladium-catalyzed cross-couplings (the Pd<sup>0</sup>–Pd<sup>II</sup>–Pd<sup>0</sup> cycle).

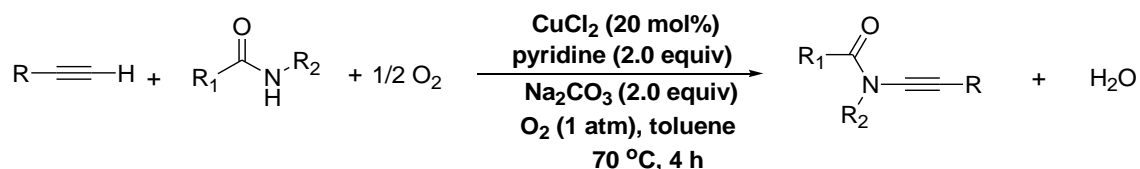
### ■ Recent Developments in Copper-Catalyzed Aerobic Cross-Dehydrogenative Coupling Reactions

Inspired by the above-described Glaser–Hay alkyne homo-coupling and Chan–Lam–Evans reaction, dramatic advances in the field of copper catalyzed aerobic cross-dehydrogenative coupling reactions have been achieved in recent years.<sup>[54–67]</sup> The coupling partners of these reactions often have acidic C–H or X–H bonds, and these reactions have been carried out in the presence of appropriate bases (organic or inorganic) and ligands (mainly nitrogen-based ligands) using molecular oxygen as the terminal oxidant (Scheme 1-16).

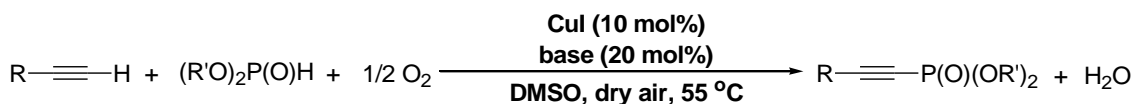
In spite of the significant progress in the development of copper-catalyzed cross-dehydrogenative coupling reactions, their fundamental mechanism is currently unclear. Most of the reports have only provided plausible reaction mechanisms without enough experimental evidences, and the reactions have been supposed to proceed

through the paths of typical oxidative cross-coupling of two different nucleophiles, as described in section 1.2.3.2 (Scheme 1-4).<sup>[54–67]</sup>

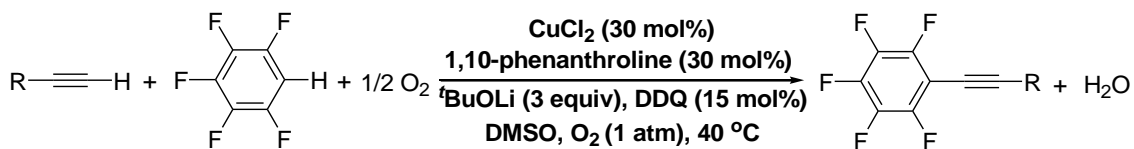
**Stahl et al. (2008)<sup>[54]</sup>**



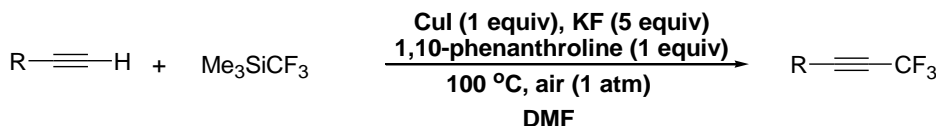
**Han et al. (2009)<sup>[55]</sup>**



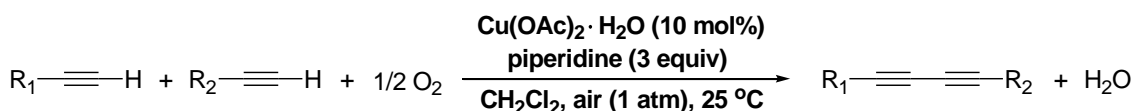
**Hong et al. (2010)<sup>[56]</sup>, Miura et al. (2010)<sup>[57]</sup>**



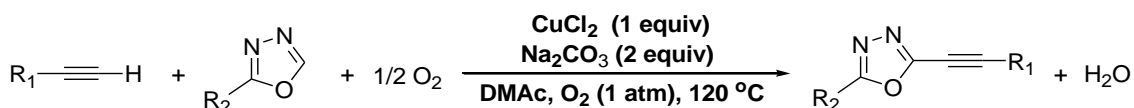
**Qing et al. (2010)<sup>[58]</sup>**



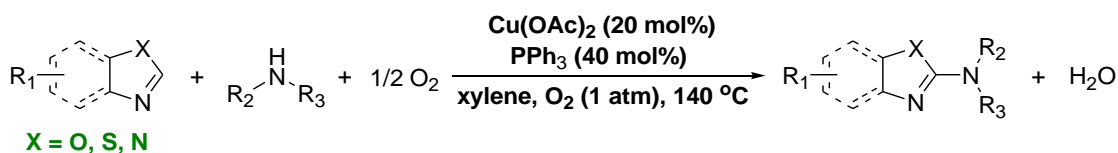
**Kesavan et al. (2010)<sup>[59]</sup>**



**Miura et al. (2010)<sup>[60]</sup>**

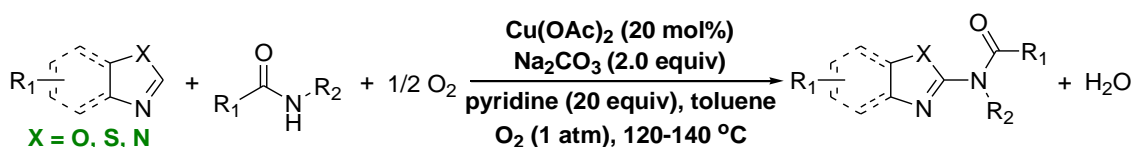


**Mori et al. (2009)<sup>[61]</sup>**

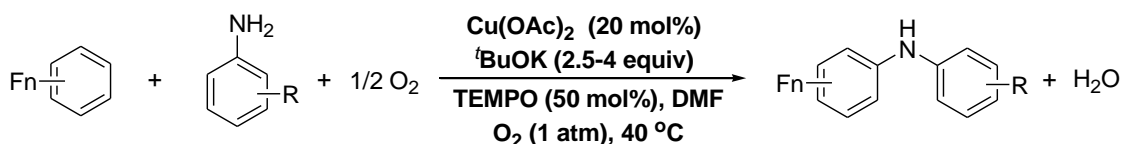




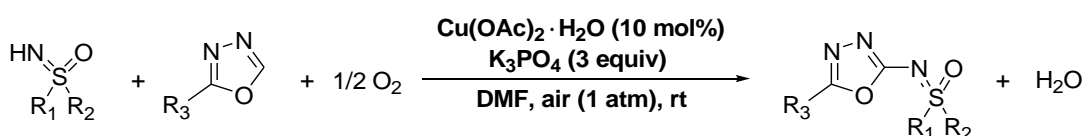
Schreiber et al. (2009)<sup>[62]</sup>



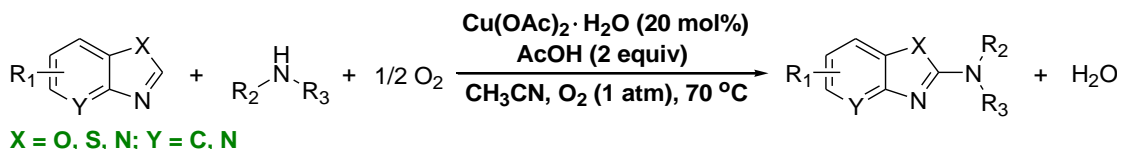
Su et al. (2010)<sup>[63]</sup>



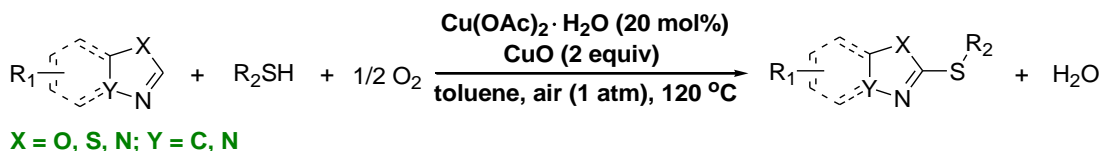
Bolm and Miura et al. (2010)<sup>[64]</sup>



Li and Duan et al. (2011)<sup>[65]</sup>



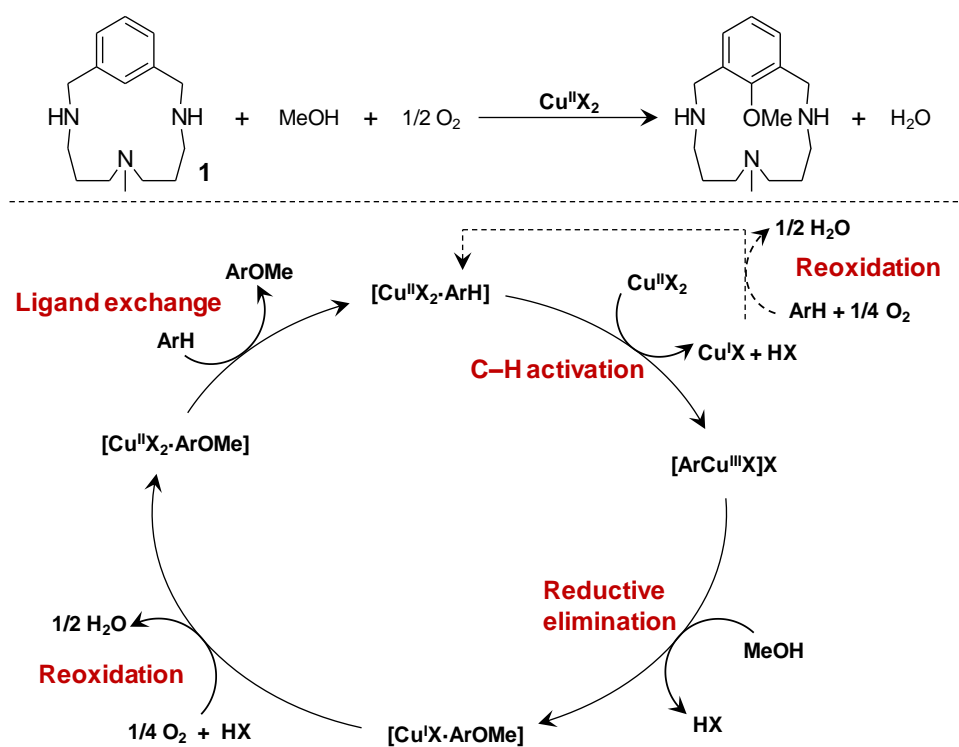
Liu et al. (2011)<sup>[66]</sup>, Huang and Liu et al. (2011)<sup>[67]</sup>



**Scheme 1-16.** Selected examples of copper-catalyzed aerobic cross-dehydrogenative coupling reactions.

Stahl and co-workers have studied the reaction mechanism for the aerobic cross-dehydrogenative coupling of the macrocyclic arene (**1**) and methanol.<sup>[53]</sup> The direct observation of the Cu<sup>III</sup> species **2** by *in situ* UV-Vis spectroscopy and the facile reaction of **2** with methanol to give an aryl ether strongly indicated the involvement of **2** in the reaction (Scheme 1-14). Kinetic studies showed that oxidation of Cu<sup>I</sup> by molecular oxygen was faster than other steps. Collective data from kinetic studies, EPR analysis, and UV-Vis spectroscopy suggested that the rates of the C–H bond activation

and C–O bond formation steps were closely matched. Based on these studies, a catalytic cycle containing sequential C–H bond activation/reductive elimination/reoxidation steps was proposed, as shown in Scheme 1-17.



**Scheme 1-17.** Proposed reaction mechanism for the aerobic oxidative methoxylation of a macrocyclic arene (**1**).<sup>[53]</sup>

Although the special macrocyclic arene was employed as the model substrate for the aerobic oxidative cross-coupling, it is a good indication that the above-described cross-coupling reactions of two acidic C–H or X–H bonds also possibly proceed through Cu<sup>III</sup> species in light of the similarity of these reactions. Apparently, further elucidation of the reaction mechanism for copper-catalyzed aerobic cross-dehydrogenative coupling reactions is still needed for the development of novel reactions or more efficient catalyst systems.

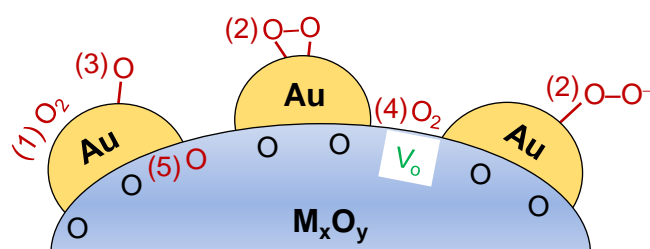
#### 1.2.4. Gold Nanoparticles for Aerobic Oxidative Bond-Forming Reactions

Gold has long been recognized as an inert metal against chemical reactions, however, discoveries by Haruta<sup>[68]</sup> and Hutchings<sup>[69]</sup> have dramatically led chemists to reevaluate its potential utility as catalysts in chemical synthesis. Haruta and co-workers found that gold nanoparticles supported on metal oxides were able to catalyze oxidation of CO even at low temperature ( $-70\text{ }^{\circ}\text{C}$ ).<sup>[68]</sup> Hutchings discovered that supported gold catalysts could promote hydrochlorination of acetylene.<sup>[69]</sup> Since these pioneering work, the great progress in the field of gold catalysis has been achieved either in homogeneous or heterogeneous systems.<sup>[70-74]</sup>

Supported gold nanoparticles on various metal oxides, for example, Au/Al<sub>2</sub>O<sub>3</sub>, Au/TiO<sub>2</sub>, Au/Fe<sub>3</sub>O<sub>4</sub>, Au/CeO<sub>2</sub>, Au/MgO, etc., or on carbonaceous materials (Au/C) are typically prepared by incipient wetness impregnation or deposition-precipitation method using appropriate gold precursors such as HAuCl<sub>4</sub> or NaAuCl<sub>4</sub> followed by reduction of the Au<sup>III</sup> species.<sup>[70]</sup> The supported gold nanoparticles can exist as various oxidation states, e.g., Au<sup>0</sup>, Au<sup>δ-</sup> or Au<sup>δ+</sup> (Au<sup>I</sup> or Au<sup>III</sup>).<sup>[71]</sup> However, the actual catalytically active species is still under debate. The preparative method can strongly affect the particle size which is one of the most important parameters to determine the catalytic activity.<sup>[70]</sup> Another important factor for the activity is gold nanoparticle-support interaction.<sup>[72]</sup> An appropriate choice of the support for a specific reaction can greatly accelerate the reaction.

Supported gold nanoparticle catalysts are particularly effective for many oxidation reactions, such as low-temperature CO oxidation, olefin epoxidation, the water-gas shift reaction, and other related oxidations.<sup>[70]</sup> Apart from these gas phase reactions, the liquid phase oxidations by gold nanoparticles have also rapidly been developed in

recent years.<sup>[73]</sup> The versatility of supported gold nanoparticles in oxidation catalysis can partly be attributed to their ability of activation of molecular oxygen. However, the identification of the nature of the active oxygen species is a quite complicated problem. In addition, the active site of supported gold nanoparticles for oxygen activation and the location of the active oxygen species, for example, on the gold nanoparticles, on the support surface, and/or at the perimeter of the interface between them, are still controversial.<sup>[75]</sup> Several modes for oxygen activation have been proposed based on theoretical and experimental studies (Figure 1-3); (1) weakly adsorbed molecular oxygen on gold nanoparticle surface at low temperature indicated by theoretical studies, (2) negatively charged oxygen species such as superoxide or peroxide identified by EPR and Raman spectroscopy, (3) atomically adsorbed oxygen species indicated by model studies, (4) molecular oxygen adsorbed at support vacancies, and (5) lattice oxygen of the support, especially for readily reducible oxides, e.g., TiO<sub>2</sub>, Fe<sub>3</sub>O<sub>4</sub>, Co<sub>3</sub>O<sub>4</sub>, CeO<sub>2</sub>, MnO<sub>2</sub>, etc.<sup>[74]</sup> However, The direct dissociative adsorption of molecular oxygen on gold nanoparticles at temperatures lower than 400 °C is strongly inhibited by the high dissociation barrier.<sup>[76]</sup>



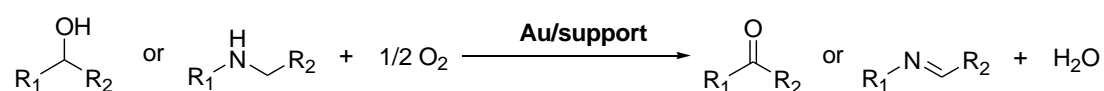
**Figure 1-3.** Active oxygen species on supported gold nanoparticle catalysts. V<sub>o</sub> = oxygen vacancy.<sup>[74]</sup>

Gold nanoparticles immobilized on different supports can have different modes for oxygen activation. With the reducible oxide supports at relatively higher reaction

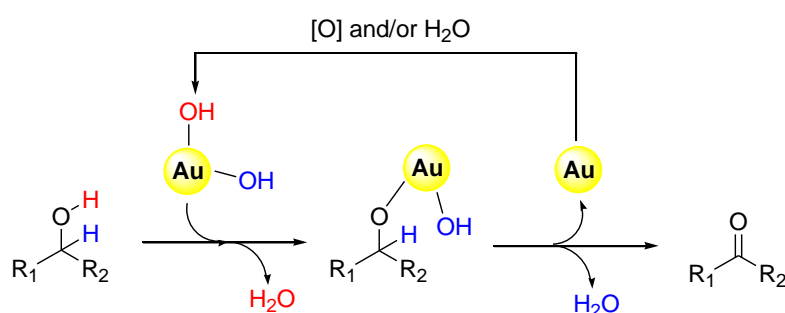
temperature for CO oxidation, the active oxygen species are likely located at the lattice sites of the oxides, and the reaction occurring at the perimeter of the interface. Otherwise, for the non-reducible supports such as  $\text{Al}_2\text{O}_3$ , the active oxygen species are likely located on the nanoparticle surface and CO oxidation also occurs on the surface.<sup>[74]</sup> At relatively lower reaction temperature, for example, lower than room temperature, removal of the lattice oxygen is increasingly inhibited, and thus the weakly adsorbed molecular oxygen on the nanoparticle surface will dominate the active oxygen species.<sup>[74]</sup> The presence of a trace amount of water can greatly accelerate CO oxidation, likely by (1) maintenance of catalytically active cationic gold species, (2) direct participation of  $\text{H}_2\text{O}$  or  $\text{OH}^-$  species in the reaction, (3) facilitation of oxygen activation, and (4) transformation of the carbonate intermediate to the bicarbonate species.<sup>[75]</sup>

One of the most extensively studied liquid phase oxidation reactions by the supported gold nanoparticle catalysts is aerobic oxidation of alcohols/amines to carbonyls/imines.<sup>[73]</sup> The presence of water also benefits the aerobic oxidation of alcohols likely through formation of surface hydroxy species, which can promote abstraction of protons from alcohols to form alkoxy species, also can assist subsequent  $\beta$ -hydride elimination to give the carbonyl products (Scheme 1-19).<sup>[77]</sup> By applying the ability of gold nanoparticles for aerobic oxidation of alcohols, various novel aerobic synthetic procedures for several valuable chemicals such as amides and esters have been developed.<sup>[73]</sup> For example, Kobayashi<sup>[78]</sup> and Wang<sup>[79]</sup> independently developed a novel efficient synthetic procedure for secondary or tertiary amides starting from readily available and easily handled alcohols and amines. The reaction was proposed to proceed through the following several sequential reactions; (1) oxidation of an alcohol to an aldehyde, (2) nucleophilic addition of an amine to the aldehyde to form a hemiaminal

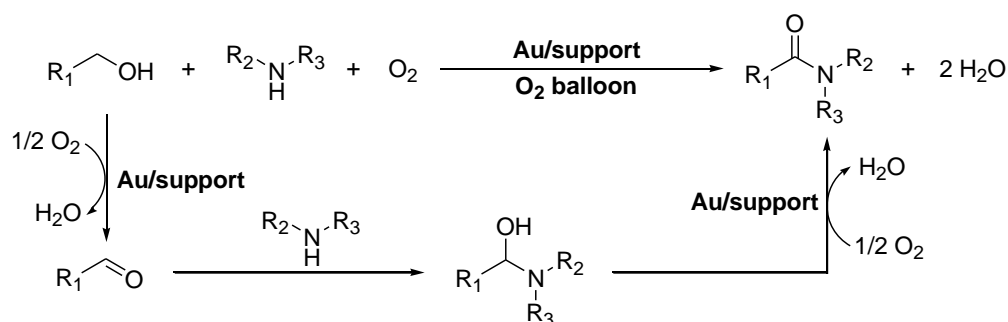
intermediate, and (3) oxidation of the hemiaminal to give an amide as the final product (Scheme 1-20). Esters have also successfully been synthesized via the process similar to that of the amide synthesis in which amines were replaced by alcohols.<sup>[80]</sup> In addition to these aerobic oxidative functional group transformations, quite recently, Corma and co-workers have developed several C–C bond forming reactions (Scheme 1-21).<sup>[81–83]</sup> However, these reactions were typically carried out under rather harsh conditions, e.g., high temperature and oxygen pressure.



**Scheme 1-18.** Aerobic oxidation of alcohols and amines by supported gold nanoparticles.<sup>[73]</sup>

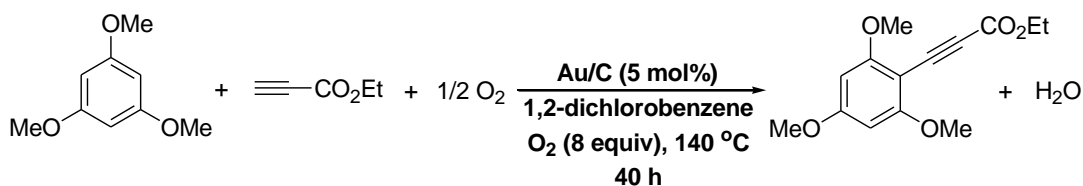


**Scheme 1-19.** Schematic illustration of aerobic oxidation of alcohols promoted by surface hydroxy species on gold nanoparticles.<sup>[77]</sup>

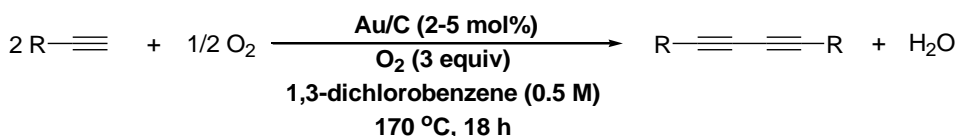


**Scheme 1-20.** Synthesis of amides by supported gold nanoparticles.<sup>[78–79]</sup>

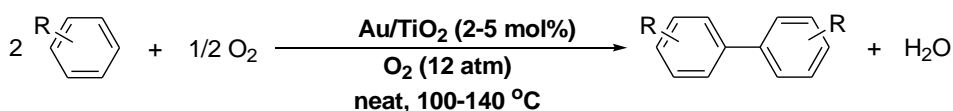
Corma et al. (2013)<sup>[81]</sup>



Corma et al. (2014)<sup>[82]</sup>



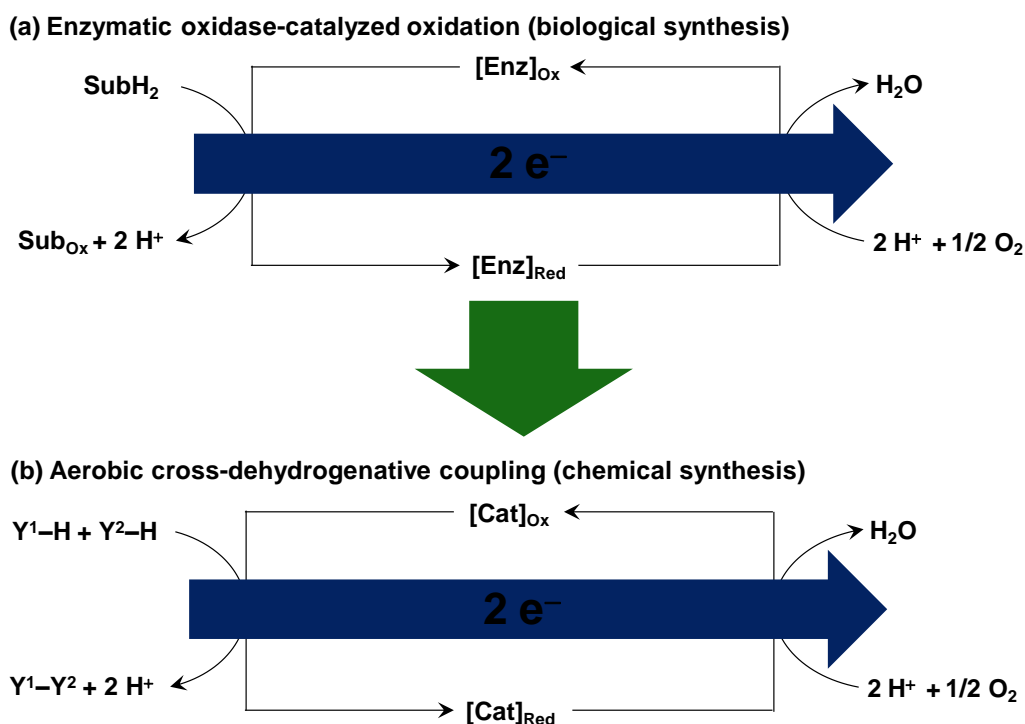
Corma et al. (2014)<sup>[83]</sup>



**Scheme 1-21.** Supported gold nanoparticle-catalyzed aerobic dehydrogenative C–C bond forming reactions.

### 1.3. Overview of This Thesis

A large quantity of waste is often generated in the process of fine chemical synthesis, causing significant increase of the environmental burden. With the growth of global population, ever-increasing demand of chemicals requires chemists to seek more efficient synthetic procedures that can eventually revolutionize future manufacture processes. Aerobic cross-dehydrogenative coupling reactions of ubiquitous C–H and/or X–H bonds to construct C–C, C–X, or X–X bonds have great potential to change the way of synthesizing a large variety of valuable chemicals. These cross-dehydrogenative couplings can be regarded as oxidase-type reactions, because the oxidative dehydrogenation is accompanied by reduction of molecular oxygen without oxygen atom transfer to substrates, and consequently, net electron transfer occurring concomitantly between the substrates and molecular oxygen (Figure 1-4).<sup>[84]</sup>



**Figure 1-4.** Schematic illustration of electron transfer processes in (a) enzymatic oxidase-catalyzed oxidation and (b) aerobic cross-dehydrogenative coupling. Cat = catalyst, Enz = Enzyme.<sup>[84]</sup>

The main purpose of this thesis is to develop novel late-transition metal-catalyzed aerobic cross-dehydrogenative coupling reactions. Considering the electron transfer processes in aerobic cross-dehydrogenative coupling reactions (Figure 1-4), the key factor for the successful employment of molecular oxygen as the terminal oxidant is the activation of substrates as well as molecular oxygen through one or multiple electron transfer between substrates, catalysts, and molecular oxygen. In this study, copper-based catalysts, supported gold nanoparticles, as well as readily reducible metal oxides such as manganese oxide based catalysts have mainly been utilized, because of their rich oxidation chemistry when using molecular oxygen as the terminal oxidant. Specifically, the following several reactions have successfully been developed; (1) copper-catalyzed



cross-coupling of terminal alkynes or *H*-phosphonates with amides through a sequential nucleophilic substitution or coordination-deprotonation/reductive elimination/reoxidation pathway (Figure 1-5, strategy 1), (2) heterogeneously gold-catalyzed aerobic oxidative amination of  $\alpha,\beta$ -unsaturated aldehydes by a sequential nucleophilic addition/aerobic oxidative dehydrogenation pathway (Figure 1-5, strategy 2), and (3) zinc and OMS-2 (manganese oxide-based octahedral molecular sieves) co-catalyzed cross-coupling of terminal alkynes and tertiary amines by a sequential oxidation/nucleophilic addition pathway (Figure 1-5, strategy 3).

In chapter 2, Cu(OH)<sub>2</sub>-catalyzed selective aerobic cross-dehydrogenative coupling of terminal alkynes and amides to ynamides is described. High yields and selectivities to ynamides are achieved even without slow addition of alkynes (56–93% yields). The substrate scope with respect to both terminal alkynes and amides is very broad. Meanwhile, a novel green synthetic route to imides via the oxidative cross-coupling followed by the hydration of ynamides to imides by Sn–W mixed oxide catalysts is also developed (80–92% yields).

In chapter 3, Cu(OAc)<sub>2</sub>-catalyzed aerobic cross-dehydrogenative coupling of *H*-phosphonates and amides to *N*-acylphosphoramidates is described. Cu(OAc)<sub>2</sub> in combination with an appropriate base is revealed to efficiently promote the oxidative cross-coupling of *H*-phosphonates and amides using air as the terminal oxidant. Various dialkyl *H*-phosphonates can efficiently react with nitrogen nucleophiles, such as oxazolidinone, lactam, pyrrolidinone, urea, indole, and sulfonamide derivatives, to give the corresponding *N*-acylphosphoramidates in moderate to high yields (52–99% yields).

In chapter 4, Au/OMS-2-catalyzed  $\beta$ -amination of  $\alpha,\beta$ -unsaturated aldehydes is

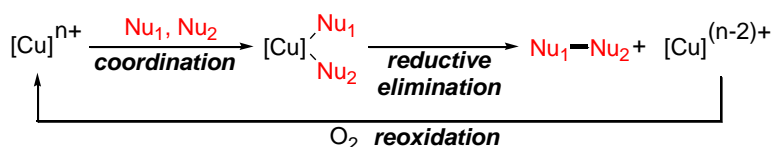
described. In the presence of Au/OMS-2 (average particle size of gold: 4.1 nm), the aerobic dehydrogenative amination of  $\alpha,\beta$ -unsaturated aldehydes with amines efficiently proceeds to give the corresponding enaminals in moderate to high yields (50–97% yields). The catalysis is truly heterogeneous, and Au/OMS-2 can be reused several times.

In chapter 5,  $\text{ZnBr}_2$  and OMS-2 co-catalyzed aerobic cross-dehydrogenative coupling of terminal alkynes and tertiary amines to propargylamines is described. In the presence of catalytic amounts of  $\text{ZnBr}_2$  and OMS-2, various combinations of terminal alkynes (aromatic and aliphatic) and tertiary methyl amines selectively give the corresponding propargylamines in moderate to high yields under 1 atm of molecular oxygen (22–88% yields).

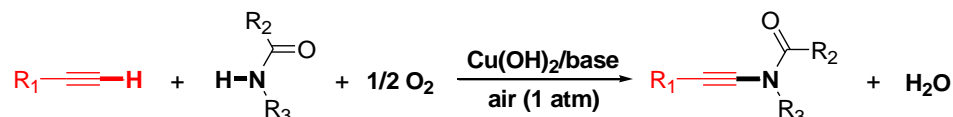
In chapter 6, general conclusions and outlooks of this thesis are described.

## ■ Aerobic Cross-Dehydrogenative Coupling of Two Different Nucleophiles

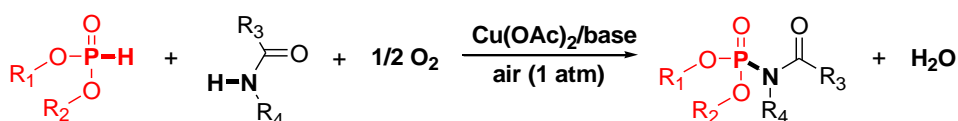
### Strategy 1: Coordination/Reductive elimination/Reoxidation



### Chapter 2: Cu(OH)<sub>2</sub>-Catalyzed Cross-Coupling of Terminal Alkynes and Amides

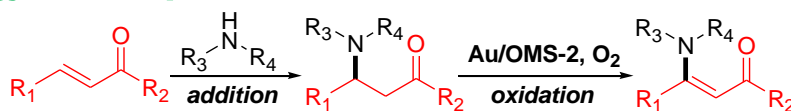


### Chapter 3: Cu(OAc)<sub>2</sub>-Catalyzed Cross-Coupling of *H*-Phosphonates and Amides

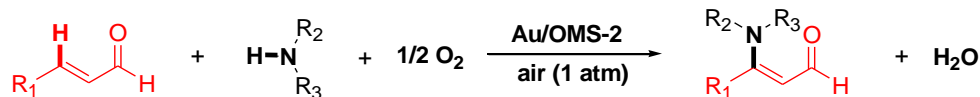


## ■ Aerobic Cross-Dehydrogenative Coupling of a Nucleophile and an Electrophile

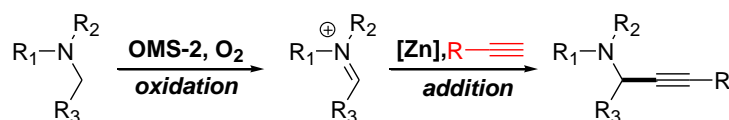
### Strategy 2: Nucleophilic addition/Oxidation



### Chapter 4: Au/OMS-Catalyzed $\beta$ -Amination of $\alpha,\beta$ -Unsaturated Aldehydes



### Strategy 3: Oxidation/Nucleophilic addition



### Chapter 5: Zn<sup>2+</sup> and OMS-2 Co-catalyzed Aerobic Cross-Dehydrogenative Coupling of Terminal Alkynes and Tertiary Amines

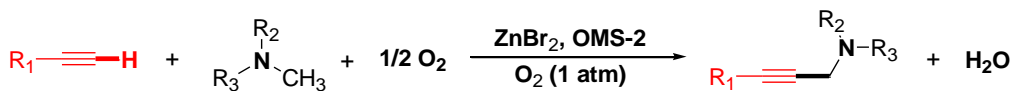


Figure 1-5. Outline of this study.

#### 1.4. References

- [1] P. Tundo, P. Anastas, *Green Chemistry: challenging perspectives*, Oxford Univ. Press, Oxford, **2000**.
- [2] a) P. T. Anastas, J. Warner, *Green Chemistry Theory and Practice*, Oxford Univ. Press, Oxford, **1998**.
- [3] M. Poliakoff, J. M. Fitzpatrick, T. R. Farren, P. T. Anastas, *Science* **2002**, 297, 807.
- [4] a) R. A. Sheldon, *Industrial Environmental Chemistry*, D. T. Sawyer and A. E. Martell (Eds.), Plenum, New York, **1992**; b) R. A. Sheldon, *Precision Process Technology*, M. P. C. Weijnen and A. A. H. Drinkenburg (Eds.), Kluwer, Dordrecht, **1993**; c) R. A. Sheldon, I. Arends, U. Hanefeld, *Green Chemistry and Catalysis*, Wiley-VCH, Weinheim, **2007**; d) C. G. Brundtland, *Our Common Future, The World Commission on Environmental Development*, Oxford University Press, Oxford, **1987**.
- [5] a) M. J. Mulvihill, E. S. Beach, J. B. Zimmerman, P. T. Anastas, *Annu. Rev. Environ. Resour.* **2011**, 36, 271; b) R. A. Sheldon, *J. Mol. Catal. A* **1996**, 107, 75.
- [6] a) B. M. Trost, *Science* **1991**, 254, 1471; b) B. M. Trost, *Angew. Chem. Int. Ed. Engl.* **1995**, 34, 259.
- [7] N. Miyaura, A. Suzuki, *Chem. Rev.* **1995**, 95, 2457.
- [8] a) V. J. Inglezakis, S. G. Pouloupoulos, *Adsorption, Ion Exchange and Catalysis: Design of Operations and Environmental Applications*, Elsevier, Oxford, **2006**;  
b) A. D. McNaught, A. Wilkinson, *IUPAC Compendium of Chemical Terminology (2nd ed., the "Gold Book")*, Blackwell Scientific Publications, Oxford, **1997**.

- [9] a) J. Hartwig, *Organotransition Metal Chemistry: From Bonding to Catalysis*, Univ. Sci. Books, Sausalito, **2010**; b) J. R. H. Ross, *Heterogeneous Catalysis: Fundamentals and Applications*, Elsevier, Oxford, **2012**; c) G. W. Parshall, R. E. Putscher, *J. Chem. Educ.* **1986**, *63*, 189;
- [10] a) G. Ertl, *Angew. Chem. Int. Ed. Engl.* **1990**, *29*, 1219; b) H.-J. Freund, G. Meijer, M. Scheffler, R. Schlögl, M. Wolf, *Angew. Chem. Int. Ed.* **2011**, *50*, 10064; c) G. Ertl, *Angew. Chem. Int. Ed.* **2008**, *47*, 3524.
- [11] a) Glaser, *Ber. Dtsch. Chem. Ges.* **1869**, *2*, 422; b) F. Ullmann, *J. Ber. Dtsch. Chem. Ges.* **1901**, *34*, 2174;
- [12] a) E. Negishi, *Handbook of Organopalladium Chemistry for Organic Synthesis*, Wiley-Interscience, New York, **2002**; b) A. Meijere, F. Diederich, *Metal-Catalyzed Cross-Coupling Reactions*, Wiley-VCH, Weinheim, **2004**.
- [13] C. C. C. Johansson Seechurn, M. O. Kitching, T. J. Colacot, V. Snieckus, *Angew. Chem. Int. Ed.* **2012**, *51*, 5062.
- [14] a) H. Meerwein, E. Buchner, K. van Emsterk, *J. Prakt. Chem.* **1939**, *152*, 237; b) W. Chodkiewicz, P. Cadot, *C. R. Hebd. Seances Acad. Sci.* **1955**, *241*, 1055; c) G. Eglinton, A. R. Galbraith, *Chem. Ind. (London)* **1956**, 737; d) A. S. Hay, *J. Org. Chem.* **1962**, *27*, 3320; e) C. E. Castro, R. D. Stephens, *J. Org. Chem.* **1963**, *28*, 2163; f) D. M. T. Chan, K. L. Monaco, R.-P. Wang, M. P. Winters, *Tetrahedron Lett.* **1998**, *39*, 2933; g) P. Y. S. Lam, C. G. Clark, S. Saubern, J. Adams, M. P. Winters, D. M. T. Chan, A. Combs, *Tetrahedron Lett.* **1998**, *39*, 2941; h) D. A. Evans, J. L. Katz, T. R. West, *Tetrahedron Lett.* **1998**, *39*, 2937.
- [15] a) M. Tamura, J. K. Kochi, *J. Am. Chem. Soc.* **1971**, *93*, 1487; b) R. J. P. Corriu, J. P. Masse, *J. Chem. Soc., Chem. Commun.* **1972**, 144; c) K. Tamao, K.

- Sumitani, M. Kumada, *J. Am. Chem. Soc.* **1972**, *94*, 4374; d) E. Negishi, S. Baba, *J. Chem. Soc., Chem. Commun.* **1976**, 596.
- [16] a) J. Tsuji, H. Takahashi, M. Morikawa, *Tetrahedron Lett.* **1965**, 4387; b) B. M. Trost, T. J. Fullerton, *J. Am. Chem. Soc.* **1973**, *95*, 292; c) I. Moritani, Y. Fujiwara, *Tetrahedron Lett.* **1967**, *8*, 1119; d) T. Mizoroki, K. Mori, A. Ozaki, *Bull. Chem. Soc. Jpn.* **1971**, *44*, 581; e) R. F. Heck, J. P. Nolley, Jr., *J. Org. Chem.* **1972**, *37*, 2320; f) K. Sonogashira, Y. Tohda, N. Hagihara, *Tetrahedron Lett.* **1975**, *50*, 4467; g) M. Yamamura, I. Moritani, S. Murahashi, *J. Organometal. Chem.* **1975**, *91*, C39; h) D. Azarian, S. S. Dua, C. Eaborn, D. R. M. Walton, *J. Organometal. Chem.* **1976**, *117*, C55; i) M. Kosugi, K. Sasazawa, Y. Shimizu, T. Migita, *Chem. Lett.* **1977**, 301; j) D. Milstein, J. K. Stille, *J. Am. Chem. Soc.* **1978**, *100*, 3636; k) S. Baba, E. Negishi, *J. Am. Chem. Soc.* **1976**, *98*, 6729; l) E. Negishi, A. O. King, N. Okukado, *J. Org. Chem.* **1977**, *42*, 1821; m) N. Miyaura, K. Yamada, A. Suzuki, *Tetrahedron Lett.* **1979**, *20*, 3437; n) Y. Hatanaka, T. Hiyama, *J. Org. Chem.* **1988**, *53*, 918; o) F. Paul, J. Patt, J. F. Hartwig, *J. Am. Chem. Soc.* **1994**, *116*, 5969; p) A. S. Guram, S. L. Buchwald, *J. Am. Chem. Soc.* **1994**, *116*, 7901; q) T. Ishiyama, M. Murata, N. Miyaura, *J. Org. Chem.* **1995**, *60*, 7508; r) T. Ishiyama, J. Takagi, K. Ishida, N. Miyaura, N. R. Anastasi, J. F. Hartwig, *J. Am. Chem. Soc.* **2002**, *124*, 390.
- [17] a) E.-i. Negishi, *Angew. Chem. Int. Ed.* **2011**, *50*, 6738; b) A. Suzuki, *Angew. Chem. Int. Ed.* **2011**, *50*, 6722.
- [18] a) E. E. I. Knappe, S. Grupe, D. Gärtner, M. Corpet, C. Gosmini, A. J. Wangelin, *Chem. Eur. J.* **2014**, *20*, 6828; b) S. Z. Tasker, E. A. Standley, T. F. Jamison, *Nature* **2014**, *509*, 299.

- [19] D. A. Everson, D. J. Weix, *J. Org. Chem.* **2014**, *79*, 4793.
- [20] a) M. Amatore, C. Gosmini, *Angew. Chem. Int. Ed.* **2008**, *47*, 2089; b) J.-M. Bégouin, C. Gosmini, *J. Org. Chem.* **2009**, *74*, 3221; c) J.-M. Bégouin, S. Claudel, C. Gosmini, *Synlett* **2009**, 3192; d) W. M. Czaplik, M. Mayer, A. Jacobi von Wangelin, *Synlett* **2009**, 2931; e) J.-M. Bégouin, M. Rivard, C. Gosmini, *Chem. Commun.* **2010**, *46*, 5972; f) A. Moncomble, P. Le Floch, A. Lledos, C. Gosmini, *J. Org. Chem.* **2012**, *77*, 5056.
- [21] a) C. Gosmini, C. Bassene-Ernst, M. Durandetti, *Tetrahedron* **2009**, *65*, 6141; b) D. A. Everson, R. Shrestha, D. J. Weix, *J. Am. Chem. Soc.* **2010**, *132*, 920; c) X. Yu, T. Yang, S. Wang, H. Xu, H. Gong, *Org. Lett.* **2011**, *13*, 2138; d) L. L. Anka-Lufford, M. R. Prinsell, D. J. Weix, *J. Org. Chem.* **2012**, *77*, 9989; e) Y. Dai, F. Wu, Z. Zang, H. You, H. Gong, *Chem. Eur. J.* **2012**, *18*, 808; f) D. A. Everson, B. A. Jones, D. J. Weix, *J. Am. Chem. Soc.* **2012**, *134*, 6146; g) S. Wang, Q. Qian, H. Gong, *Org. Lett.* **2012**, *14*, 3355; h) C.-S. Yan, Y. Peng, X.-B. Xu, Y.-W. Wang, *Chem. Eur. J.* **2012**, *18*, 6039; i) S. Biswass, D. J. Weix, *J. Am. Chem. Soc.* **2013**, *135*, 16192; j) A. H. Cherney, S. E. Reisman, *J. Am. Chem. Soc.* **2014**, *136*, 14365.
- [22] a) W. M. Czaplik, M. Mayer, A. Jacobi von Wangelin, *Angew. Chem. Int. Ed.* **2009**, *48*, 607; b) W. M. Czaplik, M. Mayer, A. Jacobi von Wangelin, *ChemCatChem* **2011**, *3*, 135.
- [23] a) L. Wang, Y. Zhang, L. Liu, Y. Wang, *J. Org. Chem.* **2006**, *71*, 1284; b) A. Krasovskiy, C. Duplais, B. H. Lipshutz, *J. Am. Chem. Soc.* **2009**, *131*, 15592; c) A. Krasovskiy, C. Duplais, B. H. Lipshutz, *Org. Lett.* **2010**, *12*, 4742; d) C. Duplais, A. Krasovskiy, A. Wattenberg, B. H. Lipshutz, *Chem. Commun.* **2010**,

- 46, 562; e) V. Krasovskaya, A. Krasovskiy, A. Bhattacharjya, B. H. Lipshutz, *Chem. Commun.* **2011**, 47, 5717; f) C. Duplais, A. Krasovskiy, B. H. Lipshutz, *Organometallics* **2011**, 30, 6090.
- [24] a) C. Liu, H. Zhang, W. Shi, A. Lei, *Chem. Rev.* **2011**, 111, 1780. b) C. Liu, L. Jin, A. Lei, *Synlett* **2010**, 17, 2527; c) W. Shi, C. Liu, A. Lei, *Chem. Soc. Rev.* **2011**, 40, 2761.
- [25] C. S. Yeung, V. M. Dong, *Chem. Rev.* **2011**, 111, 1215.
- [26] a) Z. Li, C.-J. Li, *J. Am. Chem. Soc.* **2004**, 126, 11810; b) S. A. Girard, T. Knauber, C.-J. Li, *Angew. Chem. Int. Ed.* **2014**, 53, 74; c) C.-J. Li, *Acc. Chem. Res.* **2009**, 42, 335; d) C. J. Scheuermann, *Chem. Asian. J.* **2010**, 5, 436.
- [27] a) Y. Fujiwara, I. Moritani, M. Matsuda, *Tetrahedron*, **1968**, 24, 4819; b) Y. Fujiwara, I. Moritani, M. Matsuda, S. Teranishi, *Tetrahedron Lett.* **1968**, 24, 633; c) Y. Fujiwara, I. Moritani, S. Danno, R. Asano, S. Teranishi, *J. Am. Chem. Soc.* **1969**, 91, 7166.
- [28] a) S. Murai, F. Kakiuchi, S. Sekine, Y. Tanaka, A. Kamatani, M. Sonoda, N. Chatani, *Nature* **1993**, 366, 529; b) F. Kakiuchi, S. Murai, *Acc. Chem. Res.* **2002**, 35, 826; c) T. W. Lyons, M. S. Sanford, *Chem. Rev.* **2010**, 110, 1147.
- [29] A. R. Dick, K. L. Hull, M. S. Sanford, *J. Am. Chem. Soc.* **2004**, 126, 2300.
- [30] O. Daugulis, V. G. Zaitsev, *Angew. Chem. Int. Ed.* **2005**, 44, 4046.
- [31] R. Giri, N. Maugel, J.-J. Li, D.-H. Wang, S. P. Breazzano, L. B. Saunders, J.-Q. Yu, *J. Am. Chem. Soc.* **2007**, 129, 3510.
- [32] M. D. K. Boele, G. P. F. van Strijdonck, A. H. M. de Vries, P. C. J. Kamer, J. G. de Vries, P. W. N. M. van Leeuwen, *J. Am. Chem. Soc.* **2002**, 124, 1586.
- [33] D.-H. Wang, K. M. Engle, B.-F. Shi, J.-Q. Yu, *Science* **2010**, 327, 315.



- [34] K. L. Hull, M. S. Sanford, *J. Am. Chem. Soc.* **2007**, *129*, 11904.
- [35] B.-J. Li, S.-L. Tian, Z. Fang, Z.-J. Shi, *Angew. Chem. Int. Ed.* **2008**, *47*, 1115.
- [36] X. Zhao, C. S. Yeung, V. M. Dong, *J. Am. Chem. Soc.* **2010**, *132*, 5837.
- [37] Y. Aihara, M. Tobisu, Y. Fukumoto, N. Chatani, *J. Am. Chem. Soc.* **2014**, *136*, 15509.
- [38] C. Liang, F. Robert-Peillard, C. Fruit, P. Müller, R. H. Dodd, P. Dauban, *Angew. Chem. Int. Ed.* **2006**, *45*, 4641.
- [39] D. R. Stuart, K. Fagnou, *Science* **2007**, *316*, 1172.
- [40] T. de Haro, C. Nevado, *J. Am. Chem. Soc.* **2010**, *132*, 1512.
- [41] H. Peng, Y. Xi, N. Ronaghi, B. Dong, N. G. Akhmedov, X. Shi, *J. Am. Chem. Soc.* **2014**, *136*, 13174.
- [42] L. Yang, L. Zhao, C.-J. Li, *Chem. Commun.* **2010**, *46*, 4184.
- [43] W. Yin, C. He, M. Chen, H. Zhang, A. Lei, *Org. Lett.* **2009**, *11*, 709.
- [44] Y.-H. Zhang, B.-F. Shi, J.-Q. Yu, *J. Am. Chem. Soc.* **2009**, *131*, 5072.
- [45] K.-T. Yip, R. Y. Nimje, M. V. Leskinen, P. M. Pihko, *Chem. Eur. J.* **2012**, *18*, 12590.
- [46] S. E. Allen, R. R. Walvoord, R. Padilla-Salinas, M. C. Kozlowski, *Chem. Rev.* **2013**, *113*, 6234.
- [47] a) S. V. Ley, A. W. Thomas, *Angew. Chem. Int. Ed.* **2003**, *42*, 5400; b) G. Evano, N. Blanchard, M. Toumi, *Chem. Rev.* **2008**, *108*, 3054; c) C. A. de Parrodi, P. J. Walsh, *Angew. Chem. Int. Ed.* **2009**, *48*, 4679; d) Z. Shao, F. Peng, *Angew. Chem. Int. Ed.* **2010**, *49*, 9566; e) A. E. Wendlandt, A. M. Suess, S. S. Stahl, *Angew. Chem. Int. Ed.* **2011**, *50*, 11062; f) K. Hirano, M. Miura, *Chem. Commun.* **2012**, *48*, 10704.

- [48] a) K. Kamata, S. Yamaguchi, M. Kotani, K. Yamaguchi, N. Mizuno, *Angew. Chem. Int. Ed.* **2008**, *47*, 2407; b) K. Yamaguchi, K. Kamata, S. Yamaguchi, M. Kotani, N. Mizuno, *J. Catal.* **2008**, *258*, 121.
- [49] a) T. Oishi, T. Katayama, K. Yamaguchi, N. Mizuno, *Chem. Eur. J.* **2009**, *15*, 7539; b) K. Yamaguchi, T. Oishi, T. Katayama, N. Mizuno, *Chem. Eur. J.* **2009**, *15*, 10464; c) G. Zhang, H. Yi, G. Zhang, Y. Deng, R. Bai, H. Zhang, J. T. Miller, A. J. Kropf, E. E. Bunel, A. Lei, *J. Am. Chem. Soc.* **2014**, *136*, 924; d) R. Bai, G. Zhang, H. Yi, Z. Huang, X. Qi, C. Liu, J. T. Miller, A. J. Kropf, E. E. Bunel, Y. Lan, A. Lei, *J. Am. Chem. Soc.* **2014**, *136*, 16760.
- [50] a) K. S. Rao, T.-S. Wu, *Tetrahedron*, **2012**, *68*, 7735; b) J. X. Qiao, P. Y. S. Lam, *Synthesis* **2011**, *6*, 829; c) F. Luo, C. Pan, J. Cheng, *Synlett* **2012**, *23*, 357.
- [51] a) A. E. King, B. L. Ryland, T. C. Brunold, S. S. Stahl, *Organometallics* **2012**, *31*, 7948; b) A. E. King, T. C. Brunold, S. S. Stahl, *J. Am. Chem. Soc.* **2009**, *131*, 5044.
- [52] a) X. Ribas, D. A. Jackson, B. Donnadieu, J. Mahía, T. Parella, R. Xifra, B. Hedman, K. O. Hodgson, A. Llobet, T. D. P. Stack, *Angew. Chem. Int. Ed.* **2002**, *41*, 2991; b) R. Xifra, X. Ribas, A. Llobet, A. Poater, M. Duran, M. Solà, T. D. P. Stack, J. Benet-Buchholz, B. Donnadieu, J. Mahía, T. Parella, *Chem. Eur. J.* **2005**, *11*, 5146.
- [53] A. E. King, L. M. Huffman, A. Casitas, M. Costas, X. Ribas, S. S. Stahl, *J. Am. Chem. Soc.* **2010**, *132*, 12068.
- [54] T. Hamada, X. Ye, S. S. Stahl, *J. Am. Chem. Soc.* **2008**, *130*, 833.
- [55] Y. Gao, G. Wang, L. Chen, P. Xu, Y. Zhao, Y. Zhou, L. Han, *J. Am. Chem. Soc.* **2009**, *131*, 7956.

- [56] Y. Wei, H. Zhao, J. Kan, W. Su, M. Hong, *J. Am. Chem. Soc.* **2010**, *132*, 2522.
- [57] N. Matsuyama, M. Kitahara, K. Hirano, T. Satoh, M. Miura, *Org. Lett.* **2010**, *12*, 2358.
- [58] L. Chu, F. Qing, *J. Am. Chem. Soc.* **2010**, *132*, 7262.
- [59] K. Balaraman, V. Kesavan, *Synthesis*, **2010**, *20*, 3461.
- [60] M. Kitahara, K. Hirano, H. Tsurugi, T. Satoh, M. Miura, *Chem. Eur. J.* **2010**, *16*, 1772.
- [61] D. Monoguchi, T. Fujiwara, H. Furukawa, A. Mori, *Org. Lett.* **2009**, *11*, 1607.
- [62] Q. Wang, S. L. Schreiber, *Org. Lett.* **2009**, *11*, 5178.
- [63] H. Zhao, M. Wang, W. Su, M. Hong, *Adv. Synth. Catal.* **2010**, *352*, 1301.
- [64] M. Miyasaka, K. Hirano, T. Satoh, R. Kowalczyk, C. Bolm, M. Miura, *Org. Lett.* **2011**, *13*, 359.
- [65] Y. Li, Y. Xie, R. Zhang, K. Jin, X. Wang, C. Duan, *J. Org. Chem.* **2011**, *76*, 5444.
- [66] A.-X. Zhou, X.-Y. Liu, K. Yang, S.-C. Zhao, Y.-M. Liang, *Org. Biomol. Chem.* **2011**, *9*, 5456.
- [67] S. Ranjit, R. Lee, D. Heryadi, C. Shen, J. Wu, P. Zhang, K.-W. Huang, X. Liu, *J. Org. Chem.* **2011**, *76*, 8999.
- [68] a) M. Haruta, T. Kobayashi, H. Sano, N. Yamada, *Chem. Lett.* **1987**, 405; b) M. Haruta, N. Yamada, T. Kobayashi, S. Iijima, *J. Catal.* **1989**, *115*, 301.
- [69] G. J. Hutchings, *J. Catal.* **1985**, *96*, 292.
- [70] G. C. Bond, C. Louis, D. T. Thompson, *Catalysis by Gold*, Imperial College Press, London, **2006**.
- [71] M. Stratakis, H. Garcia, *Chem. Rev.* **2012**, *112*, 4469.

- [72] a) Z. Ma, S. Dai, *ACS Catal.* **2011**, *1*, 805; b) T. Mitsudome, K. Kaneda, *Green Chem.* **2013**, *15*, 2636; c) M. Flytzani-Stephanopoulos, *Acc. Chem. Res.* **2014**, *47*, 783.
- [73] a) C. D. Pina, E. Falletta, L. Prati, M. Rossi, *Chem. Soc. Rev.* **2008**, *37*, 2077; b) S. Yamazoe, K. Koyasu, T. Tsukuda, *Acc. Chem. Res.* **2014**, *47*, 816; c) X. Liu, L. He, Y.-M. Liu, Y. Cao, *Acc. Chem. Res.* **2014**, *47*, 793.
- [74] a) M. M. Schubert, S. Hackenberg, A. C. van Veen, M. Muhler, V. Plzak, R. J. Behm, *J. Catal.* **2001**, *197*, 113; b) D. Widmann, R. J. Behm, *Acc. Chem. Res.* **2014**, *47*, 740.
- [75] a) M. Daté, M. Haruta, *J. Catal.* **2001**, *201*, 221; b) M. Daté, M. Okumura, S. Tsubota, M. Haruta, *Angew. Chem. Int. Ed.* **2004**, *43*, 2129; c) T. Fujitani, I. Nakamura, *Angew. Chem. Int. Ed.* **2011**, *50*, 10144; d) T. Fujitani, I. Nakamura, M. Haruta, *Catal. Lett.* **2014**, *144*, 1475.
- [76] N. D. S. Canning, D. Outka, R. J. Madix, *Surf. Sci.* **1984**, *141*, 240.
- [77] a) B. N. Zope, D. D. Hibbitts, M. Neurock, R. J. Davis, *Science* **2010**, *330*, 74; b) M. S. Ide, R. J. Davis, *Acc. Chem. Res.* **2014**, *47*, 825.
- [78] J.-F. Soulé, H. Miyamura, S. Kobayashi, *J. Am. Chem. Soc.* **2011**, *133*, 18550.
- [79] Y. Wang, D. Zhu, L. Tang, S. Wang, Z. Wang, *Angew. Chem. Int. Ed.* **2011**, *50*, 8917.
- [80] a) K. J. Stowers, R. J. Madix, C. M. Friend, *J. Catal.* **2013**, *308*, 131; b) X. Li, Y. Cui, X. Yang, W.-L. Dai, K. Fan, *Angew. Chem. Int. Ed.* **2013**, *458*, 63; c) X. Wan, W. Deng, Q. Zhang, Y. Wang, *Catal. Today* **2014**, *233*, 147; d) K. Suzuki, T.

- Yamaguchi, K. Matsushita, C. Iitsuka, J. Miura, T. Akaogi, H. Ishida, *ACS Catal.* **2013**, *3*, 1845; e) V. V. Costa, M. Estrada, Y. Demidova, I. Prosvirin, V. Kriventsov, R. F. Cotta, S. Fuentes, A. Simakov, E. V. Gusevskaya, *J. Catal.* **2012**, *292*, 148; f) B. Xu, R. J. Madix, C. M. Friend, *J. Am. Chem. Soc.* **2010**, *132*, 16571;
- [81] A. Leyva-Pérez, J. Oliver-Meseguer, J. R. Cabrero-Antonino, P. Rubio-Marqués, P. Serna, S. I. Al-Resayes, A. Corma, *ACS Catal.* **2013**, *3*, 1865.
- [82] M. Boronat, S. Laursen, A. Leyva-Pérez, J. Oliver-Meseguer, D. Combata, A. Corma, *J. Catal.* **2014**, *315*, 6.
- [83] a) P. Serna, A. Corma, *J. Catal.* **2014**, *315*, 41; b) P. Serna, A. Corma, *ChemSusChem* **2014**, *7*, 2136.
- [84] a) S. S. Stahl, *Angew. Chem. Int. Ed.* **2004**, *43*, 3400; b) S. S. Stahl, *Science* **2005**, *309*, 1824.

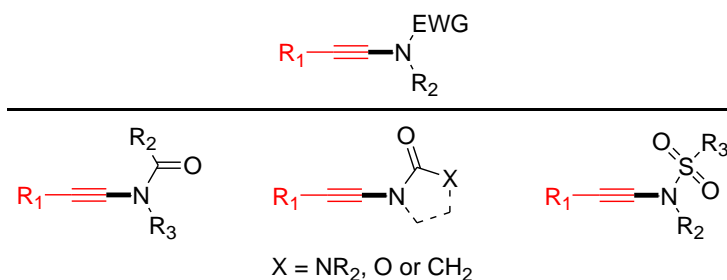


**Chapter 2**  
**Cu(OH)<sub>2</sub>-Catalyzed Aerobic**  
**Cross-Dehydrogenative Coupling of**  
**Terminal Alkynes and Amides**

## 2-1 Cu(OH)<sub>2</sub>-Catalyzed Selective Aerobic Cross-Dehydrogenative Coupling of Terminal Alkynes and Amides to Ynamides

### 2-1.1. Introduction

Alkyne moiety is one of the most important functionalities that is widely included in numerous natural products, bioactive compounds, and organic materials.<sup>[1]</sup> *N*-Substituted alkynes, namely ynamines or ynamides, represent one of the most useful alkyne derivatives (Figure 2-1-1). They provide a novel way to introduce nitrogen-based functionalities into organic molecules, including natural products and medicines.

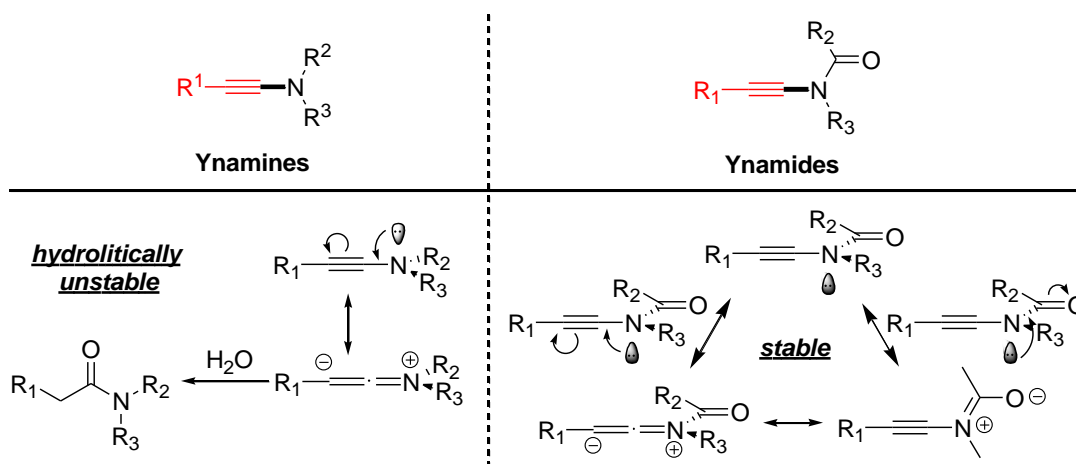


**Figure 2-1-1.** The structure of ynamides.<sup>[2,3]</sup>

Despite the potential synthetic utility of ynamines, their uses within the synthetic organic community are rather limited, likely because of their difficult preparation, handling, and especially, low stability (Figure 2-1-2).<sup>[2,3]</sup> In recent years, ynamides have received considerable attention and become versatile synthons in organic synthesis because of their superior stability over ynamines.<sup>[2,3]</sup> The stability of ynamides derives from the electron-withdrawing carbonyl group adjacent to the nitrogen atom (most of them are stable towards aqueous workups, silica gel, heating, etc.). The electron-withdrawing group partially diminishes electron density of the triple bond



through inductive effects, thus providing the enhanced stability of ynamides against moisture (Figure 2-1-2).

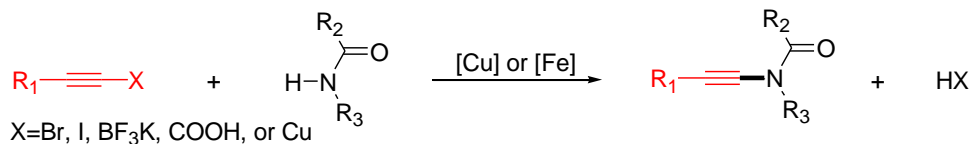


**Figure 2-1-2.** Hydrolytic stability of ynamines and ynamides.<sup>[2,3]</sup>

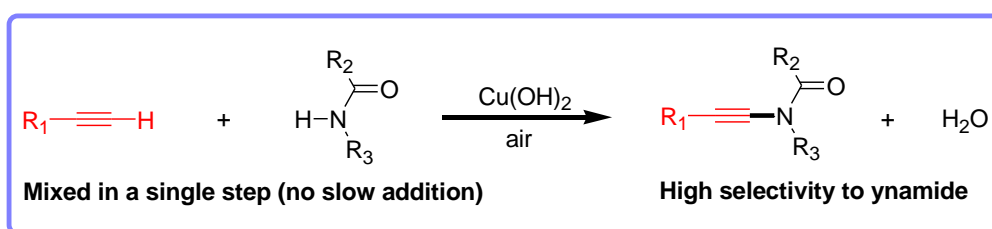
Despite the notable development in the field of ynamide chemistry, the lack of general methods to prepare these compounds is still a bottleneck for further progress. To date, a number of synthetic procedures for ynamides have been developed.<sup>[4-11]</sup> Among them, cross-coupling of alkynyl halides with amides independently developed by Hsung and Danheiser is the most widely utilized procedure.<sup>[4-6]</sup> Recently, copper-catalyzed cross-coupling of other alkyne derivatives such as alkynyl trifluoroboronates<sup>[7]</sup>, carboxylic acids<sup>[8]</sup>, and copper acetylides<sup>[9]</sup> have also been developed (Scheme 2-1-1). However, all these procedures require pre-functionalization of terminal alkynes, and a large quantity of waste is generated. The direct catalytic cross-coupling of terminal alkynes and amides without the pre-functionalization<sup>[12-14]</sup> should provide the most convenient route to ynamides. Recent progress in copper-mediated cross-coupling reactions, as described in chapter 1, suggests that copper catalysts would provide a great

opportunity for the achievement of the direct cross-coupling of terminal alkynes and amides.<sup>[15,16]</sup>

**(a) Classical procedure<sup>[4-11]</sup>**



**(b) This work**

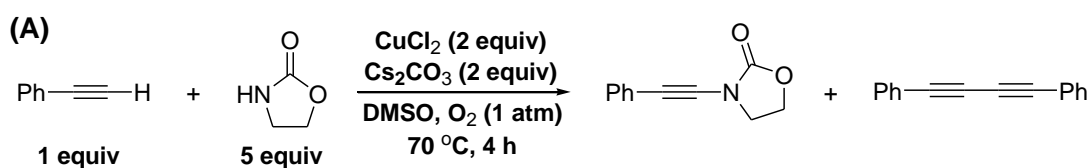


**Scheme 2-1-1.** Synthesis of ynamides.

The direct cross-coupling of terminal alkynes and amides to ynamides first reported by Stahl and co-workers, could efficiently proceed in the presence of CuCl<sub>2</sub> (20 mol%), Na<sub>2</sub>CO<sub>3</sub> (2 equiv), and pyridine (2 equiv).<sup>[11]</sup> As described in chapter 1, copper salts in combination with nitrogen-based ligands are also particularly effective for the Glaser–Hay alkyne homo-coupling. In order to suppress the alkyne homo-coupling, slow addition of terminal alkynes to the reaction mixture containing large excess amounts of amides (at least 5 equiv with respect to terminal alkynes) was required in Stahl's system.<sup>[11]</sup> For example, the cross-coupling of phenylacetylene (1 equiv) and 2-oxazolidinone (5 equiv) in the presence of CuCl<sub>2</sub> (2 equiv) and Cs<sub>2</sub>CO<sub>3</sub> (2 equiv) in DMSO gave the desired ynamide in 53% yield together with 24% yield of the diyne byproduct (Scheme 2-1-2, A). When the slow addition technique was employed, the yield of the ynamide increased up to 89% yield with the diyne byproduct produced only

in 4% yield (Scheme 2-1-2, A). Upon reducing the amount of  $\text{CuCl}_2$  to 0.2 equiv, although 2-oxazolidinone was efficiently reacted with phenylacetylene, other nitrogen nucleophiles such as sulphonamides, indoles were not the effective substrates (Scheme 2-1-2, B). The substrate scope for nitrogen nucleophiles was substantially broadened by addition of a stoichiometric amount of pyridine (2 equiv); sulphonamides and indoles were also reacted well with various electron-rich aliphatic and aromatic alkynes (Scheme 2-1-2, C). However, electron-deficient alkynes such as ethyl propiolate and 4-nitrophenylacetylene were less effective substrates, and gave the corresponding ynamides in low yields (typically,  $\leq 10\%$  and  $35\%$ , respectively) (Scheme 2-1-2, D).

The reaction mechanism for the cross-coupling is unclear at this point. Stahl and co-workers proposed a catalytic cycle including (1) successive coordination/deprotonation of an alkyne and an amide to the copper center, (2) reductive elimination to give an ynamide, and (3) reoxidation of the reduced copper species by molecular oxygen to close the catalytic cycle (Scheme 2-1-3).<sup>[11]</sup>



Two coupling partners mixed in a single step

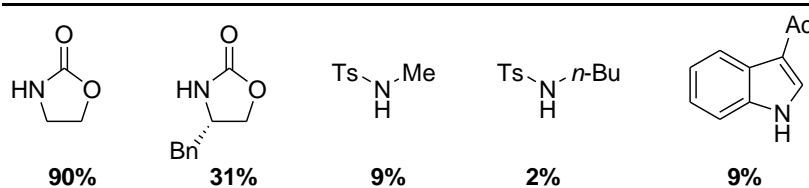
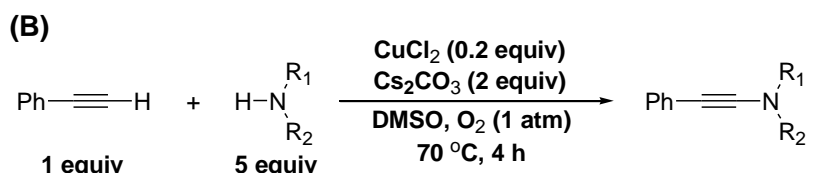
53%

24%

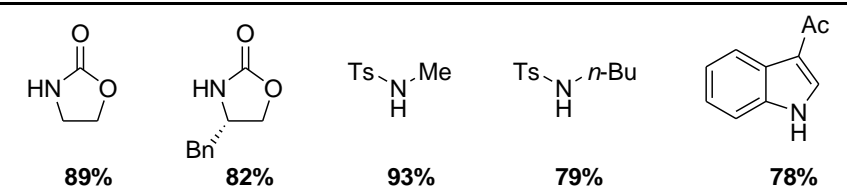
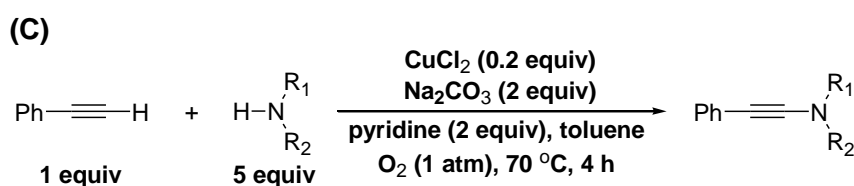
Slow addition of phenylacetylene to the reaction mixture

89%

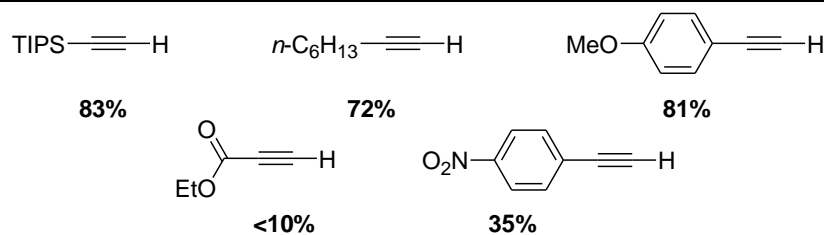
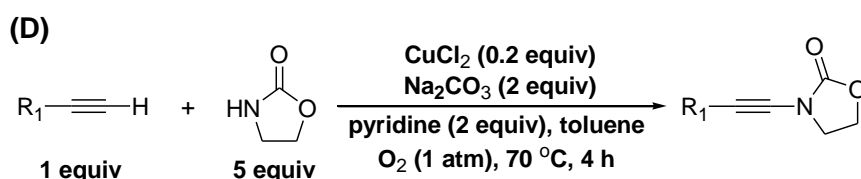
4%



Ts = tosyl; slow addition of phenylacetylene to the reaction mixture

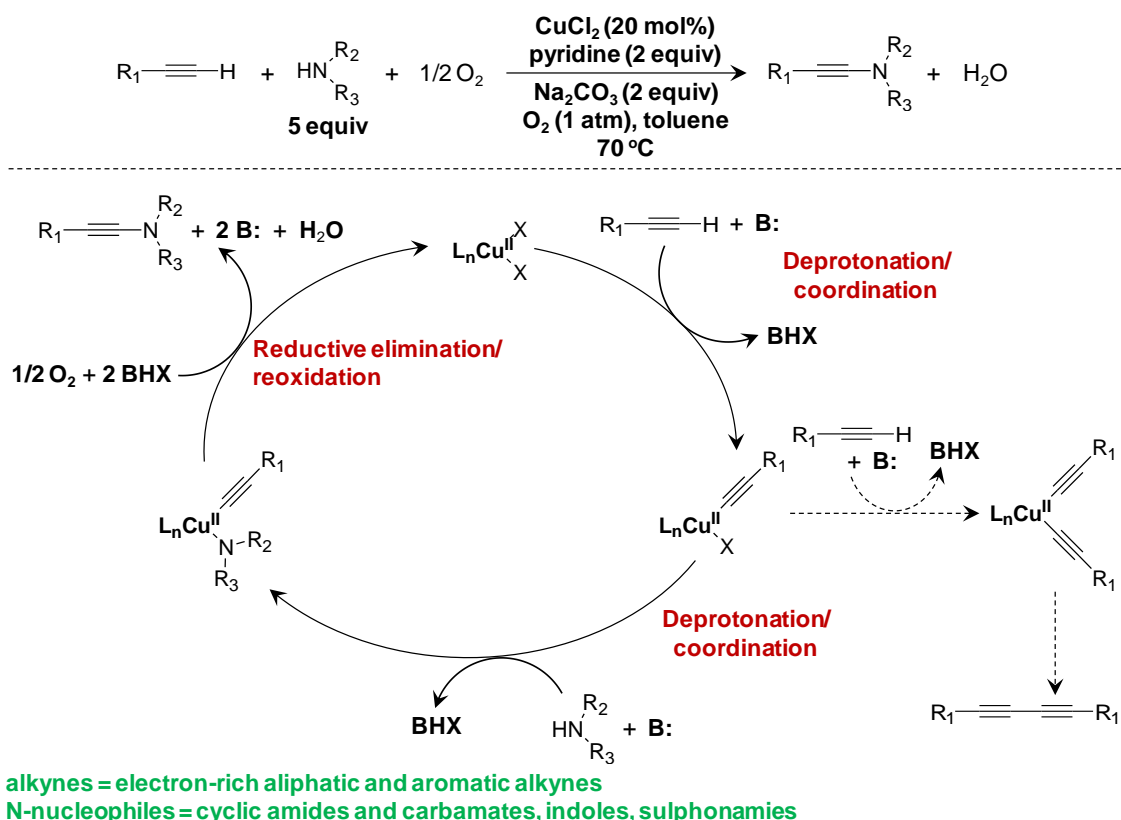


Ts = tosyl; Ac = acetyl; slow addition of phenylacetylene to the reaction mixture



TIPS = triisopropylsilyl; slow addition of alkynes to the reaction mixture

**Scheme 2-1-2.** Reaction conditions and substrate scope for the Stahl's system.<sup>[11]</sup>



**Scheme 2-1-3.** Stahl's system for the aerobic cross-dehydrogenative coupling of terminal alkynes and amides to ynamides.<sup>[11]</sup>

In this study, heterogeneous copper hydroxide-based catalysts are considered to be suitable for the selective cross-coupling, because (1) hydroxyl groups on the surface would facilitate the abstraction of protons from acidic C(sp)-H and N-H bonds and (2) they are likely less active for the alkyne homo-coupling compared to homogeneous systems (especially in the presence of nitrogen donors).

In this chapter, Cu(OH)<sub>2</sub> is turned out to selectively promote the aerobic cross-dehydrogenative coupling of terminal alkynes and amides to ynamides without employing the tedious slow addition technique (Scheme 2-1-1). The present Cu(OH)<sub>2</sub>-catalyzed procedure has several outstanding features in comparison with Stahl's system; (1) various kinds of structurally diverse ynamides can selectively be

synthesized by simply mixing catalytic amounts of  $\text{Cu}(\text{OH})_2$  and inorganic bases as well as the two coupling partners in a single step (without slow addition), (2) reduced amounts of amides are utilized (3 equiv or less), (3) readily available and inexpensive  $\text{Cu}(\text{OH})_2$  is used as the catalyst, (4) ligands are not necessary, (5) catalytic amounts of inorganic bases (20 mol% or less) are sufficient to promote the cross-coupling, (6) catalyst/product separation is very easy (heterogeneous catalysis), (7) air instead of pure molecular oxygen can be used as the terminal oxidant, and (8) water is the sole by-product.

## 2-1.2. Experimental Section

### 2-1.2.1. General

GC analyses were performed on Shimadzu GC-2014 with a FID detector equipped with a Rtx-200 capillary column. Mass spectra were recorded on Shimadzu GCMS-QP2010 equipped with a TC-5HT capillary column at an ionization voltage of 70 eV. Liquid-state NMR spectra were recorded on JEOL JNM-EX-270.  $^1\text{H}$  and  $^{13}\text{C}$  NMR spectra were measured at 270 and 67.8 MHz, respectively. UV/Vis spectra were recorded on a Jasco V-570 spectrometer. The XRD pattern was recorded on a Rigaku Multiflex diffractometer ( $\text{Cu}_{\text{K}\alpha}$ ,  $\lambda = 1.5405 \text{ \AA}$ , 40 kV–50 mA). Copper salts, bases, substrates and solvents were commercially obtained from TCI, Wako, or Aldrich (reagent grade), and purified prior to the use, if necessary.<sup>[17]</sup> Supported copper hydroxide catalysts,  $\text{Cu}(\text{OH})_x/\text{TiO}_2$  and  $\text{Cu}(\text{OH})_x/\text{Al}_2\text{O}_3$ , were prepared according to the literature procedure.<sup>[18]</sup>

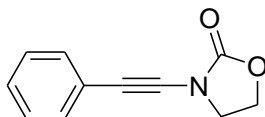
### 2-1.2.2. General Procedure for the Cross-Coupling of Terminal Alkynes and Amides

**0.1 mmol scale:** Into a Pyrex-glass screw cap vial (volume: ca. 20 mL) were successively placed  $\text{Cu}(\text{OH})_2$  (0.005 mmol, 5 mol% with respect to an alkyne), a base (5–20 mol% with respect to an alkyne), an alkyne (0.1 mmol), an amide (2–3 equiv. with respect to an alkyne), and mesitylene (1 mL). A Teflon-coated magnetic stir bar was added and the reaction mixture was vigorously stirred at 100–120 °C, under 1 atm of air. After the reaction was completed, biphenyl was added as an internal standard to the reaction mixture. Then, the conversion of the alkyne and the yield of the product were analyzed by gas chromatography. As for the isolation of the ynamide product, the internal standard was not added and the crude reaction mixture was directly subjected to silica gel column chromatography (Silica Gel 60N (63–210  $\mu\text{m}$ ), Kanto Chemical, 2.5 cm ID $\times$ 15 cm length, initial: *n*-hexane only, after mesitylene, the alkyne and the diyne byproduct were eluted: *n*-hexane/ethyl acetate = 9/1 to 3/2 (v/v)), giving the pure ynamide. The isolated products were identified by GC mass and  $^1\text{H}$  and  $^{13}\text{C}$  NMR.

**10 mmol scale:** Into a 300 mL three neck round bottom flask, were successively placed  $\text{Cu}(\text{OH})_2$  (48.8 mg, 0.5 mmol),  $\text{K}_2\text{CO}_3$  (34.6 mg, 0.25 mmol), phenylacetylene (1.02 g, 10 mmol), 2-oxazolidinone (2.61 g, 30 mmol), and mesitylene (100 mL). A Teflon-coated magnetic stir bar was added and the reaction mixture was stirred vigorously at 100 °C in oil bath for 11 h, under an open air condition. After the reaction was completed, the crude reaction mixture was directly subjected to silica gel column chromatography (Silica Gel 60N (63–210  $\mu\text{m}$ ), Kanto Chemical, 4.0 cm ID $\times$ 10 cm length, initial: *n*-hexane only, after mesitylene, phenylacetylene and the diyne byproduct

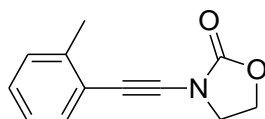
were eluted: *n*-hexane/ethyl acetate = 9/1 to 3/2 (v/v)), giving the ynamide in >99 purity (by GC and <sup>1</sup>H NMR).

### 2-1.2.3. Spectral Data of Ynamides



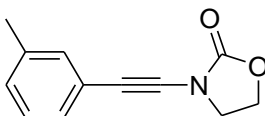
**3aa**

**3-(phenylethynyl)oxazolidin-2-one (3aa):** Solid. <sup>1</sup>H NMR (270 MHz, CDCl<sub>3</sub>, TMS): δ 3.98–4.03 (m, 2H), 4.45–4.51 (m, 2H), 7.26–7.35 (m, 3H), 7.41–7.48 (m, 2H). <sup>13</sup>C{<sup>1</sup>H} NMR (67.8 MHz, CDCl<sub>3</sub>, TMS): δ 47.01, 63.00, 71.16, 78.91, 122.12, 128.17, 128.27, 131.54, 155.86. MS (EI): *m/z* (%) : 188 (12), 187 (100) [*M*<sup>+</sup>], 143 (36), 142 (22), 128 (66), 117 (20), 116 (30), 115 (84), 114 (20), 89 (15), 88 (22), 77 (17), 64 (11), 63 (14), 62 (13).



**3ba**

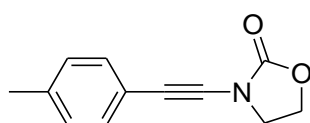
**3-(*o*-tolylethynyl)oxazolidin-2-one (3ba):** Solid. <sup>1</sup>H NMR (270 MHz, CDCl<sub>3</sub>, TMS): δ 2.44 (s, 3H), 3.99–4.05 (m, 2H), 4.46–4.52 (m, 2H), 7.08–7.26 (m, 3H), 7.38–7.41 (m, 1H). <sup>13</sup>C{<sup>1</sup>H} NMR (67.8 MHz, CDCl<sub>3</sub>, TMS): δ 20.69, 47.12, 62.95, 70.12, 82.68, 121.94, 125.50, 128.12, 129.39, 131.62, 139.90, 155.81. MS (EI): *m/z* (%) : 201 (57) [*M*<sup>+</sup>], 156 (16), 142 (11), 129 (24), 128 (16), 116 (13), 115 (100), 103 (10), 102 (24), 77 (10), 58 (10).



**3ca**

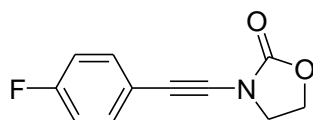


**3-(*m*-tolylethynyl)oxazolidin-2-one (3ca):** Solid.  $^1\text{H}$  NMR (270 MHz,  $\text{CDCl}_3$ , TMS):  $\delta$  2.32 (s, 3H), 3.97–4.03 (m, 2H), 4.45–4.51 (m, 2H), 7.10–7.27 (m, 4H).  $^{13}\text{C}\{^1\text{H}\}$  NMR (67.8 MHz,  $\text{CDCl}_3$ , TMS):  $\delta$  21.14, 47.02, 62.98, 71.31, 78.58, 121.89, 128.15, 128.52, 129.04, 132.10, 137.96, 155.88. MS (EI):  $m/z$  (%) : 202 (13), 201 (100) [ $M^+$ ], 157 (39), 156 (19), 143 (10), 142 (80), 131 (12), 130 (17), 129 (47), 128 (28), 116 (12), 115 (36), 103 (23), 102 (33), 101 (10), 91 (11), 78 (14), 77 (18), 76 (13), 70 (10), 63 (11), 51 (11).



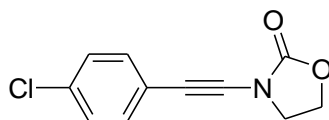
**3da**

**3-(*p*-tolylethynyl)oxazolidin-2-one (3da):** Solid.  $^1\text{H}$  NMR (270 MHz,  $\text{CDCl}_3$ , TMS):  $\delta$  2.34 (s, 3H), 3.96–4.02 (m, 2H), 4.44–4.50 (m, 2H), 7.09–7.13 (m, 2H), 7.32–7.35 (m, 2H).  $^{13}\text{C}\{^1\text{H}\}$  NMR (67.8 MHz,  $\text{CDCl}_3$ , TMS):  $\delta$  21.42, 47.05, 62.97, 71.15, 78.23, 118.95, 129.02, 131.57, 138.37, 155.93. MS (EI):  $m/z$  (%) : 202 (13), 201 (100) [ $M^+$ ], 157 (34), 156 (22), 142 (59), 130 (23), 129 (54), 128 (26), 115 (34), 103 (24), 102 (29), 101 (10), 78 (12), 77 (16), 76 (12), 51 (10).



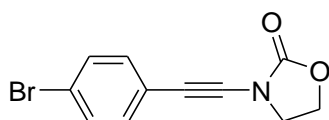
**3ea**

**3-((4-fluorophenyl)ethynyl)oxazolidin-2-one (3ea):** Solid.  $^1\text{H}$  NMR (270 MHz,  $\text{CDCl}_3$ , TMS):  $\delta$  3.98–4.03 (m, 2H), 4.47–4.53 (m, 2H), 6.96–7.05 (m, 2H), 7.39–7.46 (m, 2H).  $^{13}\text{C}\{^1\text{H}\}$  NMR (67.8 MHz,  $\text{CDCl}_3$ , TMS):  $\delta$  46.96, 63.03, 70.13, 78.55, 115.57 (d,  $J = 21.7$  Hz), 118.15 (d,  $J = 3.9$  Hz), 133.64 (d,  $J = 8.3$  Hz), 155.88, 162.48 (d,  $J = 249.2$  Hz). MS (EI):  $m/z$  (%) : 206 (11), 205 (88) [ $M^+$ ], 161 (38), 160 (17), 146 (64), 135 (18), 134 (30), 133 (100), 132 (22), 126 (13), 107 (14), 106 (17), 57 (10).



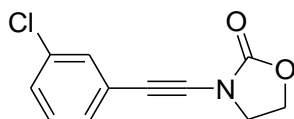
**3fa**

**3-((4-chlorophenyl)ethynyl)oxazolidin-2-one (3fa):** Solid.  $^1\text{H}$  NMR (270 MHz,  $\text{CDCl}_3$ , TMS):  $\delta$  3.98–4.04 (m, 2H), 4.49–4.55 (m, 2H), 7.26–7.30 (m, 2H), 7.34–7.40 (m, 2H).  $^{13}\text{C}\{^1\text{H}\}$  NMR (67.8 MHz,  $\text{CDCl}_3$ , TMS):  $\delta$  46.93, 63.05, 70.24, 79.78, 120.67, 128.63, 132.73, 134.19, 155.75. MS (EI):  $m/z$  (%) : 223 (33), 222 (13), 221 (100) [ $M^+$ ], 179 (11), 177 (36), 164 (18), 162 (57), 151 (32), 150 (15), 149 (43), 142 (14), 127 (11), 126 (15), 116 (12), 115 (59), 114 (85), 98 (10), 89 (11), 88 (21), 87 (21), 75 (13), 73 (17), 63 (16), 62 (10).



**3ga**

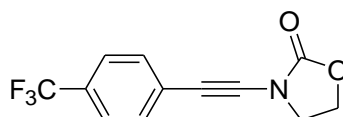
**3-((4-fluorophenyl)ethynyl)oxazolidin-2-one (3ga):** Solid.  $^1\text{H}$  NMR (270 MHz,  $\text{CDCl}_3$ , TMS):  $\delta$  3.98–4.04 (m, 2H), 4.47–4.53 (m, 2H), 7.27–7.32 (m, 2H), 7.42–7.7.46 (m, 2H).  $^{13}\text{C}\{^1\text{H}\}$  NMR (67.8 MHz,  $\text{CDCl}_3$ , TMS):  $\delta$  46.92, 63.06, 73.34, 79.97, 121.15, 122.36, 131.55, 132.91, 155.73. MS (EI):  $m/z$  (%) : 267 (53), 265 (53) [ $M^+$ ], 223 (23), 221 (23), 208 (23), 206 (23), 195 (18), 193 (11), 127 (26), 116 (14), 115 (66), 114 (100), 89 (12), 88 (25), 87 (20), 64 (11), 63 (18), 62 (12).



**3ha**

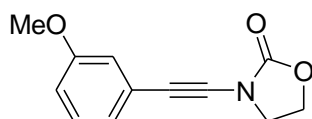
**3-((3-chlorophenyl)ethynyl)oxazolidin-2-one (3ha):** Solid.  $^1\text{H}$  NMR (270 MHz,  $\text{CDCl}_3$ , TMS):  $\delta$  3.98–4.04 (m, 2H), 4.47–4.53 (m, 2H), 7.20–7.33 (m, 3H), 7.41–7.43

(m, 1H).  $^{13}\text{C}\{^1\text{H}\}$  NMR (67.8 MHz,  $\text{CDCl}_3$ , TMS):  $\delta$  46.88, 63.08, 70.10, 80.07, 123.93, 128.34, 129.49, 129.51, 131.17, 134.07, 155.68. MS (EI):  $m/z$  (%) : 223 (33), 222 (13), 221 (100) [ $M^+$ ], 179 (13), 177 (39), 176 (10), 164 (24), 162 (74), 151 (29), 149 (31), 142 (12), 127 (12), 126 (14), 116 (16), 115 (58), 114 (80), 88 (19), 87 (16), 75 (12), 63 (14).



**3ia**

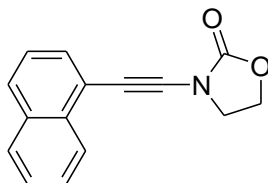
**3-((4-(trifluoromethyl)phenyl)ethynyl)oxazolidin-2-one (3ia):** Solid.  $^1\text{H}$  NMR (270 MHz,  $\text{CDCl}_3$ , TMS):  $\delta$  4.01–4.07 (m, 2H), 4.49–4.55 (m, 2H), 7.50–7.58 (m, 4H).  $^{13}\text{C}\{^1\text{H}\}$  NMR (67.8 MHz,  $\text{CDCl}_3$ , TMS):  $\delta$  46.86, 63.14, 70.40, 81.33, 114.14, 117.86, 121.87, 125.13, 125.18, 125.24, 125.30, 125.87, 125.15, 126.18, 129.03, 129.42, 129.90, 130.13, 131.32, 137.50, 155.62. MS (EI):  $m/z$  (%) : 256 (14), 255 (100) [ $M^+$ ], 236 (11), 211 (58), 210 (15), 197 (12), 196 (96), 185 (17), 183 (41), 176 (12), 163 (13), 145 (10), 142 (14), 133 (14), 115 (20), 114 (12), 88 (10), 81 (19).



**3ja**

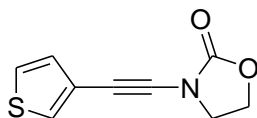
**3-((3-methoxyphenyl)ethynyl)oxazolidin-2-one (3ja):** Solid.  $^1\text{H}$  NMR (270 MHz,  $\text{CDCl}_3$ , TMS):  $\delta$  3.79 (s, 3H), 3.98–4.04 (m, 2H), 4.46–4.51 (m, 2H), 6.84–6.88 (m, 1H), 6.96–6.98 (m, 1H), 7.01–7.05 (m, 1H), 7.18–7.27 (m, 1H).  $^{13}\text{C}\{^1\text{H}\}$  NMR (67.8 MHz,  $\text{CDCl}_3$ , TMS):  $\delta$  46.98, 55.25, 63.02, 71.15, 78.75, 114.80, 116.20, 123.13, 123.95, 129.32, 155.84, 159.26. MS (EI):  $m/z$  (%) : 218 (13), 217 (100) [ $M^+$ ], 173 (35), 158 (33), 146 (10), 145 (19), 143 (14), 130 (24), 116 (22), 115 (24), 103 (15), 102 (19),

90 (13), 89 (12), 88 (12), 77 (11), 76 (14), 75 (16), 51 (11).



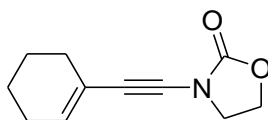
**3ka**

**3-(naphthalene-1-ylethynyl)oxazolidin-2-one (3ka):** Solid.  $^1\text{H}$  NMR (270 MHz,  $\text{CDCl}_3$ , TMS):  $\delta$  4.04–4.10 (m, 2H), 4.48–4.53 (m, 2H), 7.38–7.67 (m, 4H), 7.79–7.85 (m, 2H), 8.33 (dd,  $J = 8.1$  and  $0.8$  Hz, 1H).  $^{13}\text{C}\{^1\text{H}\}$  NMR (67.8 MHz,  $\text{CDCl}_3$ , TMS):  $\delta$  47.07, 63.06, 69.53, 83.59, 119.84, 125.13, 126.06, 126.40, 126.81, 128.20, 128.51, 129.90, 132.96, 133.10, 155.87. MS (EI):  $m/z$  (%) : 238 (16), 237 (100) [ $M^+$ ], 193 (19), 192 (12), 178 (33), 166 (18), 165 (71), 164 (39), 152 (12), 151 (31), 150 (11), 139 (13), 138 (18), 97 (13), 89 (17), 76 (14).



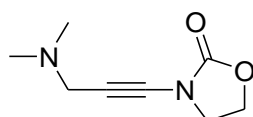
**3la**

**3-(thiophen-3-ylethynyl)oxazolidin-2-one (3la):** Solid.  $^1\text{H}$  NMR (270 MHz,  $\text{CDCl}_3$ , TMS):  $\delta$  3.96–4.02 (m, 2H), 4.45–4.51 (m, 2H), 7.12 (dd,  $J = 4.9$  and  $1.1$  Hz, 1H), 7.25–7.28 (m, 1H), 7.46 (dd,  $J = 3.0$  and  $1.1$  Hz, 1H).  $^{13}\text{C}\{^1\text{H}\}$  NMR (67.8 MHz,  $\text{CDCl}_3$ , TMS):  $\delta$  46.98, 63.02, 66.34, 78.32, 120.85, 125.28, 129.15, 130.04, 155.91. MS (EI):  $m/z$  (%) : 194 (11), 193 (100) [ $M^+$ ], 149 (24), 148 (17), 134 (50), 123 (15), 122 (28), 121 (58), 96 (10), 95 (14), 94 (28), 70 (12), 69 (10), 63 (10).



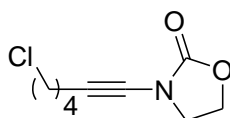
**3ma**

**3-(cyclohexenylethynyl)oxazolidin-2-one (3ma):** Oil.  $^1\text{H}$  NMR (270 MHz,  $\text{CDCl}_3$ , TMS):  $\delta$  1.53–1.69 (m, 4H), 1.99–2.06 (m, 4H), 3.57 (s, 2H), 3.99–4.05 (m, 2H), 4.38–4.44 (m, 2H), 5.54–5.55 (m, 1H).  $^{13}\text{C}\{^1\text{H}\}$  NMR (67.8 MHz,  $\text{CDCl}_3$ , TMS):  $\delta$  21.93, 22.67, 25.24, 28.65, 42.51, 43.32, 61.84, 125.76, 130.92, 153.38, 171.61. MS (EI):  $m/z$  (%) : 209 (13) [ $M^+$ ], 122 (100), 94 (27), 88 (16), 79 (21).



**3na**

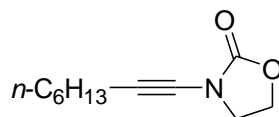
**3-(3-(dimethylamino)prop-1-ynyl)oxazolidin-2-one (3na):** Oil.  $^1\text{H}$  NMR (270 MHz,  $\text{CDCl}_3$ , TMS):  $\delta$  2.30 (s, 6H), 3.39 (s, 2H), 3.89–3.95 (m, 2H), 4.42–4.47 (m, 2H).  $^{13}\text{C}\{^1\text{H}\}$  NMR (67.8 MHz,  $\text{CDCl}_3$ , TMS):  $\delta$  44.05, 46.85, 47.83, 62.86, 66.24, 74.66, 156.29. MS (EI):  $m/z$  (%) : 168 (76) [ $M^+$ ], 167 (79), 125 (14), 124 (30), 123 (10), 96 (38), 95 (16), 82 (56), 81 (90), 80 (94), 68 (13), 67 (21), 66 (14), 58 (37), 56 (17), 55 (15), 54 (59), 53 (100), 52 (45).



**3oa**

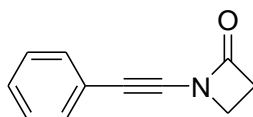
**3-(6-chlorohex-1-ynyl)oxazolidin-2-one (3oa):** Oil.  $^1\text{H}$  NMR (270 MHz,  $\text{CDCl}_3$ , TMS):  $\delta$  1.64–1.75 (m, 2H), 1.85–1.95 (m, 2H), 2.37 (t,  $J = 7.0$  Hz, 2H), 3.57 (t,  $J = 6.6$  Hz, 2H), 3.85–3.91 (m, 2H), 4.39–4.45 (m, 2H).  $^{13}\text{C}\{^1\text{H}\}$  NMR (67.8 MHz,  $\text{CDCl}_3$ , TMS):  $\delta$  17.70, 25.84, 31.46, 44.49, 46.91, 62.79, 70.22, 70.60, 156.55. MS (EI):  $m/z$  (%) : 201 (2) [ $M^+$ ], 167 (10), 166 (98), 164 (23), 138 (11), 130 (14), 126 (13), 124 (11), 122 (41), 120 (16), 106 (12), 94 (25), 93 (17), 88 (13), 81 (31), 80 (70), 79 (60), 78 (13), 77 (18), 69 (13), 68 (13), 67 (47), 66 (33), 65 (21), 55 (13), 54 (44), 53 (100), 52 (40),

51 (13).



**3pa**

**3-(oct-1-ynyl)oxazolidin-2-one (3pa):** Oil.  $^1\text{H}$  NMR (270 MHz,  $\text{CDCl}_3$ , TMS):  $\delta$  0.89 (t,  $J = 6.9$  Hz, 3H), 1.21–1.44 (m, 6H), 1.47–1.58 (m, 2H), 2.30 (t,  $J = 7.0$  Hz, 2H), 3.85–3.90 (m, 2H), 4.39–4.44 (m, 2H).  $^{13}\text{C}\{^1\text{H}\}$  NMR (67.8 MHz,  $\text{CDCl}_3$ , TMS):  $\delta$  13.98, 18.34, 22.47, 28.47, 28.70, 31.26, 47.00, 62.74, 69.94, 71.19, 156.62. MS (EI):  $m/z$  (%) : 195 (1) [ $M^+$ ], 167 (14), 166 (20), 152 (24), 139 (16), 138 (12), 136 (17), 127 (12), 126 (100), 124 (38), 122 (47), 109 (14), 108 (76), 107 (11), 106 (13), 97 (19), 95 (21), 94 (34), 93 (38), 91 (12), 88 (44), 82 (23), 81 (48), 80 (69), 79 (49), 78 (14), 77 (10), 69 (15), 68 (27), 67 (78), 66 (22), 65 (19), 56 (13), 55 (69), 54 (60), 53 (96), 52 (43).



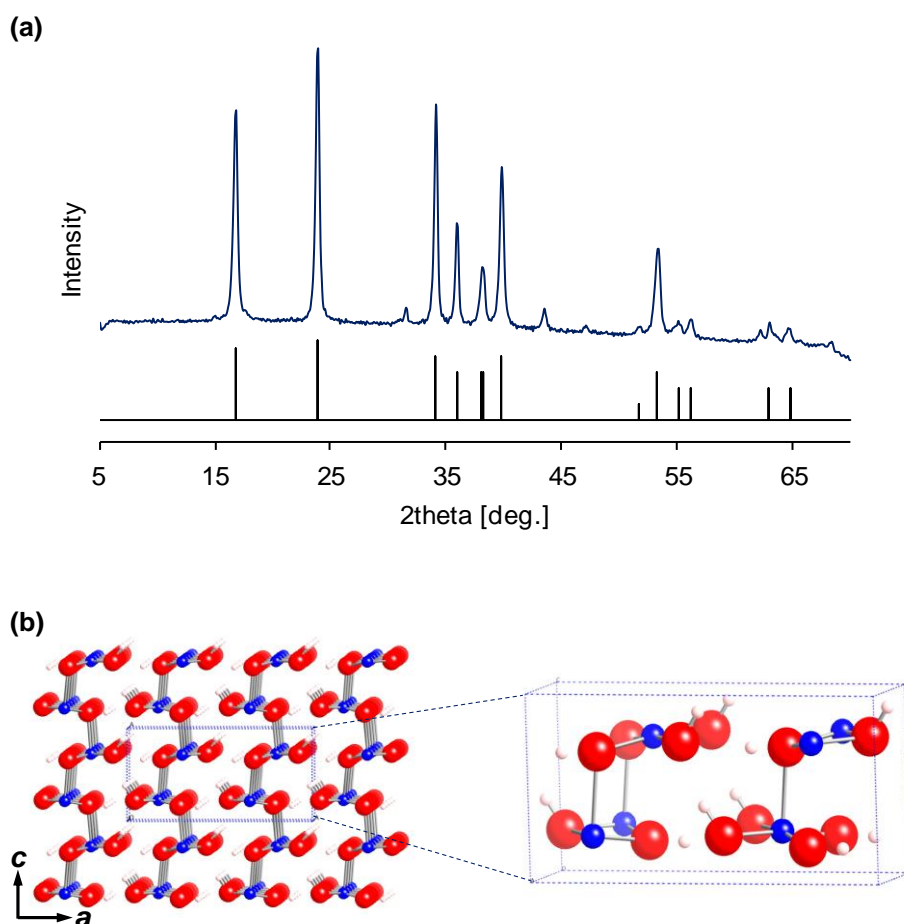
**3ac**

**3-(phenylethynyl)-1,3-oxazetidin-2-one (3ac):** Solid.  $^1\text{H}$  NMR (270 MHz,  $\text{CDCl}_3$ , TMS):  $\delta$  3.91 (t,  $J = 4.9$  Hz, 2H), 3.72 (t,  $J = 4.7$  Hz, 2H), 7.26–7.35 (m, 3H), 7.38–7.45 (m, 2H).  $^{13}\text{C}\{^1\text{H}\}$  NMR (67.8 MHz,  $\text{CDCl}_3$ , TMS):  $\delta$  37.96, 43.13, 69.86, 78.68, 122.17, 128.10, 128.29, 131.44, 166.65. MS (EI):  $m/z$  (%) : 171 (24) [ $M^+$ ], 144 (10), 143 (100), 129 (46), 128 (29), 115 (61), 114 (11), 103 (14), 102 (34), 89 (11), 88 (14), 78 (13), 77 (10), 63 (14), 62 (11).

## 2-1.3. Results and Discussion

### 2-1.3.1. Characterization of $\text{Cu}(\text{OH})_2$

The XRD pattern and crystal structure of  $\text{Cu}(\text{OH})_2$  are shown in Figure 2-1-3. The XRD pattern is in a good agreement with orthorhombic  $\text{Cu}(\text{OH})_2$  (JCPDS No 13-420) (Figure 2-1-3, a).  $\text{Cu}(\text{OH})_2$  has the structure containing corrugated layers of distorted  $\text{Cu}(\text{OH})_6$  octahedron (Figure 2-1-3, b). Copper(II) is actually surrounded pentahedrally by five  $\text{OH}^-$  ions, and the sixth  $\text{OH}^-$  ion is located too long distance to be involved in the copper octahedron.<sup>[19,20]</sup>



**Figure 2-1-3.** (a) XRD pattern and (b) crystal structure of  $\text{Cu}(\text{OH})_2$ . Red, blue, and light-red balls represent oxygen, copper, and hydrogen atoms, respectively.

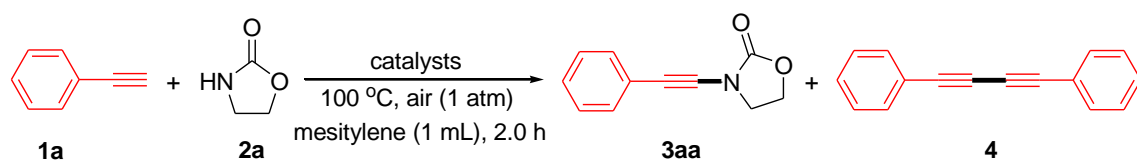
### 2-1.3.2. Optimization of the Reaction Conditions

At the beginning of the study, various kinds of copper-based catalysts were examined for the cross-coupling of ethynylbenzene (**1a**) and 2-oxazolidinone (**2a**) to produce 3-(phenylethynyl)oxazolidin-2-one (**3aa**) in 1 atm air (Table 2-1-1). Under the reaction conditions described in Table 2-1-1, no reaction proceeded in the absence of catalysts. Among various copper catalysts applied, such as  $\text{Cu}(\text{OH})_2$ ,  $\text{Cu}(\text{OH})_2 \cdot \text{CuCO}_3$ ,  $\text{CuO}$ ,  $\text{Cu}(\text{acac})_2$  (acac = acetylacetonate),  $\text{Cu}(\text{OTf})_2$  (OTf = triflate),  $\text{Cu}(\text{OAc})_2 \cdot \text{H}_2\text{O}$  (OAc = acetate),  $\text{CuI}$ ,  $\text{CuCl}_2$ , and  $\text{CuSO}_4 \cdot 5\text{H}_2\text{O}$ ,  $\text{Cu}(\text{OH})_2$  was the most effective catalyst in terms of the activity and selectivity.  $\text{Cu}_2\text{O}$  showed almost the same activity and selectivity as  $\text{Cu}(\text{OH})_2$ . Although  $\text{Cu}(\text{OH})_2 \cdot \text{CuCO}_3$ ,  $\text{Cu}(\text{acac})_2$ , and  $\text{CuSO}_4 \cdot 5\text{H}_2\text{O}$  showed the high selectivities to **3aa**, the activities of these catalysts were lower than that of  $\text{Cu}(\text{OH})_2$ . No reaction proceeded in the presence of  $\text{CuO}$ . Supported copper(II) hydroxide catalysts such as  $\text{Cu}(\text{OH})_x/\text{TiO}_2$  and  $\text{Cu}(\text{OH})_x/\text{Al}_2\text{O}_3$ <sup>[18]</sup> were not effective for the cross-coupling.

The cross-coupling was efficiently proceeded in the presence of catalytic amounts of  $\text{Cu}(\text{OH})_2$  (5 mol% with respect to **1a**) and  $\text{KHCO}_3$  (10 mol%). In this case, **3aa** was obtained in 92% yield with 99% selectivity upon simply mixing the two coupling partners in a single step without the slow addition procedure (Table 2-1-1). In a separate experiment, it is revealed that  $\text{Cu}(\text{OH})_2$  was inactive for the Glaser–hay alkyne homo-coupling, which is likely the key point to attain the high selectivity.



**Table 2-1-1.** Cross-coupling of phenylacetylene (**1a**) and 2-oxazolidinone (**2a**) by various catalysts.<sup>[a]</sup>



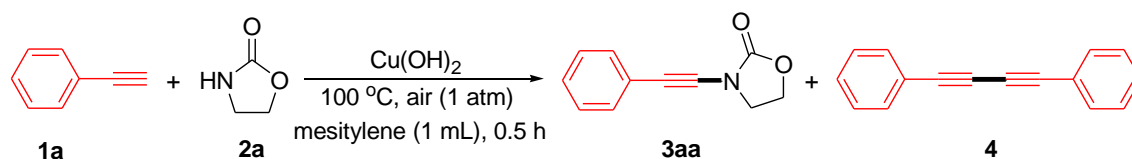
Entry	Catalyst	Conv. of <b>1</b> [%] <sup>[b]</sup>	Yield [%] <sup>[b]</sup>	
			<b>3aa</b>	<b>4</b>
<b>1</b>	<b>Cu(OH)<sub>2</sub></b>	<b>93</b>	<b>92</b>	<b>1</b>
<b>2</b>	<b>Cu<sub>2</sub>O</b>	<b>94</b>	<b>91</b>	<b>2</b>
3	Cu(OH) <sub>2</sub> ·CuCO <sub>3</sub>	80	77	2
4	CuO	<1	nd	nd
5	Cu(acac) <sub>2</sub>	57	53	2
6	Cu(OTf) <sub>2</sub>	60	8	48
7	Cu(OAc) <sub>2</sub> ·H <sub>2</sub> O	95	75	20
8	CuI	83	51	31
9	CuCl <sub>2</sub>	86	61	24
10	CuSO <sub>4</sub> ·5H <sub>2</sub> O	27	18	2
11	Cu(OH) <sub>x</sub> /TiO <sub>2</sub>	13	10	2
12	Cu(OH) <sub>x</sub> /Al <sub>2</sub> O <sub>3</sub>	<1	nd	nd
13	none	<1	nd	nd

[a] Reaction conditions: Catalyst (Cu: 5 mol%), **1a** (0.1 mmol), **2a** (0.3 mmol), KHCO<sub>3</sub> (10 mol %), mesitylene (1 mL), 100 °C, under air (1 atm), 2.0 h. [b] Conversion and yields were determined by GC analysis. nd = not detected.

Different bases were also examined for the cross-coupling of **1a** and **2a** using Cu(OH)<sub>2</sub> as the catalyst (Table 2-1-2). Among various bases examined, such as Na<sub>2</sub>CO<sub>3</sub>, K<sub>2</sub>CO<sub>3</sub>, Cs<sub>2</sub>CO<sub>3</sub>, NaHCO<sub>3</sub>, KHCO<sub>3</sub>, K<sub>3</sub>PO<sub>4</sub>·*n*H<sub>2</sub>O, triethylamine (Et<sub>3</sub>N), and 1,8-diazabicyclo[5.4.0]undec-7-ene (DBU), K<sub>2</sub>CO<sub>3</sub> was the most suitable base. Inorganic bases were turned out to be superior to organic bases. Generally, at least stoichiometric amounts of bases are required for the cross-coupling of alkynyl halides<sup>[4-6]</sup> or terminal alkynes<sup>[11]</sup> with amides. In the present Cu(OH)<sub>2</sub>-catalyzed

system, 5 mol% of  $\text{K}_2\text{CO}_3$  was sufficient to effectively promote the cross-coupling of **1a** and **2a** (Table 2-1-3).

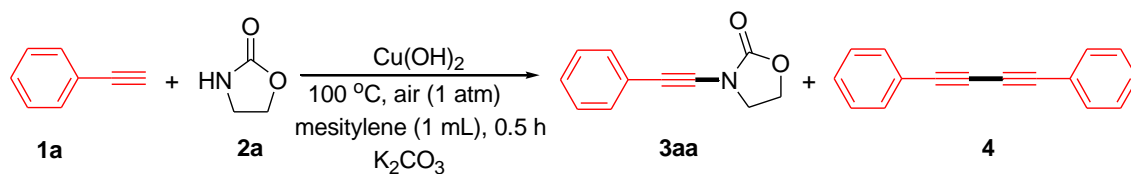
**Table 2-1-2.** Cross-coupling of phenylacetylene (**1a**) and 2-oxazolidinone (**2a**) with different bases.<sup>[a]</sup>



Entry	Base	Conv. of <b>1</b> [%] <sup>[b]</sup>	Yield [%] <sup>[b]</sup>	
			<b>3</b>	<b>4</b>
1	$\text{Na}_2\text{CO}_3$	15	13	<1
2	<b><math>\text{K}_2\text{CO}_3</math></b>	<b>75</b>	<b>73</b>	<b>1</b>
3	$\text{Cs}_2\text{CO}_3$	26	17	2
4	$\text{NaHCO}_3$	28	25	<1
5	$\text{KHCO}_3$	67	65	1
6	$\text{K}_3\text{PO}_4 \cdot n\text{H}_2\text{O}$	46	42	2
7	$\text{Et}_3\text{N}$	<1	nd	nd
8	DBU	27	16	8
9	none	<1	nd	nd

[a] Reaction conditions:  $\text{Cu}(\text{OH})_2$  (5 mol%), **1a** (0.1 mmol), **2a** (0.3 mmol), base (10 mol %), mesitylene (1 mL), 100 °C, under air (1 atm), 0.5 h. [b] Conversion and yields were determined by GC analysis. nd = not detected.

**Table 2-1-3.** Cross-coupling of phenylacetylene (**1a**) and 2-oxazolidinone (**2a**) with different amount of  $K_2CO_3$ .<sup>[a]</sup>

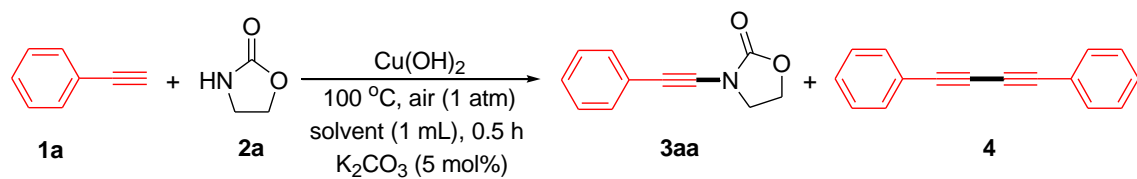


Entry	$K_2CO_3$ (mol %)	Conv. of <b>1</b> [%] <sup>[b]</sup>	Yield [%] <sup>[b]</sup>	
			<b>3aa</b>	<b>4</b>
1	2.5	48	47	1
2	5	76	75	1
3	10	75	73	1

[a] Reaction conditions:  $Cu(OH)_2$  (5 mol%), **1a** (0.1 mmol), **2a** (0.3 mmol), mesitylene (1 mL),  $100\text{ }^\circ\text{C}$ , under air (1 atm), 0.5 h. [b] Conversion and yields were determined by GC analysis.

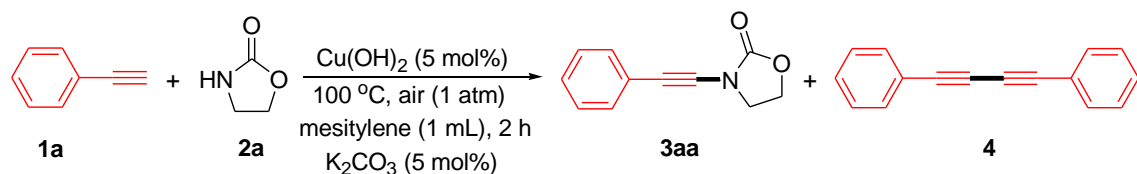
Examination of various solvents showed that mesitylene was the best one, and the reaction hardly proceeded in polar solvents such as dimethylformamide (DMF), dimethylsulfoxide (DMSO), acetonitrile, 2-propanol, ethyl acetate, and 1,4-dioxane (Table 2-1-4). 3 Equiv of **2a** were optimal for the high yield of **3aa** (Table 2-1-5).

For the  $Cu(OH)_2$ -catalyzed cross-coupling, no further conversions of substrates were observed upon removal of the catalyst by hot filtration during the reaction. Therefore, the contribution to the observed catalysis from leached copper species can be ruled out, and the catalysis is truly heterogeneous.

**Table 2-1-4.** Solvent screening.<sup>[a]</sup>

Entry	Solvent	Conv. of <b>1</b> [%] <sup>[b]</sup>	Yield [%] <sup>[b]</sup>	
			<b>3aa</b>	<b>4</b>
<b>1</b>	<b>mesitylene</b>	<b>76</b>	<b>75</b>	<b>1</b>
2 <sup>[c]</sup>	mesitylene	65	52	1
3 <sup>[d]</sup>	mesitylene	5	nd	nd
4	1,2-dichloroethane	<1	nd	nd
5	1,4-dioxane	<1	nd	nd
6	ethylacetate	<1	nd	nd
7	2-propanol	<1	nd	nd
8	acetonitrile	<1	nd	nd
9	dimethylsulfoxide	1	nd	1
10	dimethylformamide	6	2	nd

[a] Reaction conditions:  $\text{Cu}(\text{OH})_2$  (5 mol%), **1a** (0.1 mmol), **2a** (0.3 mmol), solvent (1 mL),  $\text{K}_2\text{CO}_3$  (5 mol%), 100 °C, under air (1 atm), 0.5 h. [b] Conversion and yields were determined by GC analysis. [c]  $\text{O}_2$  (1 atm). [d] Ar (1 atm). nd = not detected.

**Table 2-1-5.** Cross-coupling with different amount of 2-oxazolidinone (**2a**).<sup>[a]</sup>

Entry	<b>2a</b> (equiv)	Conv. of <b>1</b> [%] <sup>[b]</sup>	Yield [%] <sup>[b]</sup>	
			<b>3aa</b>	<b>4</b>
1	1	22	11	nd
2	2	40	29	2
<b>3</b>	<b>3</b>	<b>94</b>	<b>92</b>	<b>1</b>
4	4	96	72	3

[a] Reaction conditions:  $\text{Cu}(\text{OH})_2$  (5 mol%), **1a** (0.1 mmol), **2a** (0.3 mmol), mesitylene (1 mL), 100 °C, under air (1 atm), 2 h. [b] Conversion and yields were determined by GC analysis. nd = not detected.

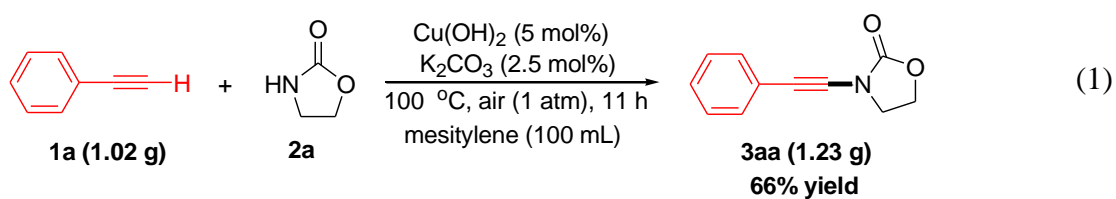
### 2-1.3.3. Substrate Scope

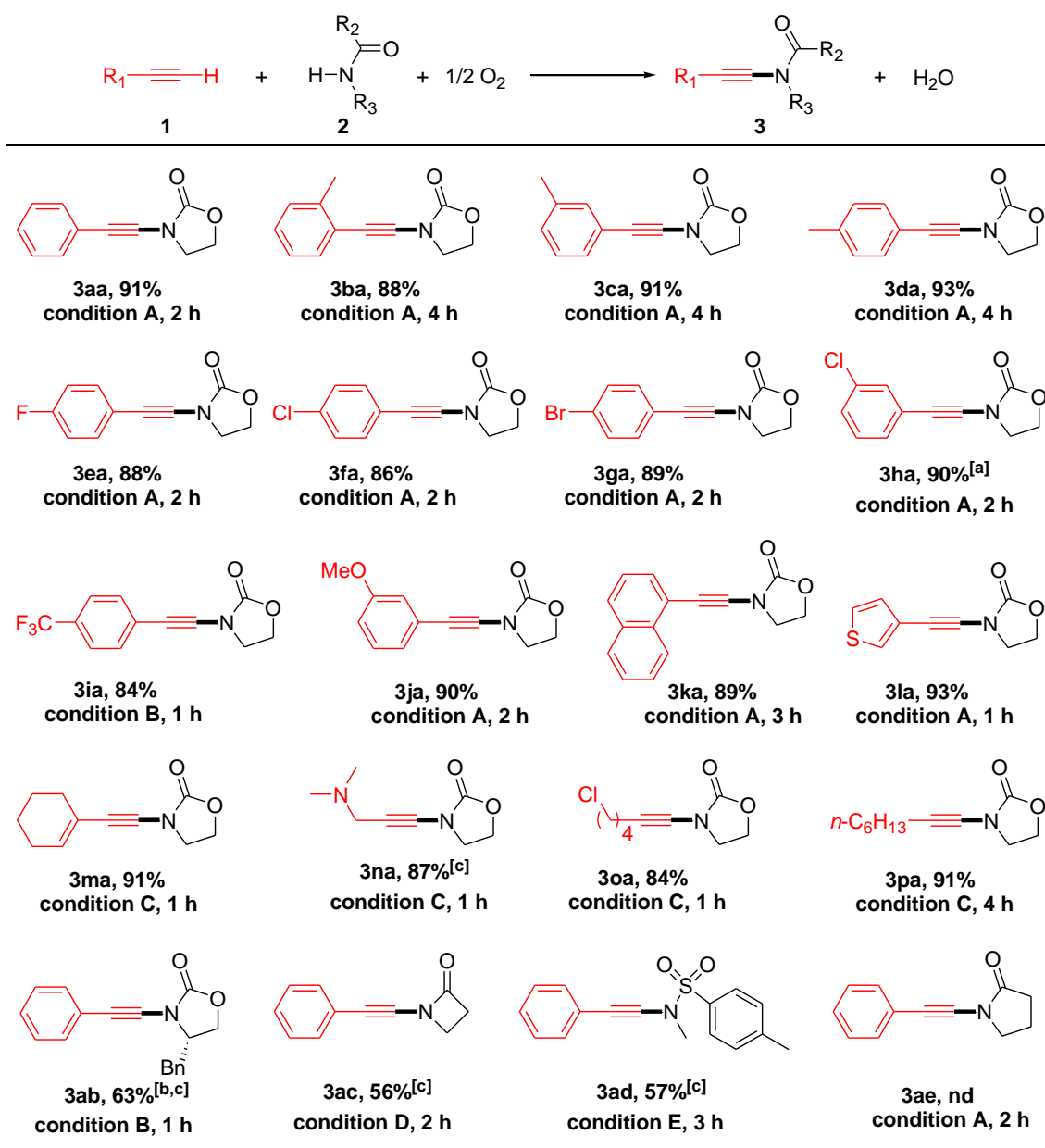
The substrate scope for the aerobic cross-dehydrogenative coupling of terminal alkynes and amides was investigated. The suitable reaction conditions were variable according to the substrates employed. By using the present Cu(OH)<sub>2</sub>-catalyzed system, various kinds of structurally diverse ynamides could be synthesized using air as the terminal oxidant (Scheme 2-1-4). After the cross-coupling, the insoluble Cu(OH)<sub>2</sub> and bases were separated by simple filtration, and the ynamide products were easily purified by directly loading the filtrate onto a short silica gel column.

Aromatic alkynes with electron-donating as well as electron-withdrawing substituents were all good substrates. It is noticeable that the cross-coupling worked well with aromatic alkynes containing electron-withdrawing substituents such as *p*-F, *p*-Cl, *p*-Br, and *p*-CF<sub>3</sub>, which are likely poor substrates in Stahl's and other related systems.<sup>[4-8,11]</sup> 2-, 3-, and 4-Ethynyltoluenes all reacted well with **2a** and almost equal yields of the corresponding ynamides were obtained, suggesting that the steric effect of substituents on aromatic rings is negligible. For halo-substituted aromatic alkynes, the corresponding ynamides were obtained in high yields without dehalogenation. Thus, it would be possible to further functionalize the ynamide products by utilizing these halo-substituents. Alkynes containing heteroatoms such as 3-ethynylthiophene and *N,N*-dimethylpropargylamine also efficiently reacted with **2a**. An enynamide could also be synthesized by the reaction of an enyne and **2a**. Apart from aromatic alkynes, aliphatic ones were also good coupling partners. In this case, the amount of **2a** could be reduced to 2 equiv with respect to the alkyne coupling partner without the deterioration of the high selectivity to the corresponding ynamides. As for nitrogen nucleophiles, oxazolidinone, azetidinone, and sulfonamide derivatives could be utilized as coupling

partners in the present  $\text{Cu}(\text{OH})_2$ -catalyzed system. However, pyrrolidone was not the effective substrate for the present cross-coupling.

In addition, a gram scale synthesis of **3aa** was also carried out (100-fold scale up, Eq. 1). In this case, 1.23 g (66% yield based on **1a**) of **3aa** was obtained. This result further demonstrates the potential utility and practicability of the present cross-coupling.





**Scheme 2-1-4.** Oxidative cross-coupling of terminal alkynes and amides. The isolated yields (based on **1**) are reported (unless otherwise noted). Conditions B–E are consistent with condition A unless otherwise noted. Reaction conditions: A: **1** (0.1 mmol), **2** (0.3 mmol), Cu(OH)<sub>2</sub> (0.5 mg, 5 mol%), K<sub>2</sub>CO<sub>3</sub> (5 mol%), mesitylene (1 mL), 100 °C, under air (1 atm). B: Cu(OH)<sub>2</sub> (1.0 mg, 10 mol%), Cs<sub>2</sub>CO<sub>3</sub> (5 mol%). C: **1** (0.2 mmol), **2** (0.4 mmol), Cu(OH)<sub>2</sub> (1.0 mg, 10 mol%), Cs<sub>2</sub>CO<sub>3</sub> (5 mol%), 110 °C. D: Cu(OH)<sub>2</sub> (1.0 mg, 10 mol%), CsOH (5 mol%), 110 °C. E: Cu<sub>2</sub>O (1.4 mg, 20 mol%), Cs<sub>2</sub>CO<sub>3</sub> (20 mol%), 120 °C. [a] Cu(OH)<sub>2</sub> (1.0 mg, 10 mol%). [b] 110 °C. [c] Yields were determined by GC using biphenyl as an internal standard. nd = not detected.

### 2-1.3.4. Reaction Mechanism

An H/D exchange reaction of [D<sub>1</sub>]ethynylbenzene (**1a'**) in the presence of 1 equiv of Cu(OH)<sub>2</sub> and K<sub>2</sub>CO<sub>3</sub> at 20 °C for 6 h in [D<sub>8</sub>]toluene resulted in a 47% decrease of the deuterium content (determined by <sup>1</sup>H NMR analysis) (Table 2-1-6). In contrast, K<sub>2</sub>CO<sub>3</sub> alone resulted in only 10% decrease of the deuterium content, and 13% decrease was observed in the presence of Cu(OH)<sub>2</sub> alone (Table 2-1-6). These results suggest a copper(II) acetylide species is likely formed through cooperative activation of alkynes by Cu(OH)<sub>2</sub> and a base.

**Table 2-1-6.** H/D exchange experiments under different reaction conditions.

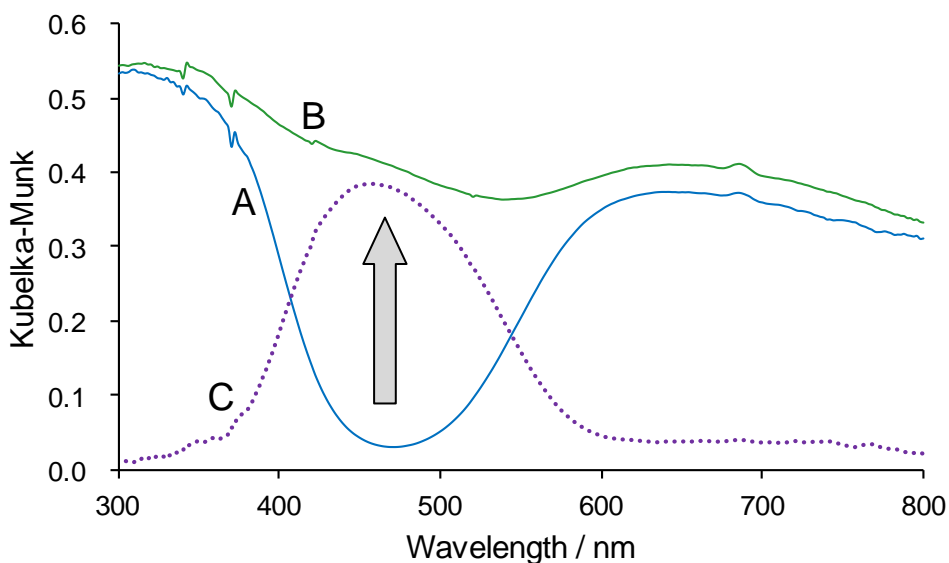
Entry	Cu(OH) <sub>2</sub> [mmol]	K <sub>2</sub> CO <sub>3</sub> [mmol]	Yield of <b>1a</b> [%]
1	0.1	0.1	47
2	0.1	-	13
3	-	0.1	10
4	-	-	0

[a] Reaction conditions: **1a'** (0.1 mmol), [D<sub>8</sub>]toluene (1 mL), 20 °C, under air (1 atm), 6 h. [b] Yields were determined by <sup>1</sup>H NMR analysis.

The possible involvement of the copper(II) acetylide species was further confirmed by UV/Vis spectrum of the catalyst. After the Cu(OH)<sub>2</sub> catalyst (5 mol% with respect to **1a**) was treated with **1a** in the presence of 5 mol% K<sub>2</sub>CO<sub>3</sub> in mesitylene at 100 °C for 1 h under an air atmosphere, the UV/Vis spectrum of the retrieved catalyst was measured (Figure 2-1-4). A new broad absorption band around 450 nm attributed possibly to ligand to metal charge transfer (LMCT)<sup>[21]</sup> of the copper acetylide species was observed.



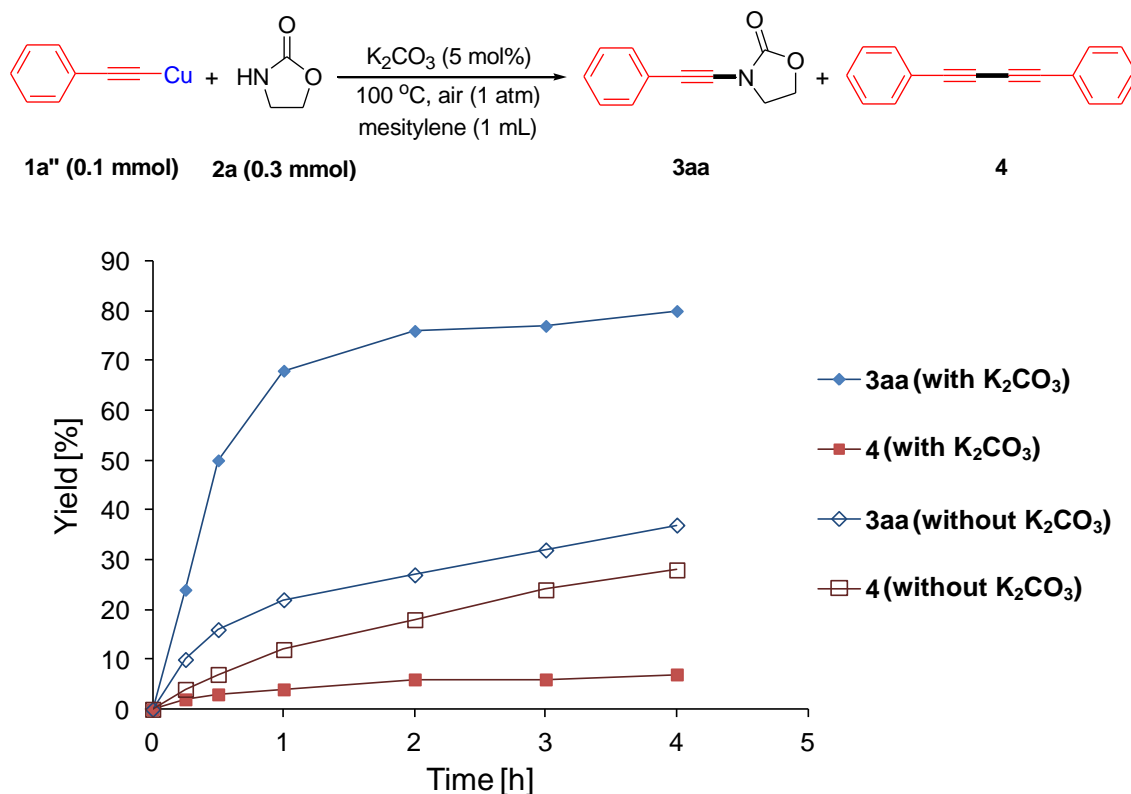
In addition, the intensity of the absorption band around 650 nm assignable to the d-d transition of copper(II) species<sup>[22]</sup> almost unchanged compared to the fresh Cu(OH)<sub>2</sub> catalyst. These results suggest that the valence state of the copper acetylide species is possibly +2.



**Figure 2-1-4.** The UV/Vis spectra of fresh Cu(OH)<sub>2</sub> catalyst (spectrum A), the catalyst retrieved after the treatment with **1a** (spectrum B), and the difference spectrum between A and B (spectrum C).

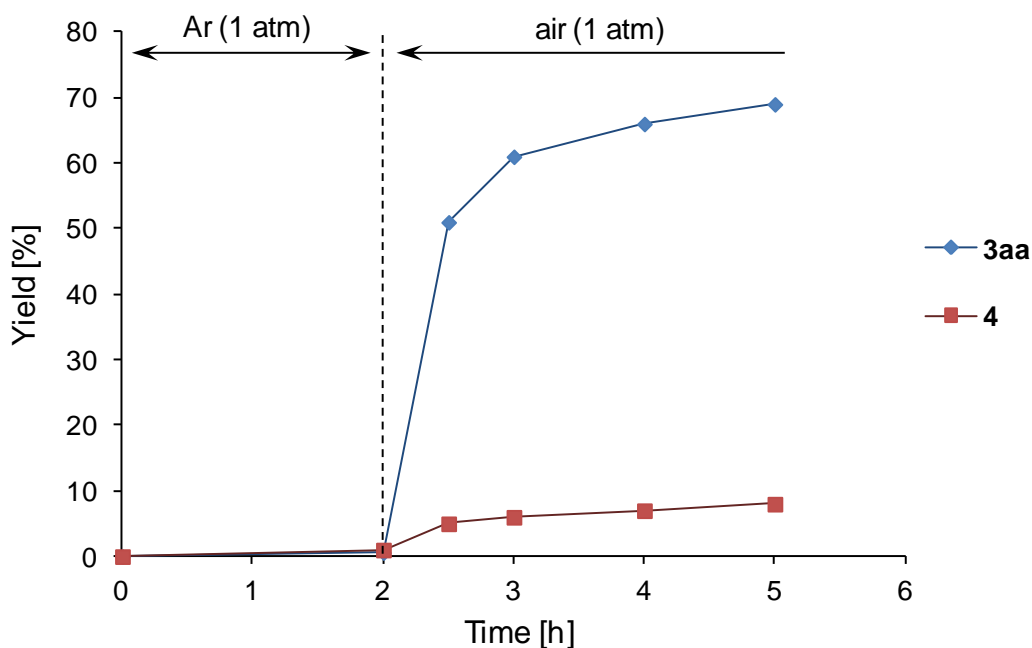
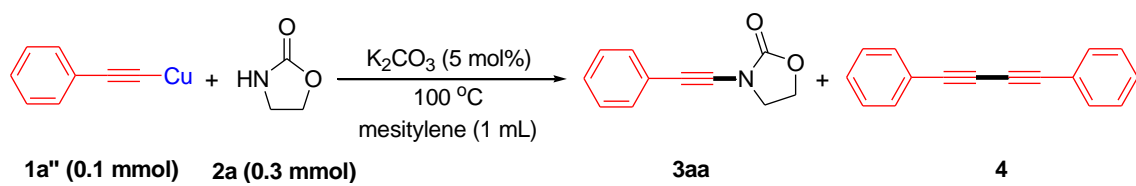
A stoichiometric reaction of copper(I) phenylacetylide (**1a'**) with **2a** efficiently proceeded to give **3aa** in a high yield and selectivity (Figure 2-1-5). This result suggests that a copper(I) acetylide species is also a possible intermediate in the present cross-coupling. In addition, this reaction was promoted greatly by the presence of 5 mol% of K<sub>2</sub>CO<sub>3</sub>, indicating the essential role of the base to facilitate deprotonative coordination of **2a** to the active copper center (Figure 2-1-5). The presence of the catalytic amount of K<sub>2</sub>CO<sub>3</sub> also resulted in the higher selectivity to **3aa**, likely because

of the facile deprotonative coordination of **2a** to the copper center to suppress the Glaser–Hay homo-coupling of **1a''** (Figure 2-1-5).



**Figure 2-1-5.** Reaction profiles for the stoichiometric reaction of copper(I) phenylacetylide (**1a''**) and 2-oxazolidinone (**2a**) in the presence or absence of  $K_2CO_3$ . Yields were determined by GC analysis using biphenyl as an internal standard.

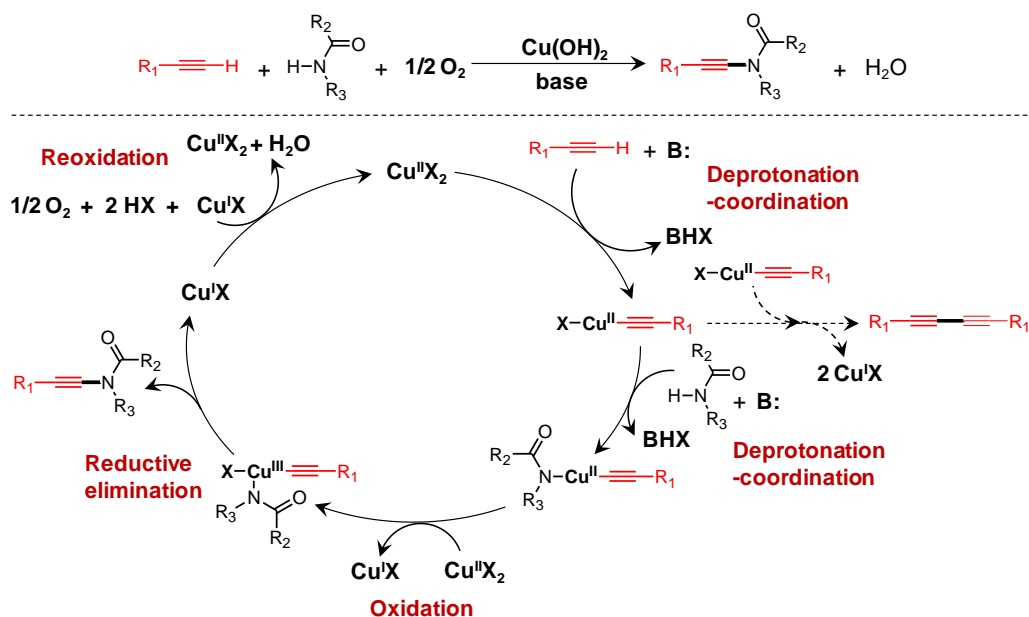
Furthermore, the reaction of **1a''** and **2a** did not proceed at all under 1 atm Ar. Upon introducing 1 atm of air to the reaction system, however, the reaction proceeded well to give **3aa** in a good yield and selectivity (Figure 2-1-6). These results suggest that the C–N bond forming reductive elimination takes place from a higher valence copper species.<sup>[23]</sup>



**Figure 2-1-6.** Reaction profiles for the stoichiometric reaction of copper(I) phenylacetylide (**1a''**) and 2-oxazolidinone (**2a**) under different atmospheric conditions. Yields were determined by GC analysis using biphenyl as an internal standard.

Based on the above results and literature reports<sup>[23]</sup> on copper-catalyzed aerobic oxidative coupling reactions (see also section 1.2.3.4), a plausible reaction mechanism is depicted in Scheme 2-1-5. This reaction likely proceeds through sequential coordination/deprotonation of an alkyne and an amide to the active copper center, followed by reductive elimination of C–N bond from the copper(III) species. Reoxidation of the resulting copper(I) species by air can regenerate the active copper catalyst. The high selectivity for the present catalyst system can be attributed to the inertness of  $\text{Cu}(\text{OH})_2$  for the Glaser-Hay alkyne homo-coupling. The  $pK_a$  value of the substrates might be an important factor for the effectiveness of different nitrogen

nucleophiles in the present cross-coupling, because the deprotonative coordination of an amide to the active copper center promoted by a base plays a vital role for the achievement of both the high yield and selectivity.



**Scheme 2-1-5.** The proposed reaction mechanism for the present cross-coupling. B: = base.

## 2-1.4. Conclusion

In conclusion, the  $Cu(OH)_2$ -catalyzed selective aerobic oxidative cross-coupling of terminal alkynes and amides to ynamides has successfully been developed. The substrate scope for the present procedure is quite broad with respect to both terminal alkynes and amides, and various kinds of structurally diverse ynamides can be synthesized in moderate to high yields (56–93% yields) even upon simply mixing the two coupling partners in a single step. The procedure is simple, efficient and practicable, providing an easy access to ynamides.

## 2-1.5. References

- [1] F. Diederich, P. J. Stang, R. R. Tykwinski, *Acetylene Chemistry: Chemistry, Biology, and Material Science*, Wiley-VCH, Weinheim, **2005**.
- [2] G. Evano, A. Coste, K. Jouvin, *Angew. Chem. Int. Ed.* **2010**, *49*, 2840.
- [3] K. A. DeKorver, H. Li, A. G. Lohse, R. Hayashi, Z. Lu, Y. Zhang, R. P. Hsung, *Chem. Rev.* **2010**, *110*, 5064.
- [4] a) M. O. Frederick, J. A. Mulder, M. R. Tracey, R. P. Hsung, J. Huang, K. C. M. Kurtz, L. Shen, C. J. Douglas, *J. Am. Chem. Soc.* **2003**, *125*, 2368; b) J. R. Dunetz, R. L. Danheiser, *Org. Lett.* **2003**, *5*, 4011.
- [5] Y. Zhang, R. P. Hsung, M. R. Tracey, K. C. M. Kurtz, E. L. Vera, *Org. Lett.* **2004**, *6*, 1151.
- [6] B. Yao, Z. Liang, T. Niu, Y. Zhang, *J. Org. Chem.* **2009**, *74*, 4630.
- [7] K. Jouvin, F. Couty, G. Evano, *Org. Lett.* **2010**, *12*, 3272.
- [8] W. Jia, N. Jiao, *Org. Lett.* **2010**, *12*, 2000.
- [9] K. Jouvin, J. Heimburger, G. Evano, *Chem. Sci.* **2012**, *3*, 756.
- [10] A. Coste, G. Karthikeyan, F. Couty, G. Evano, *Angew. Chem. Int. Ed.* **2009**, *48*, 4381.
- [11] T. Hamada, X. Ye, S. S. Stahl, *J. Am. Chem. Soc.* **2008**, *130*, 833.
- [12] D. R. Stuart, K. Fagnou, *Science* **2007**, *316*, 1172.
- [13] D.-H. Wang, K. M. Engle, B.-F. Shi, J.-Q. Yu, *Science* **2010**, *327*, 315.
- [14] R. J. Phipps, M. J. Gaunt, *Science* **2009**, *323*, 1593.
- [15] C. A. Parrodi, P. J. Walsh, *Angew. Chem. Int. Ed.* **2009**, *48*, 4679.
- [16] Z. Shao, F. Peng, *Angew. Chem. Int. Ed.* **2010**, *49*, 9566.
- [17] *Purification of Laboratory Chemicals*, 3rd ed. (Eds.: D. D. Perrin, W. L. F.

Armarego), Pergamon Press, Oxford, **1988**.

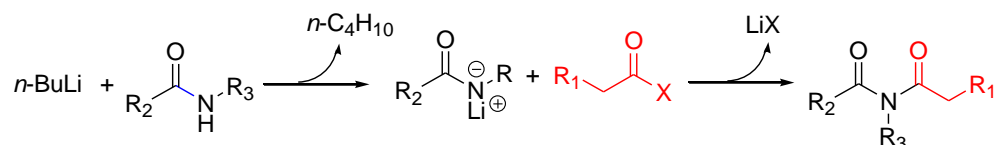
- [18] T. Oishi, T. Katayama, K. Yamaguchi, N. Mizuno, *Chem. Eur. J.* **2009**, *15*, 7539.
- [19] H. R. Oswald, A. Reller, H. W. Schmalle, E. Dubler, *Acta Cryst.* **1990**, 2279.
- [20] Y. Cudennec, A. Lecerf, *Solid State Sciences* **2003**, *5*, 1471.
- [21] V. W.-W. Yam, K. K.-W. Lo, K. M.-C. Wong, *J. Organomet. Chem.* **1999**, 578, 3.
- [22] B. J. Hathaway, D. E. Billing, *Coord. Chem. Rev.* **1970**, *5*, 143.
- [23] a) A. E. King, B. L. Ryland, T. C. Brunold, S. S. Stahl, *Organometallics* **2012**, *31*, 7948; b) A. E. King, T. C. Brunold, S. S. Stahl, *J. Am. Chem. Soc.* **2009**, *131*, 5044; c) A. E. King, L. M. Huffman, A. Casitas, M. Costas, X. Ribas, S. S. Stahl, *J. Am. Chem. Soc.* **2010**, *132*, 12068.

## 2-2 One-pot Synthesis of Imides by the Oxidative Cross-coupling to Ynamides Followed by Their Successive Hydration

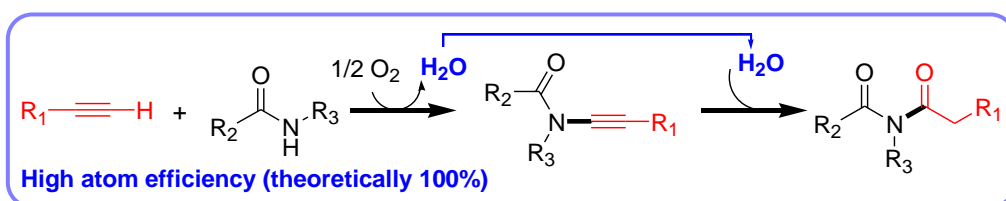
### 2-2.1. Introduction

Imides are very important key motifs in many pharmaceuticals and natural products and play a huge role in modern organic chemistry.<sup>[1]</sup> They have generally been synthesized by “non-green” two-step procedures of deprotonation of amides with strong bases such as *n*-butyllithium followed by acylation with acyl halides (Scheme 2-2-1, a).<sup>[1]</sup> However, in the classical procedure, generation of stoichiometric amounts of wastes such as *n*-butane and inorganic halides is inevitable. Hence, the development of more environmentally-friendly routes to these important compounds is highly desirable.

#### (a) Classical procedure<sup>[1]</sup>



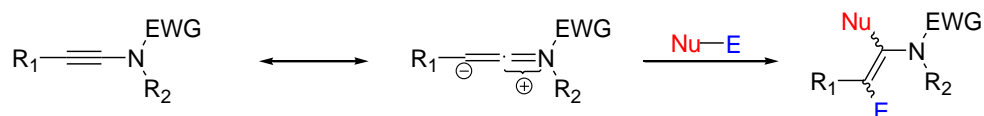
#### (b) This work



Scheme 2-2-1. Synthesis of imides.

In the previous section, the  $\text{Cu(OH)}_2$ -catalyzed highly selective cross-dehydrogenative coupling of terminal alkynes and amides to ynamides has been described. The nitrogen atom in the ynamides strongly polarizes the triple bonds due to its electron-donating ability, which allows an exceptionally high level of reactivity together with a strong differentiation of the two *sp*-hybridized carbon atoms (Scheme

2-2-2).<sup>[2,3]</sup> The substitution of amide functionalities to terminal alkynes to form ynamides can allow the formal “umpolung” reactivities of the triple bonds compared to terminal alkynes. These unique reactivities of ynamides have allowed various highly regio- and stereo-selective transformations to be realized in the past decades <sup>[4–17]</sup>.



**Scheme 2-2-2.** The reactivity of ynamides. EWG = electron-withdrawing group.<sup>[2,3]</sup>

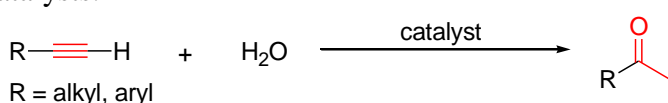
After the successful development of the aerobic cross-dehydrogenative coupling of terminal alkynes and amides, a novel one-pot synthetic procedure for imides by the successive regioselective hydration of ynamides was considered (Scheme 2-2-1, b). The hydration of alkynes can be promoted by acidic reagents, which possesses long history, dating back to Kucherov’s observation in 1881.<sup>[18]</sup> However, the acid-mediated hydration generally requires a large quantity of acidic reagents (typically  $\geq 100$  mol%) and/or highly toxic mercury(II) salts/oxide additives.<sup>[18]</sup>

Several homogeneous transition-metal salts or complexes-mediated catalytic hydration procedures have recently been developed.<sup>[18,19]</sup> However, these systems have several shortcomings, such as difficulties in the recovery and reuse of the (expensive) catalysts and/or the requirement of large amounts of acidic reagents as co-catalysts. Therefore, the development of easily recoverable and recyclable heterogeneous catalysts for the hydration of alkynes has received a particular research interest.<sup>[20]</sup> To date, a number of mercury-free<sup>[21]</sup> hydration using heterogeneous catalysts, for example, metal cation-exchanged acidic resins (M-resins; M = Cu(II), Pd(II), and Ru(III)),<sup>[22]</sup> Au(I)-containing mesoporous silica (Au(I)-MS),<sup>[23]</sup> and polystyrene-supported sulfonic



acid (PS-SO<sub>3</sub>H) have been developed (Table 2-2-1).<sup>[24]</sup> These heterogeneous systems, however, have several drawbacks, such as low activity or narrow substrate scope. Therefore, the development of efficient and widely applicable heterogeneous hydration systems without any additives is still a challenging subject.

**Table 2-2-1.** Previously reported hydration of alkynes by mercury-free heterogeneous catalysts.<sup>[22–24]</sup>

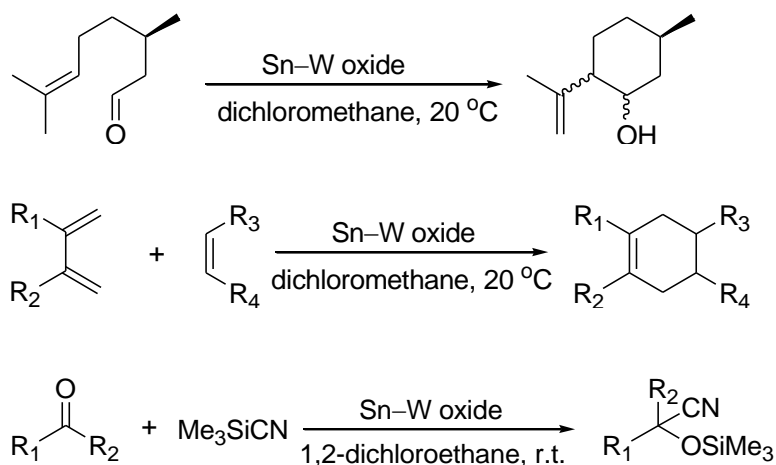


Catalyst	Additives	Temp [°C]	Time [h]	Yield [%]	Ref.
M-resins <sup>[a]</sup>	-	80	117-238	49-98	[22]
Au(I)-MS <sup>[b]</sup>	H <sub>2</sub> SO <sub>4</sub> (10 mol%)	100	7	91	[23]
PS-SO <sub>3</sub> H <sup>[c]</sup>	-	100	48	81	[24]

[a] Metal-cation-exchange-acidic resins (M = Cu<sup>II</sup>, Pd<sup>II</sup>, and Ru<sup>III</sup>). [b] Polystyrene-supported sulfonic acid. [c] Au<sup>I</sup>-containing mesoporous silica.

In the present study, the Sn–W mixed oxide catalyst, which is known to be an efficient Brønsted acid catalyst for various C–C bond-forming reactions, has successfully been applied to the hydration of alkynes (Scheme 2-2-3).<sup>[25]</sup> The catalysis is truly heterogeneous, and the retrieved Sn–W oxide catalyst after the hydration can be reused at least three times without an appreciable loss of its high catalytic performance. These characteristics feature the present catalyst system as the environmentally benign hydration.

Finally, by the combination of the Cu(OH)<sub>2</sub>-catalyzed aerobic cross-dehydrogenative coupling and the Sn–W mixed oxide catalyzed hydration, the one-pot synthetic procedure for imides has successfully been developed (Scheme 2-2-1, b). This procedure generates no wastes and the atom efficiency is theoretically 100%.



**Scheme 2-2-3.** The Sn–W mixed oxide-catalyzed C–C bond forming reactions.<sup>[25]</sup>

## 2-2.2. Experimental Section

### 2-2.2.1. General

GC analyses were performed on Shimadzu GC-2014 with a FID detector equipped with a DB-WAX ETR or an Rtx-200 capillary column. Mass spectra were recorded on Shimadzu GCMS-QP2010 equipped with a TC-5HT capillary column at an ionization voltage of 70 eV. Liquid-state NMR spectra were recorded on JEOL JNM-EX-270.  $^1\text{H}$  and  $^{13}\text{C}$  NMR spectra were measured at 270 and 67.8 MHz, respectively. The ICP-AES analyses were performed with Shimadzu ICPS-8100.

H-MOR (JRC-Z-HM15,  $\text{SiO}_2/\text{Al}_2\text{O}_3 = 14.9$ ) and  $\text{SO}_4^{2-}/\text{ZrO}_2$  (JRC-SZ-1) were supplied from the Catalysis Society of Japan. H-Y (CBV400,  $\text{SiO}_2/\text{Al}_2\text{O}_3 = 5.1$ ) was supplied from Zeolyst. Nafion (Nafion® NR-50) and Amberlyst-15 were purchased from Wako and ORGANO, respectively. Substrates and solvents were commercially obtained from TCI, Wako, or Aldrich (reagent grade), and purified prior to the use if necessary.<sup>[26]</sup>

#### **2.2.2.2. General Procedure for the Preparation of the Sn–W Mixed Oxides**

The Sn–W mixed oxide catalysts were prepared according to the following procedure.<sup>[25]</sup> First, the Sn–W mixed hydroxide precursors (Sn/W molar ratio of 2 as an example) were prepared by the following co-precipitation method. In deionized water (15 mL), Na<sub>2</sub>WO<sub>4</sub>·2H<sub>2</sub>O (2.47 g, 7.5 mmol) was dissolved, followed by addition of SnCl<sub>4</sub>·5H<sub>2</sub>O (5.26 g, 15 mmol) in a single step. After stirring the solution for 1 h at room temperature (ca. 22–23 °C), deionized water (60 mL) was added to the solution in a single step, and the colorless solution gradually became white slurry. After stirring the white slurry for 24 h at room temperature, the resulting white precipitate of the Sn–W hydroxide was filtered off, washed with a large amount of deionized water (ca. 2.0 L), and dried in vacuo to afford the Sn–W hydroxide precursor as a white powder (4.5 g). The contents of Sn and W were 38.3 and 33.6 wt%, respectively (the Sn/W molar ratio of 1.8). The elemental analysis indicated that the Sn/W molar ratio of the hydroxide was in good agreement with that of the starting metal solution. Five kinds of Sn–W hydroxides with different Sn/W molar ratios (Sn/W = 1, 1.5, 2, 5, and 10) were prepared by changing the molar ratios of the starting metal solutions. By the calcination of the corresponding hydroxide precursors at different temperatures (400–1000 °C) for 3 h under an air atmosphere, eight kinds of Sn–W oxide catalysts were prepared. The properties of Sn–W oxide catalysts are summarized in Table 2-2-2.

#### **2-2.2.3 General Procedure for the Catalytic Alkyne Hydration**

In this study, the Sn–W oxide prepared by the calcination of the hydroxide precursor with Sn/W molar ratio of 2 at 800 °C, denoted as SnW2-800, was mainly used for the hydration. The catalytic reactions were carried out as follows. Into a Pyrex-glass

screw cap vial (volume: ca. 20 mL) were successively placed the Sn–W oxide catalyst (50–100 mg), an alkyne (0.5 mmol), water (1–20 equiv with respect to an alkyne), and cyclooctane (2 mL). A Teflon-coated magnetic stir bar was added and the reaction mixture was vigorously stirred at 100–120 °C. After the reaction was completed, the catalyst was separated by filtration. Then, an internal standard (biphenyl) was added to the filtrate and analyzed by GC. As for the isolation of the products (ketones), the internal standard was not added and the crude filtrate was directly subjected to column chromatography on silica gel (Silica Gel 60N (63–210 μm), Kanto Chemical, 2.5 cm ID × 20 cm length, initial: *n*-hexane only, after cyclooctane and an alkyne were eluted: *n*-hexane/diethyl ether = 1/1 (v/v)). The isolated products were identified by GC-MS and <sup>1</sup>H and <sup>13</sup>C NMR analyses. The retrieved catalyst was washed with a small portion of acetone, and dried in vacuo prior to reuse.

**Table 2-2-2.** Properties of the Sn–W oxide catalysts.<sup>[25]</sup>

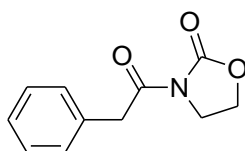
Catalyst	Sn/W ratio	Calcination temp. [°C]	BET <sup>[a]</sup> [m <sup>2</sup> g <sup>-1</sup> ]	Amount of acidic sites <sup>[b]</sup> [μmol g <sup>-1</sup> ]	Ratio of Brønsted acid sites / Lewis acid sites <sup>[c]</sup>
SnW2-400	2	400	143	290	43/57
SnW2-600	2	600	118	189	54/46
SnW1-800	1	800	35.8	73	58/42
SnW1.5-800	1.5	800	77.4	124	66/34
SnW2-800	2	800	73.6	134	73/27
SnW5-800	5	800	68.8	78	— <sup>[d]</sup>
SnW10-800	10	800	49.4	55	— <sup>[d]</sup>
SnW2-1000	2	1000	29.5	27	— <sup>[d]</sup>

[a] From the N<sub>2</sub> adsorption isotherm. [b] Amounts of total acidic sites were determined by NH<sub>3</sub>-TPD measurements. The values contain ca. 10% experimental errors. [c] The ratios were determined by IR spectra of pyridine adsorbed on the Sn–W oxides. [d] IR spectra of pyridine adsorbed on these Sn–W oxides could not be measured because of the low transmittance (nearly 0%).

#### 2-2.2.4 General Procedure for the Synthesis of Imides

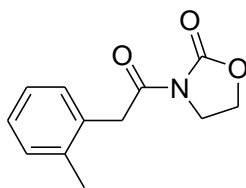
After the completion of the cross-coupling of a terminal alkyne with 2-oxazolidinone (see section 2-1.2.2 for the detailed procedures),  $\text{Cu}(\text{OH})_2$ , bases, and the remaining 2-oxazolidinone are filtered off. Then, the filtrate was added to a Pyrex-glass screw cap vial (volume: ca. 20 mL) containing Sn–W oxide (50 mg) and water (0.3 mmol). A Teflon-coated magnetic stir bar was added and the reaction mixture was vigorously stirred at 100 °C. After the reaction was completed, the crude reaction mixture was directly subjected to column chromatography on silica gel (Silica Gel 60N (63–210  $\mu\text{m}$ ), Kanto Chemical, 2.5 cm ID  $\times$  15 cm length, initial: *n*-hexane only, after mesitylene, an alkyne and a diyne byproduct were eluted: *n*-hexane/ethyl acetate = 9/1 to 2/3 (v/v)), giving the pure imide. The isolated products were identified by GC-MS and  $^1\text{H}$  and  $^{13}\text{C}$  NMR.

#### 2-2.2.5. Spectral Data of Imides



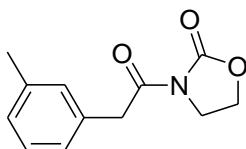
**4aa**

**3-(2-phenylacetyl)oxazolidin-2-one (4aa):** Solid.  $^1\text{H}$  NMR (270 MHz,  $\text{CDCl}_3$ , TMS):  $\delta$  3.98–4.04 (m, 2H), 4.28 (s, 2H), 4.36–4.42 (m, 2H), 7.23–7.38 (m, 5H).  $^{13}\text{C}\{^1\text{H}\}$  NMR (67.8 MHz,  $\text{CDCl}_3$ , TMS):  $\delta$  41.04, 42.67, 61.94, 127.15, 128.51, 129.69, 133.51, 153.45, 171.25. MS (EI):  $m/z$  (%) : 205 (25) [ $M^+$ ], 119 (10), 118 (100), 91 (41), 90 (32), 65 (13).



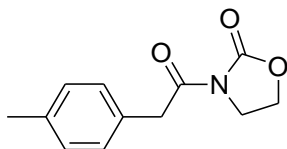
**4ba**

**3-(2-*o*-tolylacetyl)oxazolidin-2-one (4ba):** Solid.  $^1\text{H}$  NMR (270 MHz,  $\text{CDCl}_3$ , TMS):  $\delta$  2.28 (s, 3H), 4.01–4.07 (m, 2H), 4.28 (s, 2H), 4.39–4.45 (m, 2H), 7.13–7.21 (m, 4H).  $^{13}\text{C}\{^1\text{H}\}$  NMR (67.8 MHz,  $\text{CDCl}_3$ , TMS):  $\delta$  19.57, 39.38, 42.65, 62.06, 126.03, 127.44, 130.08, 130.30, 132.32, 137.13, 153.64, 171.01. MS (EI):  $m/z$  (%) : 219 (21) [ $M^+$ ], 133 (10), 132 (100), 105 (31), 104 (39), 103 (13), 79 (10), 78 (10), 77 (15).



**4ca**

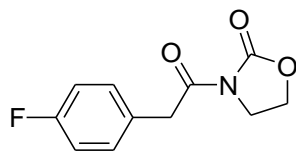
**3-(2-*m*-tolylacetyl)oxazolidin-2-one (4ca):** Solid.  $^1\text{H}$  NMR (270 MHz,  $\text{CDCl}_3$ , TMS):  $\delta$  2.34 (s, 3H), 3.98–4.04 (m, 2H), 4.25 (s, 2H), 4.36–4.42 (m, 2H), 7.07–7.26 (m, 4H).  $^{13}\text{C}\{^1\text{H}\}$  NMR (67.8 MHz,  $\text{CDCl}_3$ , TMS):  $\delta$  21.34, 40.94, 42.67, 61.93, 126.71, 127.96, 128.41, 130.41, 133.36, 138.17, 153.45, 171.39. MS (EI):  $m/z$  (%) : 219 (20) [ $M^+$ ], 133 (10), 132 (100), 105 (23), 104 (25), 103 (10), 77 (13).



**4da**

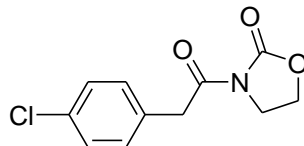
**3-(2-*p*-tolylacetyl)oxazolidin-2-one (4da):** Solid.  $^1\text{H}$  NMR (270 MHz,  $\text{CDCl}_3$ , TMS):  $\delta$  2.33 (s, 3H), 3.98–4.04 (m, 2H), 4.24 (s, 2H), 4.35–4.41 (m, 2H), 7.11–7.26 (m, 4H).  $^{13}\text{C}\{^1\text{H}\}$  NMR (67.8 MHz,  $\text{CDCl}_3$ , TMS):  $\delta$  21.06, 40.65, 42.67, 61.93, 129.23, 129.56,

130.40, 136.83, 153.46, 171.48. MS (ED):  $m/z$  (%) : 219 (20) [ $M^+$ ], 133 (10), 132 (100), 105 (27), 104 (31), 103 (10), 77 (13).



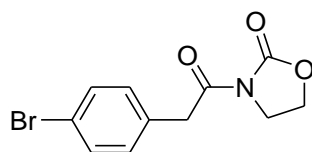
**4ea**

**3-(2-(4-fluorophenyl)acetyl)oxazolidin-2-one (4ea):** Solid.  $^1\text{H}$  NMR (270 MHz,  $\text{CDCl}_3$ , TMS):  $\delta$  4.00–4.06 (m, 2H), 4.25 (s, 2H), 4.39–4.45 (m, 2H), 6.97–7.05 (m, 2H), 7.24–7.31 (m, 2H).  $^{13}\text{C}\{^1\text{H}\}$  NMR (67.8 MHz,  $\text{CDCl}_3$ , TMS):  $\delta$  40.25, 42.65, 62.01, 115.38 (d,  $J = 21.8$  Hz), 129.12 (d,  $J = 3.3$  Hz), 131.29 (d,  $J = 7.8$  Hz), 153.46, 162.08 (d,  $J = 245.3$  Hz), 171.12. MS (ED):  $m/z$  (%) : 223 (16) [ $M^+$ ], 136 (100), 109 (49), 108 (40), 107 (10), 83 (15).



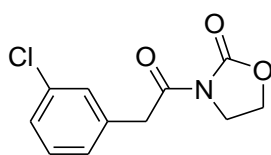
**4fa**

**3-(2-(4-chlorophenyl)acetyl)oxazolidin-2-one (4fa):** Solid.  $^1\text{H}$  NMR (270 MHz,  $\text{CDCl}_3$ , TMS):  $\delta$  3.99–4.05 (m, 2H), 4.25 (s, 2H), 4.38–4.44 (m, 2H), 7.23–7.31 (m, 4H).  $^{13}\text{C}\{^1\text{H}\}$  NMR (67.8 MHz,  $\text{CDCl}_3$ , TMS):  $\delta$  40.44, 42.64, 62.02, 128.67, 131.09, 131.89, 133.19, 153.43, 170.83. MS (ED):  $m/z$  (%) : 239 (18) [ $M^+$ ], 154 (32), 152 (100), 125 (30), 124 (22), 89 (25).



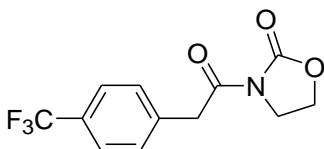
**4ga**

**3-(2-(4-bromophenyl)acetyl)oxazolidin-2-one (4ga):** Solid.  $^1\text{H}$  NMR (270 MHz,  $\text{CDCl}_3$ , TMS):  $\delta$  4.00–4.06 (m, 2H), 4.24 (s, 2H), 4.39–4.45 (m, 2H), 7.18–7.21 (m, 2H), 7.43–7.48 (m, 2H).  $^{13}\text{C}\{^1\text{H}\}$  NMR (67.8 MHz,  $\text{CDCl}_3$ , TMS):  $\delta$  40.52, 42.65, 62.02, 121.32, 131.47, 131.64, 132.41, 153.42, 170.71. MS (EI):  $m/z$  (%) : 285 (20), 283 (21) [ $M^+$ ], 198 (99), 196 (100), 171 (26), 170 (17), 169 (27), 168 (16), 90 (41), 89 (77), 88 (13), 63 (21).



**4ha**

**3-(2-(3-chlorophenyl)acetyl)oxazolidin-2-one (4ha):** Solid.  $^1\text{H}$  NMR (270 MHz,  $\text{CDCl}_3$ , TMS):  $\delta$  4.00–4.06 (m, 2H), 4.26 (s, 2H), 4.39–4.45 (m, 2H), 7.17–7.27 (m, 3H), 7.28–7.32 (m, 1H).  $^{13}\text{C}\{^1\text{H}\}$  NMR (67.8 MHz,  $\text{CDCl}_3$ , TMS):  $\delta$  40.67, 42.63, 62.02, 127.45, 128.00, 129.72, 129.80, 134.26, 135.33, 153.42, 170.57. MS (EI):  $m/z$  (%) : 239 (19) [ $M^+$ ], 154 (32), 152 (100), 125 (29), 124 (17), 89 (29), 88 (12).

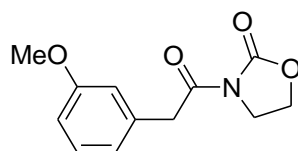


**4ia**

**3-(2-(4-(trifluoromethyl)phenyl)acetyl)oxazolidin-2-one (4ia):** Solid.  $^1\text{H}$  NMR (270 MHz,  $\text{CDCl}_3$ , TMS):  $\delta$  4.01–4.07 (m, 2H), 4.35 (s, 2H), 4.40–4.46 (m, 2H), 7.43 (d,  $J = 7.8$  Hz, 2H), 7.59 (d,  $J = 8.1$  Hz, 2H).  $^{13}\text{C}\{^1\text{H}\}$  NMR (67.8 MHz,  $\text{CDCl}_3$ , TMS):  $\delta$  40.92, 42.63, 62.07, 122.11, 125.35, 125.41, 125.46, 125.51, 126.11, 129.30, 130.13, 137.44,

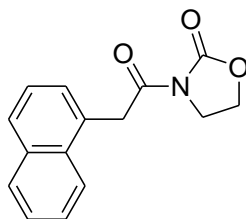


153.44, 170.41. MS (EI):  $m/z$  (%) : 273 (22) [ $M^+$ ], 187 (11), 186 (100), 159 (37), 158 (37), 109 (17), 88 (29).



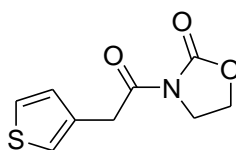
**4ja**

**3-(2-(3-methoxyphenyl)acetyl)oxazolidin-2-one (4ja):** Solid.  $^1\text{H}$  NMR (270 MHz,  $\text{CDCl}_3$ , TMS):  $\delta$  3.80 (s, 3H), 3.99–4.06 (m, 2H), 4.26 (s, 2H), 4.37–4.43 (m, 2H), 6.79–6.92 (m, 3H), 7.21–7.27 (m, 1H).  $^{13}\text{C}\{^1\text{H}\}$  NMR (67.8 MHz,  $\text{CDCl}_3$ , TMS):  $\delta$  41.03, 42.67, 55.17, 61.93, 112.82, 115.25, 122.03, 129.47, 134.91, 153.42, 159.65, 171.10. MS (EI):  $m/z$  (%) : 235 (21) [ $M^+$ ], 149 (11), 148 (100), 121 (15), 91 (17).



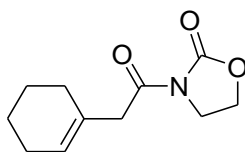
**4ka**

**3-(2-(naphthalen-1-yl)acetyl)oxazolidin-2-one (4ka):** Solid.  $^1\text{H}$  NMR (270 MHz,  $\text{CDCl}_3$ , TMS):  $\delta$  4.03–4.09 (m, 2H), 4.42–4.48 (m, 2H), 4.74 (s, 2H), 7.26–7.56 (m, 4H), 7.78–7.95 (m, 3H).  $^{13}\text{C}\{^1\text{H}\}$  NMR (67.8 MHz,  $\text{CDCl}_3$ , TMS):  $\delta$  38.82, 42.74, 62.11, 123.82, 125.43, 125.71, 126.30, 128.19, 128.24, 128.74, 130.14, 132.31, 133.82, 153.75, 171.06. MS (EI):  $m/z$  (%) : 255 (21) [ $M^+$ ], 169 (13), 168 (100), 141 (33), 140 (39), 139 (19), 115 (21).



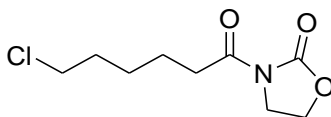
#### 4la

**3-(2-(thiophen-3-yl)acetyl)oxazolidin-2-one (4la):** Solid.  $^1\text{H}$  NMR (270 MHz,  $\text{CDCl}_3$ , TMS):  $\delta$  4.00–4.06 (m, 2H), 4.31 (s, 2H), 4.38–4.44 (m, 2H), 7.12 (dd,  $J = 5.1$  and 1.4 Hz, 1H), 7.21–7.23 (m, 1H), 7.26–7.30 (m, 1H).  $^{13}\text{C}\{^1\text{H}\}$  NMR (67.8 MHz,  $\text{CDCl}_3$ , TMS):  $\delta$  35.83, 42.61, 61.97, 123.61, 125.54, 128.75, 132.95, 153.42, 170.71. MS (EI):  $m/z$  (%) : 211 (25) [ $M^+$ ], 124 (100), 97 (39), 96 (26).



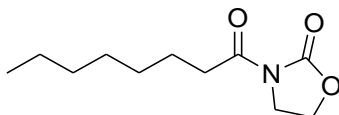
#### 4ma

**3-(2-cyclohexenylacetyl)oxazolidin-2-one (4ma):** Oil.  $^1\text{H}$  NMR (270 MHz,  $\text{CDCl}_3$ , TMS):  $\delta$  1.46–1.62 (m, 4H), 1.92–1.99 (m, 4H), 3.50 (s, 2H), 3.92–3.98 (m, 2H), 4.31–4.37 (m, 2H), 5.47–5.48 (m, 1H).  $^{13}\text{C}\{^1\text{H}\}$  NMR (67.8 MHz,  $\text{CDCl}_3$ , TMS):  $\delta$  21.93, 22.67, 25.24, 28.65, 42.51, 43.32, 61.84, 125.76, 130.92, 153.38, 171.61. MS (EI):  $m/z$  (%) : 209 (13) [ $M^+$ ], 122 (100), 94 (27), 88 (16), 79 (21).



#### 4oa

**3-(6-chlorohexanoyl)oxazolidin-2-one (4oa):** Oil.  $^1\text{H}$  NMR (270 MHz,  $\text{CDCl}_3$ , TMS):  $\delta$  1.46–1.57 (m, 2H), 1.65–1.87 (m, 4H), 2.94 (t,  $J = 7.3$  Hz, 2H), 3.55 (t,  $J = 6.8$  Hz, 2H), 3.99–4.05 (m, 2H), 4.39–4.45 (m, 2H).  $^{13}\text{C}\{^1\text{H}\}$  NMR (67.8 MHz,  $\text{CDCl}_3$ , TMS):  $\delta$  23.37, 26.25, 32.18, 34.80, 42.43, 44.72, 61.98, 153.48, 173.08. MS (EI):  $m/z$  (%) : 220 (0.1) [ $M^+$ ], 184 (18), 142 (48), 135 (10), 133 (30), 129 (100), 101 (26), 88 (47), 70 (11), 69 (78), 55 (29).



**4pa**

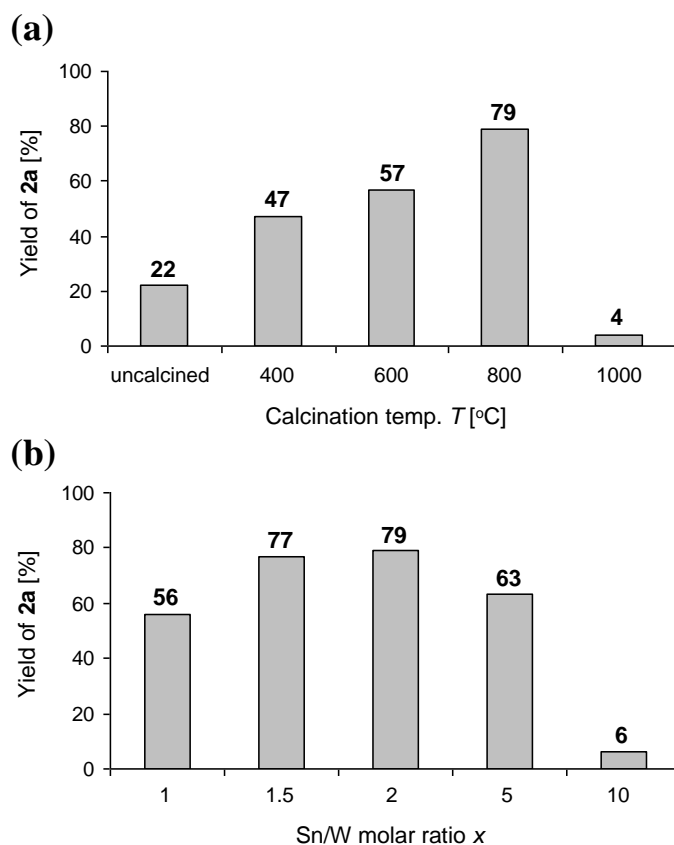
**3-octanoyloxazolidin-2-one (4pa):** Oil.  $^1\text{H}$  NMR (270 MHz,  $\text{CDCl}_3$ , TMS):  $\delta$  0.88 (t,  $J = 6.8$  Hz, 3H), 1.28–1.43 (m, 8H), 1.66 (quin,  $J = 7.4$  Hz, 2H), 2.91 (t,  $J = 7.4$  Hz, 2H), 3.99–4.05 (m, 2H), 4.38–4.44 (m, 2H).  $^{13}\text{C}\{^1\text{H}\}$  NMR (67.8 MHz,  $\text{CDCl}_3$ , TMS):  $\delta$  14.01, 22.54, 24.20, 28.96, 29.02, 31.61, 35.04, 42.47, 61.94, 153.51, 173.57. MS (EI):  $m/z$  (%) : 213 (0.4) [ $M^+$ ], 142 (69), 129 (100), 127 (24), 101 (38), 88 (61), 57 (66), 55 (37).

## 2-2.3. Results and Discussion

### 2-2.3.1. Optimization of the Reaction Conditions

Initially, optimization of the reaction conditions for the hydration of a simple terminal alkyne using various solid acid catalysts was carried out in order to evaluate the activity of these catalysts for the hydration, and thus, to find the most suitable catalyst for the hydration of ynamides. The Sn–W mixed oxide catalyst with a Sn/W molar ratio of  $x$  prepared by calcination of its hydroxide precursor at  $T$  °C is denoted as  $\text{SnW}_x\text{-}T$  (Table 2-2-2). These Sn–W mixed oxide catalysts were applied to the hydration of ethynylbenzene (**1a**) to acetophenone (**2a**). The results shown in Figure 2-2-1 indicate that the catalytic activity is largely dependent on the calcination temperature and the Sn/W molar ratio. The reaction rate with  $\text{SnW}_x\text{-}T$  increased with an increase in  $x$  and  $T$ , reached a maximum at  $x = 2$  and  $T = 800$  °C, and then decreased (Figure 2-2-4).

Thus, SnW2-800 was the most active catalyst for the hydration. The high catalytic activity of SnW2-800 for the hydration can be attributed to the strong Brønsted acid sites generated on the aggregated polytungstate species in the Sn–W mixed oxide.<sup>[25]</sup>

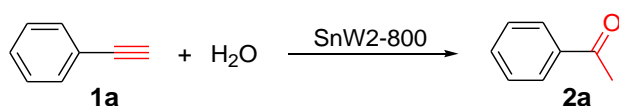


**Figure 2-2-1.** Effects of (a) calcination temperatures (Sn–W hydroxide with Sn/W molar ratio of 2 calcined at  $T$  [°C], SnW2- $T$ ) and (b) Sn/W molar ratios (Sn–W hydroxides with Sn/W molar ratio of  $x$  calcined at 800 °C, SnW $_x$ -800) on the Hydration of **1a** to **2a**. Reaction conditions: catalyst (50 mg), **1a** (0.5 mmol), water (2.5 mmol), cyclooctane (2 mL), 100 °C, 15 min. Yields were determined by GC using diphenyl as an internal standard.

Studies on the solvent effects showed that non-polar and non-aromatic solvents such as cyclooctane and *n*-octane were suitable for the hydration ( $\geq 96\%$  selectivities) (Table 2-2-3, entries 1 and 2). Due to the Friedel–Crafts-type vinylation ( $\sim 18\%$ ) of

toluene with **1a**, the hydration in toluene gave **2a** in 80% yield (Table 2-2-3, entry 3). Protic or polar solvents, such as ethanol, acetonitrile, 1,4-dioxane, and *N,N*-dimethylformamide, were not effective likely because of the strong coordination of these solvents to the active site(s) (Table 2-2-3, entries 4–7). The amount of water used up to 5 equiv had no significant effect on the reaction rate (Table 2-2-3, entries 1, 8, and 9). However, upon the addition of a large amount of water ( $\geq 10$  equiv with respect to **1a**), the hydration was completely inhibited (Table 2-2-3, entries 11 and 12).

**Table 2-2-3.** Optimization of reaction conditions for the hydration of **1a** to **2a**.<sup>[a]</sup>



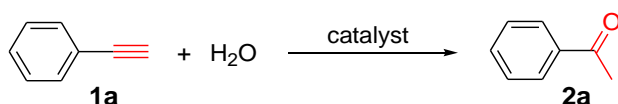
Entry	Water/ <b>1a</b>	Solvent	Conv. of <b>1a</b> [%]	Yield of <b>2a</b> [%]
1	5/1	cyclooctane	98	94
2	5/1	<i>n</i> -octane	49	49
3 <sup>[b]</sup>	5/1	toluene	>99	80 <sup>[c]</sup>
4	5/1	ethanol	<1	nd
5	5/1	acetonitrile	<1	nd
6	5/1	1,4-dioxane	1	1
7	5/1	<i>N,N</i> -dimethylformamide	<1	nd
8	1/1	cyclooctane	98	90
9	2/1	cyclooctane	97	92
10	7/1	cyclooctane	40	38
11	10/1	cyclooctane	<1	nd
12	20/1	cyclooctane	<1	nd

[a] Reaction conditions: SnW2-800 (50 mg), **1a** (0.5 mmol), water (0.5–10 mmol), cyclooctane (2 mL), 100 °C, 30 min. Yields were determined by GC using biphenyl as an internal standard. nd = not detected. [b] 20 min. [c] The Friedel–Crafts-type vinylation of toluene with **1a** proceeded to some extent (~18%).

Among various acid catalysts examined for the hydration of **1a** to **2a**, SnW2-800 showed the highest catalytic activity (Table 2-2-4, entry 1). Notably, when the amount

of SnW2-800 was reduced from 50 to 5 mg (0.13 mol% acidic sites and 9.8 mass% with respect to **1a**), the reaction also proceeded efficiently. In this case, the hydration of **1a** (0.5 mmol) carried out at 100 °C for 6 h gave **2a** in 88% yield (in this case, 0.1 mmol of water was added to the reaction mixture every 30 min). The hydration of **1a** did not proceed in the absence of a catalyst (Table 2-2-4, entry 15). No hydration occurred in the presence of SnO<sub>2</sub>, WO<sub>3</sub>, H<sub>2</sub>WO<sub>4</sub>, or a physical mixture of SnO<sub>2</sub> and WO<sub>3</sub> (Table 2-2-4, entries 2–5). SnW2-800 was more active than its Sn–W hydroxide precursor (Table 2-2-4, entry 6).

**Table 2-2-4.** Hydration of **1a** to **2a** with various catalysts.<sup>[a]</sup>

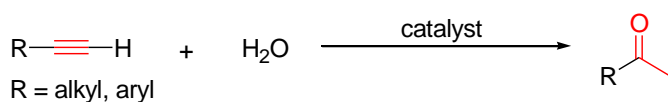


Entry	Catalyst	Conv. of <b>1a</b> [%]	Yield of <b>2a</b> [%]
1	SnW2-800	80	79
2	SnO <sub>2</sub>	<1	nd
3	WO <sub>3</sub>	<1	nd
4	H <sub>2</sub> WO <sub>4</sub>	1	nd
5 <sup>[b]</sup>	SnO <sub>2</sub> + WO <sub>3</sub>	4	nd
6 <sup>[c]</sup>	Sn–W hydroxide <sup>[c]</sup>	22	22
7	H-mordenite	6	6
8	H-Y	33	12
9	SO <sub>4</sub> <sup>2-</sup> /ZrO <sub>2</sub>	29	27
10	Nafion	6	1
11 <sup>[d]</sup>	Amberlyst-15	<1	nd
12 <sup>[d]</sup>	H <sub>2</sub> SO <sub>4</sub>	1	nd
13 <sup>[d]</sup>	<i>p</i> -TsOH	2	nd
14 <sup>[d]</sup>	H <sub>3</sub> PW <sub>12</sub> O <sub>40</sub>	3	nd
15	none	<1	nd

[a] Reaction conditions: catalyst (50 mg), **1a** (0.5 mmol), water (2.5 mmol), cyclooctane (2 mL), 100 °C, 15 min. Yields were determined by GC using biphenyl as an internal standard. nd = not detected. [b] A mixture of SnO<sub>2</sub> (25 mg) and WO<sub>3</sub> (25 mg). [c] The precursor of Sn–W oxide. [d] Catalyst (H<sup>+</sup>: 1.3 mol% with respect to **1a**). The amount was the same as that of the acid sites in the Sn–W oxide used in entry 1.

When SnW2-800 was employed as the catalyst, the turnover frequency (TOF) reached up to 246 h<sup>-1</sup> (based on the amount of acidic sites, 1.3 mol% with respect to **1a**), which is much higher than those of the previously reported (mercury-free) heterogeneous catalysts: M-resins (0.12–0.36 h<sup>-1</sup>),<sup>[22]</sup> Au(I)-MS (4.1–6.7 h<sup>-1</sup>),<sup>[23]</sup> and PS-SO<sub>3</sub>H (0.17 h<sup>-1</sup>) (Table 2-2-5).<sup>[24]</sup>

**Table 2-2-5.** Comparison of catalytic activity.



Catalyst	Additives	Temp [°C]	Time [h]	Yield [%]	TOF [h <sup>-1</sup> ]	Ref.
<b>Sn-W oxide</b>	-	<b>100</b>	<b>0.5</b>	<b>92</b>	<b>246</b>	<b>This work</b>
M-resins <sup>[a]</sup>	-	80	117-238	49-98	0.1–0.4	[22]
Au(I)-MS <sup>[b]</sup>	H <sub>2</sub> SO <sub>4</sub> (10 mol%)	100	7	91	0.2	[23]
PS-SO <sub>3</sub> H <sup>[c]</sup>	-	100	48	81	4.1–6.7	[24]

[a] Metal-cation-exchange-acidic resins (M = Cu<sup>II</sup>, Pd<sup>II</sup>, and Ru<sup>III</sup>). [b] Polystyrene-supported sulfonic acid. [c] Au<sup>I</sup>-containing mesoporous silica.

It is noticeable that SnW2-800 was much more active than commonly utilized heterogeneous acid catalysts, such as zeolites (H-mordenite and H-Y), SO<sub>4</sub><sup>2-</sup>/ZrO<sub>2</sub>, Nafion, and Amberlyst-15 (Table 2-2-4, entries 7–11). The hydration did not proceed in the presence of catalytic amounts (H<sup>+</sup>: 1.3 mol%) of H<sub>2</sub>SO<sub>4</sub>, *p*-toluenesulfonic acid, and H<sub>3</sub>PW<sub>12</sub>O<sub>40</sub> (Table 2-2-4, entries 12–14). The hydration has typically been carried out using alcohol or cyclic ether as the solvent.<sup>[18]</sup> However, no hydration proceeded in ethanol at reflux or 1,4-dioxane at 100 °C using catalytic amounts (H<sup>+</sup>: 1.3 mol%) of H<sub>2</sub>SO<sub>4</sub>, *p*-toluenesulfonic acid, or H<sub>3</sub>PW<sub>12</sub>O<sub>40</sub>. The catalytic activity of SnW2-800 was much higher than that of pure Brønsted acid catalysts such as the heteropoly acid (H<sub>3</sub>PW<sub>12</sub>O<sub>40</sub>) and sulfuric acid (Table 2-2-4). The higher catalytic activity of SnW2-800

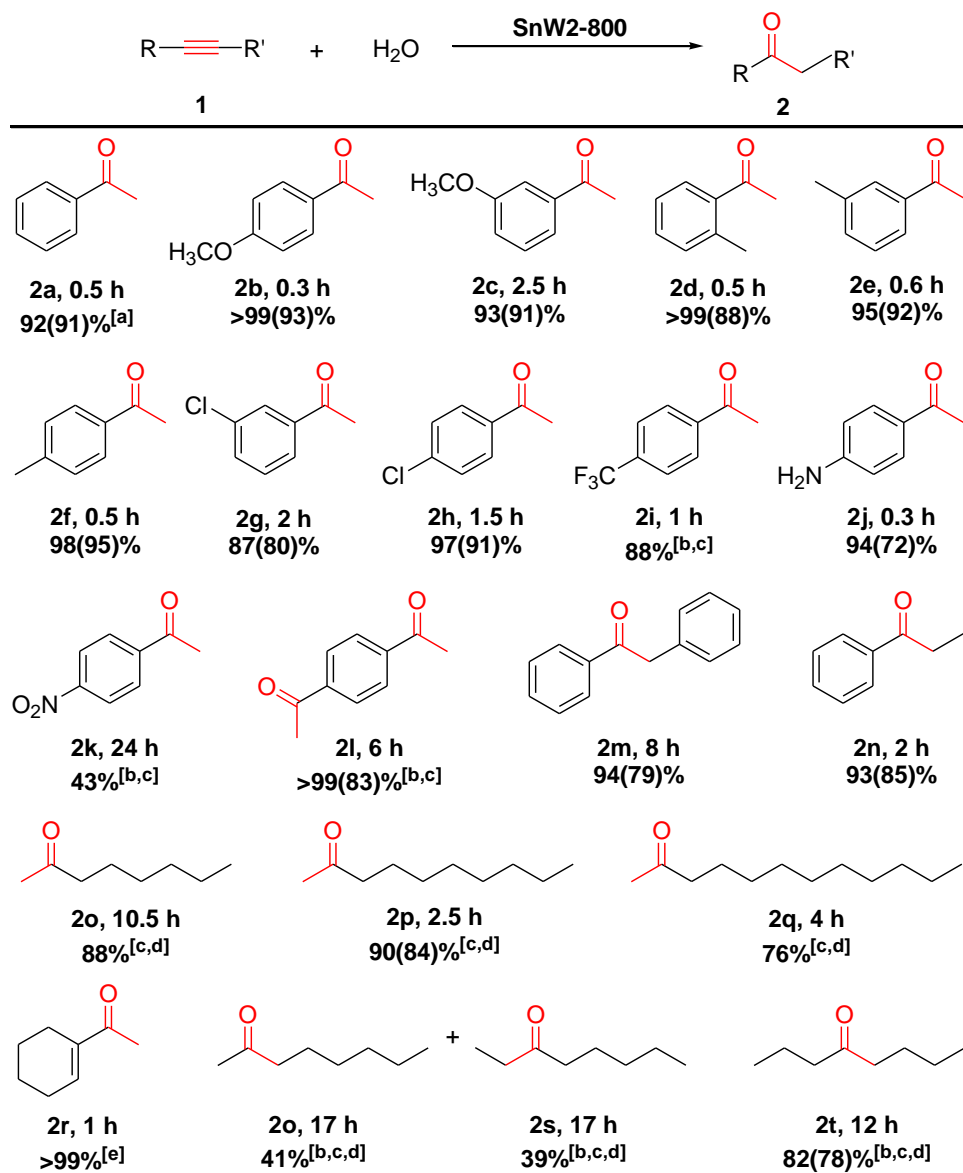
is possibly due to the Lewis acid sites on the catalyst to activate water molecule to form more nucleophilic hydroxo species.

### 2-2.3.2. Substrate Scope

The substrate scope of the SnW2-800-catalyzed hydration of alkynes to ketones was investigated. The hydration of various structurally diverse terminal and internal alkynes, such as aromatic, aliphatic, and double bond-containing ones efficiently proceeded to give the corresponding ketones in moderate to high yields (Scheme 2-2-4). The hydration of terminal alkynes gave ketones (Markovnikov hydration) as the final product without formation of the corresponding aldehydes (*anti*-Markovnikov hydration<sup>[27]</sup>). Ethynylbenzene derivatives with electron-donating or electron-withdrawing substituents were efficiently hydrated to give the corresponding acetophenone derivatives in moderate to high yields (Scheme 2-2-4, **2a–2k**). Aromatic alkynes with electron-donating substituents ( $-\text{CH}_3$  and  $-\text{OCH}_3$ ) were hydrated faster than those with electron-withdrawing substituents ( $-\text{Cl}$  and  $-\text{CF}_3$ ), indicating the electrophilic nature of the present hydration. Aromatic alkynes with reactive functional groups, such as amino and nitro groups, also reacted well (Scheme 2-2-4, **2j** and **2k**). 1,4-diethynylbenzene was also a good substrate, giving exclusively 1,4-diacetylbenzene (**2l**). Internal aromatic alkynes were also efficiently hydrated (Scheme 2-2-4, **2m** and **2n**), although longer reaction times were required in this case compared to terminal alkynes. It is noticeable that the hydration of methylphenylacetylene exclusively gave propiophenone (**2n**). The stabilization of a transitory formed vinyl cation through conjugation with the  $\pi$ -electrons of the aromatic ring is likely responsible for the high regioselectivity. The hydration of aliphatic terminal and internal alkynes can also



efficiently proceed to give the corresponding ketones (Scheme 2-2-4, **2o–2t**). The hydration of an enyne chemoselectively occurred at the alkyne functionality with the double bond remained intact (Scheme 2-2-4, **2r**).

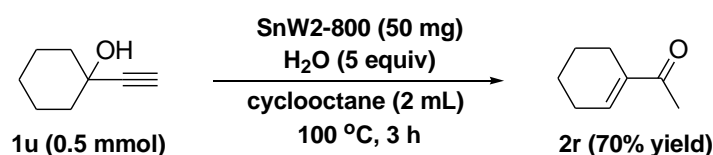


**Scheme 2-2-4.** Hydration of various alkynes with SnW2-800. Reaction conditions: SnW2-800 (50 mg), alkyne (0.5 mmol), water (2.5 mmol), cyclooctane (2 mL), 100 °C. Yields were determined by GC using biphenyl as an internal standard. Values in the parentheses are the isolated yields. [a] Water (1 mmol). [b] SnW2-800 (100 mg). [c] 120 °C. [d] Water (1.5 mmol). [e] Toluene (2 mL).

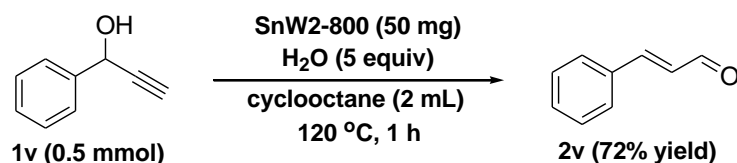
### 2-2.3.3. Sn–W Mixed Oxide-Catalyzed Rupe and Meyer–Schuster Rearrangements

For the hydration of propargylic alcohols with SnW2-800, the main products were  $\alpha,\beta$ -unsaturated carbonyl compounds. Specifically, 1-ethynylcyclohexanol (**1u**) was hydrated to give the corresponding enone (**2r**), likely via the hydration of an enyne formed by the dehydration of **1u** (Rupe rearrangement) (Scheme 2-2-5, a).<sup>[28]</sup> Similarly, the hydration of 1-phenyl-2-propyn-1-ol mainly gave the corresponding  $\alpha,\beta$ -unsaturated aldehyde (**2v**), likely via the formation of an allenyl cation, followed by hydration (Meyer–Schuster rearrangement) (Scheme 2-2-5, b).<sup>[28]</sup>

#### (a) Rupe rearrangement



#### (b) Meyer–Schuster rearrangement

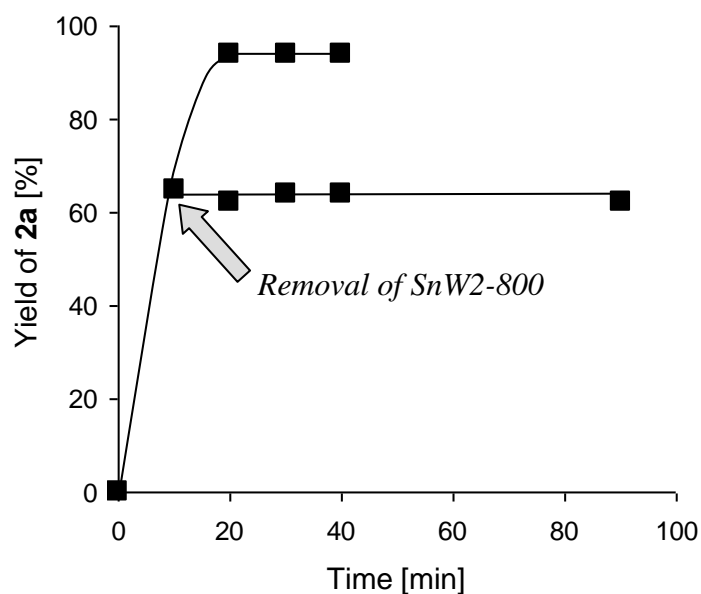


**Scheme 2-2-5.** SnW2-800-catalyzed Rupe and Meyer–Schuster Rearrangements.

### 2-2.3.4. Recyclability and Heterogeneous Catalysis of the Sn–W Mixed Oxide Catalyst

In order to verify whether the observed catalysis is intrinsically heterogeneous, SnW2-800 was separated by hot filtration, and the reaction was carried out with the filtrate under the same conditions. The hydration was completely stopped by removal of the catalyst (Figure 2-2-6). Furthermore, it was confirmed by the inductively coupled plasma atomic emission spectroscopy (ICP-AES) analysis that both Sn and W species

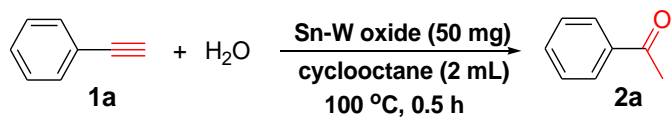
were hardly detected in the filtrate (under detection limit: Sn: <0.0013%; W: <0.0015%). These results indicate that the nature of the observed catalysis is intrinsically heterogeneous.<sup>[29]</sup>



**Figure 2-2-2.** The effect of removal of the SnW2-800 catalyst. The reaction conditions are the same as those described in Scheme 2-2-4.

In addition, the catalyst can easily be retrieved by simple filtration, and can be reused at least three times without an appreciable loss of its high catalytic activity (Table 2-2-7).

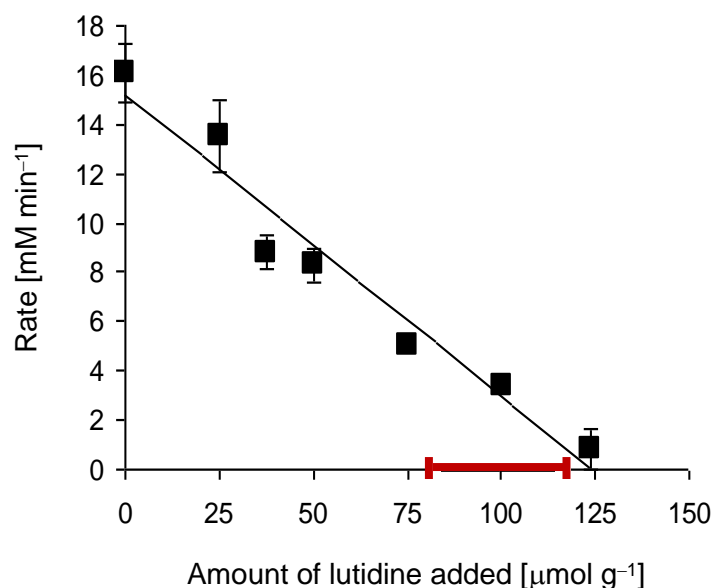
**Table 2-2-7.** Recycling of SnW2-800 for the hydration of **1a** to **2a**. The reaction conditions are the same as those described in Scheme 2-2-4.



Run	Yield of <b>2a</b> [%]
1 (fresh)	92
2	92
3	90
4	88

### 2-2.3.5. Reaction Mechanism

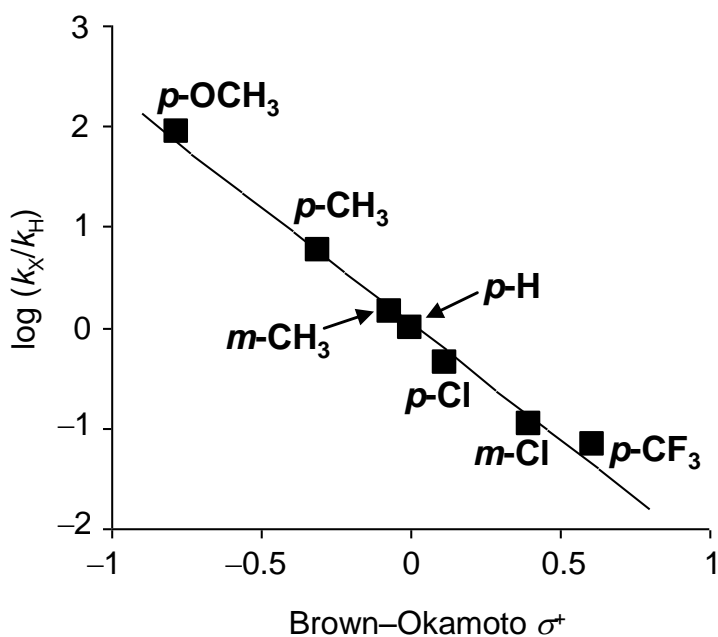
The hydration of **1a** in the presence of 2,6-lutidine, which is well known to selectively interact with Brønsted acid sites in the presence of Lewis acid sites due to the steric hindrance of methyl groups, was carried out to clarify the active sites of SnW2-800.<sup>[30]</sup> The hydration of **1a** was almost completely suppressed by an equimolar amount of 2,6-lutidine with respect to that of the Brønsted acid sites, indicating that the hydration is mainly promoted by the Brønsted acid sites in the SnW2-800 catalyst (Figure 2-2-3).



**Figure 2-2-3.** The dependence of the reaction rate on the amount of 2,6-lutidine added to the SnW2-800-catalyzed hydration of **1a**. The red bar in the  $x$  axis indicates the amount of Brønsted acid sites in the SnW2-800 catalyst (indicated with an experimental error). Reaction conditions: SnW2-800 (15 mg), **1a** (0.5 mmol), water (0.5 mmol), 2,6-lutidine, cyclooctane (2 mL), 100 °C.

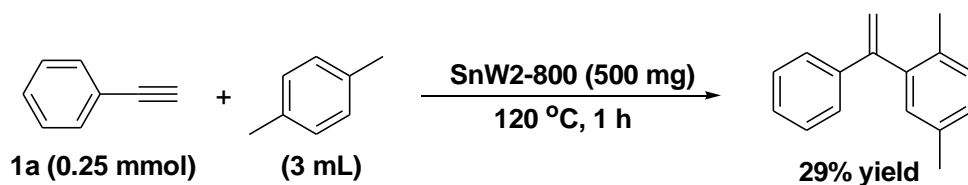
The SnW2-800-catalyzed competitive hydration reactions of  $p$ - and  $m$ -substituted ethynylbenzene derivatives show that the reactivity order is as follows:  $p\text{-OCH}_3$  ( $k_X/k_H = 85.7$ ) >  $p\text{-CH}_3$  (5.9) >  $m\text{-CH}_3$  (1.4) >  $p\text{-H}$  (1.0) >  $p\text{-Cl}$  (0.44) >  $m\text{-Cl}$  (0.11) >  $p\text{-CF}_3$

(0.067). In addition, a linear relationship between  $\log(k_X/k_H)$  and Brown–Okamoto  $\sigma^+$  is observed, and the slope (Hammett  $\rho^+$  value) is  $-2.31$  (Figure 2-2-4).<sup>[31]</sup> The large negative value of  $\rho^+$  indicates an electrophilic nature of the present hydration, in which the hydration likely proceeds through a positively charged transition state, for example, a vinyl cation.<sup>[32]</sup>



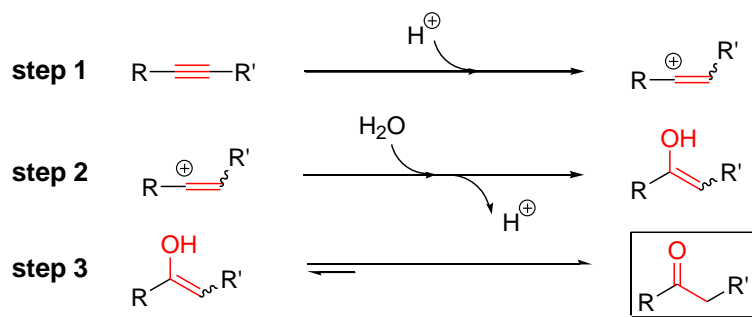
**Figure 2-2-4.** Hammett plot for the competitive hydration of *p*- and *m*-substituted ethynylbenzene derivatives ( $X = p\text{-OCH}_3, p\text{-CH}_3, m\text{-CH}_3, p\text{-H}, p\text{-Cl}, m\text{-Cl},$  and  $p\text{-CF}_3$ );  $\log(k_X/k_H)$  vs. Brown–Okamoto  $\sigma^+$  plot. Reaction conditions: SnW2-800 (100 mg), ethynylbenzene (0.5 mmol), substituted ethynylbenzene (0.5 mmol), water (1 mmol), cyclooctane (2 mL), 100 °C. Slope (Hammett  $\rho^+$  value) =  $-2.31$  ( $R^2 = 0.99$ ).

The reaction of **1a** with *p*-xylene in the presence of SnW2-800 gave a Friedel–Crafts-type vinylation product, 1,4-dimethyl-2-(1-phenylethenyl)benzene, under dehydrated conditions, which also indicates the formation of the vinyl cation intermediate (Scheme 2-2-6).<sup>[33]</sup>



**Scheme 2-2-6.** The Friedel–Crafts-type vinylation of **1a** with *p*-xylene in the presence of SnW2-800.

The above experimental results strongly support that the present SnW2-800-catalyzed hydration proceeds through (1) protonation of an alkyne to a vinyl cation (Scheme 2-2-7, step 1), (2) nucleophilic attack of water to the transitory formed vinyl cation to generate a vinylic alcohol (Scheme 2-2-7, step 2), and (3) tautomerization of the vinylic alcohol to give the corresponding ketone as the final product (Scheme 2-2-7, step 3).

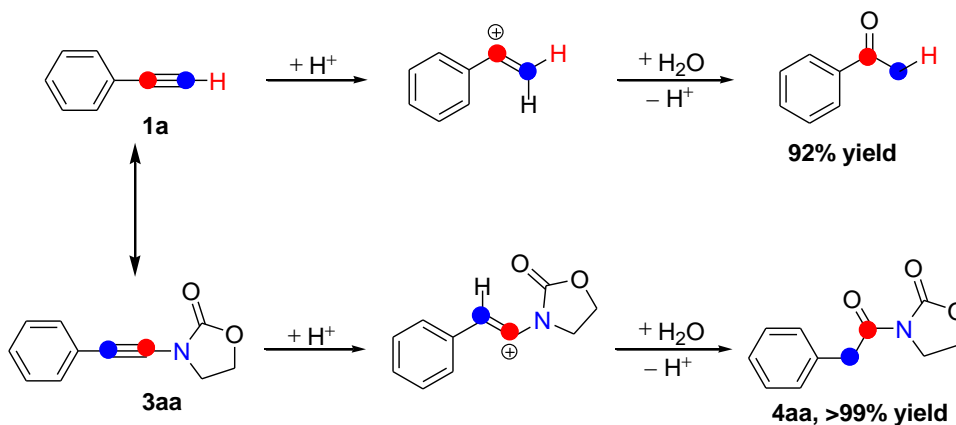


**Scheme 2-2-7.** A plausible reaction mechanism for the present hydration.

### 2-2.3.6. New Green Synthetic Procedure for Imides

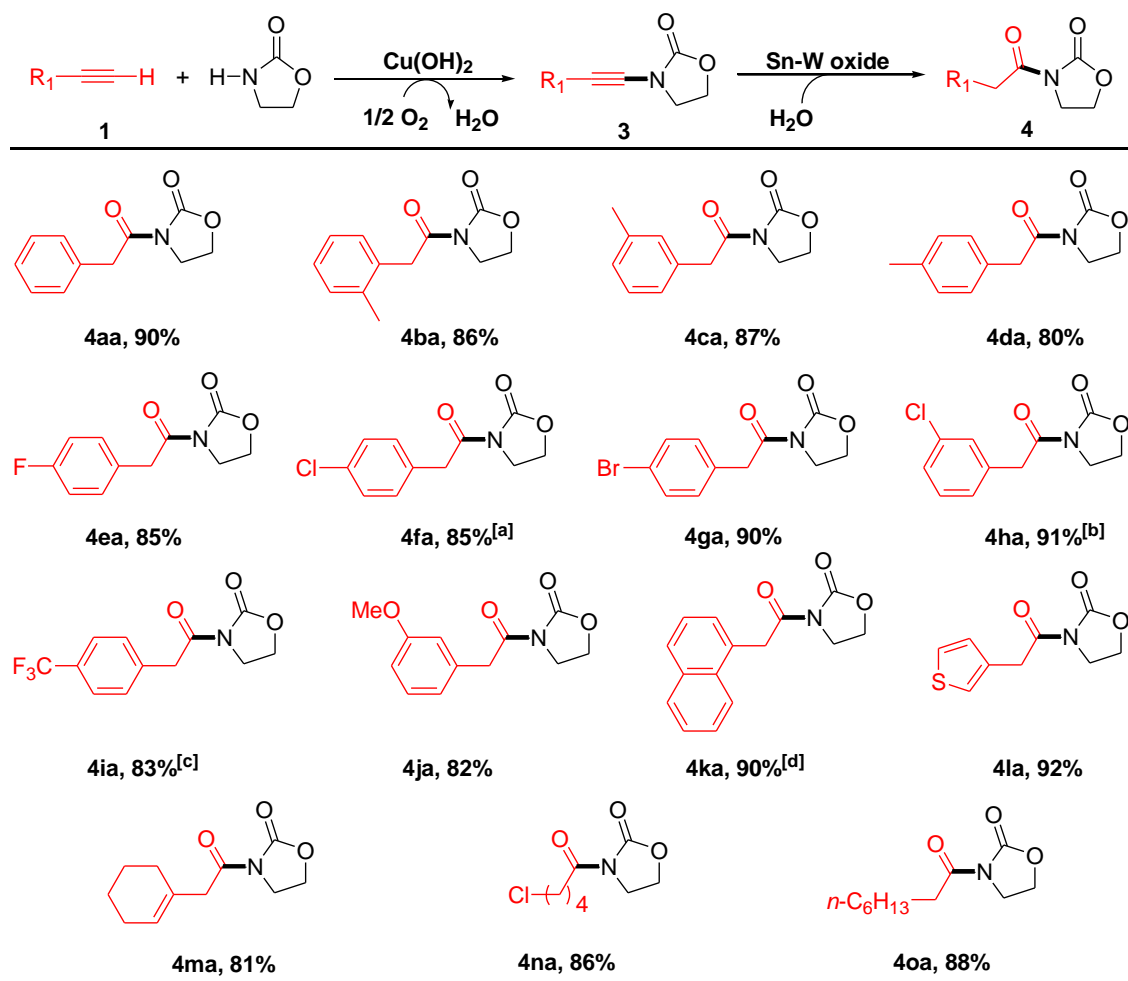
The one-pot synthesis of imides from terminal alkynes and amides was carried out. Initially, the SnW2-800-catalyzed hydration of 3-(phenylethynyl)oxazolidin-2-one (**3aa**) was carried out. In this case, the regioselectivity for the hydration of **3aa** was completely opposite to that for a terminal alkyne **1a**, and the hydration of **3aa**

regioselectively gave 3-(2-phenylacetyl)oxazolidin-2-one (**4aa**) in >99% yield (Scheme 2-2-8).



**Scheme 2-2-8.** The SnW2-800-catalyzed hydration of **1a** and **3aa**. Yields were determined by gas chromatography using biphenyl as an internal standard. Reaction conditions for **3aa**: **3aa** (0.1 mmol), SnW2-800 (50 mg), H<sub>2</sub>O (0.3 mmol), mesitylene (1 ml), 100 °C, under air (1 atm). Reaction conditions for **1a**: **1a** (0.5 mmol), Sn–W mixed oxide (50 mg), H<sub>2</sub>O (1.0 mmol), cyclooctane (2 mL), 100 °C, under air (1 atm).

Next, the one-pot synthesis of imides was carried out through the Cu(OH)<sub>2</sub>-catalyzed cross-coupling of terminal alkynes and amides to ynamides followed by the SnW2-800-catalyzed regioselective hydration (Scheme 2-2-9). Intrinsically no waste is generated from this new synthetic route, and the procedure is very simple. After the cross-coupling, Cu(OH)<sub>2</sub>, bases, and the remaining amides were filtered off, then the filtrate was added to the same reactor charged with SnW2-800 and water. Therefore, an additional isolation procedure of ynamides after the cross-coupling is not required for the present system. Various structurally diverse imides can successfully be synthesized by this new green synthetic procedure (Scheme 2-2-9).



**Scheme 2-2-9.** The sequential synthesis of imides. The isolated yields (based on **1**) are reported. Reaction conditions for the cross-coupling step, see Scheme 2-1-4, and for the hydration step, Sn–W oxide (50 mg), H<sub>2</sub>O (0.3 mmol), 100 °C, 1 h. [a] 3 h. [b] 5 h. [c] 24 h. [d] 2 h.



#### 2-2.4. Conclusion

The Sn–W mixed oxides, especially SnW2-800, can act as an efficient heterogeneous catalyst for the hydration of various structurally diverse alkynes, including aromatic, aliphatic, and double bond-containing ones. As for the hydration of propargylic alcohols, Rupe or Meyer–Schuster rearrangements proceeded to give the corresponding  $\alpha,\beta$ -unsaturated carbonyl compounds. The catalytic activity of SnW2-800 was much higher than those of previously reported heterogeneous catalysts including M-resins, Au(I)-MS, PS-SO<sub>3</sub>H, and commonly utilized acid catalysts. The catalysis was truly heterogeneous, and SnW2-800 could be reused several times without a significant loss of its high catalytic performance.

In addition, a new green synthetic procedure for imides has successfully been developed. Various structurally diverse imides were synthesized in high yields through the cross-coupling of terminal alkynes and amides followed by the hydration of ynamides. This new procedure is environmentally benign, and atom efficiency is theoretically 100%. The procedure is also very simple because the isolation of ynamide intermediates is not required.

## 2-2.5. References

- [1] J. Sperry, *Synthesis* **2011**, 22, 3569.
- [2] G. Evano, A. Coste, K. Jouvin, *Angew. Chem. Int. Ed.* **2010**, 49, 2840.
- [3] K. A. DeKorver, H. Li, A. G. Lohse, R. Hayashi, Z. Lu, Y. Zhang, R. P. Hsung, *Chem. Rev.* **2010**, 110, 5064.
- [4] J. Huang, H. Xiong, R. P. Hsung, C. Rameshkumar, J. A. Mulder, T. P. Grebe, *Org. Lett.* **2002**, 4, 2417.
- [5] N. Saito, Y. Sato, M. Mori, *Org. Lett.* **2002**, 4, 803.
- [6] Y. Zhang, K. A. DeKorver, A. G. Lohse, Y. S. Zhang, J. Huang, R. P. Hsung, *Org. Lett.* **2009**, 11, 899.
- [7] S. Couty, C. Meyer, J. Cossy, *Angew. Chem. Int. Ed.* **2006**, 45, 6726.
- [8] M. Movassaghi, M. D. Hill, O. K. Anmad, *J. Am. Chem. Soc.* **2007**, 129, 10096.
- [9] K. Tanaka, K. Takeishi, K. Noguchi, *J. Am. Chem. Soc.* **2006**, 128, 4586.
- [10] B. Witulski, T. Stengel, *Angew. Chem. Int. Ed.* **1998**, 37, 489.
- [11] J. A. Mulder, R. P. Hsung, M. O. Frederick, M. R. Tracey, C. A. Zifcick, *Org. Lett.* **2002**, 4, 1383.
- [12] K. C. M. Kurtz, R. P. Hsung, Y. Zhang, *Org. Lett.* **2006**, 8, 231.
- [13] B. Gourdet, H. W. Lam, *J. Am. Chem. Soc.* **2009**, 131, 3802.
- [14] J. P. Das, H. Chechik, I. Marek, *Nat. Chem.* **2009**, 1, 128.
- [15] C. Schotes, A. Mezzetti, *Angew. Chem. Int. Ed.* **2011**, 50, 3072.
- [16] S. Kramer, Y. Odabachian, J. Overgaard, M. Rottländer, F. Gagosz, T. Skrydstrup, *Angew. Chem. Int. Ed.* **2011**, 50, 5090.
- [17] P. W. Davies, A. Cremonesi, L. Dumitrescu, *Angew. Chem. Int. Ed.* **2011**, 50, 8931.

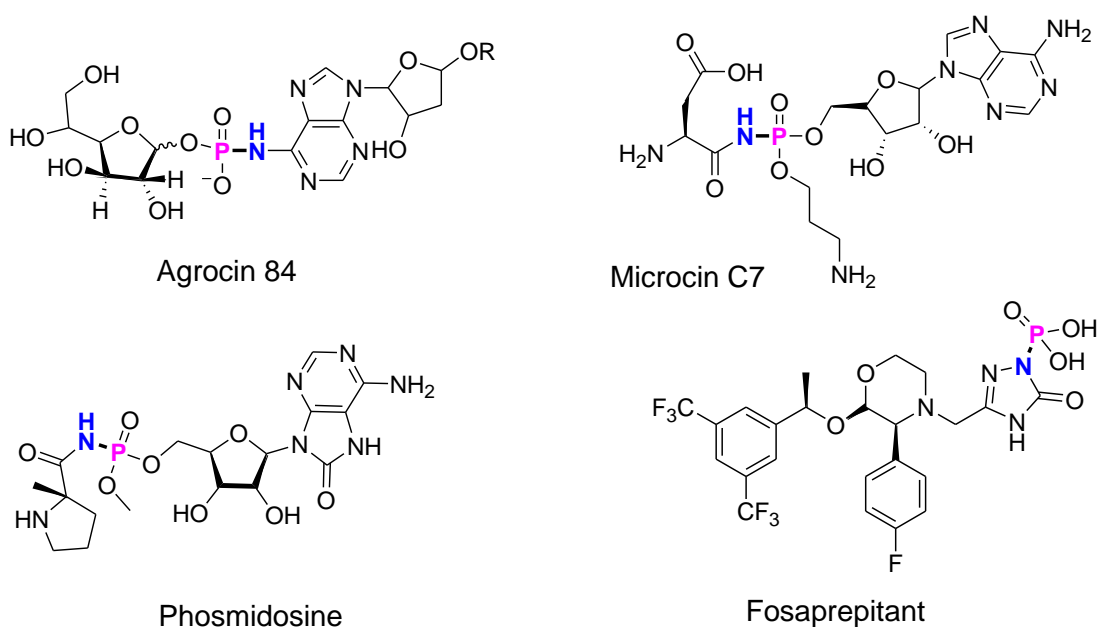
- [18] a) L. Hintermann, A. Labonne, *Synthesis* **2007**, 1121; b) F. Alonso, I. P. Beletskaya, M. Yus, *Chem. Rev.* **2004**, *104*, 3079, and references cited therein.
- [19] a) N. Marion, R. S. Ramón, S. P. Nolan, *J. Am. Chem. Soc.* **2009**, *131*, 448; b) A. Leyva, A. Corma, *J. Org. Chem.* **2009**, *74*, 2067; c) E. Mizushima, K. Sato, T. Hayashi, M. Tanaka, *Angew. Chem. Int. Ed.* **2002**, *41*, 4563.
- [20] a) P. T. Anastas, J. C. Warner, *Green Chemistry: Theory and Practice*, Oxford University Press, London, **1998**; b) R. A. Sheldon, *Green Chem.* **2000**, *2*, G1; c) P. T. Anastas, L. B. Bartlett, M. M. Kirchoff, T. C. Williamson, *Catal. Today* **2000**, *55*, 11; d) R. A. Sheldon, H. van Bekkum, *Fine Chemicals through Heterogeneous Catalysis*, Wiley, Weinheim, **2001**.
- [21] G. A. Olah, D. Meidar, *Synthesis* **1978**, 671.
- [22] I. K. Meier, J. A. Marsella, *J. Mol. Catal.* **1993**, *78*, 31.
- [23] J. Huang, F. Zhu, W. He, F. Zhang, W. Wang, H. Li, *J. Am. Chem. Soc.* **2010**, *132*, 1492.
- [24] S. Iimura, K. Manabe, S. Kobayashi, *Org. Biomol. Chem.* **2003**, *1*, 2416.
- [25] Y. Ogasawara, S. Uchida, K. Yamaguchi, N. Mizuno, *Chem. Eur. J.* **2009**, *15*, 4343.
- [26] *Purification of Laboratory Chemicals*, 3rd ed. (Eds.: D. D. Perrin, W. L. F. Armarego), Pergamon Press, Oxford, **1988**.
- [27] M. Tokunaga, Y. Wakatsuki, *Angew. Chem. Int. Ed.* **1998**, *37*, 2867.
- [28] S. Swaminathan, K. V. Narayanan, *Chem. Rev.* **1971**, *71*, 429.
- [29] R. A. Sheldon, M. Wallau, I. W. C. E. Arends, U. Schuchardt, *Acc. Chem. Res.* **1998**, *31*, 485.
- [30] A. Corma, *Chem. Rev.* **1995**, *95*, 559, and references cited therein.

- [31] H. C. Brown, Y. Okamoto, *J. Am. Chem. Soc.* **1958**, *80*, 4979.
- [32] K. A. Connors, *Chemical Kinetics, The Study of Reaction Rates in Solution*, VCH Publishers, Inc., New York, **1990**.
- [33] M. A. Rahman, O. Ogawa, J. Oyamada, T. Kitamura, *Synthesis* **2008**, 3755.

**Chapter 3**  
**Cu(OAc)<sub>2</sub>-Catalyzed Aerobic**  
**Cross-Dehydrogenative Coupling of**  
***H*-Phosphonates and Amides**

### 3.1. Introduction

In continuation of chapter 2 on the copper-catalyzed cross-coupling of terminal alkynes and amides, a novel synthetic procedure for *N*-acylphosphoramidates via the aerobic cross-dehydrogenative coupling of *H*-phosponates and amides was successfully developed by applying the copper-catalyzed aerobic cross-dehydrogenative coupling strategy.



**Figure 3-1.** Several biologically active compounds containing *N*-acylphosphoramidate units.<sup>[1-4]</sup>

*N*-Acylphosphoramidates are very important compounds that have been found in a large variety of natural products and pharmaceuticals such as Agrocin 84,<sup>[1]</sup> Microcin C7,<sup>[2]</sup> Phosmidosin,<sup>[3]</sup> and Fosaprepitant,<sup>[4]</sup> which are known to have antifungal, antitumor, and antiemetic activities (Figure 3-1). The synthesis of *N*-acylphosphoramidates often employs multi-step non-green procedures. For example, one of the most generally utilized procedures is nucleophilic substitution of

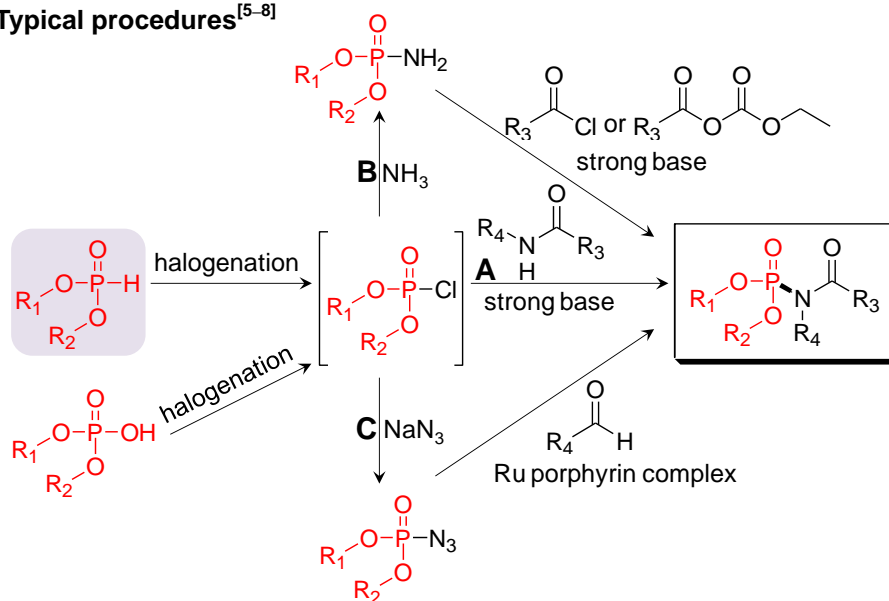
chlorophosphonates with amides in the presence of strong bases, such as *n*-BuLi (Scheme 3-1, A).<sup>[5]</sup> Nucleophilic substitution of acyl chlorides or mixed anhydrides with phosphoramides is also developed for the synthesis of *N*-acylphosphoramidates. (Scheme 3-1, B).<sup>[6]</sup> Che and co-workers have reported phosphoramidation of aldehydes with phosphoryl azides by a ruthenium(IV) porphyrine complex (Scheme 3-1, C).<sup>[7]</sup> However, all of these procedures utilize chlorophosphonates as starting materials, which are generally prepared by chlorination of *H*-phosphonates or phosphates using hazardous reagents, such as Cl<sub>2</sub>, COCl<sub>2</sub>, or SO<sub>2</sub>Cl<sub>2</sub>.<sup>[8]</sup> Subsequently, the procedures developed to date possess several drawbacks, which include tedious multi-step procedures, handling of toxic reagents, production of a large amount of waste during both phosphorylation and chlorination steps. Therefore, the development of novel green synthetic procedures for *N*-acylphosphoramidates directly from *H*-phosphonates is highly desirable, because they are more readily available and easy-to-handle compared to chlorophosphonates, and more importantly, pre-functionalization of *H*-phosphonates is not required, which results in the great improvement of the overall synthetic efficiency of *N*-acylphosphoramidates.

The starting point of the research described in this chapter is that the C(sp)-H, N-H, and P(O)-H bonds in alkynes, amides and *H*-phosphonates, respectively, are all activated and readily dissociated by the assistance of transition metals and bases.<sup>[9-11]</sup> To date, there is remarkable progress in the development of P-C<sup>[9]</sup> and P-X<sup>[10]</sup> bond forming reactions via direct activation of the P-H bond. Because of the effectiveness of copper catalysts for the cross-coupling of two activated nucleophiles to construct C-C and C-X bonds (including P-C and N-C bonds),<sup>[11]</sup> as described in chapter 1, copper catalysts were considered to be able to promote the aerobic cross-dehydrogenative

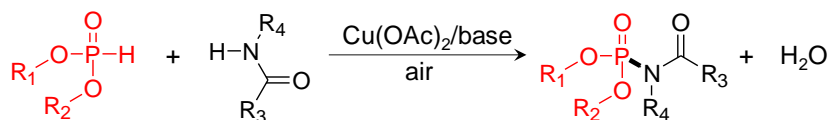
coupling of *H*-phosphonates and amides.

In this study,  $\text{Cu}(\text{OAc})_2$  ( $\text{OAc}$  = acetate) was turned out to be a suitable catalyst for the synthesis of *N*-acylphosphoramidates directly from *H*-phosphonates and amides. The present catalyst system employs air as the terminal oxidant and produces water as a sole byproduct, providing a quite simple, efficient, and green synthetic route to highly important *N*-acylphosphoramidates (Scheme 3-1, b). The present work is the first example of the metal-catalyzed aerobic cross-dehydrogenative coupling of phosphorus and nitrogen nucleophiles to form P–N bonds.

(a) Typical procedures<sup>[5–8]</sup>



(b) This work



**Scheme 3-1.** Synthesis of *N*-acylphosphoramidates.



## 3.2. Experimental Section

### 3.2.1. General

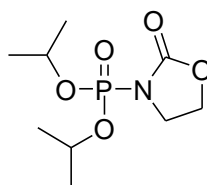
GC analyses were performed on Shimadzu GC-2014 with a FID detector equipped with an Rtx-200 capillary column. Mass spectra were recorded on Shimadzu GCMS-QP2010 equipped with a TC-5HT capillary column at an ionization voltage of 70 eV. Liquid-state NMR spectra were recorded on JEOL JNM-EX-270.  $^1\text{H}$  and  $^{13}\text{C}$  NMR spectra were measured at 270 and 67.8 MHz, respectively, using tetramethylsilane (TMS) as an internal reference.  $^{31}\text{P}$  NMR spectra were measured at 109.3 MHz, using 85%  $\text{H}_3\text{PO}_4$  in  $\text{D}_2\text{O}$  as an external reference. Copper salts, bases, substrates, and solvents were commercially obtained from TCI, Wako, or Across (reagent grade), and purified prior to use, if necessary.<sup>[12]</sup> Molecular sieves 4A (MS 4A) was pretreated at 350 °C in vacuo prior to use.

### 3.2.2. General Procedure for the Cross-Coupling of *H*-Phosphonates and Amides

The cross-coupling was carried out via the following procedure. Into a Pyrex glass test tube (volume: ca. 20 mL) were successively placed  $\text{Cu}(\text{OAc})_2$  (10 mol % with respect to a *H*-phosphonate **1**), a base (1–4 equiv. with respect to **1**), an amide (**2**, 3 equiv with respect to **1**), MS 4 A (100 mg), toluene (1 mL), and a Teflon-coated magnetic stir bar. After stirring the reaction mixture for 5 min, a toluene solution of **1** (0.2 M, 1 mL) was added to the reaction mixture over 30 min by a syringe pump at 80 °C, and the reaction mixture was stirred for further 10–60 min at 80 °C under an open air condition. After the reaction was completed, an internal standard (naphthalene) was added to the reaction mixture, and the conversion of **1** and the yield of the product

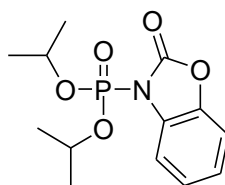
were determined by GC analysis. As for the isolation of *N*-acylphosphoramidates, the internal standard was not added. After the reaction, the base and MS 4 A were filtered off, and then the filtrate was concentrated by evaporation of toluene. The crude product was subjected to column chromatography on silica gel (Silica Gel 60N (63–210  $\mu\text{m}$ ), Kanto Chemical, 2.5 cm ID $\times$ 15 cm length, typically chloroform/acetone = 5:1 (v/v); diethylether/*n*-hexane = 2:1 (v/v) for **3ab**, **3am**, and **3ao**; chloroform/acetone = 10:1 (v/v) for **3an** and **3ap**), giving the pure *N*-acylphosphoramidates. The products were identified by GC-MS and NMR ( $^1\text{H}$ ,  $^{13}\text{C}$ , and  $^{31}\text{P}$ ) analyses.

### 3.2.3. Spectral Data of *N*-Acylphosphoramidates



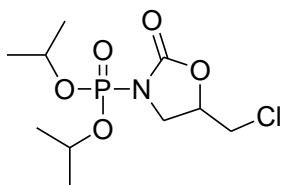
**3aa**

**diisopropyl(2-oxooxazolidin-3-yl)phosphonate (3aa):** Colorless oil.  $^1\text{H}$  NMR (270 MHz,  $\text{CDCl}_3$ , TMS):  $\delta$  1.36–1.41 (m, 12H), 3.95 (t,  $J = 8.0$  Hz, 2H), 4.41 (t,  $J = 8.0$  Hz, 2H), 4.69–4.87 (m, 2H).  $^{13}\text{C}\{^1\text{H}\}$  NMR (67.8 MHz,  $\text{CDCl}_3$ , TMS):  $\delta$  23.48 (d,  $J = 5.0$  Hz), 23.62 (d,  $J = 5.0$  Hz), 45.04 (d,  $J = 4.5$  Hz), 63.45 (d,  $J = 8.9$  Hz), 73.76 (d,  $J = 6.1$  Hz), 155.45 (d,  $J = 8.9$  Hz).  $^{31}\text{P}$  NMR (109.3 MHz,  $\text{CDCl}_3$ ):  $\delta$  -5.55 (t,  $J = 7.2$  Hz). MS (ED):  $m/z$  (%) : 251 (0.1) [ $M^+$ ], 209 (13), 194 (42), 168 (100), 151 (34), 150 (29), 123 (28), 106 (10), 88 (52).



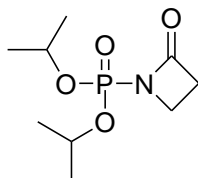
**3ab**

**diisopropyl(2-oxobenzo[*d*]oxazol-3(2*H*)-yl)phosphonate (3ab):** Colorless oil.  $^1\text{H}$  NMR (270 MHz,  $\text{CDCl}_3$ , TMS):  $\delta$  1.35 (d,  $J = 6.2$  Hz, 6H), 1.44 (d,  $J = 6.2$  Hz, 6H), 4.79–4.96 (m, 2H), 7.15–7.28 (m, 3H), 7.73–7.79 (m, 1H).  $^{13}\text{C}\{^1\text{H}\}$  NMR (67.8 MHz,  $\text{CDCl}_3$ , TMS):  $\delta$  23.42 (d,  $J = 5.0$  Hz), 23.64 (d,  $J = 5.6$  Hz), 75.10 (d,  $J = 6.1$  Hz), 109.81, 113.98 (d,  $J = 1.2$  Hz), 123.98, 124.34, 129.82 (d,  $J = 6.7$  Hz). 143.31 (d,  $J = 11.1$  Hz), 152.4 (d,  $J = 7.3$  Hz).  $^{31}\text{P}$  NMR (109.3 MHz,  $\text{CDCl}_3$ ):  $\delta$  -9.72 (t,  $J = 7.0$  Hz). MS (EI):  $m/z$  (%) : 299 (24) [ $M^+$ ], 257 (12), 242 (16), 216 (11), 215 (85), 171 (24), 136 (12), 135 (100), 106 (10).



**3ac**

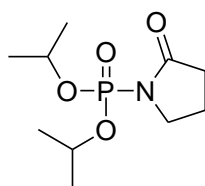
**diisopropyl(5-chloromethyl)-2-oxooxazolidin-3-yl)phosphonate (3ac):**  $^1\text{H}$  NMR (270 MHz,  $\text{CDCl}_3$ , TMS):  $\delta$  1.36–1.41 (m, 12H), 3.67–4.08 (m, 4H), 4.70–4.90 (m, 3H).  $^{13}\text{C}\{^1\text{H}\}$  NMR (67.8 MHz,  $\text{CDCl}_3$ , TMS):  $\delta$  23.41, 23.49, 23.56, 23.62, 23.64, 23.69, 44.67, 47.61 (d,  $J = 4.5$  Hz), 73.95 (q,  $J = 6.1$  Hz), 154.23 (d,  $J = 8.3$  Hz).  $^{31}\text{P}$  NMR (109.3 MHz,  $\text{CDCl}_3$ ):  $\delta$  -6.21 (t,  $J = 7.3$  Hz). MS (EI):  $m/z$  (%) : 299 (0.1) [ $M^+$ ], 257 (12), 244 (14), 242 (42), 218 (33), 216 (100), 201 (12), 199 (37), 198 (11), 178 (15), 166 (13), 162 (11), 136 (49), 123 (11), 99 (36), 86 (17), 75 (10), 56 (15).



**3ad**

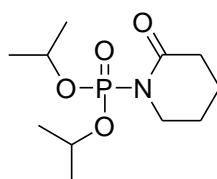
**diisopropyl(2-oxoazetidin-1-yl)phosphonate (3ad):** Colorless oil.  $^1\text{H}$  NMR (270 MHz,  $\text{CDCl}_3$ , TMS):  $\delta$  1.37 (d,  $J = 3.0$  Hz, 6H), 1.38 (d,  $J = 2.7$  Hz, 6H), 3.10–3.15 (m, 2H),

3.53–3.56 (m, 2H), 4.66–4.82 (m, 2H).  $^{13}\text{C}\{^1\text{H}\}$  NMR (67.8 MHz,  $\text{CDCl}_3$ , TMS):  $\delta$  23.56 (d,  $J = 5.0$  Hz), 23.72 (d,  $J = 5.0$  Hz), 38.10 (d,  $J = 9.5$  Hz), 38.50, 73.09 (d,  $J = 6.2$  Hz), 166.82 (d,  $J = 4.5$  Hz).  $^{31}\text{P}$  NMR (109.3 MHz,  $\text{CDCl}_3$ ):  $\delta$  -10.952–-10.739 (m). MS (EI):  $m/z$  (%) : 235 (0.1) [ $M^+$ ], 178 (12), 152 (16), 151 (36), 136 (10), 124 (100).



**3ae**

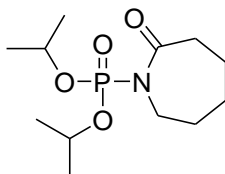
**diisopropyl(2-oxopyrrolidin-1-yl)phosphonate (3ae):** Colorless oil.  $^1\text{H}$  NMR (270 MHz,  $\text{CDCl}_3$ , TMS):  $\delta$  1.34 (d,  $J = 6.2$  Hz, 6H), 1.37 (d,  $J = 5.9$  Hz, 6H), 2.04–2.14 (m, 2H), 2.46 (t,  $J = 8.0$  Hz, 2H), 3.74 (t,  $J = 7.0$  Hz, 2H), 4.68–4.84 (m, 2H).  $^{13}\text{C}\{^1\text{H}\}$  NMR (67.8 MHz,  $\text{CDCl}_3$ , TMS):  $\delta$  20.14 (d,  $J = 8.4$  Hz), 23.47 (d,  $J = 5.0$  Hz), 23.67 (d,  $J = 5.0$  Hz), 32.55 (d,  $J = 9.5$  Hz), 47.84 (d,  $J = 4.5$  Hz), 72.90 (d,  $J = 6.2$  Hz), 177.66 (d,  $J = 1.6$  Hz).  $^{31}\text{P}$  NMR (109.3 MHz,  $\text{CDCl}_3$ ):  $\delta$  -4.20 (t,  $J = 7.3$  Hz). MS (EI):  $m/z$  (%) : 249 (0.7) [ $M^+$ ], 208 (13), 207 (15), 192 (27), 166 (100), 165 (55), 149 (82), 148 (45), 124 (24), 110 (13), 86 (43), 85 (26), 84 (53), 56 (27).



**3af**

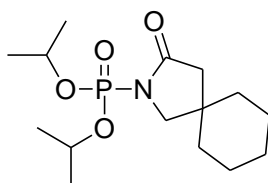
**diisopropyl(2-oxopiperidin-1-yl)phosphonate (3af):**  $^1\text{H}$  NMR (270 MHz,  $\text{CDCl}_3$ , TMS):  $\delta$  1.32 (d,  $J = 6.5$  Hz, 6H), 1.36 (d,  $J = 6.2$  Hz, 6H), 1.80–1.83 (m, 4H), 2.43–2.48 (m, 2H), 3.64–3.70 (m, 2H), 4.69–4.86 (m, 2H).  $^{13}\text{C}\{^1\text{H}\}$  NMR (67.8 MHz,  $\text{CDCl}_3$ , TMS):  $\delta$  20.17, 22.86 (d,  $J = 5.6$  Hz), 23.40 (d,  $J = 5.0$  Hz), 23.67 (d,  $J = 5.6$

Hz), 33.33 (d,  $J = 6.2$  Hz), 46.52 (d,  $J = 2.2$  Hz), 72.80 (d,  $J = 6.2$  Hz), 173.57 (d,  $J = 1.7$  Hz).  $^{31}\text{P}$  NMR (109.3 MHz,  $\text{CDCl}_3$ ):  $\delta -0.615$  (brs). MS (EI):  $m/z$  (%) : 263 (7) [ $M^+$ ], 221 (15), 180 (49), 179 (100), 178 (11), 163 (40), 162 (59), 124 (26), 123 (20), 110 (27), 99 (59), 98 (39), 82 (59), 81 (36), 55 (35).



**3ag**

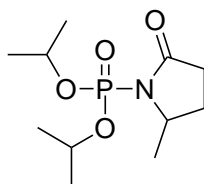
**diisopropyl(2-oxoazepan-1-yl)phosphonate (3ag):**  $^1\text{H}$  NMR (270 MHz,  $\text{CDCl}_3$ , TMS):  $\delta$  1.31 (d,  $J = 6.2$  Hz, 6H), 1.36 (d,  $J = 6.5$  Hz, 6H), 1.743 (brs, 6H), 2.60–2.62 (br, 2H), 3.76–3.79 (br, 2H), 4.64–4.81 (m, 2H).  $^{13}\text{C}\{^1\text{H}\}$  NMR (67.8 MHz,  $\text{CDCl}_3$ , TMS):  $\delta$  23.31, 23.51 (d,  $J = 5.0$  Hz), 23.68 (d,  $J = 5.0$  Hz), 29.39, 29.85 (d,  $J = 1.7$  Hz), 38.73 (d,  $J = 7.8$  Hz), 46.67 (d,  $J = 2.8$  Hz), 72.61 (d,  $J = 6.2$  Hz), 178.38.  $^{31}\text{P}$  NMR (109.3 MHz,  $\text{CDCl}_3$ ):  $\delta$  0.281 (quint,  $J = 9.3$  Hz). MS (EI):  $m/z$  (%) : 277 (11) [ $M^+$ ], 236 (11), 235 (11), 194 (22), 193 (45), 177 (13), 176 (38), 152 (24), 137 (11), 136 (15), 124 (53), 123 (12), 110 (91), 99 (15), 96 (100), 95 (53), 84 (17), 69 (10), 67 (11), 56 (13), 55 (37).



**3ah**

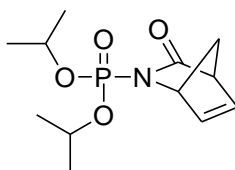
**diisopropyl(3-oxo-2-azaspiro[4,5]decan-2-yl)phosphonate (3ah):** Colorless oil.  $^1\text{H}$  NMR (270 MHz,  $\text{CDCl}_3$ , TMS):  $\delta$  1.34 (d,  $J = 6.2$  Hz, 6H), 1.37 (d,  $J = 6.2$  Hz, 6H), 1.45–1.51 (br, 10H), 2.32 (s, 2H), 3.49 (s, 2H), 4.66–4.82 (m, 2H).  $^{13}\text{C}\{^1\text{H}\}$  NMR (67.8 MHz,  $\text{CDCl}_3$ , TMS):  $\delta$  22.61, 23.54 (d,  $J = 5.0$  Hz), 23.68 (d,  $J = 5.0$  Hz), 25.49, 35.93,

37.77 (d,  $J = 6.7$  Hz), 45.08 (d,  $J = 8.9$  Hz), 58.48 (d,  $J = 2.2$  Hz), 72.84 (d,  $J = 6.1$  Hz), 176.82 (d,  $J = 1.1$  Hz).  $^{31}\text{P}$  NMR (109.3 MHz,  $\text{CDCl}_3$ ):  $\delta$  -4.42 (t,  $J = 7.3$  Hz). MS (EI):  $m/z$  (%) : 317 (4) [ $M^+$ ], 276 (16), 275 (12), 260 (19), 235 (11), 234 (100), 233 (65), 232 (15), 217 (75), 216 (21), 177 (18), 154 (14), 153 (28), 152 (50), 135 (13), 124 (16), 110 (70), 95 (21), 94 (13), 81 (17), 67 (20), 55 (11).



**3ai**

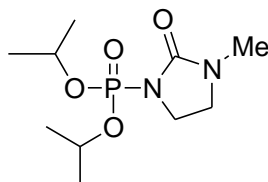
**diisopropyl(2-methyl-5-oxopyrrolidin-1-yl)phosphonate (3ai):** Colorless oil.  $^1\text{H}$  NMR (270 MHz,  $\text{CDCl}_3$ , TMS):  $\delta$  1.31–1.41 (m, 15H), 1.70–1.78 (m, 1H), 2.23–2.66 (m, 3H), 4.21–4.26 (m, 1H), 4.69–4.83 (m, 2H).  $^{13}\text{C}\{^1\text{H}\}$  NMR (67.8 MHz,  $\text{CDCl}_3$ , TMS):  $\delta$  21.75, 23.39, 23.46, 23.53, 23.60, 23.69, 23.77, 27.62 (d,  $J = 8.9$  Hz), 30.96 (d,  $J = 9.5$  Hz), 55.87 (d,  $J = 4.5$  Hz), 72.70 (t,  $J = 6.1$  Hz), 177.50 (d,  $J = 2.2$  Hz).  $^{31}\text{P}$  NMR (109.3 MHz,  $\text{CDCl}_3$ ):  $\delta$  -4.30 (t,  $J = 7.5$  Hz). MS (EI):  $m/z$  (%): 263 (2) [ $M^+$ ], 248 (12), 222 (12), 206 (40), 180 (49), 179 (35), 164 (100), 163 (31), 162 (29), 124 (53), 100 (11), 99 (15), 98 (41), 84 (50), 82 (13), 81 (10), 56 (10), 55 (25).



**3aj**

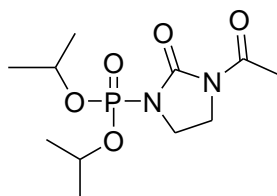
**diisopropyl(3-oxo-2-azabicyclo[2.2.1]hept-5-en-2-yl)phosphonate (3aj):** Colorless oil.  $^1\text{H}$  NMR (270 MHz,  $\text{CDCl}_3$ , TMS):  $\delta$  1.24 (d,  $J = 6.2$  Hz, 3H), 1.30–1.38 (m, 9H), 2.18–2.23 (m, 1H), 2.40–2.43 (m, 1H), 3.39 (s, 1H), 4.46–4.59 (m, 1H), 4.63–4.78 (m, 1H), 4.93 (s, 1H), 6.67–6.70 (m, 1H), 6.93–6.96 (m, 1H).  $^{13}\text{C}\{^1\text{H}\}$  NMR (67.8 MHz,

CDCl<sub>3</sub>, TMS):  $\delta$  23.33, 23.41, 23.49, 23.63, 23.67, 23.69, 23.73, 54.56 (d,  $J = 7.8$  Hz), 58.02 (d,  $J = 5.6$  Hz), 64.96 (d,  $J = 3.3$  Hz), 72.35, 72.44, 72.67, 72.76, 137.69, 140.82, 179.91 (d,  $J = 1.1$  Hz). <sup>31</sup>P NMR (109.3 MHz, CDCl<sub>3</sub>):  $\delta$  -4.23 (t,  $J = 7.2$  Hz). MS (EI): 150 (35), 124 (100), 66 (35), 65 (13).



**3ak**

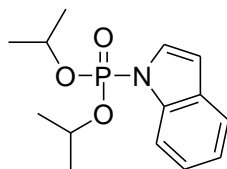
**diisopropyl(3-methyl-2-oxoimidazolidin-1-yl)phosphonate (3ak):** <sup>1</sup>H NMR (270 MHz, CDCl<sub>3</sub>, TMS):  $\delta$  1.33–1.38 (m, 12H), 2.82 (s, 3H), 3.42 (t,  $J = 8.0$  Hz, 2H), 3.74 (t,  $J = 8.0$  Hz, 2H), 4.66–4.85 (m, 2H). <sup>13</sup>C{<sup>1</sup>H} NMR (67.8 MHz, CDCl<sub>3</sub>, TMS):  $\delta$  23.53 (d,  $J = 5.0$  Hz), 23.67 (d,  $J = 5.0$  Hz), 30.59, 41.58 (d,  $J = 3.4$  Hz), 45.44 (d,  $J = 7.8$  Hz), 72.60 (d,  $J = 6.1$  Hz), 157.35 (d,  $J = 7.9$  Hz). <sup>31</sup>P NMR (109.3 MHz, CDCl<sub>3</sub>):  $\delta$  -3.17 (t,  $J = 7.3$  Hz). MS (EI):  $m/z$  (%): 264 (7) [ $M^+$ ], 222 (10), 207 (13), 181 (37), 180 (53), 179 (21), 164 (20), 163 (53), 124 (22), 101 (38), 100 (94), 99 (100), 58 (10), 57 (98), 56 (14).



**3al**

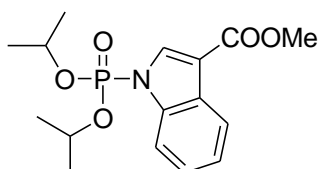
**diisopropyl(3-acetyl-2-oxoimidazolidin-1-yl)phosphonate (3al):** <sup>1</sup>H NMR (270 MHz, CDCl<sub>3</sub>, TMS):  $\delta$  1.36–1.41 (m, 12H), 2.51 (s, 3H), 3.72–3.81 (m, 2H), 3.83–3.91 (m, 2H), 4.72–4.88 (m, 2H). <sup>13</sup>C{<sup>1</sup>H} NMR (67.8 MHz, CDCl<sub>3</sub>, TMS):  $\delta$  23.56 (d,  $J = 5.0$  Hz), 23.67 (d,  $J = 4.5$  Hz), 40.65, 40.77 (d,  $J = 2.8$  Hz), 40.84, 73.55 (d,  $J = 6.1$  Hz), 153.46 (d,  $J = 8.9$  Hz), 170.79. <sup>31</sup>P NMR (109.3 MHz, CDCl<sub>3</sub>):  $\delta$  -4.77 (t,  $J = 7.3$  Hz).

MS (EI):  $m/z$  (%) : 292 (2) [ $M^+$ ], 251 (14), 250 (32), 235 (18), 209 (41), 208 (78), 193 (17), 192 (23), 191 (13), 180 (19), 167 (57), 166 (100), 165 (16), 149 (38), 129 (11), 128 (11), 124 (10), 123 (32), 110 (91), 87 (15), 85 (30), 68 (10).



**3am**

**diisopropyl-1H-indol-1-ylphosphonate (3am):** Yellow oil.  $^1\text{H}$  NMR (270 MHz,  $\text{CDCl}_3$ , TMS):  $\delta$  1.10 (d,  $J = 6.2$  Hz, 6H), 1.41 (d,  $J = 6.2$  Hz, 6H), 4.58–4.70 (m, 2H), 6.62–6.64 (m, 1H), 7.18–7.30 (m, 2H), 7.46–7.48 (m, 1H), 7.59–7.62 (m, 1H), 7.74–7.77 (m, 1H).  $^{13}\text{C}\{^1\text{H}\}$  NMR (67.8 MHz,  $\text{CDCl}_3$ , TMS):  $\delta$  23.25 (d,  $J = 5.0$  Hz), 23.82 (d,  $J = 5.0$  Hz), 73.12 (d,  $J = 5.0$  Hz), 106.91 (d,  $J = 8.3$  Hz), 113.88, 120.86 (d,  $J = 1.1$  Hz), 121.89, 123.19, 128.82 (d,  $J = 7.3$  Hz), 130.98 (d,  $J = 10.0$  Hz), 136.95 (d,  $J = 5.0$  Hz).  $^{31}\text{P}$  NMR (109.3 MHz,  $\text{CDCl}_3$ ):  $\delta$  -4.69. MS (EI):  $m/z$  (%) : 281 (16) [ $M^+$ ], 198 (10), 197 (100), 179 (21), 117 (17), 116 (19), 89 (11).

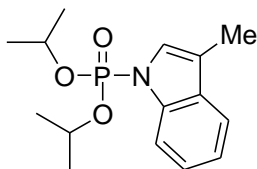


**3an**

**methyl-1-(diisopropoxyphosphoryl)-1H-indole-3-carboxylate (3an):**  $^1\text{H}$  NMR (270 MHz,  $\text{CDCl}_3$ , TMS):  $\delta$  1.11 (d,  $J = 6.2$  Hz, 6H), 1.43 (d,  $J = 5.9$  Hz, 6H), 3.93 (s, 3H), 4.61–4.77 (m, 2H), 7.27–7.37 (m, 2H), 7.71–7.78 (m, 1H), 8.15–8.22 (m, 2H).  $^{13}\text{C}\{^1\text{H}\}$  NMR (67.8 MHz,  $\text{CDCl}_3$ , TMS):  $\delta$  23.22 (d,  $J = 5.0$  Hz), 23.76 (d,  $J = 5.0$  Hz), 51.28, 74.01 (d,  $J = 5.6$  Hz), 112.33 (d,  $J = 8.3$  Hz), 113.97, 121.70 (d,  $J = 1.2$  Hz), 123.40, 124.21, 128.14 (d,  $J = 8.9$  Hz), 135.60 (d,  $J = 7.3$  Hz), 137.12 (d,  $J = 4.5$  Hz), 164.67 (d,

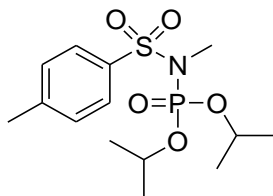


$J = 1.2$  Hz).  $^{31}\text{P}$  NMR (109.3 MHz,  $\text{CDCl}_3$ ):  $\delta -5.93$  (d,  $J = 6.9$  Hz). MS (EI):  $m/z$  (%) : 339 (17) [ $M^+$ ], 256 (12), 255 (100), 224 (46), 206 (12), 144 (10).



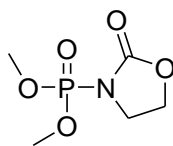
**3ao**

**diisopropyl(3-methyl-1H-indol-1-yl)phosphonate (3ao):**  $^1\text{H}$  NMR (270 MHz,  $\text{CDCl}_3$ , TMS):  $\delta$  1.10 (d,  $J = 6.2$  Hz, 6H), 1.40 (d,  $J = 6.2$  Hz, 6H), 2.29 (d,  $J = 1.1$  Hz, 3H), 4.56–4.68 (m, 2H), 7.20–7.30 (m, 3H), 7.51–7.54 (m, 1H), 7.71–7.74 (m, 1H).  $^{13}\text{C}\{^1\text{H}\}$  NMR (67.8 MHz,  $\text{CDCl}_3$ , TMS):  $\delta$  9.57, 23.32 (d,  $J = 5.0$  Hz), 23.83 (d,  $J = 5.0$  Hz), 72.87 (d,  $J = 5.0$  Hz), 113.87, 115.93 (d,  $J = 8.9$  Hz), 118.93 (d,  $J = 1.2$  Hz), 121.44, 123.16, 125.58 (d,  $J = 7.3$  Hz), 131.77 (d,  $J = 10.0$  Hz), 137.33.  $^{31}\text{P}$  NMR (109.3 MHz,  $\text{CDCl}_3$ ):  $\delta -4.44$  (d,  $J = 7.0$  Hz). MS (EI):  $m/z$  (%) : 295 (16) [ $M^+$ ], 212 (11), 211 (100), 193 (12), 130 (38).



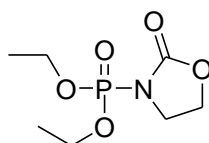
**3ap**

**diisopropylmethyl(tosyl)phosphoramidate (3ap):**  $^1\text{H}$  NMR (270 MHz,  $\text{CDCl}_3$ , TMS):  $\delta$  1.32 (d,  $J = 6.2$  Hz, 6H), 1.40 (d,  $J = 6.2$  Hz, 6H), 2.43 (s, 3H), 3.03 (d,  $J = 8.1$  Hz, 3H), 4.63–4.79 (m, 2H), 7.27–7.33 (m, 2H), 7.85–7.90 (m, 2H).  $^{13}\text{C}\{^1\text{H}\}$  NMR (67.8 MHz,  $\text{CDCl}_3$ , TMS):  $\delta$  21.53, 23.46 (d,  $J = 5.0$  Hz), 23.61 (d,  $J = 5.0$  Hz), 34.51 (d,  $J = 2.2$  Hz), 73.39 (d,  $J = 6.1$  Hz), 127.97, 129.34, 136.06, 144.07.  $^{31}\text{P}$  NMR (109.3 MHz,  $\text{CDCl}_3$ ):  $\delta -2.81$  (sext,  $J = 7.6$  Hz). MS (EI):  $m/z$  (%) : 285 (10), 248 (14), 243 (19), 201 (100), 202 (14), 155 (12), 120 (14), 119 (21), 110 (11), 108 (28), 91 (36), 65 (11).



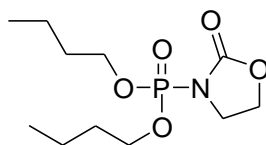
**3ba**

**dimethyl(2-oxooxazolidin-3-yl)phosphonate (3ba):**  $^1\text{H}$  NMR (270 MHz,  $\text{CDCl}_3$ , TMS):  $\delta$  3.90 (d,  $J = 11.3$  Hz, 6H), 3.97 (t,  $J = 8.0$  Hz, 2H), 4.45 (t,  $J = 8.0$  Hz, 2H).  $^{13}\text{C}\{^1\text{H}\}$  NMR (67.8 MHz,  $\text{CDCl}_3$ , TMS):  $\delta$  44.78 (d,  $J = 4.5$  Hz), 54.68 (d,  $J = 6.2$  Hz), 63.74 (d,  $J = 8.9$  Hz), 155.50 (d,  $J = 9.4$  Hz).  $^{31}\text{P}$  NMR (109.3 MHz,  $\text{CDCl}_3$ ):  $\delta$  -0.30 (sep,  $J = 11.7$  Hz). MS (EI):  $m/z$  (%) : 195 (0.7) [ $M^+$ ], 151 (39), 136 (32), 110 (95), 109 (100), 80 (17), 79 (47), 56 (17).



**3ca**

**diethyl(2-oxooxazolidin-3-yl)phosphonate (3ca):**  $^1\text{H}$  NMR (270 MHz,  $\text{CDCl}_3$ , TMS):  $\delta$  1.36–1.42 (m, 6H), 3.96 (t,  $J = 8.0$  Hz, 2H), 4.15–4.35 (m, 4H), 4.43 (t,  $J = 8.0$  Hz, 2H).  $^{13}\text{C}\{^1\text{H}\}$  NMR (67.8 MHz,  $\text{CDCl}_3$ , TMS):  $\delta$  15.95 (d,  $J = 6.7$  Hz), 44.90 (d,  $J = 4.5$  Hz), 63.58 (d,  $J = 8.5$  Hz), 64.61 (d,  $J = 6.1$  Hz), 155.47 (d,  $J = 8.9$  Hz).  $^{31}\text{P}$  NMR (109.3 MHz,  $\text{CDCl}_3$ ):  $\delta$  -3.24 (quint,  $J = 8.0$  Hz). MS (EI):  $m/z$  (%) : 196 (58), 180 (12), 179 (47), 168 (70), 164 (19), 152 (12), 151 (67), 150 (55), 138 (50), 136 (25), 124 (26), 123 (52), 111 (17), 110 (25), 109 (43), 107 (14), 106 (30), 93 (13), 91 (22), 88 (100), 87 (36), 86 (19), 82 (44), 81 (67), 80 (13), 79 (18), 70 (17), 65 (23), 56 (14).



**3da**

**dibutyl(2-oxooxazolidin-3-yl)phosphonate (3da):**  $^1\text{H}$  NMR (270 MHz,  $\text{CDCl}_3$ , TMS):  $\delta$  0.94 (t,  $J = 7.4$  Hz, 6H), 1.36–1.50 (m, 4H), 1.65–1.76 (m, 4H), 3.95 (t,  $J = 8.0$  Hz, 2H), 4.09–4.26 (m, 4H), 4.43 (t,  $J = 8.0$  Hz, 2H).  $^{13}\text{C}\{^1\text{H}\}$  NMR (67.8 MHz,  $\text{CDCl}_3$ , TMS):  $\delta$  13.44, 18.50, 32.08 (d,  $J = 7.3$  Hz), 44.98 (d,  $J = 4.5$  Hz), 63.57 (d,  $J = 8.9$  Hz), 68.26 (d,  $J = 6.6$  Hz), 155.45 (d,  $J = 8.9$  Hz).  $^{31}\text{P}$  NMR (109.3 MHz,  $\text{CDCl}_3$ ):  $\delta$  -3.03 (quint,  $J = 7.4$  Hz). MS (EI):  $m/z$  (%) : 224 (13), 194 (12), 168 (100), 150 (10), 88 (30).

### 3.3. Results and Discussion

#### 3.3.1. Optimization of the Reaction Conditions

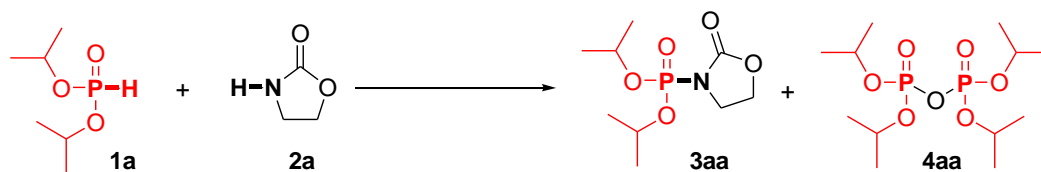
The optimization of the reaction conditions by using  $\text{Cu}(\text{OAc})_2$  (10 mol %) as the catalyst for the cross-coupling of diisopropylphosphonate (**1a**) and 2-oxazolidinone (**2a**) to diisopropyl(2-oxooxazolidin-3-yl)phosphonate (**3aa**) was carried out. The cross-coupling of **1a** and **2a** (1:2, mixed in a single step) in the presence of  $\text{Cu}(\text{OAc})_2$  and triethylamine ( $\text{Et}_3\text{N}$ ) in 1 atm of air gave **3aa** in 17% yield (Table 3-1, entry 1). In this case, a low yield of **3aa** was obtained due to the decomposition of **1a** to unidentified byproducts. Upon the addition of molecular sieves 4 A (MS 4 A) to the reaction mixture, the yield of **3aa** increased up to 51% together with a trace amount of a pyrophosphate (**4aa**) formed by the oxygenative dimerization of **1a** (Table 3-1, entry 2). By the slow addition of **1a** to the reaction mixture containing  $\text{Cu}(\text{OAc})_2$ ,  $\text{Et}_3\text{N}$ , and MS 4 A under open air conditions, the yield of **3aa** improved up to 81% (Table 3-1, entry 3). The steady increase of the yield of **3aa** could be attributed to the successful suppression of the hydrolytic decomposition of **1a** by the use of MS 4 A and the slow addition of **1a**. Further increase of the yield of **3aa** up to 90% was achieved by changing the molar ratio of **1a** to **2a** from 1:2 to 1:3, (Table 3-1, entry 4). The amount of

Cu(OAc)<sub>2</sub> could be reduced to 5 mol % with only a slight decrease in the yield of **3aa** (Table 3-1, entry 5). When the amount of **2a** was increased to 5 equiv, no further improvement of the yield of **3aa** was observed (Table 2-2-1, entry 6). When 1 equiv of **2a** with respect to **1a** was employed, the cross-coupling also proceeded, giving **3aa** in a moderate yield (Table 3-1, entry 7).

Among various copper catalysts examined, such as Cu(OAc)<sub>2</sub>, Cu(OTf)<sub>2</sub> (OTf = triflate), [Cu( $\mu$ -OH)(tmen)]<sub>2</sub>Cl<sub>2</sub> (tmen = *N,N,N',N'*-tetramethylethylenediamine), CuCl<sub>2</sub>, Cu(acac)<sub>2</sub>, CuI, CuSO<sub>4</sub>·5H<sub>2</sub>O, Cu(OH)<sub>2</sub>, and Cu<sub>2</sub>O, Cu(OAc)<sub>2</sub> showed the highest activity and selectivity for the cross-coupling of **1a** and **2a** (Table 3-1, entry 4, 8–15). Cu(OTf)<sub>2</sub> showed as high activity and selectivity as Cu(OAc)<sub>2</sub> (Table 3-1, entry 8). Other copper catalysts, such as [Cu( $\mu$ -OH)(tmen)]<sub>2</sub>Cl<sub>2</sub>, CuCl<sub>2</sub>, Cu(acac)<sub>2</sub>, CuI, and CuSO<sub>4</sub>·5H<sub>2</sub>O, showed lower activities and/or selectivities than those of Cu(OAc)<sub>2</sub> (Table 3-1, entries 9–13). Cu(OH)<sub>2</sub> and Cu<sub>2</sub>O, which have shown high activity for the cross-coupling of terminal alkynes and amides (see chapter 2), were not effective for the present cross-coupling (Table 3-1, entries 14 and 15). Other metal acetates, such as Ni(OAc)<sub>2</sub>·4H<sub>2</sub>O, Co(OAc)<sub>2</sub>·4H<sub>2</sub>O, Fe(OAc)<sub>2</sub>, Mn(OAc)<sub>2</sub>·4H<sub>2</sub>O, and Pd(OAc)<sub>2</sub> were not able to promote the present cross-coupling (Table 3-1, entries 16–20).

Both inorganic and organic bases could effectively promote the cross-coupling, giving **3aa** in high yields (Table 3-2). Among various bases examined, such as Et<sub>3</sub>N, Na<sub>2</sub>CO<sub>3</sub>, K<sub>2</sub>CO<sub>3</sub>, Cs<sub>2</sub>CO<sub>3</sub>, NaHCO<sub>3</sub>, KHCO<sub>3</sub>, K<sub>3</sub>PO<sub>4</sub>·*n*H<sub>2</sub>O, pyridine, and DBU (1,8-diazabicyclo[5.4.0]undec-7-ene), K<sub>2</sub>CO<sub>3</sub> was the most suitable base for the cross-coupling of **1a** and **2a**, giving **3aa** in an almost quantitative yield (Table 3-2, entry 4). The yield of **3aa** significantly decreased in the absence of bases (Table 3-2, entry 12).

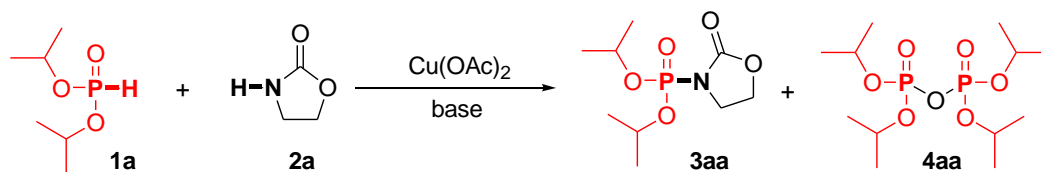
**Table 3-1.** Oxidative cross-coupling of diisopropylphosphonate (**1a**) and 2-oxazolidinone (**2a**) under various conditions.<sup>[a]</sup>



Entry	Catalyst	<b>1a/2a</b>	Conv. of <b>1a</b> [%]	Yield [%]	
				<b>3aa</b>	<b>4aa</b>
1 <sup>[b]</sup>	Cu(OAc) <sub>2</sub>	1/2	82	17	1
2 <sup>[c]</sup>	Cu(OAc) <sub>2</sub>	1/2	93	51	1
3	Cu(OAc) <sub>2</sub>	1/2	99	81	1
4	Cu(OAc) <sub>2</sub>	1/3	99	90	1
5 <sup>[d]</sup>	Cu(OAc) <sub>2</sub>	1/3	93	84	1
6	Cu(OAc) <sub>2</sub>	1/5	>99	89	1
7	Cu(OAc) <sub>2</sub>	1	93	68	6
8	Cu(OTf) <sub>2</sub>	1/3	97	89	1
9	[Cu(μ-OH)(tmen)] <sub>2</sub> Cl <sub>2</sub>	1/3	>99	62	38
10	CuCl <sub>2</sub>	1/3	>99	63	37
11	Cu(acac) <sub>2</sub>	1/3	2	1	nd
12	CuI	1/3	12	1	6
13	CuSO <sub>4</sub> ·5H <sub>2</sub> O	1/3	44	25	2
14	Cu(OH) <sub>2</sub>	1/3	3	nd	nd
15	Cu <sub>2</sub> O	1/3	<1	nd	nd
16	Ni(OAc) <sub>2</sub> ·4H <sub>2</sub> O	1/3	<1	nd	nd
17	Co(OAc) <sub>2</sub> ·4H <sub>2</sub> O	1/3	<1	nd	nd
18	Fe(OAc) <sub>2</sub>	1/3	<1	nd	nd
19	Mn(OAc) <sub>2</sub> ·4H <sub>2</sub> O	1/3	<1	nd	nd
20	Pd(OAc) <sub>2</sub>	1/3	7	nd	nd
21	none	1/3	<1	nd	nd

[a] Reaction conditions: **1a** (0.2 mmol), catalyst (10 mol %), Et<sub>3</sub>N (0.2 mmol), MS 4 A (100 mg), toluene (2 mL), 80 °C, under air (1 atm). A toluene solution of **1a** (1 mL, 0.2 M) was added to the reaction mixture over 30 min by a syringe pump, and the reaction mixture was stirred for an additional 10 min. Conversion and yield were determined by GC analysis. nd = not detected (<1%) [b] Mixed in a single step, without MS 4 A, 40 min. [c] Mixed in a single step, MS 4 A (100 mg), 40 min. [d] Cu(OAc)<sub>2</sub> (5 mol %).

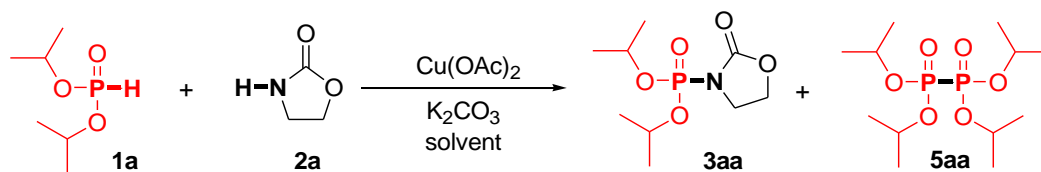
**Table 3-2.** Screening of bases for the cross-coupling of diisopropylphosphonate (**1a**) and 2-oxazolidinone (**2a**).<sup>[a]</sup>



Entry	Base [equiv]	Conv. of <b>1a</b> [%]	Yield [%]	
			<b>3aa</b>	<b>4aa</b>
1	$\text{Et}_3\text{N}$ (1)	99	90	1
2	$\text{Et}_3\text{N}$ (0.5)	95	75	1
3	$\text{Na}_2\text{CO}_3$ (1)	79	67	1
<b>4</b>	<b><math>\text{K}_2\text{CO}_3</math> (1)</b>	<b>&gt;99</b>	<b>&gt;99</b>	<b>nd</b>
<b>5</b>	<b><math>\text{K}_2\text{CO}_3</math> (0.5)</b>	<b>&gt;99</b>	<b>97</b>	<b>nd</b>
6	$\text{Cs}_2\text{CO}_3$ (1)	>99	53	nd
7	$\text{NaHCO}_3$ (1)	65	51	2
8	$\text{KHCO}_3$ (1)	97	85	1
9	$\text{K}_3\text{PO}_4 \cdot n\text{H}_2\text{O}$ (1)	>99	88	nd
10	pyridine (1)	79	61	2
11	DBU (1)	>99	77	4
12	none	57	39	2

[a] Reaction conditions: **1a** (0.2 mmol), **2a** (0.6 mmol),  $\text{Cu}(\text{OAc})_2$  (10 mol%), MS4A (100 mg), toluene (2 mL), 80 °C, under air (1 atm), 40 min. A toluene solution of **1a** (1 mL, 0.2 M) was added to the reaction mixture over 30 min by a syringe pump, and the reaction mixture was stirred for an additional 10 min. Conversion and yield were determined by GC analysis. nd = not detected (<1%).

**Table 3-3.** Screening of solvents for the cross-coupling of diisopropylphosphonate (**1a**) and 2-oxazolidinone (**2a**).<sup>[a]</sup>



Entry	Solvent	Conv. of <b>1a</b> [%]	Yield [%]	
			<b>3aa</b>	<b>5aa</b>
<b>1</b> <sup>[b]</sup>	<b>toluene</b>	>99	>99	nd
2 <sup>[c,d]</sup>	toluene	9	9	nd
3 <sup>[c]</sup>	1,2-dichloroethane	22	20	2
4 <sup>[c]</sup>	1,4-dioxane	>99	53	17
5 <sup>[c]</sup>	2-propanol	27	15	4
6 <sup>[c]</sup>	acetonitrile	60	24	24
7 <sup>[c]</sup>	dimethylsulfoxide	75	17	13
8 <sup>[c]</sup>	dimethylformamide	>99	29	21

[a] Reaction conditions: **1a** (0.2 mmol), **2a** (0.6 mmol), Cu(OAc)<sub>2</sub> (10 mol%), Et<sub>3</sub>N (0.2 mmol), MS4A (100 mg), solvent (2 mL), 80 °C, under air (1 atm), 40 min. Toluene solution of **1a** (1 mL, 0.2 M) was added to the reaction mixture over 30 min by a syringe pump, and the reaction mixture was stirred for an additional 10 min. Conversion and yields were determined by GC analysis. nd = not detected (<1%). [b] **4aa** was detected by GC (1%). [c] **4aa** was hardly detected by GC (<1%). [d] The reaction was carried out under Ar atmosphere.

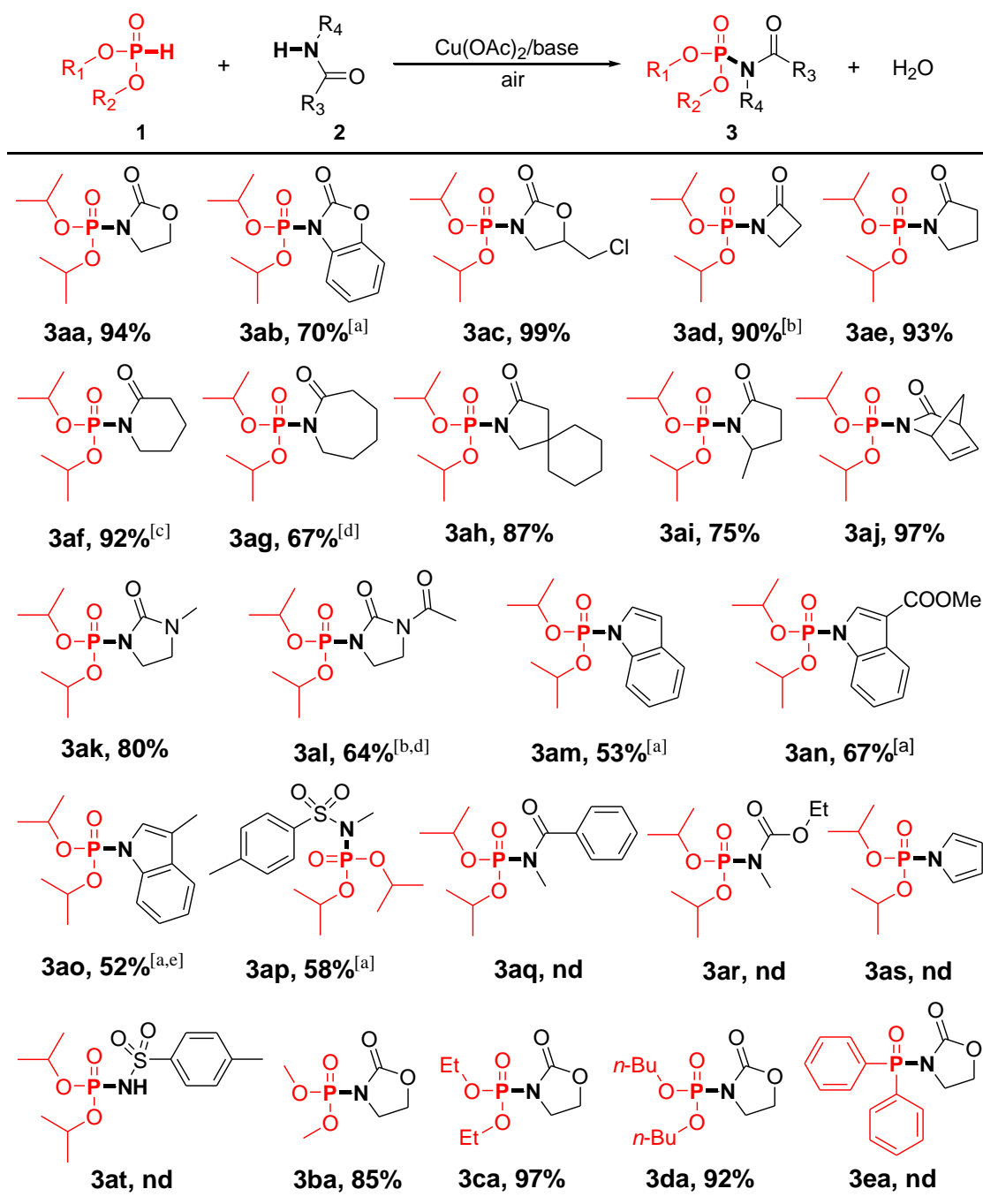
Studies on the solvent effects showed that toluene was the best one. Other solvents, such as 1,2-dichloroethane, 1,4-dioxane, 2-propanol, acetonitrile, dimethylformamide (DMF), and dimethylsulfoxide (DMSO), were not as effective as toluene (Table 3-3). The cross-coupling of **1a** and **2a** under an Ar atmosphere gave only a stoichiometric amount of **3aa** with respect to Cu(OAc)<sub>2</sub> (Table 3-3, entry 2). This result suggests that the reoxidation of the reduced copper species by O<sub>2</sub> (air) is necessary for the present cross-coupling (Scheme 3-3).

### 3.3.2. Substrate Scope

The scope of the present  $\text{Cu}(\text{OAc})_2$ -catalyzed aerobic cross-dehydrogenative coupling of *H*-phosphonates and amides to *N*-acylphosphoramidates was investigated using air as the terminal oxidant. The conditions suitable for the cross-coupling, especially bases, were largely dependent on the types of substrates. The isolation of *N*-acylphosphoramidates was very simple (section 3.2.2), and the isolated yields are summarized in Scheme 3-2.

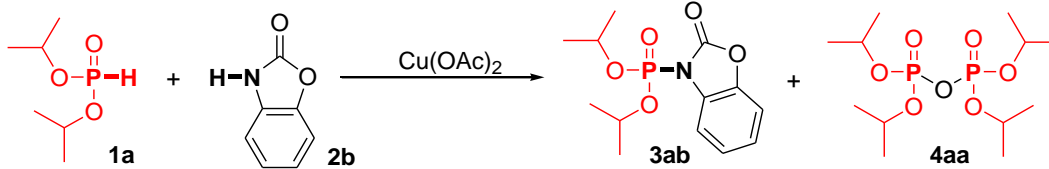
The cross-coupling of benzooxazolidinone and **1a** efficiently proceeded by using 4-methylpyridine as a base instead of  $\text{K}_2\text{CO}_3$ , giving a good yield of the corresponding *N*-acylphosphoramidate (Scheme 3-2, **3ab**, and Table 3-4). A 5-substituted oxazolidinone was also a good coupling partner of **1a** (Scheme 3-2, **3ac**). 4-, 5-, 6-, and 7-Membered lactams were efficiently reacted with **1a** to afford the corresponding *N*-acylphosphoramidates in high to excellent yields (Scheme 3-2, **3ad–3ag**). 4- and 5-Substituted pyrrolidinones also reacted well with **1a** (Scheme 3-2, **3ah** and **3ai**). A bicyclic lactam, 2-azabicyclo[2.2.1]hept-5-en-3-one, was also applicable to the present cross-coupling (Scheme 3-2, **3aj**). Apart from the above cyclic carbamates and lactams, cyclic urea derivatives also reacted well with **1a** (Scheme 3-2, **3ak** and **3al**). In addition, indole and sulfonamide derivatives were also suitable nitrogen nucleophiles for the cross-coupling (Scheme 3-2, **3am–3ap**). Other nitrogen nucleophiles, such as acyclic secondary amide and carbamate, pyrrole, and primary sulphonamide were not effective substrates for the present cross-coupling (Scheme 3-2, **3aq–3at**). With regard to the *H*-phosphonate coupling partner, various dialkyl phosphonates could be utilized, giving the corresponding *N*-acylphosphoramidates in high yields (Scheme 3-2, **3aa–3da**). Diphenylphosphine oxide was not the effective coupling partner (Scheme 3-2, **3ea**).



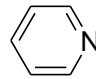
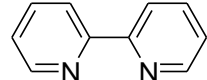
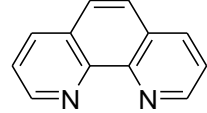
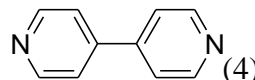
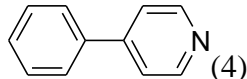

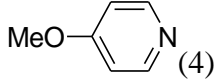
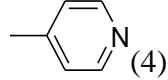


**Scheme 3-2.** Aerobic cross-dehydrogenative coupling of *H*-phosphonates and nitrogen nucleophiles. Reaction conditions: **1** (0.2 mmol), **2** (0.6 mmol), Cu(OAc)<sub>2</sub> (10 mol %), K<sub>2</sub>CO<sub>3</sub> (0.2 mmol), MS 4 A (100 mg), toluene (2 mL), 80 °C, under air (1 atm). A toluene solution of **1** (1 mL, 0.2 M) was added to the reaction mixture over 30 min by a syringe pump, and the reaction mixture was stirred for an additional 10 min (unless otherwise noted). The isolated yields (based on **1**) are reported. [a] 4-methylpyridine (0.8 mmol) instead of K<sub>2</sub>CO<sub>3</sub> (0.2 mmol). [b] 1.5 h. [c] 2,2'-bipyridyl (20 mol %). [d] 6,6'-dimethylbipyridyl (20 mol %). [e] 1 h. nd = not detected.

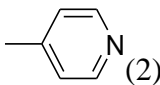
**Table 3-4.** Screening of bases for the cross-coupling of **1a** and **2b**<sup>[a]</sup>



Reaction scheme: **1a** + **2b**  $\xrightarrow{\text{Cu(OAc)}_2}$  **3ab** + **4aa**

Entry	Base [equiv.]	Conv. of <b>1a</b> [%]	Yield [%]	
			<b>3aa</b>	<b>4</b>
1	K <sub>2</sub> CO <sub>3</sub> (1)	33	2	nd
2	K <sub>2</sub> CO <sub>3</sub> (4)	28	6	nd
3	 (4)	>99	45	26
4	 (4)	46	33	1
5	 (4)	22	7	4
6	 (4)	98	52	23
7	 (4)	>99	56	15
<b>8</b>	 (4)	<b>&gt;99</b>	<b>64</b>	<b>10</b>
9	 (4)	99	42	18
10 <sup>[b]</sup>	 (4)	>99	55	1

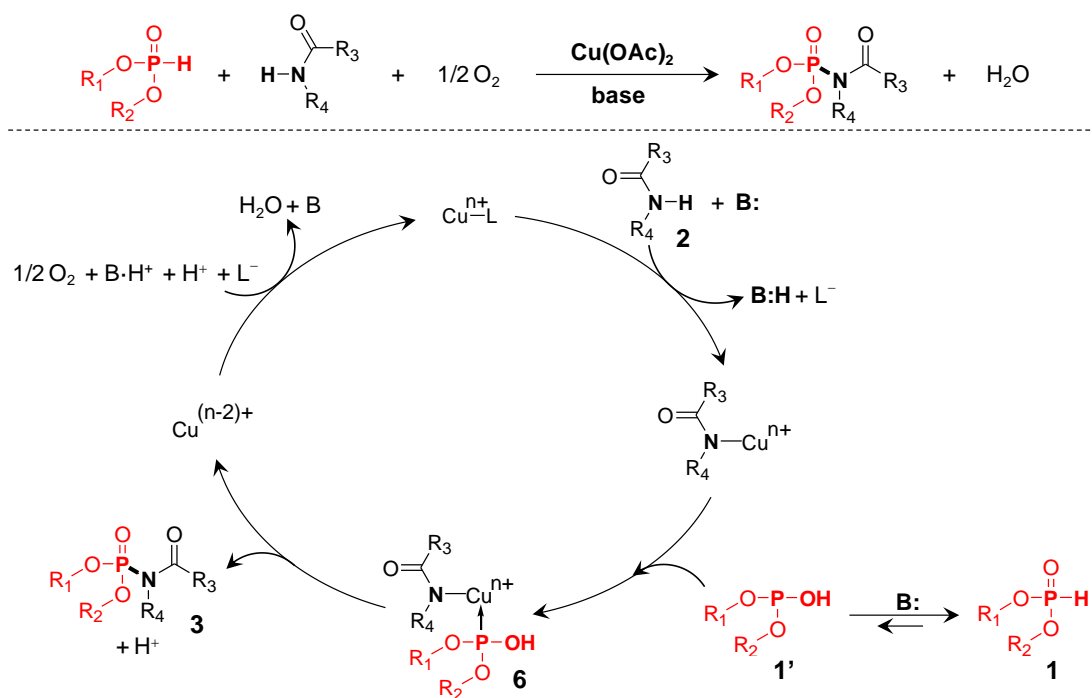
**Table 3-4.** (Continued)

Entry	Base [equiv.]	Conv. of <b>1a</b> [%]	Yield [%]	
			<b>3aa</b>	<b>4</b>
11		99	42	4

[a] Reaction conditions: **1a** (0.2 mmol), **2b** (0.6 mmol), Cu(OAc)<sub>2</sub> (10 mol%), toluene (2 mL), MS4A (100 mg), 80 °C, under air (1 atm), 40 min. Toluene solution of **1a** (1 mL, 0.2 M) was added to the reaction mixture over 30 min by a syringe pump, and the reaction mixture was stirred for an additional 10 min. Conversion and yields were determined by GC analysis. nd = not detected (<1%). [b] Cu formate (10 mol%) .

### 3.3.3. Reaction mechanism

A possible reaction mechanism is shown in Scheme 3-3. The proposed catalytic cycle consists of (1) coordination of amidate and phosphite species to the copper center to afford a Cu(phosphite)(amidate) intermediate (**6**), (2) subsequent reductive elimination to generate the corresponding *N*-acylphosphoramidates, and (3) reoxidation of the reduced copper species by O<sub>2</sub> (air) to regenerate the active copper species (Scheme 3-3). Bases likely play two important roles; (1) abstract N–H protons of amides, and (2) increase concentration of phosphite forms (**1'**) or directly deprotonate **1** to coordinate to the active copper center.



**Scheme 3-3.** A possible reaction mechanism for the copper-catalyzed oxidative cross-coupling of *H*-phosphonates and amides (L = acetate, B: = base).

### 3.4. Conclusion

In summary, the  $\text{Cu}(\text{OAc})_2$ -catalyzed aerobic oxidative cross-coupling of *H*-phosphonates and amides to *N*-acylphosphoramidates has successfully been developed. Various dialkyl *H*-phosphonates can efficiently react with nitrogen nucleophiles (including oxazolidinone, lactam, pyrrolidinone, urea, indole, and sulfonamide derivatives), giving the corresponding P–N coupling products. The present cross-coupling completely avoids the utilization of (hazardous) stoichiometric reagents (e.g., chlorophosphonates,  $\text{Cl}_2$ ,  $\text{COCl}_2$ ,  $\text{SO}_2\text{Cl}_2$ , *n*-BuLi, and/or  $\text{NaN}_3$  in conventional procedures, Scheme 3-1) and the formation of vast amounts of byproducts, providing a green, and practical synthetic route to *N*-acylphosphoramidates.

### 3.5. References

- [1] M. E. Tate, P. J. Murphy, W. P. Roberts, A. Kerr, *Nature* **1979**, 280, 697.
- [2] J. I. Guijarro, J. E. González-Pastor, F. Baleux, J. L. S. Millán, M. A. Castilla, M. Rico, F. Moreno, M. Delepierre, *J. Biol. Chem.* **1995**, 270, 23520.
- [3] M. Uramoto, C.-J. Kim, K. Shinya, H. Kusakabe, K. Isono, *J. Antibiot.* **1991**, 44, 375.
- [4] K. C. Lasseter, J. Gambale, B. Jin, A. Bergman, M. Constanzer, J. Dru, T. H. Han, A. Majumdar, J. K. Evans, M. G. Murphy, *J. Clin. Pharmacol.* **2007**, 47, 834.
- [5] P. K. Chakravarty, W. J. Greenlee, W. H. Parsons, A. A. Parchett, P. Combs, A. Roth, R. D. Busch, T. N. Mellin, *J. Med. Chem.* **1989**, 32, 1886.
- [6] L. A. Adams, R. J. Cox, J. S. Gibson, M. B. Mayo-Martin, M. Walter, W. Whittingham, *Chem. Commun.* **2002**, 2004.
- [7] W. Xiao, C.-Y. Zhou, C.-M. Che, *Chem. Commun.* **2012**, 48, 5871.
- [8] (a) G. M. Kosolapoff, L. Maier, *Organic Phosphorus Compounds*; Wiley-Interscience: New York, **1972**. (b) F. R. Hartley, *The Chemistry of Organophosphorus Compounds*; Wiley: New York, **1996**. (c) L. D. Quin, *A Guide to Organophosphorus Chemistry*; Wiley: New York, **2000**. (d) H. K. Gupta, A. Mazumder, P. Garg, P. K. Gutch, D. K. Dubey, *Tetrahedron Lett.* **2008**, 49, 6704.
- [9] For selected reviews and examples see: (a) L.-B. Han, M. Tanaka, *Chem. Commun.* **1999**, 395. (b) D. Prim, J. Campagne, D. Joseph, B. Andrioletti, *Tetrahedron* **2002**, 58, 2041. (c) A. Schwan, *Chem. Soc. Rev.* **2004**, 33, 218. (d) O. Delacroix, A. C. Gaumont, *Curr. Org. Chem.* **2005**, 9, 1851. (e) D. S. Glueck,

- Synlett* **2007**, 2627. (f) L. Coudray, J. Montchamp, *Eur. J. Org. Chem.* **2008**, 3601. (g) T. Kagayama, A. Nakano, S. Sakaguchi, Y. Ishii, *Org. Lett.* **2006**, 8, 407. (h) C. D. Hou, Y. L. Ren, R. Lang, X. X. Hu, C. G. Xia, F. W. Li, *Chem. Commun.* **2012**, 48, 5181. (i) L.-B. Han, Y. Ono, S. Shimada, *J. Am. Chem. Soc.* **2008**, 130, 2752. (j) Y. Gao, G. Wang, L. Chen, P. Xu, Y. Zhao, Y. Zhou, L.-B. Han, *J. Am. Chem. Soc.* **2009**, 131, 7956. (k) H. Ohmiya, H. Yorimitsu, K. Oshima, *Angew. Chem. Int. Ed.* **2005**, 44, 2368. (l) C.-B. Xiang, Y.-J. Bian, X.-R. Mao, Z.-Z. Huang, *J. Org. Chem.* **2012**, 77, 7706.
- [10] (a) D. W. Stephan, *Angew. Chem. Int. Ed.* **2000**, 39, 314. (b) T. J. Clark, K. Lee, I. I. Manners, *Chem. Eur. J.* **2006**, 12, 8634. (c) S. Greenberg, D. W. Stephan, *Chem. Soc. Rev.* **2008**, 37, 1482. (d) R. J. Less, R. L. Melen, V. Naseri, D. S. Wright, *Chem. Commun.* **2009**, 4929. (e) R. Waterman, *Dalton Trans.* **2009**, 18. (f) R. Waterman, *Curr. Org. Chem.* **2008**, 12, 1322. (g) H. Dorn, R. A. Singh, J. A. Massey, A. J. Lough, I. Manners, *Angew. Chem. Int. Ed.* **1999**, 38, 3321. (h) H. Dorn, R. A. Singh, J. A. Massey, J. M. Nelson, C. A. Jaska, A. J. Lough, I. Manners, *J. Am. Chem. Soc.* **2000**, 122, 6669. (i) L.-B. Han, T. D. Tilley, *J. Am. Chem. Soc.* **2006**, 128, 13698. (j) V. P. W. Böhm, M. Brookhart, *Angew. Chem. Int. Ed.* **2001**, 40, 4694. (k) R. Shu, L. Hao, J. F. Harrod, H.-G. Woo, E. Samuel, *J. Am. Chem. Soc.* **1998**, 120, 12988. (l) Y. Zhou, S. Yin, Y. Gao, Y. Zhao, M. Goto, L.-B. Han, *Angew. Chem. Int. Ed.* **2010**, 49, 6852.
- [11] (a) S. V. Ley, A. W. Thomas, *Angew. Chem. Int. Ed.* **2003**, 42, 5400. (b) G. Evano, N. Blanchard, M. Toumi, *Chem. Rev.* **2008**, 108, 3054. (c) A. E. Wendlandt, A. M. Suess, S. S. Stahl, *Angew. Chem. Int. Ed.* **2011**, 50, 11062. (d) Z. Shao, F. Peng, *Angew. Chem. Int. Ed.* **2010**, 49, 9566. (e) C. A. Parrodi, P. J.

- Walsh, *Angew. Chem. Int. Ed.* **2009**, *48*, 4679. (f) C. Liu, H. Zhang, W. Shi, A. Lei, *Chem. Rev.* **2011**, *111*, 1780. (g) K. Hirano, M. Miura, *Chem. Commun.* **2012**, *48*, 10704.
- [12] *Purification of Laboratory Chemicals*, 3rd ed. (Eds.: D. D. Perrin, W. L. F. Armarego), Pergamon Press, Oxford, **1988**.
- [13] (a) T. Hamada, X. Ye, S. S. Stahl, *J. Am. Chem. Soc.* **2008**, *130*, 833. (b) Y. Wei, H. Zhao, J. Kan, W. Su, M. Hong, *J. Am. Chem. Soc.* **2010**, *132*, 2522. (c) L. Chu, F. Qing, *J. Am. Chem. Soc.* **2010**, *132*, 7262. (d) M. Nishino, K. Hirano, T. Satoh, M. Miura, *Angew. Chem. Int. Ed.* **2012**, *51*, 6993.

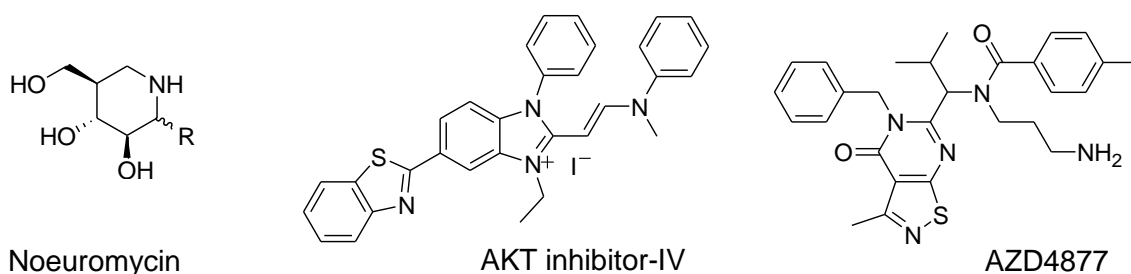




**Chapter 4**  
**Supported Gold Nanoparticle-Catalyzed**  
**Aerobic Dehydrogenative Amination of**  
 **$\alpha,\beta$ -Unsaturated Aldehydes**

## 4.1. Introduction

As a very important class of compounds, enaminals ( $\beta$ -enaminals) have been utilized for the synthesis of a large variety of heterocyclic compounds such as furans, pyrans, pyrroles, pyridines, pyrazoles, isothiazoles, and isoxazoles.<sup>[1,2]</sup> They have also been applied to the synthesis of several bioactive compounds, such as noeuromycin, AKT (protein kinase B) inhibitor-IV, and AZD4877 (a kinesin spindle protein inhibitor and potential anticancer agent) (Figure 4-1).<sup>[1,2]</sup>

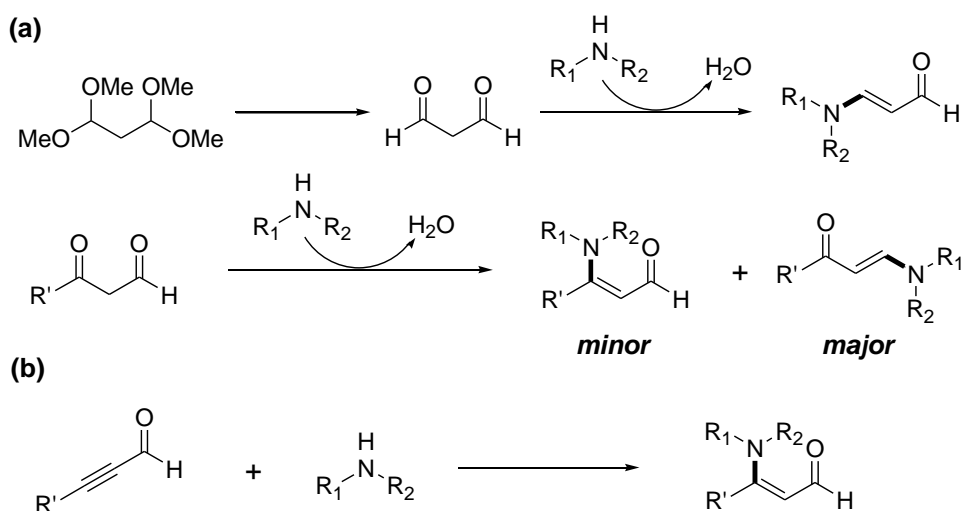


**Figure 4-1.** Several biologically active compounds using enaminals as starting materials.<sup>[1-4]</sup>

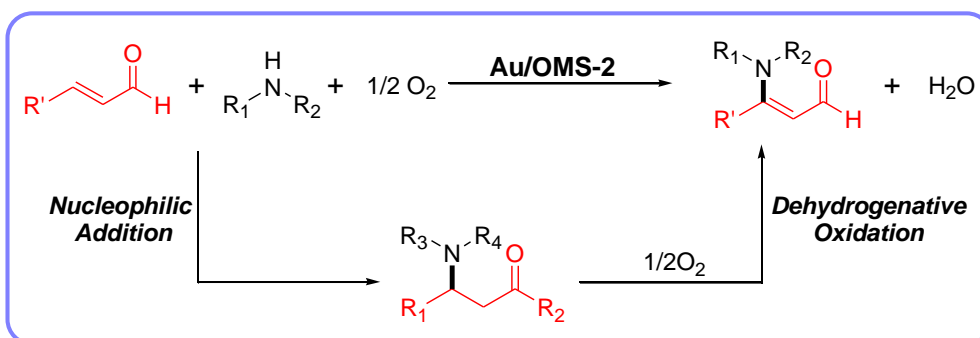
Several procedures are available for the synthesis of enaminals.<sup>[2,3]</sup> The most widely utilized procedures are (1) dehydrative condensation of amines with 1,3-dicarbonyl compounds (Scheme 4-1, a) and (2) hydroamination of propargylic aldehydes (Scheme 4-1, b). The dehydrative condensation with *in situ* generated malondialdehyde is only applicable to the synthesis of  $\beta$ -aminoacroleins. Meanwhile, the condensation with ketoaldehydes could not selectively give  $\beta$ -substituted enaminals due to the higher reactivity of aldehyde functionalities toward the condensation, consequently giving enamminones as the major products.<sup>[3e]</sup> Although a wide variety of enaminals can be synthesized by hydroamination of propargylic aldehydes, the development of alternative synthetic procedures for enaminals would be very desirable considering the limitation in

availability and/or synthesis of starting propargylic aldehydes. In this context, direct dehydrogenative amination of readily available  $\alpha,\beta$ -unsaturated aldehydes would provide a promising method for the selective synthesis of enaminals (Scheme 4-1)

### Classical procedures



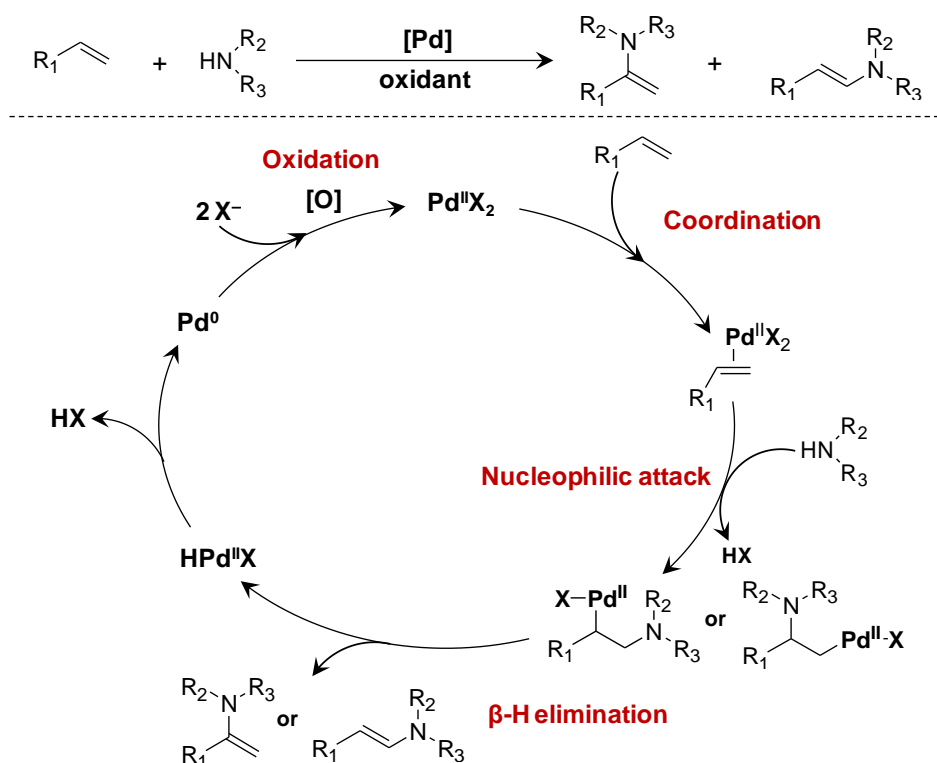
### This work



**Scheme 4-1.** Synthesis of enaminals.

As a valuable method for the construction of  $C(sp^2)$ -N bonds, dehydrogenative amination or amidation of alkenes, namely aza-Wacker-type oxidation, has generally been efficiently promoted by palladium-based catalysts, and both intra- and inter-molecular reactions have been developed.<sup>[4-6]</sup> These reactions are supposed to

proceed through the following several steps: (1) coordination of an alkene to a palladium catalyst, (2) nucleophilic attack of a nitrogen nucleophile to the palladium alkene complex, (3)  $\beta$ -H elimination to afford an enamine or an enamide, and (4) reoxidation of the reduced metal center to regenerate the initial Pd<sup>II</sup> species (Scheme 4-2).<sup>[4]</sup>



**Scheme 4-2.** Palladium-catalyzed aza-Wacker oxidation.

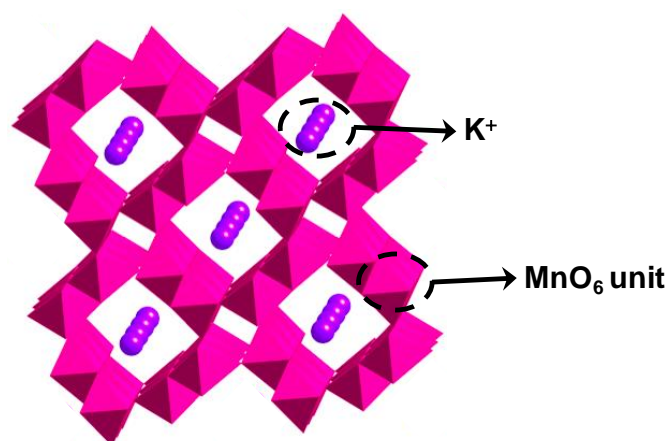
To date, the palladium-catalyzed aza-Wacker oxidation using less-basic amides, such as sulfonamides, carbamates, and lactams, has been developed.<sup>[4]</sup> Amination of alkenes using simple amines is relatively less-developed,<sup>[5,6]</sup> likely due to the severe deactivation of homogeneous metal-based catalysts by the strong coordination of amines.

Recently, Ishii<sup>[5e,h]</sup> and Ying<sup>[5g]</sup> have reported excellent palladium-catalyzed procedures for the amination of  $\alpha,\beta$ -unsaturated carbonyl compounds. However, these systems are limited to the amination of  $\alpha,\beta$ -unsaturated esters and ketones with aniline derivatives.<sup>[5e,g,h,7]</sup> Therefore, the dehydrogenative amination of  $\alpha,\beta$ -unsaturated aldehydes with a large variety of amines has never been developed to date.

To develop the  $\beta$ -amination of  $\alpha,\beta$ -unsaturated aldehydes, a reaction pathway, including (1) nucleophilic addition of an amine to an  $\alpha,\beta$ -unsaturated aldehyde to generate a  $\beta$ -amino aldehyde intermediate and (2) selective dehydrogenative oxidation of the  $\beta$ -amino aldehyde, is proposed in this study (Scheme 4-1). In order to realize the proposed reaction pathway, the design of catalysts to promote the dehydrogenation of saturated C–C single bonds would be the key for the achievement of the amination. This study is especially focused on supported gold nanoparticles to promote the dehydrogenation. The last several decades have witnessed the great success of supported gold nanoparticles for aerobic oxidative dehydrogenation reactions through activation of molecular oxygen, as described in chapter 1. In addition, they can easily be separated and reused, and are highly durable against strong coordination of nitrogen nucleophiles. These properties of supported gold nanoparticles are envisioned to promote the dehydrogenation of various saturated C–C single bonds.

Described in this chapter is a supported gold nanoparticle-catalyzed dehydrogenative amination of  $\alpha,\beta$ -unsaturated aldehydes to enaminals using air (molecular oxygen) as the sole oxidant (Scheme 4-1, this work). In the presence of gold nanoparticles supported on manganese oxide-based octahedral molecular sieves OMS-2<sup>[8]</sup> (Au/OMS-2), the amination of various  $\alpha,\beta$ -unsaturated aldehydes with a wide range of amines proceeded efficiently, affording the corresponding enaminals in

moderate to high yields (50–97 %). OMS-2 ( $\text{KMn}_8\text{O}_{16}$ ) has the  $2 \times 2$  hollandite type structure with a one-dimensional pore (Figure 4-2), which has been utilized as supports or oxidation catalysts and shown versatile oxidation catalysis for organic transformations.<sup>[8]</sup> The catalysis in the present amination was intrinsically heterogeneous, and the Au/OMS-2 catalyst could be reused at least five times without a loss of its high catalytic performance. The present Au/OMS-2-catalysed amination of  $\alpha,\beta$ -unsaturated aldehydes provides a highly efficient synthetic procedure for enaminals and reveals new oxidation catalysis of gold nanoparticles.<sup>[9,10]</sup>



**Figure 4-2.** The structure of OMS-2.<sup>[8]</sup>

## 4.2. Experimental Section

### 4.2.1. General

GC analyses were performed on Shimadzu GC-2014 with a FID detector equipped with an Rxi-5 Sil MS capillary column. GC-MS spectra were recorded on Shimadzu GCMS-QP2010 equipped with an InertCap 5 capillary column at an ionization voltage of 70 eV. Liquid-state NMR spectra were recorded on JEOL JNM-ECA-500.  $^1\text{H}$  and  $^{13}\text{C}$  NMR spectra were measured at 495.1 and 124.5 MHz, respectively, using

tetramethylsilane (TMS) as an internal reference ( $\delta = 0$  ppm). ICP-AES analyses were performed on Shimadzu ICPS-8100. XRD patterns were recorded on a Rigaku SmartLab diffractometer ( $\text{Cu}_{K\alpha}$ ,  $\lambda = 1.5405 \text{ \AA}$ , 45 kV–200 mA). TEM measurements were performed on JEOL JEM-2010HC. OMS-2 (BET surface area:  $90 \text{ m}^2 \text{ g}^{-1}$ )<sup>[11]</sup> and  $\text{Co}_3\text{O}_4$  (BET:  $182 \text{ m}^2 \text{ g}^{-1}$ )<sup>[12]</sup> were prepared according to the literature procedures.  $\text{CeO}_2$  (BET:  $111 \text{ m}^2 \text{ g}^{-1}$ , Cat. No. 544841-25G, Aldrich),  $\text{Al}_2\text{O}_3$  (BET:  $160 \text{ m}^2 \text{ g}^{-1}$ , Cat. No. KHS-24, Sumitomo Chemical), and  $\text{TiO}_2$  (BET:  $316 \text{ m}^2 \text{ g}^{-1}$ , Cat. No. ST-01, Ishihara Sangyo Kaisya) were commercially available. Various supported metal catalysts ( $\text{Pd}/\text{Al}_2\text{O}_3$ ,  $\text{Cu}/\text{Al}_2\text{O}_3$ ,  $\text{Ru}/\text{Al}_2\text{O}_3$ , and  $\text{Rh}/\text{Al}_2\text{O}_3$  for Table 3-1) were prepared according to the literature procedures.<sup>[13]</sup> Solvents and substrates were obtained from Kanto Chemical, TCI, Wako, or Aldrich (reagent grade), and purified prior to use, if necessary.<sup>[14]</sup>

#### 4.2.2. Preparation of Supported Gold Nanoparticle Catalysts

**Au/OMS-2:** An aqueous solution of  $\text{HAuCl}_4 \cdot 4\text{H}_2\text{O}$  (8.3 mM, 60 mL) containing OMS-2 (2.0 g) was vigorously stirred at room temperature. After 15 min, the pH of the solution was quickly adjusted to 10 by addition of an aqueous solution of NaOH (1.0 M), and the resulting slurry was further stirred for 24 h. The solid was then filtered off, washed with a large amount of water (4 L), and dried in vacuo to afford the supported hydroxide catalyst precursor. Then, the hydroxide precursor was calcined at  $300 \text{ }^\circ\text{C}$  for 2 h, giving Au/OMS-2 as a dark brown powder (Au content: 3.6 wt %).

**Au/ $\text{Al}_2\text{O}_3$ , Au/ $\text{TiO}_2$ , and Au/ $\text{Co}_3\text{O}_4$ :** An aqueous solution of  $\text{HAuCl}_4 \cdot 4\text{H}_2\text{O}$  (8.3 mM, 60 mL) containing  $\text{Al}_2\text{O}_3$ ,  $\text{TiO}_2$ , or  $\text{Co}_3\text{O}_4$  (2.0 g) was vigorously stirred at room temperature. After 15 min, the pH of the solution was quickly adjusted to 10 by

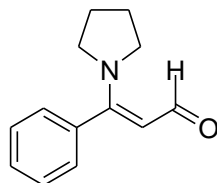
addition of an aqueous solution of NaOH (1.0 M), and the resulting slurry was further stirred for 24 h. The solid was then filtered off, washed with a large amount of water (4 L), and dried in vacuo to afford the supported hydroxide catalyst precursors. Then, the hydroxide precursors were calcined at 400 °C for 2 h, giving Au/Al<sub>2</sub>O<sub>3</sub> (Au content: 3.8 wt %), Au/TiO<sub>2</sub> (Au content: 3.6 wt %), and Au/Co<sub>3</sub>O<sub>4</sub> (Au content: 4.0 wt %) as wine red, purple, and dark black powders, respectively.

#### 4.2.3. Typical Procedure for the Dehydrogenative Amination

Into a Pyrex glass reactor (volume: ca. 20 mL) were successively placed Au/OMS-2 (3.6 mol %, 100 mg), an  $\alpha,\beta$ -unsaturated aldehyde (**1**) (0.5 mmol), an amide (**2**) (1.0 mmol), THF (1.9 mL), H<sub>2</sub>O (0.1 mL), and a Teflon-coated magnetic stir bar, and the reaction mixture was vigorously stirred at 50 °C, in 1 atm of air. After the reaction was completed, an internal standard (diphenyl) was added to the reaction mixture, and the conversion of **1** and the product yield were determined by GC analyses. As for the isolation of enaminal products, the internal standard was not added. After the reaction, the catalyst was filtered off (>97 % recovery), and then the filtrate was concentrated by evaporation of THF. The crude product was subjected to column chromatography on silica gel (typically using diethylether/acetone as an eluent), giving the pure enaminals. The products were identified by GC-MS and NMR (<sup>1</sup>H and <sup>13</sup>C) analyses. The retrieved catalyst was washed with ethanol and acetone, and calcined at 300 °C for 2 h before being used for the reuse experiment.

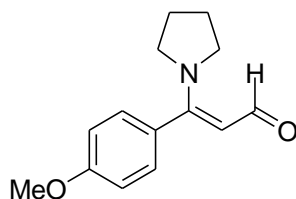


#### 4.2.4. Spectral Data of Enaminals and Enaminones



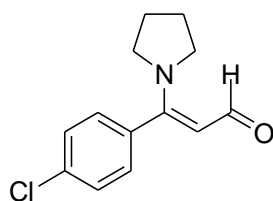
**3aa**

**3-phenyl-3-(1-pyrrolidinyl)-2-propenal (3aa):**  $^1\text{H}$  NMR (495.1 MHz,  $\text{DMSO-}d_6$ , TMS):  $\delta$  1.77 (quin,  $J = 6.8$  Hz, 2H), 1.97 (quin,  $J = 6.8$  Hz, 2H), 2.99 (t,  $J = 6.8$  Hz, 2H), 3.33 (t,  $J = 6.8$  Hz, 2H), 5.15 (d,  $J = 8.8$  Hz, 1H), 7.32–7.35 (m, 2H), 7.48–7.52 (m, 3H), 8.50 (d,  $J = 8.8$  Hz, 1H).  $^{13}\text{C}\{^1\text{H}\}$  NMR (124.5 MHz,  $\text{DMSO-}d_6$ , TMS):  $\delta$  24.48, 24.88, 48.14, 49.75, 102.04, 128.43, 128.50, 128.63, 129.12, 134.48, 164.75, 187.15. MS (EI):  $m/z$  (%) : 201 (41) [ $M^+$ ], 200 (23), 185 (14), 184 (100), 172 (23), 144 (32), 104 (16), 103 (32), 102 (21), 77 (29), 70 (39).



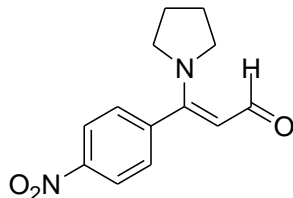
**3ba**

**3-(4-methoxyphenyl)-3-(pyrrolidin-1-yl)acrylaldehyde (3ba):**  $^1\text{H}$  NMR (495.1 MHz,  $\text{DMSO-}d_6$ , TMS):  $\delta$  1.77 (quin,  $J = 6.8$  Hz, 2H), 1.97 (quin,  $J = 6.8$  Hz, 2H), 3.02 (t,  $J = 6.8$  Hz, 2H), 3.30 (t,  $J = 6.8$  Hz, 2H), 3.81 (s, 3H), 5.13 (d,  $J = 8.5$  Hz, 1H), 7.02–7.05 (m, 2H), 7.26–7.29 (m, 2H), 8.56 (d,  $J = 8.8$  Hz, 1H).  $^{13}\text{C}\{^1\text{H}\}$  NMR (124.5 MHz,  $\text{DMSO-}d_6$ , TMS):  $\delta$  24.54, 24.88, 48.13, 49.77, 55.20, 102.24, 113.79, 126.56, 129.99, 159.67, 164.70, 187.29. MS (EI):  $m/z$  (%) : 231 (43) [ $M^+$ ], 230 (17), 215 (16), 214 (100), 202 (15), 174 (22), 134 (16), 133 (36), 132 (13), 95 (12), 89 (12), 77 (12), 70 (30).



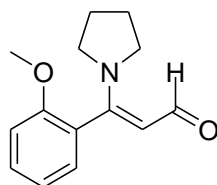
**3ca**

**3-(4-chlorophenyl)-3-(pyrrolidin-1-yl)acrylaldehyde (3ca):**  $^1\text{H}$  NMR (495.1 MHz, DMSO- $d_6$ , TMS):  $\delta$  1.78 (quin,  $J = 6.8$  Hz, 2H), 1.97 (quin,  $J = 6.8$  Hz, 2H), 3.00 (t,  $J = 6.7$  Hz, 2H), 3.32 (t,  $J = 6.8$  Hz, 2H), 5.16 (d,  $J = 8.8$  Hz, 1H), 7.38–7.41 (m, 2H), 7.55–7.58 (m, 2H), 8.52 (d,  $J = 8.8$  Hz, 1H).  $^{13}\text{C}\{^1\text{H}\}$  NMR (124.5 MHz, DMSO- $d_6$ , TMS):  $\delta$  24.46, 24.90, 48.24, 49.73, 102.23, 128.59, 130.43, 133.21, 133.96, 163.40, 186.86. MS (EI):  $m/z$  (%) : 236 (11) [ $M^+$ ], 237 (12), 235 (37), 234 (17), 220 (32), 219 (17), 218 (100), 206 (20), 180 (10), 178 (23), 143 (11), 138 (17), 137 (18), 136 (16), 102 (26), 101 (26), 95 (11), 75 (16), 70 (49).



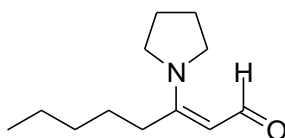
**3da**

**3-(4-nitrophenyl)-3-(pyrrolidin-1-yl)acrylaldehyde (3da):**  $^1\text{H}$  NMR (495.1 MHz, DMSO- $d_6$ , TMS):  $\delta$  1.81 (quin,  $J = 6.8$  Hz, 2H), 2.00 (quin,  $J = 6.8$  Hz, 2H), 3.00 (t,  $J = 6.8$  Hz, 2H), 3.37 (t,  $J = 7.1$  Hz, 2H), 5.21 (d,  $J = 8.8$  Hz, 1H), 7.68–7.70 (m, 2H), 8.34–8.36 (m, 2H), 8.49 (d,  $J = 8.8$  Hz, 1H).  $^{13}\text{C}\{^1\text{H}\}$  NMR (124.5 MHz, DMSO- $d_6$ , TMS):  $\delta$  24.40, 24.97, 48.42, 49.77, 102.22, 123.67, 130.18, 140.85, 147.80, 162.43, 186.56. MS (EI):  $m/z$  (%) : 246 (38) [ $M^+$ ], 245 (16), 230 (15), 229 (100), 217 (14), 199 (14), 189 (17), 183 (11), 171 (10), 143 (15), 102 (19), 70 (36).



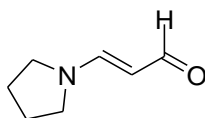
**3ea**

**3-(2-methoxyphenyl)-3-(pyrrolidin-1-yl)acrylaldehyde (3ea):**  $^1\text{H}$  NMR (495.1 MHz, DMSO- $d_6$ , TMS):  $\delta$  1.77 (quin,  $J = 6.7$  Hz, 2H), 1.90–2.02 (m, 2H), 2.92–2.99 (m, 2H), 3.31 (t,  $J = 7.1$  Hz, 2H), 5.09 (d,  $J = 8.8$  Hz, 1H), 7.03–7.06 (m, 1H), 7.15–7.17 (m, 2H), 7.45–7.48 (m, 1H), 8.50 (d,  $J = 8.8$  Hz, 1H).  $^{13}\text{C}\{^1\text{H}\}$  NMR (124.5 MHz, DMSO- $d_6$ , TMS):  $\delta$  24.52, 24.71, 47.93, 48.79, 55.62, 101.55, 111.67, 120.37, 123.05, 129.99, 130.88, 155.86, 162.14, 186.83. MS (EI):  $m/z$  (%) : 231 (62) [ $M^+$ ], 232 (10), 230 (14), 215 (16), 214 (100), 213 (17), 212 (14), 202 (16), 200 (30), 188 (15), 187 (18), 186 (13), 174 (21), 172 (10), 133 (16), 132 (16), 131 (30), 119 (14), 118 (12), 115 (11), 105 (31), 103 (19), 95 (28), 91 (20), 90 (12), 89 (18), 79 (11), 77 (30), 70 (86), 63 (11), 55 (10).



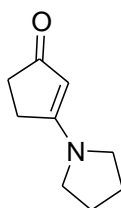
**3fa**

**3-(pyrrolidin-1-yl)oct-2-enal (3fa):**  $^1\text{H}$  NMR (495.1 MHz, DMSO- $d_6$ , TMS):  $\delta$  0.88 (t,  $J = 7.1$  Hz, 3H), 1.28–1.39 (m, 4H), 1.50 (quin,  $J = 7.6$  Hz, 2H), 1.86–1.91 (m, 4H), 2.64 (t,  $J = 7.8$  Hz, 2H), 3.15 (t,  $J = 6.2$  Hz, 2H), 3.48 (t,  $J = 6.1$  Hz, 2H), 4.77 (d,  $J = 8.5$  Hz, 1H), 9.35 (d,  $J = 4.3$  Hz, 1H).  $^{13}\text{C}\{^1\text{H}\}$  NMR (124.5 MHz, DMSO- $d_6$ , TMS):  $\delta$  13.87, 21.81, 24.24, 24.92, 28.60, 28.76, 31.11, 47.31, 48.21, 99.61, 165.18, 184.59. MS (EI):  $m/z$  (%) : 195 (34) [ $M^+$ ], 178 (21), 166 (23), 153 (11), 152 (69), 139 (46), 138 (19), 136 (14), 124 (36), 122 (26), 120 (14), 111 (79), 110 (38), 108 (12), 96 (23), 83 (58), 82 (15), 71 (11), 70 (100), 69 (13), 68 (22), 67 (11), 55 (24), 54 (11).



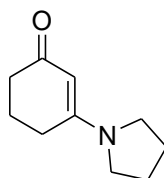
**3ga**

**3-(pyrrolidin-1-yl)acrylaldehyde (3ga):**  $^1\text{H}$  NMR (495.1 MHz, DMSO- $d_6$ , TMS):  $\delta$  1.84 (quin,  $J = 6.6$  Hz, 2H), 1.93 (quin,  $J = 6.9$  Hz, 2H), 3.11 (t,  $J = 7.1$  Hz, 2H), 3.50 (t,  $J = 6.7$  Hz, 2H), 4.89 (dd,  $J = 12.6$  and 8.6 Hz, 1H), 7.53 (d,  $J = 12.8$  Hz, 1H), 8.92 (d,  $J = 8.5$  Hz, 1H).  $^{13}\text{C}\{^1\text{H}\}$  NMR (124.5 MHz, DMSO- $d_6$ , TMS):  $\delta$  24.66, 24.83, 46.74, 51.74, 101.24, 156.56, 187.31. MS (EI):  $m/z$  (%) : 125 (100) [ $M^+$ ], 124 (17), 108 (32), 106 (16), 96 (26), 82 (12), 79 (15), 70 (18), 69 (44), 68 (44), 55 (14), 54 (17).



**3ha**

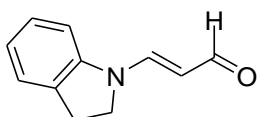
**3-(pyrrolidin-1-yl)cyclopent-2-enone (3ha):**  $^1\text{H}$  NMR (495.1 MHz, DMSO- $d_6$ , TMS):  $\delta$  1.86–1.95 (m, 4H), 2.16–2.18 (m, 2H), 2.60–2.62 (m, 2H), 3.20 (t,  $J = 6.7$  Hz, 2H), 3.43 (t,  $J = 6.5$  Hz, 2H), 4.72 (s, 1H).  $^{13}\text{C}\{^1\text{H}\}$  NMR (124.5 MHz, DMSO- $d_6$ , TMS):  $\delta$  24.65, 24.99, 27.14, 33.80, 47.32, 48.92, 98.54, 174.58, 200.68. MS (EI):  $m/z$  (%) : 151 (85) [ $M^+$ ], 123 (16), 122 (100), 108 (31), 95 (45), 94 (26), 81 (11), 70 (13), 68 (16), 67 (18), 55 (11), 53 (21).



**3ia**

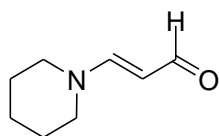
**3-(pyrrolidin-1-yl)cyclohex-2-enone (3ia):**  $^1\text{H}$  NMR (495.1 MHz, DMSO- $d_6$ , TMS):  $\delta$

1.80–1.90 (m, 6H), 2.04 (t,  $J = 6.5$  Hz, 2H), 2.46 (t,  $J = 6.2$  Hz, 2H), 3.12 (t,  $J = 6.2$  Hz, 2H), 3.43 (t,  $J = 6.2$  Hz, 2H), 4.75 (s, 1H).  $^{13}\text{C}\{^1\text{H}\}$  NMR (124.5 MHz, DMSO- $d_6$ , TMS):  $\delta$  21.76, 24.35, 24.88, 27.18, 35.86, 47.46, 47.51, 97.15, 162.90, 193.45. MS (EI):  $m/z$  (%): 165 (70) [ $M^+$ ], 137 (42), 136 (17), 109 (100), 108 (37), 94 (17), 81 (16), 70 (13), 68 (33), 67 (15).



**3gb**

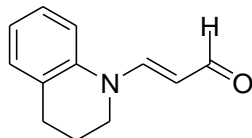
**3-(indolin-1-yl)acrylaldehyde (3gb):**  $^1\text{H}$  NMR (495.1 MHz, DMSO- $d_6$ , TMS):  $\delta$  3.20 (t,  $J = 8.5$  Hz, 2H), 3.83 (t,  $J = 8.5$  Hz, 2H), 5.31 (dd,  $J = 12.8$  and 8.2 Hz, 1H), 6.98 (td,  $J = 7.5$  and 0.8 Hz, 1H), 7.20–7.26 (m, 2H), 7.35 (d,  $J = 8.0$  Hz, 1H), 8.22 (d,  $J = 13.1$  Hz, 1H), 9.27 (d,  $J = 8.2$  Hz, 1H).  $^{13}\text{C}\{^1\text{H}\}$  NMR (124.5 MHz, DMSO- $d_6$ , TMS):  $\delta$  26.98, 47.80, 105.04, 109.24, 123.01, 125.68, 127.61, 131.50, 143.32, 148.59, 189.23. MS (EI):  $m/z$  (%) : 173 (100) [ $M^+$ ], 174 (12), 172 (30), 156 (26), 154 (11), 145 (15), 144 (64), 143 (26), 130 (38), 119 (11), 118 (24), 117 (50), 115 (18), 104 (16), 91 (25), 90 (15), 89 (17), 77 (18), 65 (13), 63 (11), 55 (17).



**3gc**

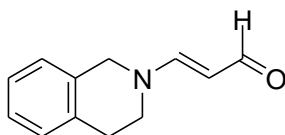
**2-(piperidin-1-yl)acrylaldehyde (3gc):**  $^1\text{H}$  NMR (495.1 MHz, DMSO- $d_6$ , TMS):  $\delta$  1.52–1.62 (m, 6H), 3.23 (brs, 2H), 3.38 (brs, 2H), 5.11 (dd,  $J = 12.8$  and 8.2 Hz, 1H), 7.28 (d,  $J = 12.7$  Hz, 1H), 8.94 (d,  $J = 8.5$  Hz, 1H).  $^{13}\text{C}\{^1\text{H}\}$  NMR (124.5 MHz, DMSO- $d_6$ , TMS):  $\delta$  23.47, 24.52, 26.10, 45.51, 53.71, 99.85, 159.72, 187.98. MS (EI):

$m/z$  (%) : 139 (64) [ $M^+$ ], 138 (19), 122 (100), 110 (24), 96 (10), 94 (11), 84 (13), 83 (15), 82 (26), 80 (15), 70 (14), 56 (13), 55 (32), 54 (18).



**3gd**

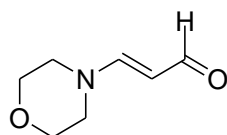
**3-(3,4-dihydroquinolin-1(2H)-yl)acrylaldehyde (3gd):**  $^1\text{H}$  NMR (495.1 MHz, DMSO- $d_6$ , TMS):  $\delta$  1.93 (quin,  $J = 6.2$  Hz, 2H), 2.72 (t,  $J = 6.1$  Hz, 2H), 3.52 (d,  $J = 6.4$  Hz, 2H), 5.49 (dd,  $J = 13.0$  and 8.2 Hz, 1H), 7.01 (td,  $J = 7.5$  and 1.6 Hz, 1H), 7.16–7.17 (m, 1H), 7.22–7.25 (m, 1H), 7.42 (d,  $J = 8.2$  Hz, 1H), 8.14 (d,  $J = 13.0$  Hz, 1H), 9.31 (d,  $J = 8.2$  Hz, 1H).  $^{13}\text{C}\{^1\text{H}\}$  NMR (124.5 MHz, DMSO- $d_6$ , TMS):  $\delta$  21.69, 26.65, 45.90, 105.66, 116.13, 122.89, 127.46, 128.54, 129.04, 139.35, 153.55, 190.46. MS (EI):  $m/z$  (%) : 187 (70) [ $M^+$ ], 188 (10), 186 (13), 171 (15), 170 (100), 158 (40), 143 (11), 131 (10), 130 (61), 117 (26), 115 (13), 103 (12), 91 (12), 77 (20).



**3ge**

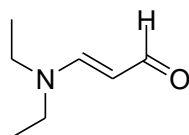
**3-(3,4-dihydroisoquinolin-2(1H)-yl)acrylaldehyde (3ge, *trans*:*cis* = 3:1):**  $^1\text{H}$  NMR (495.1 MHz, DMSO- $d_6$ , TMS): for *trans*-isomer:  $\delta$  2.89 (brs, 2H), 3.67 (brs, 2H), 4.41 (s, 2H), 5.19–5.23 (m, 1H), 7.20–7.21 (m, 4H), 7.54 (d,  $J = 12.8$  Hz, 1H), 9.02 (d,  $J = 8.2$  Hz, 1H); for *cis*-isomer:  $\delta$  2.89 (brs, 2H), 3.45 (brs, 2H), 4.62 (s, 2H), 5.19–5.23 (m, 1H), 7.20–7.21 (m, 4H), 7.54 (d,  $J = 12.8$  Hz, 1H), 9.02 (d,  $J = 8.2$  Hz, 1H).  $^{13}\text{C}\{^1\text{H}\}$  NMR (124.5 MHz, DMSO- $d_6$ , TMS): for the mixture of *cis* and *trans* isomers:  $\delta$  26.86, 28.99, 43.15, 46.67, 49.70, 53.40, 100.36, 100.94, 125.67, 126.35, 126.51, 127.00, 128.19, 128.60, 131.66, 134.03, 134.62, 159.25, 159.73, 188.08. MS (EI):  $m/z$  (%) : 187

(100) [ $M^+$ ], 188 (13), 186 (28), 170 (39), 168 (10), 158 (26), 132 (12), 131 (24), 130 (33), 129 (10), 117 (63), 116 (27), 115 (40), 105 (16), 104 (41), 103 (30), 91 (17), 78 (25), 77 (23).



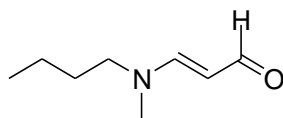
**3gf**

**3-morpholinoacrylaldehyde (3gf):**  $^1\text{H}$  NMR (495.1 MHz, DMSO- $d_6$ , TMS):  $\delta$  3.29 (brs, 2H), 3.41 (brs, 2H), 3.62 (brs, 4H), 5.18 (dd,  $J = 12.9$  and  $8.4$  Hz, 1H), 7.33 (d,  $J = 12.8$  Hz, 1H), 8.99 (d,  $J = 8.5$  Hz, 1H).  $^{13}\text{C}\{^1\text{H}\}$  NMR (124.5 MHz, DMSO- $d_6$ , TMS):  $\delta$  45.17, 52.04, 65.14, 66.30, 100.61, 159.82, 188.26. MS (EI):  $m/z$  (%) : 141 (100) [ $M^+$ ], 124 (93), 112 (18), 111 (12), 96 (12), 94 (28), 84 (36), 83 (32), 82 (34), 68 (13), 57 (10), 56 (19), 55 (92), 54 (50).



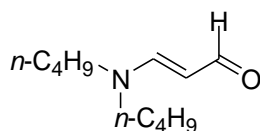
**3gg**

**3-(diethylamino)acrylaldehyde (3gg):**  $^1\text{H}$  NMR (495.1 MHz, DMSO- $d_6$ , TMS):  $\delta$  1.07 (t,  $J = 7.1$  Hz, 3H), 1.15 (t,  $J = 7.2$  Hz, 3H), 3.21 (q,  $J = 7.1$  Hz, 2H), 3.33 (q,  $J = 7.1$  Hz, 2H), 5.02 (dd,  $J = 12.7$  and  $8.5$  Hz, 1H), 7.32 (d,  $J = 12.7$  Hz, 1H), 8.94 (d,  $J = 8.5$  Hz, 1H).  $^{13}\text{C}\{^1\text{H}\}$  NMR (124.5 MHz, DMSO- $d_6$ , TMS):  $\delta$  11.31, 14.51, 42.02, 49.40, 100.15, 159.17, 187.82. MS (EI):  $m/z$  (%) : 127 (100) [ $M^+$ ], 112 (12), 110 (80), 98 (33), 94 (19), 84 (11), 82 (20), 80 (34), 71 (11), 70 (32), 68 (15), 58 (16), 56 (70), 55 (16), 54 (11).



**3gh**

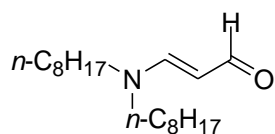
**3-(butyl(methyl)amino)acrylaldehyde (3gh, *trans:cis* = 3:1):**  $^1\text{H}$  NMR (495.1 MHz, DMSO- $d_6$ , TMS): for *trans*-isomer:  $\delta$  0.90 (t,  $J = 7.4$  Hz, 3H), 1.20–1.26 (m, 2H), 1.46–1.54 (m, 2H), 2.78 (s, 3H), 3.31 (t,  $J = 6.9$  Hz, 2H), 4.96 (dd,  $J = 12.5$  and 8.5 Hz, 1H), 7.40 (d,  $J = 12.5$  Hz, 1H), 8.95 (d,  $J = 8.5$  Hz, 1H); for *cis*-isomer:  $\delta$  0.90 (t,  $J = 7.4$  Hz, 3H), 1.26–1.31 (m, 2H), 1.46–1.54 (m, 2H), 3.08 (s, 3H), 3.14 (t,  $J = 7.4$  Hz, 2H), 5.02 (dd,  $J = 12.8$  and 8.5 Hz, 1H), 7.30 (d,  $J = 12.8$  Hz, 1H), 8.92 (d,  $J = 8.5$  Hz, 1H).  $^{13}\text{C}\{^1\text{H}\}$  NMR (124.5 MHz, DMSO- $d_6$ , TMS): for *trans*-isomer:  $\delta$  13.56, 19.04, 30.04, 34.91, 56.50, 100.34, 160.55, 187.65; for *cis*-isomer:  $\delta$  13.70, 19.50, 27.24, 42.36, 49.09, 100.12, 160.71, 187.65. MS (EI):  $m/z$  (%) : 141 (48) [ $M^+$ ], 124 (10), 112 (16), 99 (13), 98 (100), 97 (13), 84 (16), 82 (19), 70 (34), 68 (11), 57 (22), 55 (21).



**3gi**

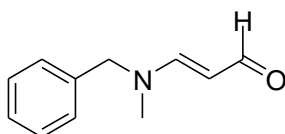
**3-(dibutylamino)acrylaldehyde (3gi):**  $^1\text{H}$  NMR (495.1 MHz, DMSO- $d_6$ , TMS):  $\delta$  0.90 (t,  $J = 7.4$  Hz, 6H), 1.22–1.33 (m, 4H), 1.45–1.55 (m, 4H), 3.13 (t,  $J = 7.6$  Hz, 2H), 3.29 (t,  $J = 7.1$  Hz, 2H), 5.00 (dd,  $J = 12.8$  and 8.5 Hz, 1H), 7.32 (d,  $J = 13.0$  Hz, 1H), 8.93 (d,  $J = 8.5$  Hz, 1H).  $^{13}\text{C}\{^1\text{H}\}$  NMR (124.5 MHz, DMSO- $d_6$ , TMS):  $\delta$  13.59, 13.69, 19.13, 19.58, 27.93, 30.62, 47.40, 54.82, 100.17, 160.03, 187.80. MS (EI):  $m/z$  (%) : 183 (47) [ $M^+$ ], 166 (43), 154 (22), 140 (73), 126 (13), 112 (27), 99 (17), 98 (100), 97 (11), 84 (73), 82 (13), 70 (36), 68 (11), 57 (47), 56 (39), 55 (21).





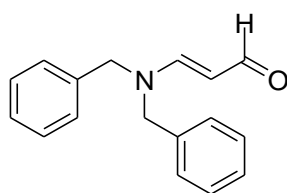
**3gj**

**3-(dioctylamino)acrylaldehyde (3gj):**  $^1\text{H}$  NMR (495.1 MHz, DMSO- $d_6$ , TMS):  $\delta$  0.86 (t,  $J = 6.9$  Hz, 6H), 1.26–1.31 (m, 20H), 1.49–1.56 (m, 4H), 3.11 (t,  $J = 7.5$  Hz, 2H), 3.27 (t,  $J = 7.1$  Hz, 2H), 4.99 (dd,  $J = 12.9$  and 8.4 Hz, 1H), 7.30 (d,  $J = 12.8$  Hz, 1H), 8.93 (d,  $J = 8.5$  Hz, 1H).  $^{13}\text{C}\{^1\text{H}\}$  NMR (124.5 MHz, DMSO- $d_6$ , TMS):  $\delta$  13.88, 22.09, 25.83, 25.86, 26.31, 28.54, 28.67, 28.75, 31.24, 47.67, 55.11, 100.19, 159.91, 187.71. MS (EI):  $m/z$  (%) : 295 (7) [ $M^+$ ], 266 (13), 253 (19), 252 (100), 210 (11), 196 (61), 168 (24), 154 (33), 140 (32), 126 (10), 98 (43), 84 (15), 70 (19), 69 (12), 57 (18), 56 (14), 55 (17).



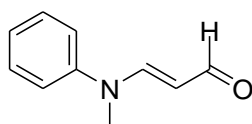
**3gk**

**3-(benzyl(methyl)amino)acrylaldehyde (3gk, *trans*:*cis* = 3:1):**  $^1\text{H}$  NMR (495.1 MHz, DMSO- $d_6$ , TMS): for *trans*-isomer:  $\delta$  2.72 (s, 3H), 4.53 (s, 2H), 5.05 (dd,  $J = 12.7$  and 8.5 Hz, 1H), 7.23–7.41 (m, 5H), 7.68 (d,  $J = 12.5$  Hz, 1H), 9.04 (d,  $J = 8.2$  Hz, 1H); for *cis*-isomer:  $\delta$  3.12 (s, 3H), 4.41 (s, 2H), 5.15 (dd,  $J = 12.5$  and 8.5 Hz, 1H), 7.23–7.41 (m, 5H), 7.47 (d,  $J = 12.7$  Hz, 1H), 8.97 (d,  $J = 8.5$  Hz, 1H).  $^{13}\text{C}\{^1\text{H}\}$  NMR (124.5 MHz, DMSO- $d_6$ , TMS): for *trans*-isomer:  $\delta$  35.07, 60.03, 101.11, 127.21, 127.54, 128.74, 136.83, 160.89, 188.02; for *cis*-isomer:  $\delta$  42.76, 52.77, 101.11, 127.40, 127.77, 128.67, 135.78, 161.22, 188.02. MS (EI):  $m/z$  (%) : 175 (27) [ $M^+$ ], 158 (31), 91 (100), 84 (16), 65 (21).



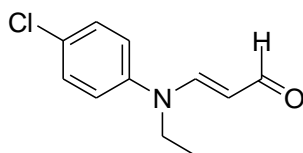
**3gl**

**3-(dibenzylamino)acrylaldehyde (3gl):**  $^1\text{H}$  NMR (495.1 MHz,  $\text{DMSO-}d_6$ , TMS):  $\delta$  4.35 (s, 2H), 4.59 (s, 2H), 5.15 (dd,  $J = 13.1$  and  $8.5$  Hz, 1H), 7.19–7.41 (m, 10H), 7.77 (d,  $J = 13.0$  Hz, 1H), 9.06 (d,  $J = 8.5$  Hz, 1H).  $^{13}\text{C}\{^1\text{H}\}$  NMR (124.5 MHz,  $\text{DMSO-}d_6$ , TMS):  $\delta$  50.85, 58.56, 102.07, 127.08, 127.32, 127.90, 128.60, 128.77, 135.75, 136.77, 160.88, 188.46. MS (EI):  $m/z$  (%) : 251 (8) [ $M^+$ ], 160 (41), 91 (100), 65 (15).



**3gm**

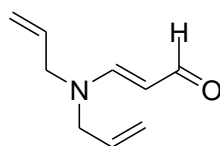
**3-(methyl(phenyl)amino)acrylaldehyde (3gm):**  $^1\text{H}$  NMR (495.1 MHz,  $\text{DMSO-}d_6$ , TMS):  $\delta$  3.29 (s, 3H), 5.41–5.45 (m, 1H), 7.18–7.21 (m, 1H), 7.35–7.37 (m, 2H), 7.40–7.44 (m, 2H), 7.90 (d,  $J = 13.0$  Hz, 1H), 9.25 (d,  $J = 8.2$  Hz, 1H).  $^{13}\text{C}\{^1\text{H}\}$  NMR (124.5 MHz,  $\text{DMSO-}d_6$ , TMS):  $\delta$  36.41, 105.59, 119.82, 124.56, 129.45, 145.64, 156.38, 190.03. MS (EI):  $m/z$  (%) : 161 (54) [ $M^+$ ], 160 (26), 145 (15), 144 (100), 132 (40), 130 (10), 118 (11), 117 (50), 107 (10), 104 (18), 91 (30), 77 (47), 65 (10), 51 (20).



**3gn**

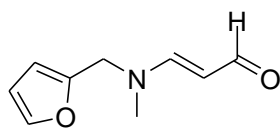
**3-((4-chlorophenyl)(ethyl)amino)acrylaldehyde (3gn):**  $^1\text{H}$  NMR (495.1 MHz,  $\text{DMSO-}d_6$ , TMS):  $\delta$  1.13 (t,  $J = 7.1$  Hz, 3H), 3.77 (q,  $J = 7.2$  Hz, 2H), 5.42 (brs, 1H), 7.35–7.38 (m, 2H), 7.44–7.47 (m, 2H), 7.77 (d,  $J = 13.3$  Hz, 1H), 9.23 (d,  $J = 8.2$  Hz,

1H).  $^{13}\text{C}\{^1\text{H}\}$  NMR (124.5 MHz, DMSO- $d_6$ , TMS):  $\delta$  11.65, 43.93, 105.51, 122.32, 128.92, 129.40, 142.94, 155.30, 190.22. MS (EI):  $m/z$  (%) : 210 (14) [ $M^+$ ], 211 (24), 209 (73), 208 (13), 194 (45), 193 (14), 192 (100), 182 (14), 180 (45), 154 (15), 153 (19), 152 (31), 151 (13), 145 (24), 140 (22), 139 (19), 138 (39), 131 (16), 130 (27), 127 (11), 125 (14), 118 (10), 117 (36), 116 (11), 113 (15), 111 (46), 103 (10), 90 (11), 89 (16), 82 (15), 77 (10), 75 (34).



**3go**

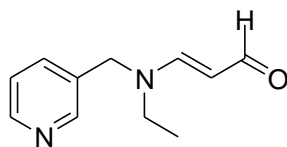
**3-(diallylamino)acrylaldehyde (3go):**  $^1\text{H}$  NMR (495.1 MHz, DMSO- $d_6$ , TMS):  $\delta$  3.79 (d,  $J = 4.8$  Hz, 2H), 3.94 (d,  $J = 5.7$  Hz, 2H), 5.07 (dd,  $J = 12.8$  and 8.5 Hz, 1H), 5.16–5.25 (m, 4H), 5.70–5.77 (m, 1H), 5.83–5.90 (m, 1H), 7.40 (d,  $J = 13.1$  Hz, 1H), 8.96 (d,  $J = 8.5$  Hz, 1H).  $^{13}\text{C}\{^1\text{H}\}$  NMR (124.5 MHz, DMSO- $d_6$ , TMS):  $\delta$  50.05, 57.35, 101.57, 117.39, 118.38, 131.28, 133.80, 160.11, 188.20. MS (EI):  $m/z$  (%) : 151 (11) [ $M^+$ ], 124 (11), 123 (94), 122 (64), 120 (13), 110 (34), 108 (100), 96 (10), 94 (19), 93 (11), 82 (63), 81 (31), 80 (93), 79 (10), 70 (27), 68 (53), 67 (42), 65 (10), 56 (14), 55 (57), 54 (36), 53 (21).



**3gp**

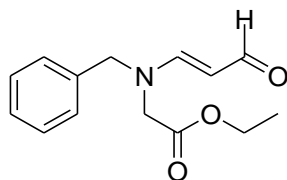
**3-((furan-2-ylmethyl)(methyl)amino)acrylaldehyde (3gp, *trans:cis* = 3:1):**  $^1\text{H}$  NMR (495.1 MHz, DMSO- $d_6$ , TMS): for *trans*-isomer:  $\delta$  2.75 (s, 3H), 4.53 (s, 2H), 5.04 (dd,  $J = 12.8$  and 8.5 Hz, 1H), 6.44–6.45 (m, 2H), 7.56 (d,  $J = 12.7$  Hz, 1H), 7.66 (s, 1H), 9.02 (d,  $J = 8.2$  Hz, 1H); for *cis*-isomer:  $\delta$  3.10 (s, 3H), 4.38 (s, 2H), 5.28 (dd,  $J = 11.9$

and 8.8 Hz, 1H), 6.44–6.45 (m, 2H), 7.34 (d,  $J = 12.5$  Hz, 1H), 7.64 (s, 1H), 8.96 (d,  $J = 7.9$  Hz, 1H).  $^{13}\text{C}\{^1\text{H}\}$  NMR (124.5 MHz,  $\text{DMSO-}d_6$ , TMS): for *trans*-isomer:  $\delta$  34.91, 52.70, 101.46, 109.02, 110.63, 143.42, 150.03, 160.57, 188.09; for *cis*-isomer:  $\delta$  42.39, 45.74, 101.46, 109.02, 110.51, 143.07, 149.27, 160.73, 188.22. MS (EI):  $m/z$  (%) : 165 (29) [ $M^+$ ], 136 (15), 81 (100), 53 (29).



**3gq**

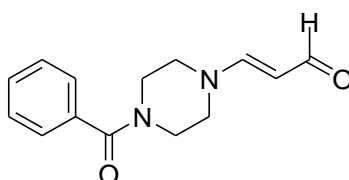
**3-(ethyl(pyridin-3-ylmethyl)amino)acrylaldehyde (3gq, *trans:cis* = 1.2:1):**  $^1\text{H}$  NMR (495.1 MHz,  $\text{DMSO-}d_6$ , TMS): for *trans*-isomer:  $\delta$  1.17 (t,  $J = 7.1$  Hz, 3H), 3.46 (q,  $J = 7.0$  Hz, 2H), 4.51 (s, 2H), 4.92 (dd,  $J = 12.5$  and 8.5 Hz, 1H), 7.22–7.30 (m, 2H), 7.58 (d,  $J = 12.5$  Hz, 1H), 8.53–8.58 (m, 2H), 8.98 (d,  $J = 8.2$  Hz, 1H); for *cis*-isomer:  $\delta$  1.00 (t,  $J = 6.8$  Hz, 3H), 3.17 (q,  $J = 6.7$  Hz, 2H), 4.59 (s, 2H), 5.17 (dd,  $J = 12.7$  and 8.7 Hz, 1H), 7.22–7.30 (m, 2H), 7.56 (d,  $J = 12.7$  Hz, 1H), 8.53–8.58 (m, 2H), 9.03 (d,  $J = 8.2$  Hz, 1H).  $^{13}\text{C}\{^1\text{H}\}$  NMR (124.5 MHz,  $\text{DMSO-}d_6$ , TMS): for the mixture of *cis* and *trans* isomers:  $\delta$  10.89, 14.37, 42.73, 49.95, 50.70, 56.51, 101.15, 101.87, 121.92, 122.50, 145.62, 146.52, 149.79, 149.97, 160.16, 160.38, 188.25, 188.39. MS (EI):  $m/z$  (%) : 190 (59) [ $M^+$ ], 173 (58), 161 (34), 133 (13), 132 (10), 106 (21), 98 (51), 93 (62), 92 (100), 80 (25), 70 (13), 65 (54), 56 (20).



**3gr**

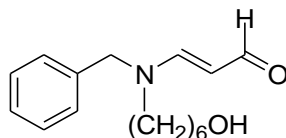
**ethyl 2-(benzyl(3-oxoprop-1-en-1-yl)amino)acetate (3gr, *trans:cis* = 1:0.9):**  $^1\text{H}$  NMR

(495.1 MHz, DMSO- $d_6$ , TMS): for *trans*-isomer:  $\delta$  1.15 (t,  $J = 7.2$  Hz, 3H), 4.00 (s, 2H), 4.07 (q,  $J = 7.1$  Hz, 2H), 4.57 (s, 2H), 4.41 (s, 2H), 5.02 (dd,  $J = 12.7$  and 8.5 Hz, 1H), 7.26–7.38 (m, 5H), 7.67 (d,  $J = 13.0$  Hz, 1H), 9.04 (d,  $J = 8.0$  Hz, 1H); for *cis*-isomer:  $\delta$  1.19 (t,  $J = 7.1$  Hz, 3H), 4.12 (q,  $J = 6.9$  Hz, 2H), 4.28 (s, 2H), 4.46 (s, 2H), 5.16 (dd,  $J = 12.5$  and 8.2 Hz, 1H), 7.26–7.38 (m, 5H), 7.47 (d,  $J = 13.0$  Hz, 1H), 8.99 (d,  $J = 8.2$  Hz, 1H).  $^{13}\text{C}\{^1\text{H}\}$  NMR (124.5 MHz, DMSO- $d_6$ , TMS): for the mixture of *cis* and *trans* isomers:  $\delta$  14.01, 49.18, 52.58, 55.84, 59.01, 60.87, 60.93, 102.20, 102.87, 127.40, 127.92, 128.13, 128.57, 128.66, 135.76, 136.37, 160.83, 161.51, 167.84, 169.45, 188.60. MS (EI):  $m/z$  (%) : 247 (12) [ $M^+$ ], 174 (21), 91 (100), 65 (12).



**3gs**

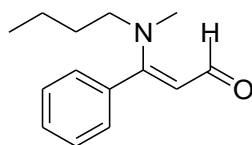
**3-(4-benzoylpiperazin-1-yl)acrylaldehyde (3gs):**  $^1\text{H}$  NMR (495.1 MHz, DMSO- $d_6$ , TMS):  $\delta$  3.38 (brs, 6H), 3.68 (brs, 2H), 5.19 (brs, 1H), 7.39 (d,  $J = 12.8$  Hz, 1H), 7.43–7.50 (m, 5H), 9.01 (d,  $J = 8.2$  Hz, 1H).  $^{13}\text{C}\{^1\text{H}\}$  NMR (124.5 MHz, DMSO- $d_6$ , TMS):  $\delta$  40.51, 41.96, 44.68, 45.85, 47.34, 51.98, 101.01, 127.03, 128.51, 129.76, 135.52, 159.73, 169.31, 188.38. MS (EI):  $m/z$  (%) : 190 (13), 134 (22), 122 (14), 105 (94), 85 (48), 77 (54), 69 (100), 58 (14), 57 (10), 56 (69), 51 (17).



**3gt**

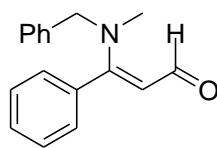
**3-(benzyl(6-hydroxyhexyl)amino)acrylaldehyde (3gt, *trans:cis* = 1:1):**  $^1\text{H}$  NMR (495.1 MHz, DMSO- $d_6$ , TMS): for *trans*-isomer:  $\delta$  1.22–1.31 (m, 4H), 1.34–1.45 (m,

4H), 3.34–3.38 (m, 4H), 4.36–4.37 (brs, 1H), 4.53 (s, 2H), 5.05 (dd,  $J = 12.8$  and  $8.5$  Hz, 1H), 7.23–7.40 (m, 5H), 7.60 (d,  $J = 12.7$  Hz, 1H), 9.01 (d,  $J = 8.5$  Hz, 1H); for *cis*-isomer:  $\delta$  1.22–1.31 (m, 4H), 1.34–1.45 (m, 2H), 1.56 (quin,  $J = 7.1$  Hz, 2H), 3.06 (t,  $J = 7.5$  Hz, 2H), 3.34–3.38 (m, 2H), 4.36–4.37 (brs, 1H), 4.44 (s, 2H), 5.10 (dd,  $J = 13.0$  and  $8.5$  Hz, 1H), 7.23–7.40 (m, 5H), 7.51 (d,  $J = 12.8$  Hz, 1H), 8.97 (d,  $J = 8.5$  Hz, 1H).  $^{13}\text{C}\{^1\text{H}\}$  NMR (124.5 MHz, DMSO- $d_6$ , TMS): for the mixture of *cis* and *trans* isomers:  $\delta$  25.19, 25.48, 25.81, 26.12, 28.44, 32.41, 47.54, 51.01, 55.44, 58.38, 60.59, 100.73, 101.44, 127.00, 127.27, 127.79, 128.61, 128.72, 136.33, 137.13, 160.59, 160.70, 188.21. MS (EI):  $m/z$  (%) : 261 (6) [ $M^+$ ], 218 (12), 91 (100), 65 (10).



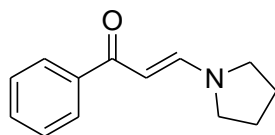
**3ah**

**3-(butyl(methyl)amino)-3-phenylacrylaldehyde (3ah, *cis:trans* = 2.8:1):**  $^1\text{H}$  NMR (495.1 MHz, DMSO- $d_6$ , TMS): for *cis*-isomer:  $\delta$  0.67 (brs, 2H), 0.99–1.00 (brs, 2H), 1.38 (brs, 3H), 2.94–2.98 (m, 5H), 5.20 (d,  $J = 7.6$  Hz, 1H), 7.30 (brs, 2H), 7.48–7.52 (m, 3H), 8.41 (d,  $J = 8.5$  Hz, 1H); for *trans*-isomer:  $\delta$  0.67 (brs, 2H), 0.99–1.00 (brs, 2H), 1.62 (brs, 3H), 2.64 (brs, 5H), 5.28 (brs, 1H), 7.30 (brs, 2H), 7.48–7.52 (m, 3H), 8.41 (d,  $J = 8.5$  Hz, 1H).  $^{13}\text{C}\{^1\text{H}\}$  NMR (124.5 MHz, DMSO- $d_6$ , TMS): for the mixture of *cis* and *trans* isomers:  $\delta$  13.40, 13.78, 19.06, 19.58, 27.27, 30.00, 37.15, 51.04, 51.68, 101.60, 102.23, 128.40, 128.80, 129.07, 129.21, 133.70, 134.14, 166.97, 167.44, 188.31. MS (EI):  $m/z$  (%) : 217 (52) [ $M^+$ ], 216 (35), 201 (11), 200 (74), 188 (45), 175 (48), 174 (54), 160 (35), 158 (44), 156 (11), 146 (30), 144 (20), 133 (1), 132 (98), 130 (10), 118 (78), 117 (18), 116 (10), 115 (13), 105 (14), 104 (22), 103 (100), 102 (24), 91 (29), 86 (15), 77 (74), 72 (40), 58 (12), 55 (10), 51 (14).



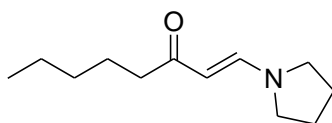
**3ak**

**3-(benzyl(methyl)amino)-3-phenylacrylaldehyde (3ak, *cis:trans* = 3:1):**  $^1\text{H}$  NMR (495.1 MHz, DMSO- $d_6$ , TMS): for *cis*-isomer:  $\delta$  2.92 (s, 3H), 4.22 (s, 2H), 5.33 (d,  $J = 7.4$  Hz, 1H), 7.11–7.47 (m, 10H), 8.52 (brs, 1H); for *trans*-isomer:  $\delta$  2.75 (s, 3H), 4.67 (s, 2H), 5.33 (d,  $J = 7.4$  Hz, 1H), 7.11–7.47 (m, 10H), 8.52 (brs, 1H).  $^{13}\text{C}\{^1\text{H}\}$  NMR (124.5 MHz, DMSO- $d_6$ , TMS): for *cis*-isomer:  $\delta$  37.45, 55.13, 102.83, 126.71, 127.34, 128.55, 128.70, 129.08, 129.43, 133.52, 136.95, 167.61, 188.81; for *trans*-isomer: 37.45, 54.67, 102.83, 126.71, 127.34, 128.55, 128.70, 129.08, 129.43, 133.52, 136.95, 167.61, 188.81. MS (EI):  $m/z$  (%) : 251 (32) [ $M^+$ ], 250 (22), 235 (18), 234 (93), 222 (21), 160 (26), 118 (88), 103 (25), 91 (100), 77 (24), 65 (25).



**5aa**

**1-phenyl-3-(pyrrolidin-1-yl)prop-2-en-1-one (5aa):**  $^1\text{H}$  NMR (495.1 MHz, DMSO- $d_6$ , TMS):  $\delta$  1.84 (quin,  $J = 6.6$  Hz, 2H), 1.95 (quin,  $J = 6.8$  Hz, 2H), 3.25 (t,  $J = 6.8$  Hz, 2H), 3.56 (t,  $J = 6.7$  Hz, 2H), 5.73 (d,  $J = 12.2$  Hz, 1H), 7.41–7.44 (m, 2H), 7.46–7.49 (m, 1H), 7.85–7.89 (m, 3H).  $^{13}\text{C}\{^1\text{H}\}$  NMR (124.5 MHz, DMSO- $d_6$ , TMS):  $\delta$  24.70, 24.82, 46.87, 51.97, 91.86, 127.15, 128.17, 130.73, 140.29, 149.79, 185.58. MS (EI):  $m/z$  (%) : 201 (100) [ $M^+$ ], 202 (15), 200 (17), 184 (22), 172 (55), 132 (27), 131 (19), 124 (34), 106 (16), 105 (41), 96 (68), 82 (12), 79 (11), 78 (10), 77 (48), 70 (59), 68 (21), 55 (12), 51 (16).



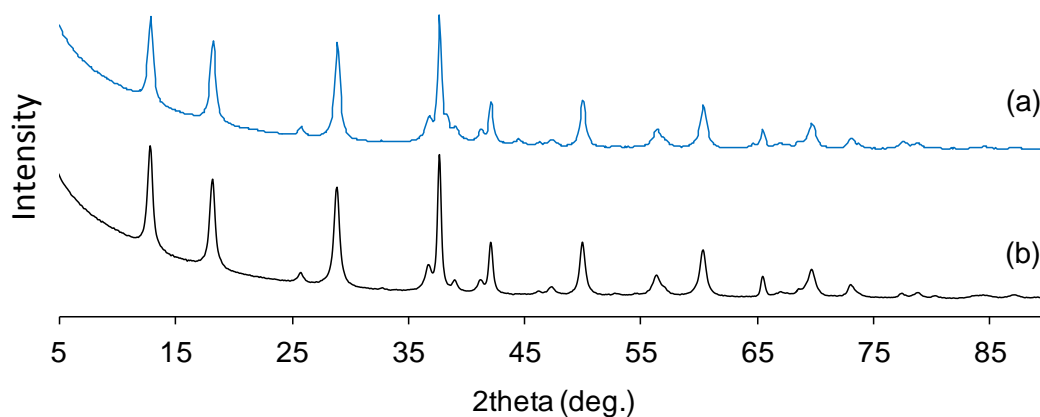
**5fa**

**1-(pyrrolidin-1-yl)oct-1-en-3-one (5fa):**  $^1\text{H}$  NMR (495.1 MHz,  $\text{DMSO-}d_6$ , TMS):  $\delta$  0.85 (t,  $J = 7.1$  Hz, 3H), 1.18–1.31 (m, 4H), 1.48 (quin,  $J = 7.4$  Hz, 2H), 1.82–1.90 (m, 4H), 2.22 (t,  $J = 7.4$  Hz, 2H), 3.06 (brs, 2H), 3.46 (brs, 2H), 4.87 (d,  $J = 12.8$  Hz, 1H), 7.65 (d,  $J = 12.7$  Hz, 1H).  $^{13}\text{C}\{^1\text{H}\}$  NMR (124.5 MHz,  $\text{DMSO-}d_6$ , TMS):  $\delta$  13.89, 22.07, 24.75, 25.00, 31.25, 46.32, 51.55, 96.46, 147.85, 195.18. MS (EI):  $m/z$  (%) : 195 (17) [ $M^+$ ], 139 (23), 124 (100), 106 (13), 97 (20), 96 (14).

### 4.3. Results and Discussion

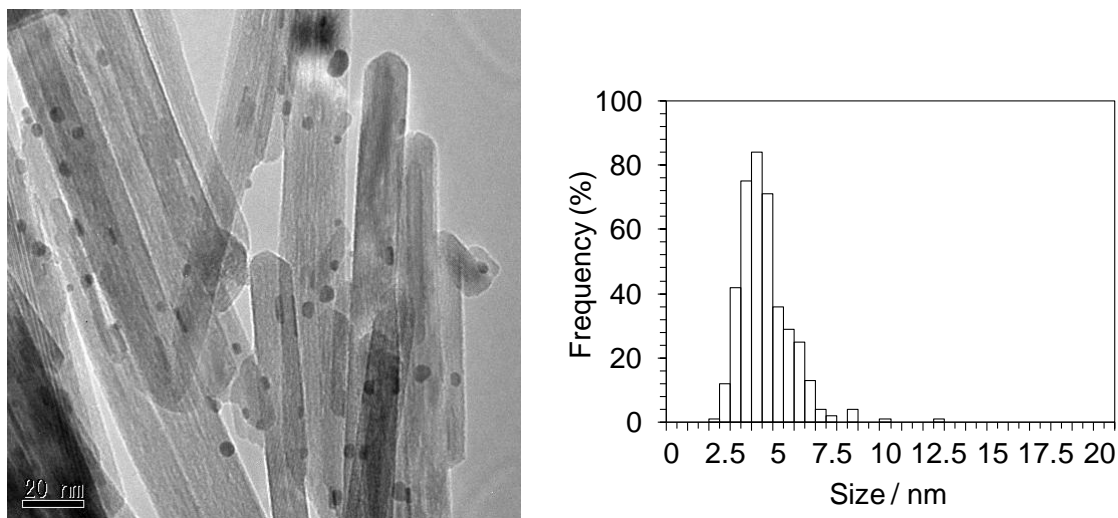
#### 4.3.1. Characterization of Au/OMS-2 Catalyst

Comparison of the XRD patterns of OMS-2 and Au/OMS-2, as shown in Figure 4-3, reveals that the structure of OMS-2 remained unchanged after immobilization of gold nanoparticles according to the procedure described in section 4.2.2. From the TEM images of Au/OMS-2, the average gold particle size was 4.1 nm (Figure 4-4).



**Figure 4-3.** XRD patterns of (a) Au/OMS-2 and (b) OMS-2.





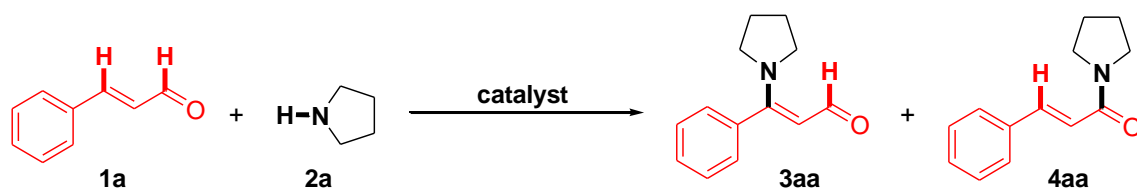
**Figure 4-4.** TEM image and Au particle size distribution of Au/OMS-2 (average: 4.1 nm,  $\sigma$ : 1.2 nm). The size distribution was determined using 400 particles.

#### 4.3.2. Optimization of the Reaction Conditions

Various supported metal catalysts (such as gold, palladium, ruthenium, rhodium, and copper on various supports; given in the format: metal/support) were initially subjected to the dehydrogenative amination of cinnamaldehyde (**1a**) with pyrrolidine (**2a**) to 3-phenyl-3-(1-pyrrolidinyl)-2-propenal (**3aa**) at 50 °C in 1 atm of air (Table 4-1). No amination proceeded in the absence of catalysts or in the presence of Pd/Al<sub>2</sub>O<sub>3</sub>, Cu/Al<sub>2</sub>O<sub>3</sub>, Ru/Al<sub>2</sub>O<sub>3</sub>, and Rh/Al<sub>2</sub>O<sub>3</sub> (Table 4-1, entries 1–4 and 13). Confirmed by a separate experiment, the homogeneous palladium-catalyzed system developed by Ishii and co-workers was turned out to be inefficient for the amination of  $\alpha,\beta$ -unsaturated aldehydes.<sup>[5e,f]</sup> Specifically, when the amination of **1a** with **2a** was carried out using a combined catalyst of PdCl<sub>2</sub>(CH<sub>3</sub>CN)<sub>2</sub> (5 mol%)/H<sub>5</sub>PV<sub>2</sub>Mo<sub>10</sub>O<sub>40</sub> (1 mol%)/hydroquinone system (20 mol%)<sup>[5e,f]</sup> under the conditions described in Table 4-1 (dimethylformamide was used as a solvent instead of THF), **1a** was mostly decomposed to benzaldehyde (retro-aldol reaction; 18 % yield) and other unidentified byproducts.<sup>[7]</sup> In contrast, when

using Au/Al<sub>2</sub>O<sub>3</sub> as the catalyst, 44 % yield of **3aa** was obtained. Among various supports examined, such as Al<sub>2</sub>O<sub>3</sub>, TiO<sub>2</sub>, Co<sub>3</sub>O<sub>4</sub>, and OMS-2, OMS-2 showed the best performance. In this case, the yield of **3aa** increased up to 83 % (Table 4-1, entry 8).<sup>[15]</sup> When the reaction was carried out under an Ar atmosphere in the presence of Au/OMS-2, 52% yield of **3aa** was obtained (Table 4-1, entry 9). In sharp contrast, only a trace amount of **3aa** was obtained when using Au/TiO<sub>2</sub> as the catalyst under an Ar atmosphere (Table 4-1, entry 10). These results indicate that OMS-2 could function as not only a support for gold nanoparticles but also an oxidant for the present amination. The oxidation ability of OMS-2 is likely responsible for the high performance of OMS-2.<sup>[8]</sup> A physical mixture of Au/TiO<sub>2</sub> and OMS-2 afforded almost the same yield of **3aa** as Au/TiO<sub>2</sub> (Table 4-1, entry 11). OMS-2 alone was not effective for the amination (Table 4-1, entry 12). Therefore, highly dispersed gold nanoparticles on OMS-2 likely play an important role for the present amination.<sup>[16]</sup>

**Table 4-1.** The amination of cinnamaldehyde (**1a**) with pyrrolidine (**2a**) in the presence of various catalysts.<sup>[a]</sup>



Entry	Catalysts	Conv. of <b>1a</b> [%]	Yield [%]	
			<b>3aa</b>	<b>4aa</b>
1	Pd/Al <sub>2</sub> O <sub>3</sub>	80	<1	1
2	Cu/Al <sub>2</sub> O <sub>3</sub>	85	<1	<1
3	Ru/Al <sub>2</sub> O <sub>3</sub>	78	<1	<1
4	Rh/Al <sub>2</sub> O <sub>3</sub>	80	<1	<1
5	Au/Al <sub>2</sub> O <sub>3</sub>	90	44	1
6	Au/TiO <sub>2</sub>	90	41	2
7	Au/Co <sub>3</sub> O <sub>4</sub>	97	69	2
8	Au/OMS-2	>99	83	4
9 <sup>[b]</sup>	Au/OMS-2	98	52	6
10 <sup>[b]</sup>	Au/TiO <sub>2</sub>	92	3	4
11 <sup>[c]</sup>	Au/TiO <sub>2</sub> + OMS-2	92	37	2
12	OMS-2	83	<1	<1
13	None	83	<1	<1

[a] Reaction conditions: **1a** (0.5 mmol), **2a** (1.0 mmol), catalyst (metal: 3.6 mol%), THF (1.9 mL), H<sub>2</sub>O (0.1 mL), 50 °C, 1.5 h, air (1 atm). Conversion and yield were determined by GC analysis. [b] Ar (1 atm). [c] A physical mixture of Au/TiO<sub>2</sub> (3.6 mol%) and OMS-2 (100 mg).

The presence of small amounts of water could significantly promote the amination. However, in the presence of large amounts of water, the corresponding amidation byproduct **4aa** largely increased (Table 4-2).

**Table 4-2.** Effect of amounts of water on the amination of cinnamaldehyde (**1a**) with pyrrolidine (**2a**).<sup>[a]</sup>

Entry	THF/H <sub>2</sub> O (v/v = mL/mL)	Conv. of <b>1a</b> [%]	Yield [%]	
			<b>3aa</b>	<b>4aa</b>
1	2:0	>99	31	Trace
2	1.95:0.05	99	73	1
3	1.9:0.1	>99	82	2
4	1.8:0.2	>99	80	5
5	1.6:0.4	>99	58	17
6 <sup>[b]</sup>	0:2	>99	21	41

[a] Reaction conditions: **1a** (0.5 mmol), **2a** (2.0 mmol), Au/OMS-2 (Au: 3.6 mol%), 50 °C, 1.5 h, air (1 atm). [b] 2 h. Conversion and yield were determined by GC analysis.

To obtain a high yield of **3aa**, at least 2 equiv of **2a** were required (Table 4-3). No significant improvement of the yield of **3aa** was observed even if the amount of **2a** was increased to 2 equiv with respect to **1a**.

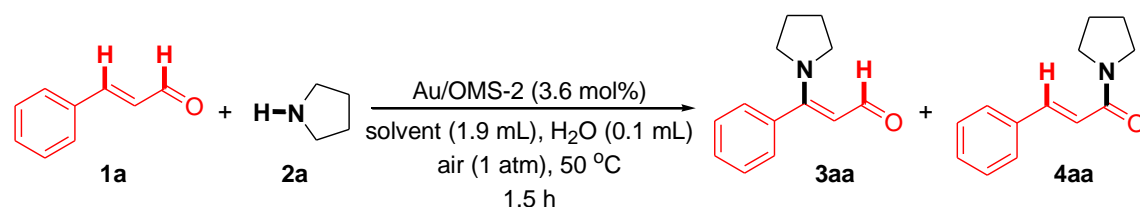
**Table 4-3.** Effect of amounts of pyrrolidine (**2a**) on the amination of cinnamaldehyde (**1a**) with (**2a**).<sup>[a]</sup>

Entry	Amount of <b>2a</b> [mmol]	Conv. of <b>1a</b> [%]	Yield [%]	
			<b>3aa</b>	<b>4aa</b>
1	0.5	78	59	2
2	1	>99	83	4
3	1.5	>99	77	3
4	2	>99	82	2

[a] Reaction conditions: **1a** (0.5 mmol), Au/OMS-2 (Au: 3.6 mol%), THF (1.9 mL), H<sub>2</sub>O (0.1 mL), 50 °C, 1.5 h, air (1 atm). Conversion and yield were determined by GC analysis.

A broad range of solvents could be utilized for the present amination. Among various solvents examined, such as tetrahydrofuran (THF), acetonitrile, *N,N*-dimethylformamide (DMF), toluene, dimethylsulfoxide (DMSO), *N*-methylpyrrolidone (NMP), *N,N*-dimethylacetamide (DMA), 1,4-dioxane, ethanol, ethyl acetate, dimethylcarbonate, and 1,2-dichloroethane, tetrahydrofuran (THF) was the most effective solvent (Table 4-4).

**Table 4-4.** Effect of solvents on the amination of cinnamaldehyde (**1a**) with (**2a**).<sup>[a]</sup>



Entry	Solvent	Conv. of <b>1a</b> [%]	Yield [%]	
			<b>3aa</b>	<b>4aa</b>
1	tetrahydrofuran	>99	83	4
2	acetonitrile	>99	18	2
3	<i>N,N</i> -dimethylformamide	>99	73	3
4 <sup>[b]</sup>	toluene	>99	85	1
5	dimethylsulfoxide	97	48	2
6	<i>N</i> -methylpyrrolidone	96	72	2
7	<i>N,N</i> -dimethylacetamide	99	68	3
8	1,4-dioxane	99	61	1
9	ethanol	>99	34	8
10	ethyl acetate	>99	68	6
11	dimethylcarbonate	>99	66	3
12	1,2-dichloroethane	>99	54	3
13 <sup>[c]</sup>	tetrahydrofuran	>99	85	8

[a] Reaction conditions: **1a** (0.5 mmol), **2a** (1.0 mmol), Au/OMS-2 (Au: 3.6 mol%), solvent (1.9 mL), H<sub>2</sub>O (0.1 mL), 50 °C, 1.5 h, air (1 atm). Conversion and yields were determined by GC analysis. [b] Without addition of H<sub>2</sub>O, 6 h. [c] 60 °C.

### 4.3.3. Substrate Scope

The scope of the present Au/OMS-2-catalyzed amination was investigated using air as the terminal oxidant. Under the optimized reaction conditions, a large variety of structurally diverse enaminals could be synthesized by using Au/OMS-2 as the catalyst (Scheme 4-3). The isolation of the desired enaminal product is very simple (see section 4-2-3), and the isolated yields are summarized in Scheme 4-3.

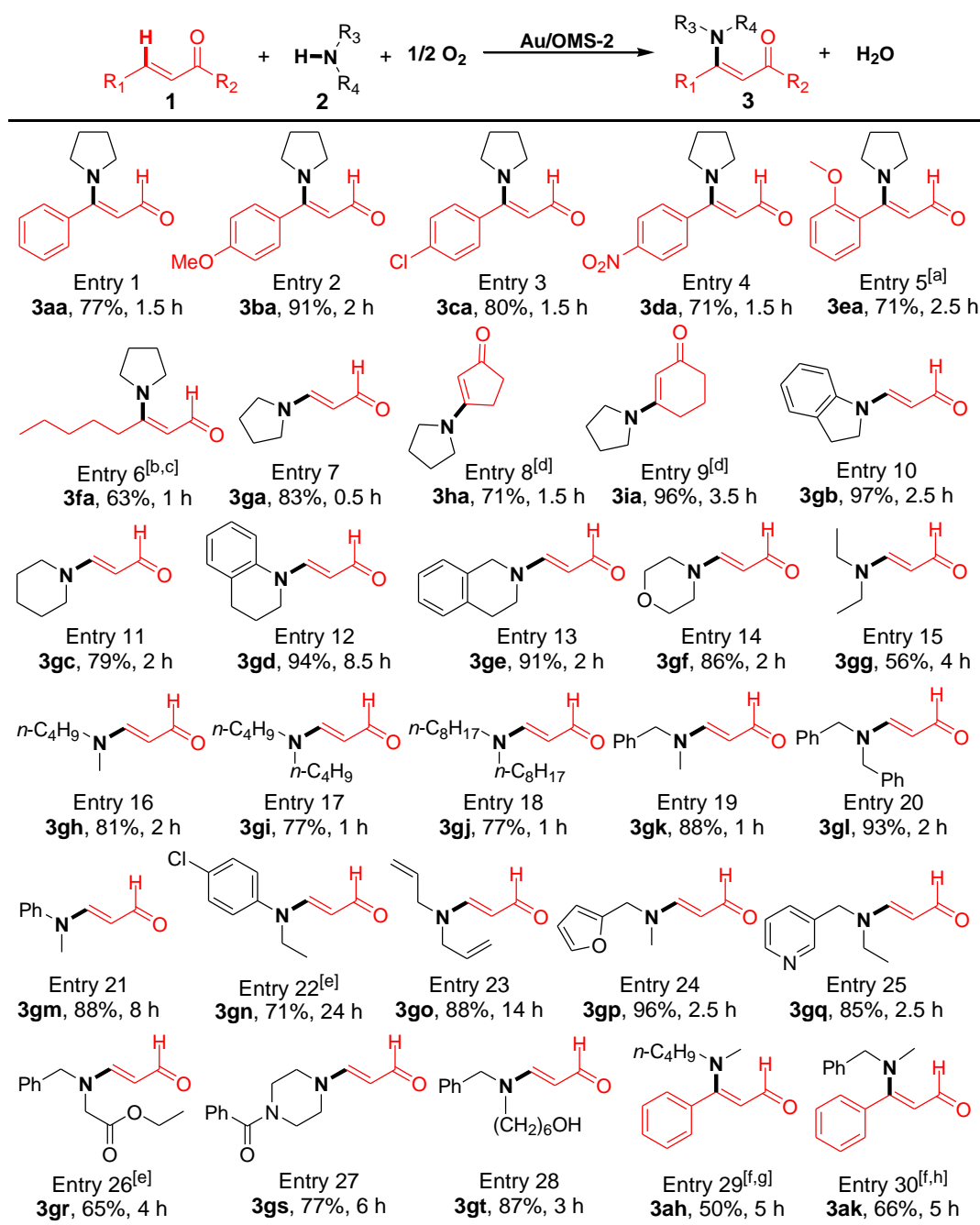
The amination of various substituted cinnamaldehydes with **2a** was efficiently proceeded to give the corresponding enaminals (Scheme 4-3, entries 1–5). An aliphatic  $\alpha,\beta$ -unsaturated aldehyde also reacted smoothly with **2a**, affording **3fa** together with a moderate yield of an enaminone (**5fa**) (Scheme 4-3, entry 6). Acrolein, which is unstable and readily polymerized or oxidized, could efficiently react with **2a** to afford the corresponding  $\beta$ -aminoacrolein in a high yield (Scheme 4-3, entry 7).  $\alpha,\beta$ -Unsaturated ketones were also good substrates for the present amination, affording the corresponding enaminoxones (Scheme 4-3, entries 8 and 9).

Considering the importance of  $\beta$ -aminoacroleins in synthetic organic chemistry,<sup>[1,2]</sup> acrolein was mainly employed as a coupling partner for the examination of the scope of amines. The amination of acrolein with various aliphatic amines efficiently proceeded to give the corresponding  $\beta$ -aminoacroleins (Scheme 4-3, entries 10–18). Benzylic amines and aniline derivatives also smoothly reacted with acrolein (Scheme 4-3, entries 19–22). The allyl group remained intact when diallylamine was subjected to the present amination (Scheme 4-3, entry 23). Amines containing heterocycles, such as furan and pyridine, were also excellent amination reagents for acrolein (Scheme 4-3, entries 24 and 25). Functionalized amines with ester and amide groups were also compatible with the present amination (Scheme 4-3, entries 26 and 27). The

amination of acrolein with a secondary amine containing an alcohol functionality also proceeded efficiently (Scheme 4-3, entry 28). The combination of **1a** with various secondary amines also gave the corresponding enaminals (Scheme 4-3, entries 29 and 30).

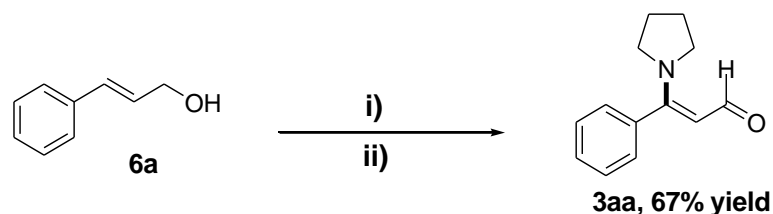
It is noticeable that **3aa** could also successfully be synthesized in 67% yield starting from cinnamylalcohol (**6a**) by a one-pot sequential procedure of oxidation of **6a** followed by amination with **2a** (Scheme 4-4). In this case, Au/OMS-2 could promote both the oxidative dehydrogenation of alcohols and the amination of  $\alpha,\beta$ -unsaturated aldehydes.

As described above, in the case of the amination of 2-octenal (**1f**) with **2a**, the corresponding enaminoone **5fa** was obtained as a byproduct, which can be regarded as a Wacker-type oxidation product. By simply adding amines and water to the reaction solution after the Au/OMS-2-catalyzed amination completed, the enaminoone products were obtained in high yields starting from  $\alpha,\beta$ -unsaturated aldehydes and pyrrolidine. Specifically, from the one-pot reaction of **1a** and **1f** with pyrrolidine, enaminoones **5aa** and **5fa** could efficiently be synthesized (Scheme 4-5). This one-pot procedure represents the first example of formal Wacker-type oxidation of  $\alpha,\beta$ -unsaturated aldehydes.<sup>[15]</sup>

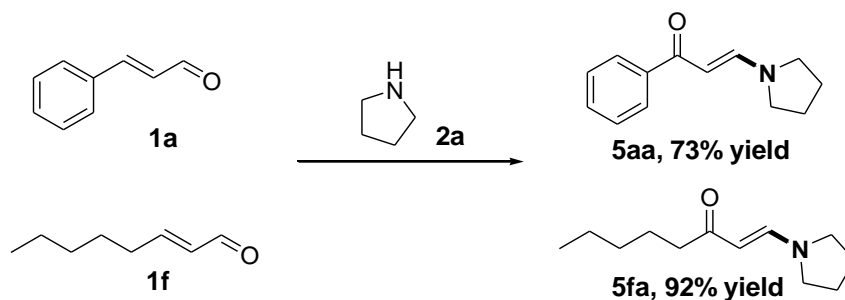


**Scheme 4-3.** Aerobic dehydrogenative amination of  $\alpha,\beta$ -unsaturated aldehydes. Reaction conditions: **1** (0.5 mmol), **2** (1.0 mmol), Au/OMS-2 (3.6 mol%), THF (1.9 mL), H<sub>2</sub>O (0.1 mL), 50 °C, air (1 atm). Yields (based on **1**) of isolated products are shown. Major byproducts were amidation products **4** (<5 % yield, except for **4ea**). See section 4.2.4 for the *E/Z* ratios of products. [a] **4ea** was obtained as an amination byproduct (24 % yield). [b] THF (2 mL), without addition of H<sub>2</sub>O. [c] **5fa** (see Scheme 4-5) was obtained as a byproduct (28 % yield). [d] **2** (2.0 mmol), THF (1.8 mL), H<sub>2</sub>O (0.2 mL). [e] THF (1.8 mL), H<sub>2</sub>O (0.2 mL). [f] Toluene (2 mL). [g] 60 °C. [h] 70 °C.





**Scheme 4-4.** One-pot synthesis of **3aa** from **6a** and **2a**. Reaction conditions: i) **6a** (0.5 mmol), Au/OMS-2 (3.6 mol%), toluene (2 mL), 100 °C, 1 h, O<sub>2</sub> (1 atm). Then, ii) **2a** (1.0 mmol) was added to the reaction mixture followed by stirring at 50 °C for an additional 6 h. Yield was determined by GC analysis.

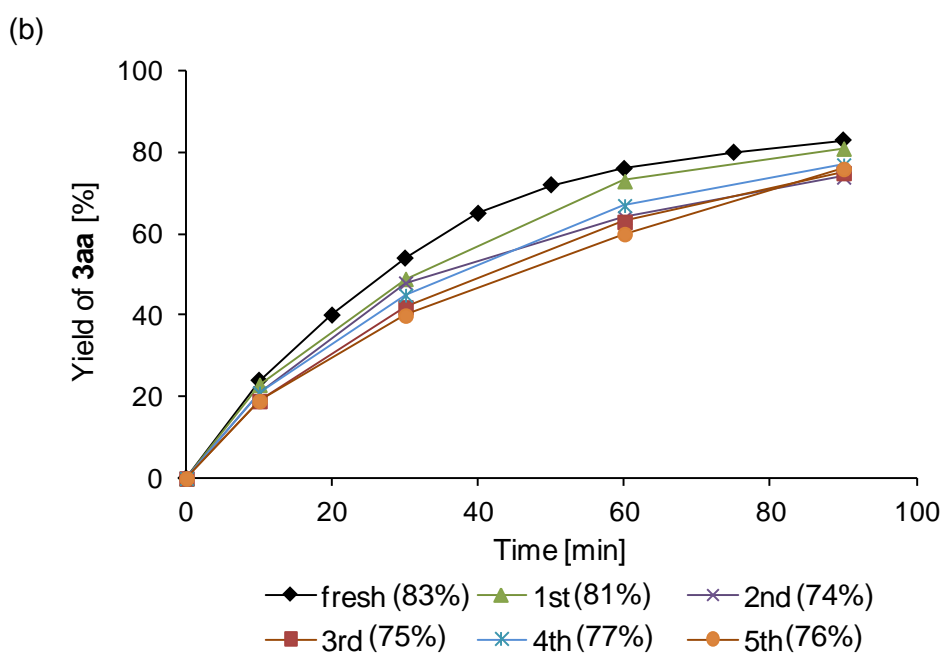
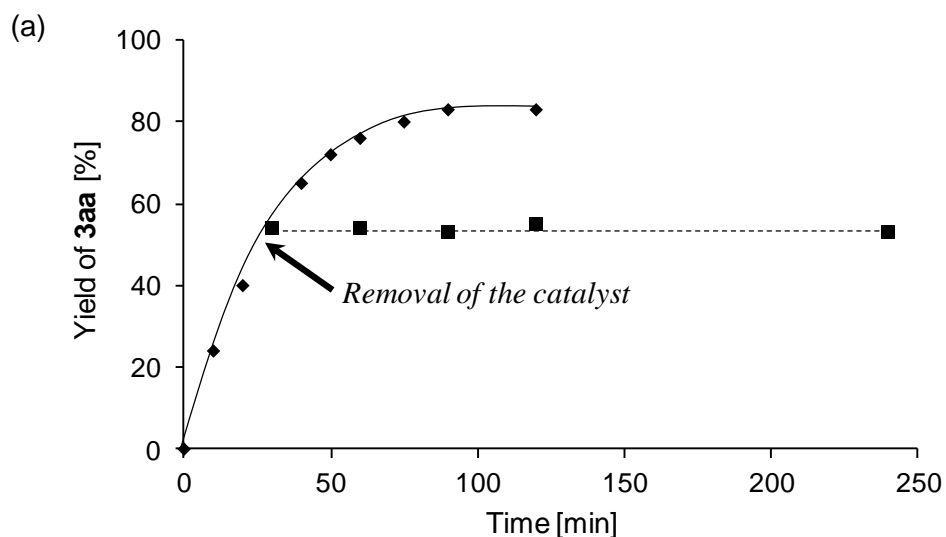
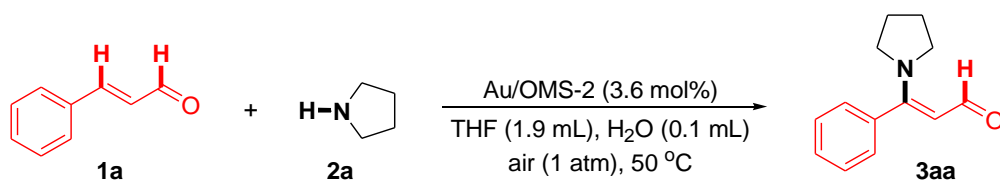


**Scheme 4-5.** One-pot synthesis of enaminones from  $\alpha,\beta$ -unsaturated aldehydes and **2a**. Reaction conditions: **1** (0.5 mmol), **2a** (1.0 mmol), Au/OMS-2 (3.6 mol%), THF (1.9 mL), H<sub>2</sub>O (0.1 mL), 50 °C, 1.5 h, air (1 atm). Then, the catalyst was filtered off, followed by the addition of **2a** (2.0 mmol) and H<sub>2</sub>O (0.1 mL) to the filtrate. For **1a**, the filtrate was stirred at 60 °C for an additional 24 h. For **1f**, 50 °C for an additional 3 h. Yields (based on **1**) of isolated products are shown.

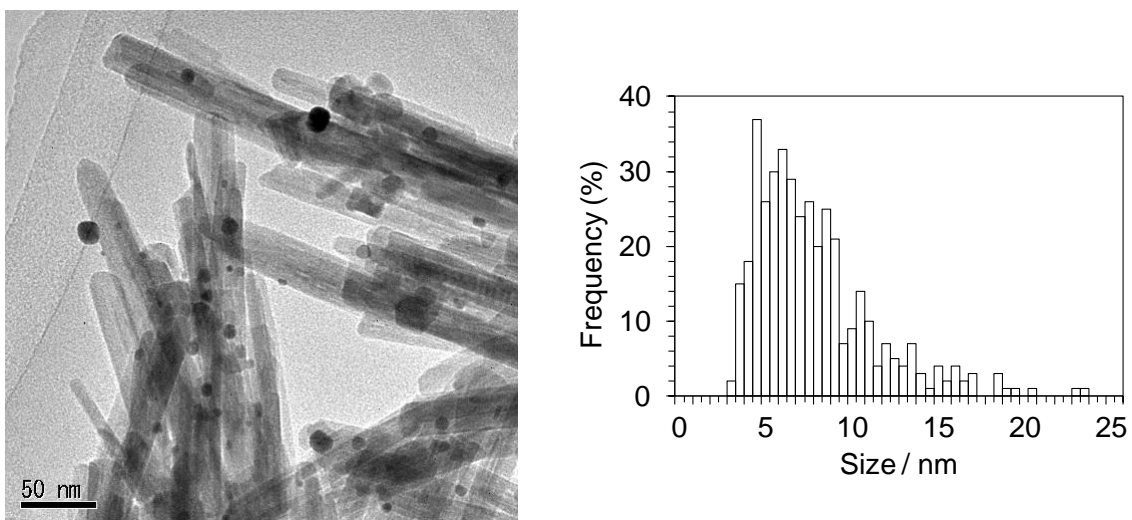
#### 4.3.4. Recyclability and Heterogeneous Catalysis of Au/OMS-2

In order to verify whether the observed catalysis was truly heterogeneous or not, the Au/OMS-2 catalyst was separated by hot filtration, and the reaction was carried out with the filtrate under the same reaction conditions described in Table 4-1. In this case, the amination of **1a** with **2a** was completely stopped by removal of the catalyst (Figure 4-4, a). In addition, gold and manganese species were barely detected in the filtrate (under detection limit: Au: <0.002 %, Mn: <0.00001 %) by inductively coupled plasma atomic emission spectroscopic (ICP-AES) analysis. These results indicate that the observed catalysis for the present amination is intrinsically heterogeneous.<sup>[16]</sup>

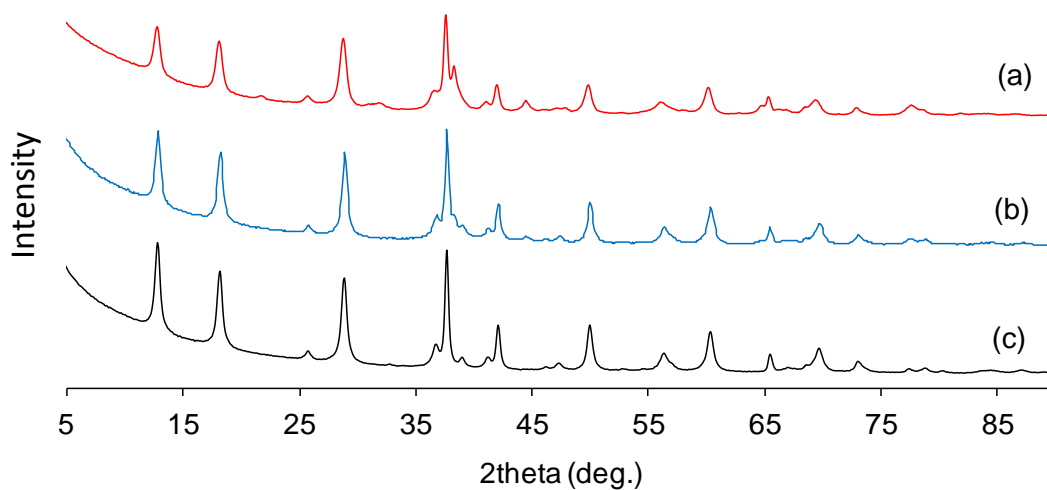
After the amination of **1a** with **2a**, the Au/OMS-2 catalyst could easily be retrieved by simple filtration with >97 % recovery, and the retrieved catalyst could be reused at least five times for the same reaction without a significant loss of its high catalytic performance. Although slight decreases in the reaction rates, for example,  $0.20 \text{ mM h}^{-1}$  for the fifth reuse experiment vs.  $0.27 \text{ mM h}^{-1}$  for the first run with the fresh catalyst, were observed, 76 % yield of **3aa** was still obtained for 1.5 h even at the fifth reuse experiment (Figure 4-4, b, 83% yield for the first run). The average particle size of gold was grown to 7.5 nm after the fifth reuse experiment with a wider size distribution ( $\sigma = 3.5 \text{ nm}$ ) in comparison with fresh Au/OMS-2 (average: 4.1 nm,  $\sigma: 1.2 \text{ nm}$ ) (Figure 4-5). In addition, the structure of OMS-2 support was unchanged after the fifth reuse experiment (Figure 4-6). Therefore, the slight decrease in the reaction rate and the final yield of **3aa** is likely due to the growth of the gold nanoparticle size.



**Figure 4-4.** Verification of heterogeneous catalysis and reuse of Au/OMS-2. (a) The effect of removal of the Au/OMS-2 catalyst, and (b) the reaction profiles for the catalyst reuse experiment. The reaction conditions were the same as those described in Table 3-1. GC yields are shown here.



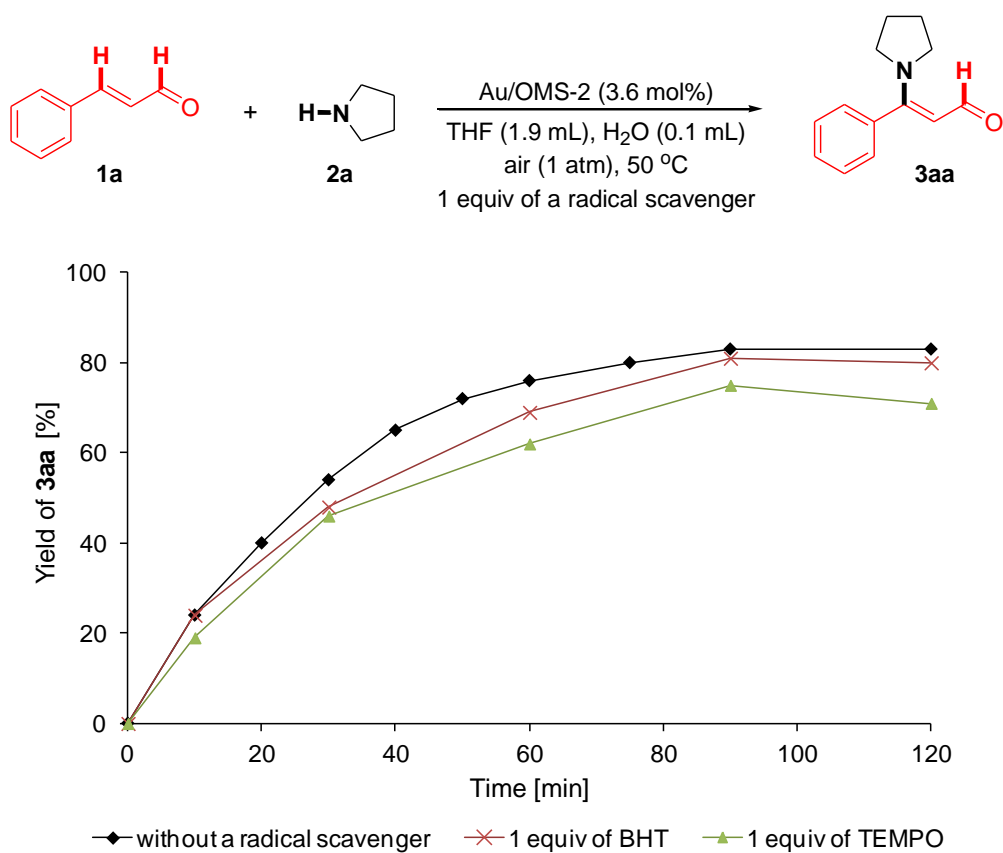
**Figure 4-5.** TEM image and Au particle size distribution of Au/OMS-2 after the fifth reuse (average: 7.5 nm,  $\sigma$ : 3.5 nm). The size distribution was determined using 400 particles.



**Figure 4-6.** XRD patterns of Au/OMS-2 and OMS-2. (a) Au/OMS-2 after fifth reuse, (b) fresh Au/OMS-2, and (c) OMS-2.

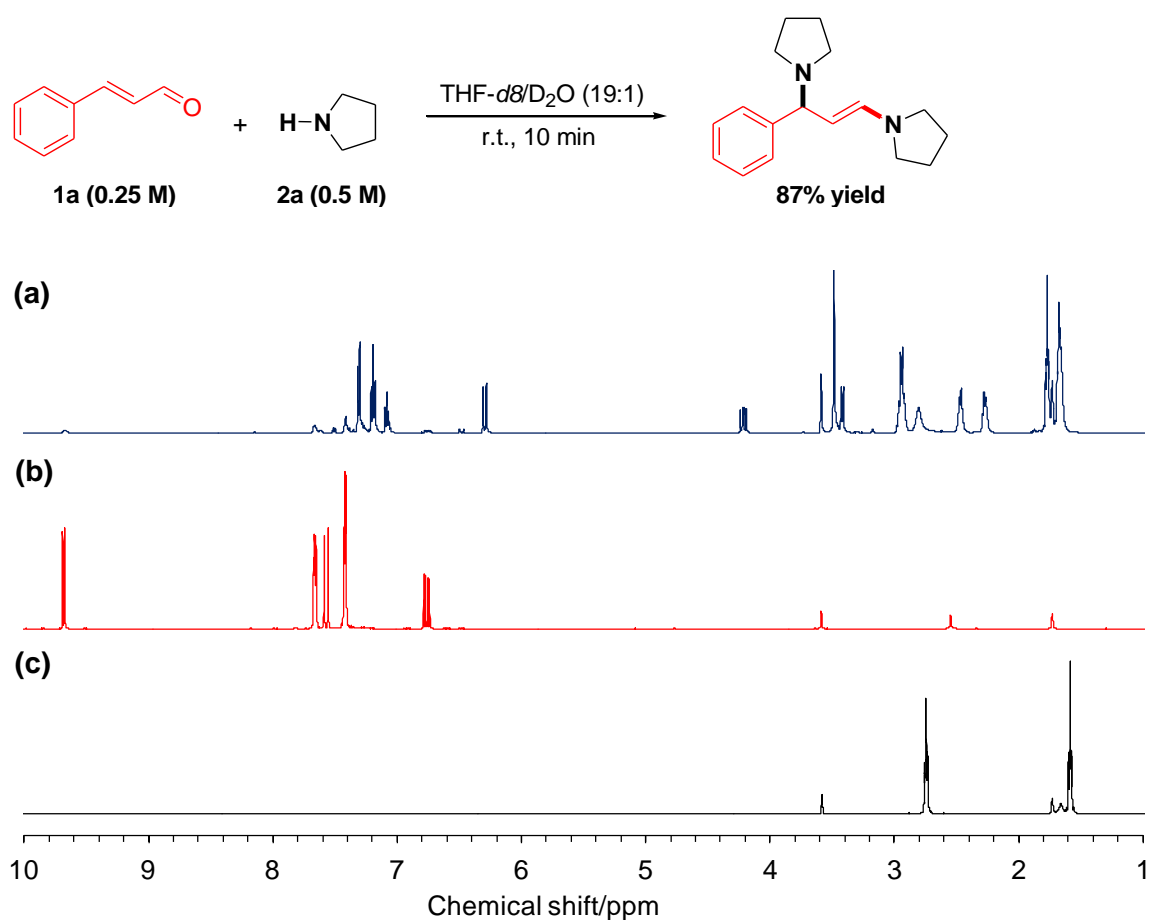
### 4.3.5. Reaction Mechanism

In the presence of stoichiometric amounts of radical scavengers such as 2,6-di-*tert*-butyl-4-methylphenol (BHT) or 2,2,6,6-tetramethylpiperidine 1-oxyl (TEMPO), the reaction rate as well as the final yield of **3aa** for the amination of **1a** with **2a** were almost unchanged (Figure 4-7). This result suggests that radical intermediates are not involved in the present amination.

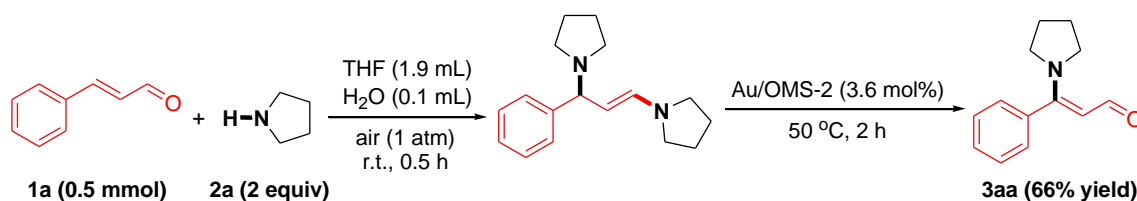


**Figure 4-7.** Effect of radical scavengers on the amination of cinnamaldehyde (**1a**) with pyrrolidine (**2a**). The reaction conditions were the same as those described in Table 4-1. GC yields are shown here.

The  $^1\text{H}$  NMR spectra of **1a** and **2a** under various conditions are shown in Figure 4-8. Upon mixing **1a** (0.25 M) and **2a** (0.5 M) in THF-*d*8/D<sub>2</sub>O (19:1), 1,1'-(3-phenyl-1-propene-1,3-diyl)bis-pyrrolidine derived from 1,2- and 1,4-addition of **2a** to **1a** was formed in 87% yield in 10 min.<sup>[18]</sup> In addition, the amination was efficiently proceeded when **1a** and **2a** had been stirred at room temperature for 0.5 h before Au/OMS-2 was added to the reaction solution (Scheme 4-6). These results indicate that a diamination intermediate is likely involved in the present amination.

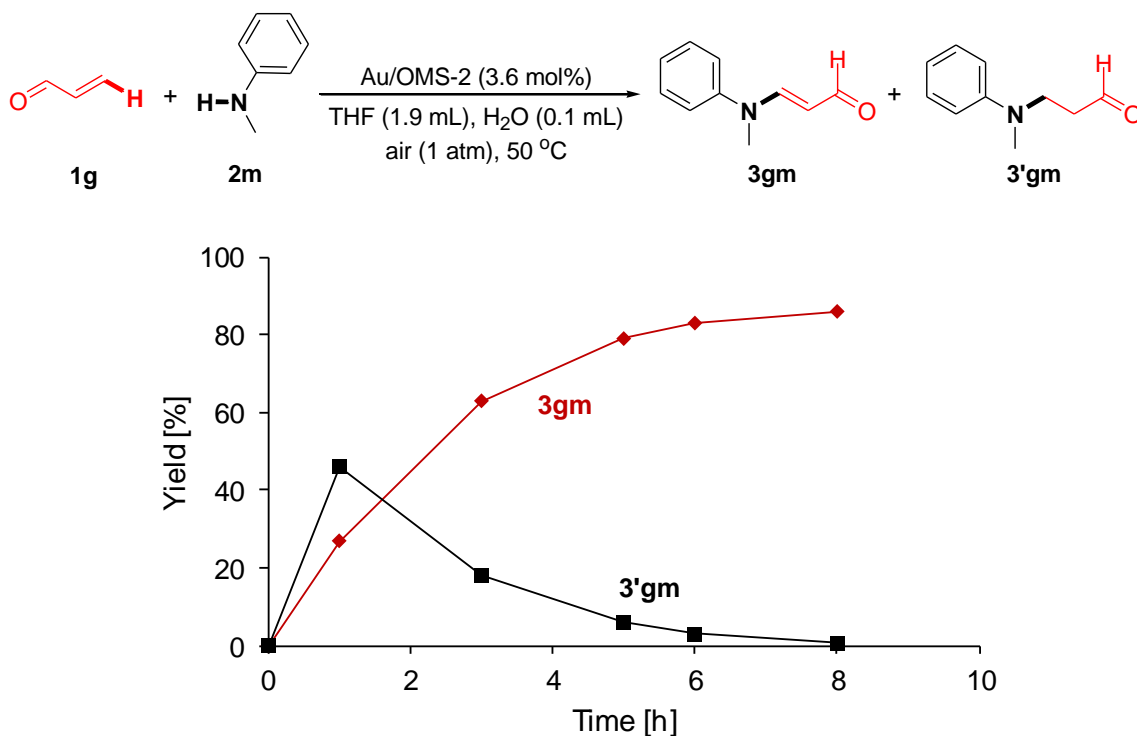


**Figure 4-8.**  $^1\text{H}$  NMR spectra of (a) **1a** (0.25 M) and **2a** (0.5 M) in THF-*d*8/D<sub>2</sub>O (19:1), (b) **1a** (0.25 M) in THF-*d*8, and (c) **2a** (0.5 M) in THF-*d*8.

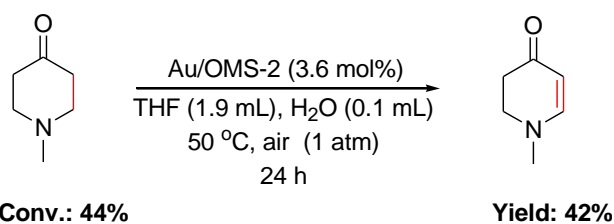


**Scheme 4-6.** Sequential synthesis of **3aa** from **1a** and **2a**.

The reaction profile for the present Au/OMS-2-catalyzed amination indicates that the amination proceeds through a  $\beta$ -aminoaldehyde intermediate (aza-Michael addition product) (Figure 4-9). In addition, a  $\beta$ -aminoketone, 1-methyl-4-piperidone, can be dehydrogenated to afford the corresponding enaminone by using Au/OMS-2 (Scheme 4-7). Even under Ar atmosphere, the amination can be promoted by Au/OMS-2, indicating OMS-2 can facilitate step 2 in Scheme 4-8.<sup>[8b]</sup>



**Figure 4-9.** Reaction profile for the reaction of **1g** and **2m**. The reaction conditions were the same as those described in Table 4-1. GC yields are shown here.



**Scheme 4-7.** Dehydrogenation of 1-methyl-4-piperidone to 1-methyl-2,3-dihydropyridin-4(1H)-one by Au/OMS-2. Reaction conditions: 1-methyl-4-piperidone (0.5 mmol), Au/OMS-2 (Au: 3.6 mol%), THF (1.9 mL), H<sub>2</sub>O (0.1 mL), 50 °C, 24 h, air (1 atm). Conversion and yield were determined by GC analysis.

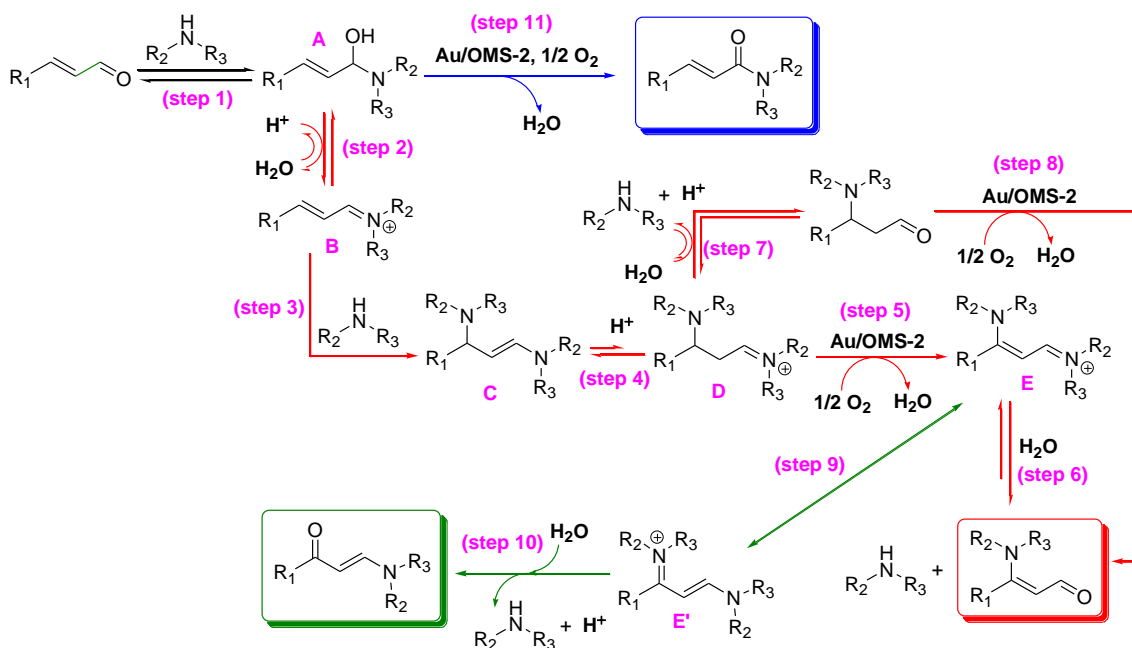
The above experimental results suggest that the present Au/OMS-2-catalyzed amination of  $\alpha,\beta$ -unsaturated aldehydes likely proceeds via the following several sequential reactions; (1) 1,2-addition of a secondary amine to  $\alpha,\beta$ -unsaturated aldehyde to give a hemiaminal intermediate **A** (Scheme 4-8, step 1), (2) dehydration of **A** to form an iminium intermediate **B** (Scheme 4-8, step 2), (3) 1,4-addition of the secondary amine to **B** to give an enamine intermediate **C** (Scheme 4-8, step 3) followed by isomerization of **C** to an iminium intermediate **D** (Scheme 4-8, step 4), and (4) oxidative dehydrogenation of **D** to give an  $\alpha,\beta$ -unsaturated iminium intermediate **E** (Scheme 4-8, step 5) followed by the kinetically favored hydrolytic decomposition of **E** to generate the corresponding enaminal. An alternative pathway, including (1) hydrolytic decomposition of **D** to a  $\beta$ -aminoaldehyde (Scheme 4-8, step 7) and (2) oxidative dehydrogenation of the  $\beta$ -aminoaldehyde promoted by Au/OMS-2 to afford the corresponding enaminal (Scheme 4-8, step 8), is also possible. The reaction mechanism for the present amination is completely different from that for the traditional palladium-catalyzed aza-Wacker oxidation, which is supposed to proceed through



migratory insertion of an amine into the palladium-alkene complex, followed by  $\beta$ -hydride elimination (Scheme 4-2).<sup>[5e,g,h]</sup>

When large amounts of an amine exist in the reaction mixture, the equilibrium in step 6 can shift toward **E**, and resonance between **E** and **E'** (Scheme 4-8, step 9) followed by hydrolytic decomposition of **E'** affords the corresponding enaminone as the final thermodynamically favored Wacker-type oxidation product (Scheme 4-8, step 10).

The amidation by-product, such as **4aa**, can be generated by oxidative dehydrogenation of **A** by Au/OMS-2 (Scheme 4-8, step 11). Upon increasing the amount of water, the equilibrium in step 2 can shift to **A**, which is likely responsible for the increase in the amount of the amidation by-product.



**Scheme 4-8.** Proposed reaction path for the present Au/OMS-2-catalyzed dehydrogenative amination of  $\alpha,\beta$ -unsaturated aldehydes and formal Wacker-type oxidation.

#### 4.4. Conclusion

In summary, the novel synthetic procedure for enaminals by the Au/OMS-2-catalyzed heterogeneous dehydrogenative amination of  $\alpha,\beta$ -unsaturated aldehydes has successfully been developed. The substrate scope for the present amination was very broad with respect to both  $\alpha,\beta$ -unsaturated aldehydes and amines.  $\alpha,\beta$ -unsaturated ketones were also good substrates, affording the corresponding enamines. In addition, the first formal Wacker-type oxidation of  $\alpha,\beta$ -unsaturated aldehydes has successfully been developed. The present amination provides a convenient procedure for synthetically important enaminals and enamines from the readily available starting materials.

#### 4.5. References

- [1] a) S. G. Zlotin, P. G. Kislitsin, A. V. Samet, E. A. Serebryakov, L. D. Konyushkin, V. V. Semenov, *J. Org. Chem.* **2000**, *65*, 8430; b) H. Liu, X. Liang, H. S  hoel, A. B  low, M. Bols, *J. Am. Chem. Soc.* **2001**, *123*, 5116; c) N. Nishiwaki, T. Ogihara, T. Takami, M. Tamura, M. Ariga, *J. Org. Chem.* **2004**, *69*, 8382; d) H. Kuwabara, K. Umihara, Y. Furugori, I. Itoh, *Chem. Lett.* **2005**, *34*, 834; e) L. E. Kiss, H. S. Ferreira, D. A. Learmonth, *Org. Lett.* **2008**, *10*, 1835; f) Q. Sun, R. Wu, S. Cai, Y. Lin, L. Sellers, K. Sakamoto, B. He, B. R. Peterson, *J. Med. Chem.* **2011**, *54*, 1126; g) M.-E Theoclitou, B. Aquila, M. H. Block, P. J. Brassil, L. Castriotta, E. Code, M. P. Collins, A. M. Davies, T. Deegan, J. Ezhuthachan, S. Filla, E. Freed, H. Hu, D. Huszar, M. Jayaraman, D. Lawson, P. M. Lewis, M. V. P. Nadella, V. Oza, M. Padmanilayam, T. Pontz, L. Ronco, D. Russell, D. Whitston, X. Zheng, *J. Med. Chem.* **2011**, *54*, 6734; h) S.

- Muthusarayanan, B. D. Bala, S. Perumal, *Tetrahedron Lett.* **2013**, *54*, 5302; i) T. R. Swaroop, H. Ila, K. S. Rangappa, *Tetrahedron Lett.* **2013**, *54*, 5288.
- [2] a) B. Stanovnik, J. Svete, *Chem. Rev.* **2004**, *104*, 2433, and references cited therein. b) A. -Z. A. Elassar, A. A. El-Khair, *Tetrahedron* **2003**, *59*, 8463; c) J. V. Greenhill. *Chem. Soc. Rev.* **1977**, *6*, 277.
- [3] a) J. Dabrowski, K. Kamienska-Trela, *J. Am. Chem. Soc.* **1976**, *98*, 2826; b) M. d'Ischia, A. Napolitano, C. Costantini, *Tetrahedron* **1995**, *51*, 9501; c) S. K. Chatterjee, W.-D. Rudolf, *Phosphorus, Sulfur and Silicon* **1998**, *133*, 251; d) J. Clayden, N. Greeves, S. Warren, *Organic Chemistry*, Oxford University Press, New York, **2012**; e) Z.-P. Lin, F. F. Wong, Y.-B. Chen, C.-H. Lin, M.-T. Hsieh, J.-C. Lien, Y.-H. Chou, H.-C. Lin, *Tetrahedron* **2013**, *69*, 3991.
- [4] a) S. S. Stahl, *Angew. Chem. Int. Ed.* **2004**, *43*, 3400; b) E. M. Beccalli, G. Brogini, M. Martinelli, S. Sottocornola, *Chem. Rev.* **2007**, *107*, 5318; c) R. I. McDonald, G. Liu, S. S. Stahl, *Chem. Rev.* **2011**, *111*, 2981.
- [5] a) J. J. Bozell, L. S. Hegedus, *J. Org. Chem.* **1981**, *46*, 2561; b) L. S. Hegedus, B. Akemark, K. Zetterberg, L. F. Olsson, *J. Am. Chem. Soc.* **1984**, *106*, 7122; c) M. Beller, M. Eichberger, H. Trauthwein, *Angew. Chem. Int. Ed.* **1997**, *36*, 2225; d) M. Beller, H. Trauthwein, M. Eichberger, C. Breindl, T. E. Muller, *Eur. J. Inorg. Chem.* **1999**, 1121; e) Y. Obora, Y. Shimizu, Y. Ishii, *Org. Lett.* **2009**, *11*, 5058; f) Y. Shimizu, Y. Obora, Y. Ishii, *Org. Lett.* **2010**, *12*, 1372; g) L. L. Chng, J. Zhang, J. Yang, M. Amoura, J. Y. Ying, *Adv. Synth. Catal.* **2011**, *353*, 2988; h) Y. Mizuta, K. Yasuda, Y. Obora, *J. Org. Chem.* **2013**, *78*, 6332; i) Y. Yang, F. Ni, W.-M. Shu, S.-B. Yu, M. Gao, A.-X. Wu, *J. Org. Chem.* **2013**, *78*, 5418; j) X. Ji, H. Huang, W. Wu, H. Jiang, *J. Am. Chem. Soc.* **2013**, *135*, 5286.

- [6] S. Ueno, R. Shimizu, R. Kuwano, *Angew. Chem. Int. Ed.* **2009**, *48*, 4543.
- [7] D. Enders, T. V. Nguyen, *Tetrahedron Lett.* **2012**, *53*, 2091.
- [8] a) Y.-C. Son, V. D. Makwana, A. R. Howell, S. L. Suib, *Angew. Chem. Int. Ed.* **2001**, *40*, 4280; b) T. Oishi, K. Yamaguchi, N. Mizuno, *ACS Catal.* **2011**, *1*, 1351; c) K. Yamaguchi, H. Kobayashi, T. Oishi, N. Mizuno, *Angew. Chem. Int. Ed.* **2012**, *51*, 544; d) K. Yamaguchi, Y. Wang, T. Oishi, Y. Kuroda, N. Mizuno, *Angew. Chem. Int. Ed.* **2013**, *52*, 5627.
- [9] J. Mielby, S. Kegnæs, P. Fristrup, *ChemCatChem* **2012**, *4*, 1037.
- [10] a) Y. Wang, D. Zhu, L. Tang, S. Wang, Z. Wang, *Angew. Chem. Int. Ed.* **2011**, *50*, 8917; b) J.-F. Soulé, H. Miyamura, S. Kobayashi, *J. Am. Chem. Soc.* **2011**, *133*, 18550; c) J. Zhu, Y. Zhang, F. Shi, Y. Deng, *Tetrahedron Lett.* **2012**, *53*, 3178.
- [11] R. N. DeGuzman, Y.-F. Shen, E. J. Neth, S. L. Suib, C.-L. O'Young, S. Levine, J. M. Newsam, *Chem. Mater.* **1994**, *6*, 815.
- [12] D. Pope, D. S. Walker, R. L. Moss, *J. Catal.* **1977**, *47*, 33.
- [13] K. Taniguchi, S. Itagaki, K. Yamaguchi, N. Mizuno, *Angew. Chem. Int. Ed.* **2013**, *52*, 8420.
- [14] *Purification of Laboratory Chemicals*, 3rd ed. (Eds.: D. D. Perrin, W. L. F. Armarego), Pergamon Press, Oxford, **1988**.
- [15] T. Mitsudome, S. Yoshida, T. Mizugaki, K. Jitsukawa, K. Kaneda, *Angew. Chem. Int. Ed.* **2013**, *52*, 5961.
- [16] R. A. Sheldon, M. Wallau, I. W. C. E. Arends, U. Schuchardt, *Acc. Chem. Res.* **1998**, *31*, 485.
- [17] a) T. Diao, S. S. Stahl, *J. Am. Chem. Soc.* **2011**, *133*, 14566; b) Y. Izawa, D. Pun, S. S. Stahl, *Science* **2011**, *333*, 209; c) T. Diao, T. J. Wadzinski, S. S. Stahl,

*Chem. Sci.* **2012**, *3*, 887; d) W. Gao, Z. He, Y. Qian, J. Zhao, Y. Huang, *Chem. Sci.* **2012**, *3*, 883; e) A. N. Campbell, S. S. Stahl, *Acc. Chem. Res.* **2012**, *45*, 851; f) Y. Izawa, C. Zheng, S. S. Stahl, *Angew. Chem. Int. Ed.* **2013**, *52*, 3672. g) T. Diao, D. Pun, S. S. Stahl, *J. Am. Chem. Soc.* **2013**, *135*, 8205, h) D. Pun, T. Diao, S. S. Stahl, *J. Am. Chem. Soc.* **2013**, *135*, 8213.

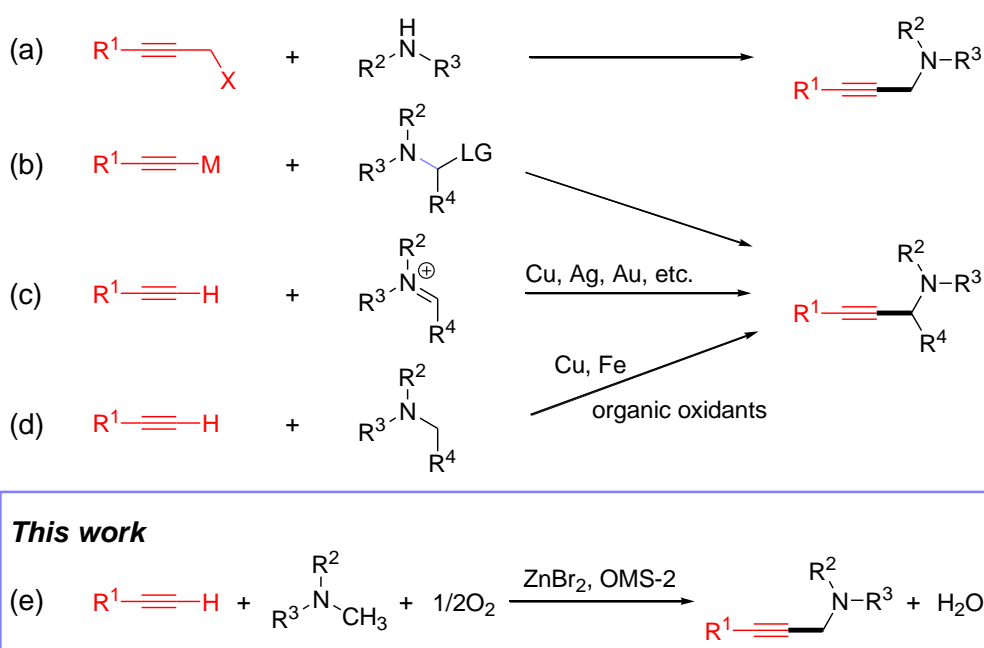
[18] J. C. Combret, J. L. Klein, M. Mouslouhouddine, *Synthesis*, **1984**, *6*, 493.



**Chapter 5**  
**Zn<sup>2+</sup> and OMS-2 Co-catalyzed Aerobic**  
**Cross-Dehydrogenative Coupling of**  
**Terminal Alkynes and Tertiary Amines**

## 5.1. Introduction

Propargylamines represent a very important class of compounds that have been key structural motifs in a number of bioactive compounds.<sup>[1]</sup> In addition, they have been utilized for the synthesis of nitrogen-containing compounds such as pyrazines, oxazoles, and pyrroles.<sup>[2]</sup>



**Scheme 5-1.** Synthesis of propargylamines (X = Cl, Br; M = Li, Mg; LG = leaving group).<sup>[3-7]</sup>

Various synthetic procedures for propargyl amines have been developed, and the most widely utilized procedures are (1) nucleophilic substitution of propargyl halides with amines (Scheme 5-1, a)<sup>[3]</sup> or of  $\alpha$ -substituted tertiary amines with metal acetylide reagents (Scheme 5-1, b),<sup>[4]</sup> (2) metal-catalyzed nucleophilic addition of terminal alkynes to iminium species generated *in situ* by dehydrative condensation of aldehydes and amines (Scheme 5-1, c),<sup>[5]</sup> and (3) cross-dehydrogenative coupling<sup>[6]</sup> of terminal



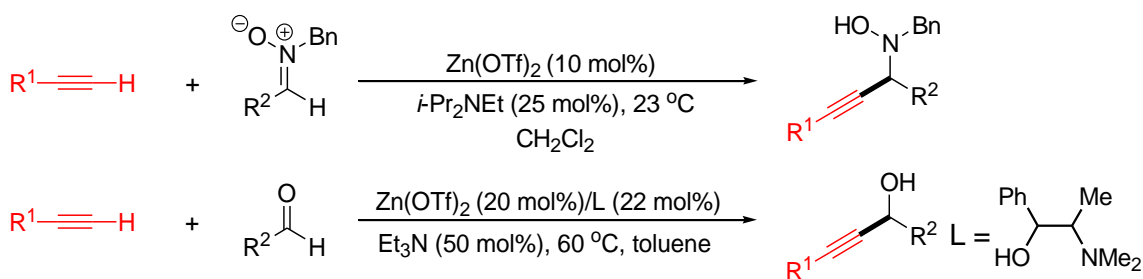
alkynes and tertiary amines (Scheme 5-1, d).<sup>[7]</sup> Among them, procedure (d), which proceeds through C–H bond activation and subsequent C–C bond formation, has become promising for the synthesis of propargylamines due to its high synthetic efficiency and environmentally benign nature.

To date, various copper-,<sup>[7a-i]</sup> iron-,<sup>[7j,k]</sup> or silver-catalyzed<sup>[7l]</sup> systems for procedure (d) have been developed. However, these systems have a drawback of the requirement of at least stoichiometric amounts of organic oxidants such as *t*-BuOOH, (*t*-BuO)<sub>2</sub>, *N*-bromosuccinimide, and diethyl azodicarboxylate, which results in the generation of a large amount of wastes during the reaction. Photoredox systems have also been applied to this type of reaction and shown high catalytic performance. For these systems, however, the scope of amines is typically limited to only tetrahydroisoquinoline derivatives.<sup>[7m-o]</sup> Therefore, the development of new catalyst systems for the cross-dehydrogenative coupling of terminal alkynes and tertiary amines, which have a wide substrate scope and utilize naturally abundant and environmentally benign molecular oxygen as the terminal oxidant, is highly desirable.

In line with the research on the aerobic cross-dehydrogenative couplings described in the previous chapters, the target of this chapter is the development of a novel catalyst system for the synthesis of propargylamines by employing the cross-dehydrogenative coupling strategy using molecular oxygen as the terminal oxidant. The strategy to achieve the target reaction is (1) to find a catalyst which can form a metal acetylide species from a terminal alkyne, and (2) to discover an oxidant that can promote the formation of an electrophilic iminium species from a tertiary amine and that can readily be reoxidized by molecular oxygen. Recently, an OMS-2-promoted aerobic oxidative  $\alpha$ -cyanation of tertiary amines has successfully been developed by Mizuno and co-workers.<sup>[8]</sup> This

reaction possibly proceeds through the formation of iminium intermediates by the step-by-step two-electron oxidation of tertiary amines by OMS-2.<sup>[8]</sup> Thus, it is envisioned that an appropriate metal source, which can generate metal acetylide species as described above, in combination with OMS-2 would promote the cross-dehydrogenative coupling of terminal alkynes and tertiary amines through nucleophilic addition of the metal acetylide species to the iminium intermediates.

In this chapter, the aerobic cross-dehydrogenative coupling of terminal alkynes and tertiary amines to propargylamines co-catalyzed by ZnBr<sub>2</sub> and OMS-2 (Scheme 5-1, e) is described. Zinc-based catalysts are versatile in nucleophilic addition of alkynes to various electrophiles, such as aldehydes and nitrons (Scheme 5-2).<sup>[9]</sup> By using the present ZnBr<sub>2</sub> and OMS-2 co-catalyzed system, various kinds of propargylamines can successfully be synthesized. In this reaction, molecular oxygen can be used as the terminal oxidant, and OMS-2 can be reused several times.



**Scheme 5-2.** Zinc-catalyzed nucleophilic addition of alkynes to electrophiles.<sup>[9]</sup>

## 5.2. Experimental Section

### 5.2.1. General

GC analyses were performed on Shimadzu GC-2014 with a FID detector equipped with an Rxi-5 Sil capillary column. GC-MS spectra were recorded on Shimadzu GCMS-QP2010 equipped with an InertCap 5 capillary column at an ionization voltage of 70 eV. Liquid-state NMR spectra were recorded on JEOL JNM-ECA-500.  $^1\text{H}$  and  $^{13}\text{C}$  NMR spectra were measured at 500.2 and 125.8 MHz, respectively, using tetramethylsilane (TMS) as an internal reference ( $\delta = 0$  ppm). OMS-2 (BET surface area:  $90\text{ m}^2\text{ g}^{-1}$ ) was prepared according to the literature procedures.<sup>[10]</sup> Activated  $\text{MnO}_2$  (Cat. No. 217646-5G, for organic oxidations, Aldrich),  $\beta\text{-MnO}_2$  (BET surface area:  $36\text{ m}^2\text{ g}^{-1}$ , Cat. No. 133-09681, Wako) were commercially available. Solvents and substrates were obtained from Kanto Chemical, TCI, Wako, or Aldrich (reagent grade), and purified prior to the use (if required).<sup>[11]</sup>

### 5.2.2. Typical Procedure for the Cross-Coupling of Terminal Alkynes and Tertiary Amines

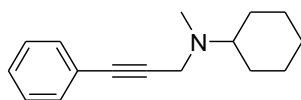
Into a Pyrex glass reactor (volume: ca. 20 mL) were successively placed  $\text{ZnBr}_2$  (11.3 mg, 0.05 mmol), OMS-2 (100 mg), an alkyne (**1**) (1 mmol), a tertiary amine (**2**) (2 mmol), cyclopentylmethylether (CPME) (2 mL), and a Teflon-coated magnetic stir bar, and the reaction mixture was purged with oxygen gas, and then vigorously stirred at  $100\text{ }^\circ\text{C}$ . After the reaction was completed, an internal standard (diphenyl) was added to the reaction mixture, and the conversion of **1** and **2** and the product yield were determined by GC analysis. As for isolation of the propargylamine product, the internal standard was not added. After the reaction, OMS-2 was filtered off (>97 % recovery),

and then the filtrate was concentrated by evaporation of CPME. The crude product was subjected to column chromatography on silica gel (typically using *n*-hexane/diethylether as the eluent), giving the pure propargylamines. The products were identified by GC-MS and NMR ( $^1\text{H}$  and  $^{13}\text{C}$ ) analyses.

### 5.2.3. Reuse Experiment of OMS-2

The cross-coupling of phenylacetylene (**1a**) and *N,N*-dimethylcyclohexylamine (**2a**) to *N*-methyl-*N*-(3-phenylprop-2-yn-1-yl)cyclohexylamine (**3aa**) was carried out with fresh OMS-2 as the above-described experimental procedure. After the reaction, OMS was retrieved by filtration, washed with acetone and water, and then calcined at 300 °C for 2 h. Into a Pyrex glass reactor (volume: ca. 20 mL) were successively placed  $\text{ZnBr}_2$  (11.3 mg, 0.05 mmol), the retrieved OMS-2 (100 mg), **1a** (1 mmol), **2a** (2 mmol), CPME (2 mL), and a Teflon-coated magnetic stir bar, and the reaction mixture was purged with oxygen gas, and then vigorously stirred at 100 °C for 8 h. After the reaction was completed, the internal standard (diphenyl) was added to the reaction mixture, and the conversion of **1a** and **2a** and the yield of **3aa** were determined by GC analysis. The reuse experiments were repeated 3 times.

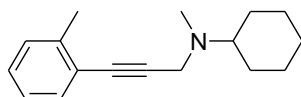
### 5.2.4. Spectral Data of Propargylamines



**3aa**

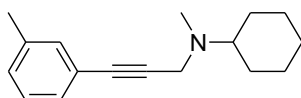
***N*-methyl-*N*-(3-phenylprop-2-yn-1-yl)cyclohexylamine (3aa):**  $^1\text{H}$  NMR (500.2 MHz,  $\text{CDCl}_3$ , TMS):  $\delta$  1.09–1.32 (m, 5H), 1.60–1.64 (m, 1H), 1.78–1.81 (m, 2H), 1.95–1.98 (m, 2H), 2.41–2.46 (m, 4H), 3.63 (s, 2H), 7.27–7.31 (m, 3H), 7.41–7.44 (m, 2H).

$^{13}\text{C}\{^1\text{H}\}$  NMR (125.8 MHz,  $\text{CDCl}_3$ , TMS):  $\delta$  25.67, 26.23, 29.96, 38.68, 43.82, 61.16, 84.92, 85.80, 123.58, 127.98, 128.32, 131.78. MS (EI):  $m/z$  (%) : 227 (11) [ $M^+$ ], 184 (19), 171 (29), 170 (35), 116 (33), 115 (100), 94 (43), 89 (11), 82 (10), 70 (21), 68 (27), 55 (18).



**3ba**

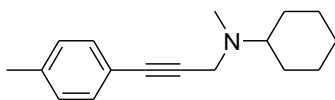
***N*-methyl-*N*-(3-(*o*-tolyl)prop-2-yn-1-yl)cyclohexanamine (3ba):**  $^1\text{H}$  NMR (500.2 MHz,  $\text{CDCl}_3$ , TMS):  $\delta$  1.10–1.31 (m, 5H), 1.60–1.63 (m, 1H), 1.78–1.80 (m, 2H), 1.98–2.00 (m, 2H), 2.43–2.48 (m, 7H), 3.70 (s, 2H), 7.10–7.14 (m, 1H), 7.17–7.21 (m, 2H), 7.39 (t,  $J = 7.5$  Hz, 1H).  $^{13}\text{C}\{^1\text{H}\}$  NMR (125.8 MHz,  $\text{CDCl}_3$ , TMS):  $\delta$  21.02, 25.63, 26.22, 30.16, 38.90, 44.00, 60.92, 83.91, 89.48, 123.42, 125.58, 127.99, 129.46, 132.12, 140.10. MS (EI):  $m/z$  (%) : 241 (29) [ $M^+$ ], 240 (12), 199 (11), 198 (42), 185 (63), 184 (64), 170 (16), 158 (11), 150 (15), 130 (18), 129 (100), 128 (95), 127 (38), 115 (19), 104 (25), 94 (68), 77 (11), 68 (15), 55 (17).



**3ca**

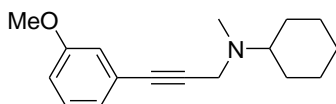
***N*-methyl-*N*-(3-(*m*-tolyl)prop-2-yn-1-yl)cyclohexanamine (3ca):**  $^1\text{H}$  NMR (500.2 MHz,  $\text{CDCl}_3$ , TMS):  $\delta$  1.09–1.32 (m, 5H), 1.60–1.64 (m, 1H), 1.77–1.81 (m, 2H), 1.95–1.97 (m, 2H), 2.32 (s, 3H), 2.40–2.46 (m, 4H), 3.63 (s, 2H), 7.09 (d,  $J = 7.5$  Hz, 1H), 7.18 (t,  $J = 7.5$  Hz, 1H), 7.22–7.26 (m, 2H).  $^{13}\text{C}\{^1\text{H}\}$  NMR (125.8 MHz,  $\text{CDCl}_3$ , TMS):  $\delta$  21.30, 25.65, 26.23, 29.98, 38.68, 43.81, 61.10, 85.08, 85.34, 123.37, 128.22, 128.84, 128.86, 132.35, 137.96. MS (EI):  $m/z$  (%) : 241 (24) [ $M^+$ ], 198 (31), 185 (52),

184 (61), 158 (11), 150 (12), 130 (22), 129 (100), 128 (35), 127 (16), 115 (18), 94 (76), 68 (14), 55 (13).



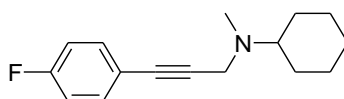
**3da**

***N*-methyl-*N*-(3-(*p*-tolyl)prop-2-yn-1-yl)cyclohexanamine (3da):**  $^1\text{H}$  NMR (500.2 MHz,  $\text{CDCl}_3$ , TMS):  $\delta$  1.09–1.31 (m, 5H), 1.60–1.63 (m, 1H), 1.77–1.80 (m, 2H), 1.95–1.97 (m, 2H), 2.33 (s, 3H), 2.40–2.46 (m, 4H), 3.61 (s, 2H), 7.09 (d,  $J = 8.0$  Hz, 2H), 7.31 (d,  $J = 8.0$  Hz, 2H).  $^{13}\text{C}\{^1\text{H}\}$  NMR (125.8 MHz,  $\text{CDCl}_3$ , TMS):  $\delta$  21.50, 25.66, 26.22, 29.93, 38.64, 43.82, 61.13, 84.95, 84.98, 120.49, 129.05, 131.63, 137.98. MS (EI):  $m/z$  (%) : 241 (23) [ $M^+$ ], 198 (26), 185 (46), 184 (56), 170 (10), 158 (11), 150 (10), 130 (19), 129 (100), 128 (36), 127 (16), 115 (14), 94 (70), 68 (11), 55 (12).



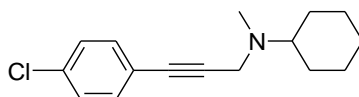
**3ea**

***N*-(3-(3-methoxyphenyl)prop-2-yn-1-yl)-*N*-methylcyclohexanamine (3ea):**  $^1\text{H}$  NMR (500.2 MHz,  $\text{CDCl}_3$ , TMS):  $\delta$  1.09–1.32 (m, 5H), 1.60–1.64 (m, 1H), 1.78–1.81 (m, 2H), 1.95–1.97 (m, 2H), 2.40–2.46 (m, 4H), 3.62 (s, 2H), 3.79 (s, 3H), 6.85 (ddd,  $J = 8.5, 2.5$  and  $1.0$  Hz, 1H), 6.96 (dd,  $J = 2.5$  and  $1.5$  Hz, 1H), 7.02 (dt,  $J = 7.5$  and  $1.0$  Hz, 1H), 7.20 (t,  $J = 8.0$  Hz, 1H).  $^{13}\text{C}\{^1\text{H}\}$  NMR (125.8 MHz,  $\text{CDCl}_3$ , TMS):  $\delta$  25.66, 26.22, 29.94, 38.68, 43.80, 55.34, 61.18, 84.81, 85.72, 114.47, 116.74, 124.32, 124.57, 129.37, 159.37. MS (EI):  $m/z$  (%) : 257 (37) [ $M^+$ ], 256 (12), 215 (10), 214 (34), 201 (66), 200 (68), 174 (12), 150 (16), 146 (27), 145 (98), 115 (24), 107 (10), 103 (15), 102 (25), 95 (10), 94 (100), 77 (10), 68 (18), 55 (17).



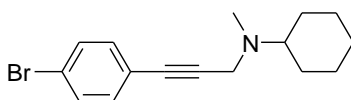
**3fa**

***N*-(3-(4-fluorophenyl)prop-2-yn-1-yl)-*N*-methylcyclohexanamine (3fa):**  $^1\text{H}$  NMR (500.2 MHz,  $\text{CDCl}_3$ , TMS):  $\delta$  1.09–1.32 (m, 5H), 1.59–1.64 (m, 1H), 1.78–1.81 (m, 2H), 1.94–1.96 (m, 2H), 2.39–2.45 (m, 4H), 3.61 (s, 2H), 6.98 (tt,  $J = 8.5$  and 2.0 Hz, 2H), 7.37–7.41 (m, 2H).  $^{13}\text{C}\{^1\text{H}\}$  NMR (125.8 MHz,  $\text{CDCl}_3$ , TMS):  $\delta$  25.65, 26.22, 29.91, 38.63, 43.76, 61.23, 83.79, 85.54, 115.53 (d,  $J = 21.6$  Hz), 119.64 (d,  $J = 3.5$  Hz), 133.58 (d,  $J = 8.3$  Hz), 162.37 (d,  $J = 249.6$  Hz). MS (EI):  $m/z$  (%) : 245 (16) [ $M^+$ ], 202 (22), 189 (37), 188 (46), 134 (20), 133 (100), 94 (51), 68 (12), 55 (11).



**3ga**

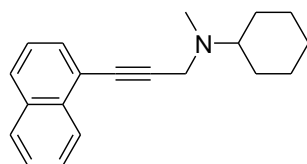
***N*-(3-(4-chlorophenyl)prop-2-yn-1-yl)-*N*-methylcyclohexanamine (3ga):**  $^1\text{H}$  NMR (500.2 MHz,  $\text{CDCl}_3$ , TMS):  $\delta$  1.09–1.31 (m, 5H), 1.60–1.63 (m, 1H), 1.78–1.81 (m, 2H), 1.93–1.95 (m, 2H), 2.39–2.44 (m, 4H), 3.61 (s, 2H), 7.26 (dt,  $J = 8.5$  and 2.0 Hz, 2H), 7.34 (dt,  $J = 9.0$  and 2.0 Hz, 2H).  $^{13}\text{C}\{^1\text{H}\}$  NMR (125.8 MHz,  $\text{CDCl}_3$ , TMS):  $\delta$  25.63, 26.20, 29.89, 38.64, 43.78, 61.24, 83.77, 86.98, 122.04, 128.62, 132.97, 133.95. MS (EI):  $m/z$  (%) : 261 (21) [ $M^+$ ], 220 (11), 218 (32), 207 (18), 206 (26), 205 (52), 204 (62), 178 (10), 170 (14), 152 (10), 151 (35), 150 (33), 149 (100), 115 (27), 114 (27), 113 (13), 94 (100), 68 (17), 55 (20).



**3ha**

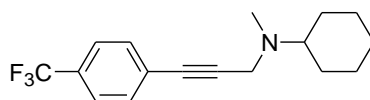
***N*-(3-(4-bromophenyl)prop-2-yn-1-yl)-*N*-methylcyclohexanamine (3ha):**  $^1\text{H}$  NMR (500.2 MHz,  $\text{CDCl}_3$ , TMS):  $\delta$  1.09–1.31 (m, 5H), 1.60–1.64 (m, 1H), 1.78–1.81 (m,

2H), 1.93–1.95 (m, 2H), 2.38–2.44 (m, 4H), 3.60 (s, 2H), 7.27 (dt,  $J = 8.5$  and  $2.0$  Hz, 2H), 7.42 (dt,  $J = 9.0$  and  $2.0$  Hz, 2H).  $^{13}\text{C}\{^1\text{H}\}$  NMR (125.8 MHz,  $\text{CDCl}_3$ , TMS):  $\delta$  25.64, 26.21, 29.90, 38.65, 43.80, 61.26, 83.85, 87.22, 122.14, 122.52, 131.56, 133.23. MS (EI):  $m/z$  (%) : 307 (19), 306 (9) [ $M^+$ ], 305 (20), 264 (23), 262 (23), 251 (45), 250 (52), 249 (47), 248 (48), 196 (16), 195 (53), 194 (15), 193 (53), 183 (10), 182 (12), 170 (17), 169 (12), 150 (18), 115 (36), 114 (42), 113 (16), 94 (100), 88 (12), 70 (10), 68 (22), 55 (20).



**3ia**

***N*-methyl-*N*-(3-(naphthalen-1-yl)prop-2-yn-1-yl)cyclohexanamine (3ia):**  $^1\text{H}$  NMR (500.2 MHz,  $\text{CDCl}_3$ , TMS):  $\delta$  1.11–1.34 (m, 5H), 1.61–1.64 (m, 1H), 1.79–1.82 (m, 2H), 2.02–2.04 (m, 2H), 2.50–2.56 (m, 4H), 3.80 (s, 2H), 7.38–7.41 (m, 1H), 7.47–7.51 (m, 1H), 7.53–7.57 (m, 1H), 7.65 (dd,  $J = 7.0$  and  $1.0$  Hz, 1H), 7.78 (d,  $J = 8.5$  Hz, 1H), 7.82 (d,  $J = 8.0$  Hz, 1H), 8.35 (d,  $J = 8.5$  Hz, 1H).  $^{13}\text{C}\{^1\text{H}\}$  NMR (125.8 MHz,  $\text{CDCl}_3$ , TMS):  $\delta$  25.63, 26.22, 30.16, 39.00, 44.14, 61.08, 83.06, 90.65, 121.28, 125.30, 126.35, 126.38, 126.69, 128.33, 128.42, 130.48, 133.28, 133.53. MS (EI):  $m/z$  (%) : 277 (20) [ $M^+$ ], 234 (18), 221 (31), 220 (38), 166 (19), 165 (100), 164 (20), 163 (14), 94 (41), 68 (11).

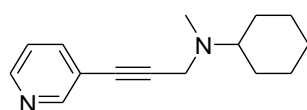


**3ja**

***N*-methyl-*N*-(3-(4-(trifluoromethyl)phenyl)prop-2-yn-1-yl)cyclohexanamine (3ja):**  $^1\text{H}$  NMR (500.2 MHz,  $\text{CDCl}_3$ , TMS):  $\delta$  1.10–1.32 (m, 5H), 1.61–1.64 (m, 1H),

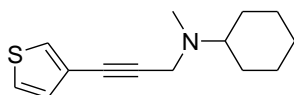


1.79–1.82 (m, 2H), 1.94–1.97 (m, 2H), 2.40–2.46 (m, 4H), 3.64 (s, 2H), 7.51–7.56 (m, 4H).  $^{13}\text{C}\{^1\text{H}\}$  NMR (125.8 MHz,  $\text{CDCl}_3$ , TMS):  $\delta$  25.65, 26.20, 29.92, 38.68, 43.79, 61.35, 83.69, 88.77, 124.07 (q,  $J = 272.0$  Hz), 125.26 (q,  $J = 4.8$  Hz), 127.41, 129.79 (q,  $J = 98.5$  Hz), 132.01. MS (EI):  $m/z$  (%) : 295 (26) [ $M^+$ ], 253 (13), 252 (52), 240 (11), 239 (83), 238 (90), 212 (12), 184 (16), 183 (97), 182 (13), 150 (15), 133 (19), 115 (12), 94 (100), 68 (12), 55 (17).



**3ka**

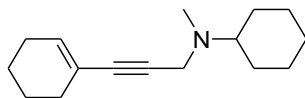
***N*-methyl-*N*-(3-(pyridin-3-yl)prop-2-yn-1-yl)cyclohexanamine (3ka):**  $^1\text{H}$  NMR (500.2 MHz,  $\text{CDCl}_3$ , TMS):  $\delta$  1.10–1.32 (m, 5H), 1.61–1.64 (m, 1H), 1.79–1.82 (m, 2H), 1.94–1.96 (m, 2H), 2.40–2.46 (m, 4H), 3.64 (s, 2H), 7.21–7.24 (m, 1H), 7.70 (dt,  $J = 8.0$  and  $2.0$  Hz, 1H), 8.50 (dd,  $J = 5.0$  and  $2.0$  Hz, 1H), 8.66 (d,  $J = 1.5$  Hz, 1H).  $^{13}\text{C}\{^1\text{H}\}$  NMR (125.8 MHz,  $\text{CDCl}_3$ , TMS):  $\delta$  25.58, 26.14, 29.85, 38.62, 43.75, 61.26, 81.56, 89.55, 120.62, 122.95, 138.57, 148.35, 152.48. MS (EI):  $m/z$  (%) : 228 (25) [ $M^+$ ], 186 (12), 185 (53), 173 (11), 172 (82), 171 (89), 150 (17), 145 (14), 144 (10), 130 (12), 119 (10), 117 (35), 116 (100), 94 (100), 90 (13), 89 (46), 82 (11), 70 (15), 68 (31), 63 (28), 55 (28).



**3la**

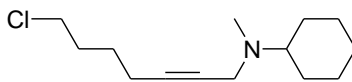
***N*-methyl-*N*-(3-(thiophen-3-yl)prop-2-yn-1-yl)cyclohexanamine (3la):**  $^1\text{H}$  NMR (500.2 MHz,  $\text{CDCl}_3$ , TMS):  $\delta$  1.09–1.31 (m, 5H), 1.60–1.63 (m, 1H), 1.77–1.81 (m, 2H), 1.93–1.96 (m, 2H), 2.39–2.45 (m, 4H), 3.60 (s, 2H), 7.09 (dd,  $J = 5.0$  and  $1.0$  Hz, 1H), 7.23 (dd,  $J = 5.0$  and  $2.8$  Hz, 1H), 7.39 (d,  $J = 3.0$  Hz, 1H).  $^{13}\text{C}\{^1\text{H}\}$  NMR (125.8

MHz, CDCl<sub>3</sub>, TMS):  $\delta$  25.65, 26.23, 29.90, 38.63, 43.81, 61.16, 79.87, 85.42, 122.55, 125.16, 128.28, 130.13. MS (EI):  $m/z$  (%) : 233 (20) [ $M^+$ ], 190 (25), 177 (45), 176 (60), 150 (17), 122 (29), 121 (100), 94 (45), 82 (10), 77 (19), 70 (12), 68 (25), 55 (20).



**3ma**

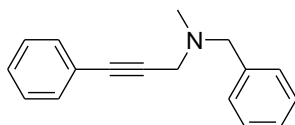
***N*-(3-(cyclohex-1-en-1-yl)prop-2-yn-1-yl)-*N*-methylcyclohexanamine (3ma):** <sup>1</sup>H NMR (500.2 MHz, CDCl<sub>3</sub>, TMS):  $\delta$  1.08–1.30 (m, 5H), 1.55–1.65 (m, 5H), 1.75–1.79 (m, 2H), 1.90–1.93 (m, 2H), 2.06–2.13 (m, 4H), 2.33–2.39 (m, 4H), 3.51 (s, 2H), 6.04–6.06 (m, 1H). <sup>13</sup>C{<sup>1</sup>H} NMR (125.8 MHz, CDCl<sub>3</sub>, TMS):  $\delta$  21.62, 22.41, 25.60, 26.18, 29.53, 29.89, 38.49, 43.68, 60.93, 82.62, 86.70, 120.77, 133.90. MS (EI):  $m/z$  (%) : 232 (10), 231 (61) [ $M^+$ ], 230 (16), 202 (10), 189 (20), 188 (69), 176 (14), 175 (97), 174 (72), 160 (34), 150 (18), 148 (22), 147 (22), 146 (37), 134 (12), 133 (12), 132 (29), 120 (30), 119 (35), 118 (12), 117 (22), 115 (15), 112 (10), 108 (16), 107 (11), 105 (15), 104 (10), 103 (12), 95 (15), 94 (79), 93 (13), 92 (22), 91 (100), 87 (10), 82 (19), 81 (48), 79 (33), 78 (15), 77 (31), 70 (36), 68 (33), 67 (12), 65 (24), 57 (10), 55 (35), 53 (12), 51 (11).



**3na**

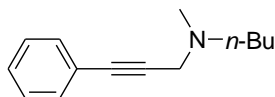
***N*-(7-chlorohept-2-yn-1-yl)-*N*-methylcyclohexanamine (3na):** <sup>1</sup>H NMR (500.2 MHz, CDCl<sub>3</sub>, TMS):  $\delta$  1.07–1.29 (m, 5H), 1.59–1.69 (m, 3H), 1.76–1.79 (m, 2H), 1.88–1.93 (m, 4H), 2.25 (tt,  $J$  = 7.0 and 2.0 Hz, 2H), 2.31–2.37 (m, 4H), 3.36 (t,  $J$  = 2.0 Hz, 2H), 3.56 (t,  $J$  = 7.0 Hz, 2H). <sup>13</sup>C{<sup>1</sup>H} NMR (125.8 MHz, CDCl<sub>3</sub>, TMS):  $\delta$  18.16, 25.67, 26.13, 26.22, 29.79, 31.69, 38.45, 43.33, 44.63, 60.97, 76.65, 83.88. MS (EI):  $m/z$  (%) :

241 (15) [ $M^+$ ], 206 (14), 200 (14), 198 (42), 185 (11), 184 (23), 164 (40), 150 (45), 148 (20), 122 (10), 120 (11), 109 (12), 108 (100), 107 (15), 95 (22), 94 (35), 91 (12), 82 (26), 81 (13), 79 (12), 77 (14), 70 (17), 68 (25), 67 (17), 65 (11), 55 (29), 54 (14), 53 (15).



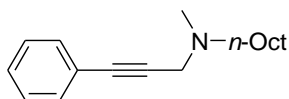
**3ab**

**N-benzyl-N-methyl-3-phenylprop-2-yn-1-amine (3ab):**  $^1\text{H}$  NMR (500.2 MHz,  $\text{CDCl}_3$ , TMS):  $\delta$  2.40 (s, 3H), 3.51 (s, 2H), 3.64 (s, 2H), 7.26 (tt,  $J = 7.0$  and  $2.0$  Hz, 1H), 7.28–7.33 (m, 5H), 7.36–7.38 (m, 2H), 7.45–7.48 (m, 2H).  $^{13}\text{C}\{^1\text{H}\}$  NMR (125.8 MHz,  $\text{CDCl}_3$ , TMS):  $\delta$  42.12, 45.89, 60.40, 84.60, 85.81, 123.46, 127.32, 128.12, 128.39, 128.44, 129.35, 131.85, 138.62. MS (EI):  $m/z$  (%) : 235 (25) [ $M^+$ ], 234 (31), 158 (43), 144 (26), 118 (10), 116 (15), 115 (100), 92 (10), 91 (60), 89 (12), 65 (16).



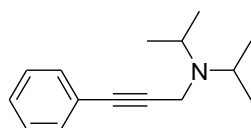
**3ac**

**N-methyl-N-(3-phenylprop-2-yn-1-yl)butan-1-amine (3ac):**  $^1\text{H}$  NMR (500.2 MHz,  $\text{CDCl}_3$ , TMS):  $\delta$  0.93 (t,  $J = 7.3$  Hz, 3H), 1.36 (sext,  $J = 7.4$  Hz, 2H), 1.45–1.51 (m, 2H), 2.36 (s, 3H), 2.45–2.49 (m, 2H), 3.54 (s, 2H), 7.26–7.31 (m, 3H), 7.41–7.45 (m, 2H).  $^{13}\text{C}\{^1\text{H}\}$  NMR (125.8 MHz,  $\text{CDCl}_3$ , TMS):  $\delta$  14.11, 20.70, 29.91, 42.08, 46.52, 55.83, 84.74, 85.27, 123.45, 127.98, 128.29, 131.76. MS (EI):  $m/z$  (%) : 201 (3) [ $M^+$ ], 158 (54), 116 (11), 115 (100).



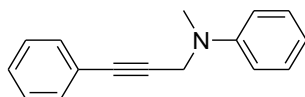
**3ad**

***N*-methyl-*N*-(3-phenylprop-2-yn-1-yl)octan-1-amine (3ad):**  $^1\text{H}$  NMR (500.2 MHz,  $\text{CDCl}_3$ , TMS):  $\delta$  0.88 (t,  $J = 7.0$  Hz, 3H), 1.27–1.31 (m, 10H), 1.49 (quin,  $J = 7.3$  Hz, 2H), 2.36 (s, 3H), 2.45–2.48 (m, 2H), 3.54 (s, 2H), 7.27–7.30 (m, 3H), 7.41–7.45 (m, 2H).  $^{13}\text{C}\{^1\text{H}\}$  NMR (125.8 MHz,  $\text{CDCl}_3$ , TMS):  $\delta$  14.21, 22.77, 27.62, 27.80, 29.39, 29.67, 31.97, 42.13, 46.54, 56.21, 84.77, 85.31, 123.49, 128.02, 128.31, 131.81. MS (EI):  $m/z$  (%) : 257 (3) [ $M^+$ ], 159 (11), 158 (86), 116 (11), 115 (100).



**3ad**

***N,N*-diisopropyl-3-phenylprop-2-yn-1-amine (3ae):**  $^1\text{H}$  NMR (500.2 MHz,  $\text{CDCl}_3$ , TMS):  $\delta$  1.15 (d,  $J = 6.5$  Hz, 12H), 3.25 (sep,  $J = 6.5$  Hz, 2H), 3.65 (s, 2H), 7.24–7.29 (m, 3H), 7.37–7.42 (m, 2H).  $^{13}\text{C}\{^1\text{H}\}$  NMR (125.8 MHz,  $\text{CDCl}_3$ , TMS):  $\delta$  20.79, 34.91, 48.62, 83.57, 89.20, 123.95, 127.78, 128.28, 131.53. MS (EI):  $m/z$  (%) : 215 (5) [ $M^+$ ], 200 (50), 116 (16), 115 (100).



**3ae**

***N*-methyl-*N*-(3-phenylprop-2-yn-1-yl)aniline (3af):** MS (EI):  $m/z$  (%) : 222 (14), 221 (81) [ $M^+$ ], 220 (69), 144 (22), 116 (12), 115 (100), 106 (11), 104 (18), 89 (15), 77 (32), 63 (10), 51 (12).

## 5.3. Results and Discussion

### 5.3.1. Optimization of the Reaction Conditions

Initially, the optimization of the reaction conditions for the cross-dehydrogenative coupling of phenylacetylene (**1a**) and *N,N*-dimethylcyclohexylamine (**2a**) to

*N*-methyl-*N*-(3-phenylprop-2-yn-1-yl)cyclohexanamine (**3aa**) was carried out using 1 atm of molecular oxygen as the terminal oxidant. Among various zinc catalysts examined, such as ZnCl<sub>2</sub>, Zn(OTf)<sub>2</sub> (OTf = triflate), ZnF<sub>2</sub>, ZnI<sub>2</sub>, and ZnBr<sub>2</sub> in toluene (Table 5-1, entries 1–5), ZnBr<sub>2</sub> in combination with OMS-2 most effectively promoted the reaction, giving **3aa** in 59 % yield (Table 5-1, entry 5). In this case, **2a** was exclusively alkynylated at the methyl position without the methine alkynylation. The cross-coupling with other metal catalysts, such as InCl<sub>3</sub>, NiCl<sub>2</sub>·6H<sub>2</sub>O, FeCl<sub>3</sub>, CuCl<sub>2</sub>·2H<sub>2</sub>O, CoCl<sub>2</sub>, and MgCl<sub>2</sub>, gave lower yields of **3aa** (Table 5-1, entries 6–11). In the case of CuCl<sub>2</sub>·2H<sub>2</sub>O as the catalyst, a significant amount of 1,4-diphenylbutadiyne derived from the Glaser–Hay homo-coupling of **1a** was generated as a byproduct (Table 5-1, entry 9, see also chapter 1). When the solvent was changed from toluene to cyclopentylmethylether (CPME), the yield of **3aa** increased to 85% (Table 5-1, entry 12, Table 5-2). Both ZnBr<sub>2</sub> and OMS-2 were indispensable for the present cross-coupling. The reaction hardly proceeded in the absence of ZnBr<sub>2</sub> or OMS-2 (Table 5-1, entries 14 and 16). The cross-coupling under 1 atm of Ar gave only 16% yield of **3aa**, which suggests that molecular oxygen is the terminal oxidant (Table 5-1, entry 13). The present cross-coupling was significantly suppressed by a radical scavenger, dibutylhydroxytoluene (BHT), which indicates that the reaction proceeds through radical intermediates (Table 5-1, entry 15).

Examination on the solvent effects showed that CPME was superior to other solvents, such as trifluorotoluene, *N*-methylpyrrolidone, dimethylformamide, dimethylacetamide, 1,4-dioxane, dimethylsulfoxide, and diethylcarbonate (Table 5-2).

OMS-2 was more active than the commercially available activated MnO<sub>2</sub> and β-MnO<sub>2</sub> (Table 5-3, entries 1–3). *t*-BuOOH was not effective for the present

cross-coupling (Table 5-3, entry 4).

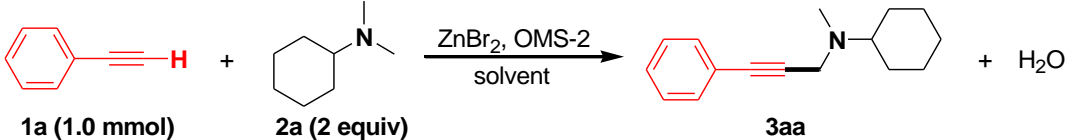
**Table 5-1.** The cross-dehydrogenative coupling of phenylacetylene (**1a**) and *N,N*-dimethylcyclohexylamine (**2a**) with various metal catalysts.<sup>[a]</sup>

**1a (1.0 mmol)** + **2a (2 equiv)**  $\xrightarrow[\text{O}_2 (1 \text{ atm})]{\text{catalyst, OMS-2}}$  **3aa** + H<sub>2</sub>O

Entry	Catalyst	Conv. [%]		Yield of <b>3aa</b> [%]
		<b>1a</b>	<b>2a</b>	
1	ZnCl <sub>2</sub>	61	36	51
2	Zn(OTf) <sub>2</sub>	24	32	8
3	ZnF <sub>2</sub>	12	23	1
4	ZnI <sub>2</sub>	29	29	4
5	ZnBr <sub>2</sub>	72	43	59
6	InCl <sub>3</sub>	37	29	24
7	NiCl <sub>2</sub> ·6H <sub>2</sub> O	21	22	7
8	FeCl <sub>3</sub>	23	28	8
9 <sup>[b]</sup>	CuCl <sub>2</sub> ·2H <sub>2</sub> O	98	41	37
10	CoCl <sub>2</sub>	58	37	43
11	MgCl <sub>2</sub>	23	28	7
12 <sup>[c]</sup>	ZnBr <sub>2</sub>	95	56	85
13 <sup>[c,d]</sup>	ZnBr <sub>2</sub>	28	8	16
14 <sup>[c,e]</sup>	ZnBr <sub>2</sub>	8	2	1
15 <sup>[c,f]</sup>	ZnBr <sub>2</sub>	68	11	14
16 <sup>[c]</sup>	none	10	23	<1

[a] Reaction conditions: catalyst (metal: 5 mol%), OMS-2 (100 mg), **1a** (1.0 mmol), **2a** (2.0 mmol), toluene (2 mL), 100 °C, O<sub>2</sub> (1 atm), 4.5 h. Conversion and yield were determined by GC analysis. [b] 1,4-Diphenylbutadiyne was formed in 43% yield. [c] CPME (2 mL), 8 h. [d] Ar (1 atm). [e] Without OMS-2. [f] BHT (2.0 mmol).

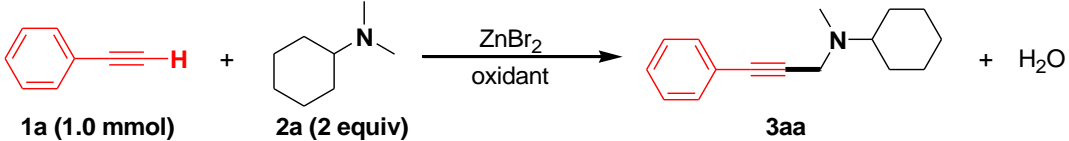
**Table 5-2.** Effect of solvents on the cross-dehydrogenative coupling of phenylacetylene (**1a**) and *N,N*-dimethylcyclohexylamine (**2a**).<sup>[a]</sup>



Entry	Solvent	Conv. [%]		Yield of <b>3aa</b> [%]
		<b>1a</b>	<b>2a</b>	
1	toluene	87	54	68
2	PhCF <sub>3</sub>	93	55	76
3	<i>N</i> -methylpyrrolidone	71	74	44
4	<i>N,N</i> -dimethylformamide	77	75	49
5	<i>N,N</i> -dimethylacetamide	79	63	58
6	1,4-dioxane	54	37	39
7	dimethylsulfoxide	81	77	48
<b>8</b>	<b>cyclopentylmethylether</b>	<b>95</b>	<b>56</b>	<b>85</b>
9	diethylcarbonate	92	67	73

[a] Reaction conditions: ZnBr<sub>2</sub> (5 mol%), OMS-2 (100 mg), **1a** (1.0 mmol), **2a** (2.0 mmol), solvent (2 mL), 100 °C, O<sub>2</sub> (1 atm), 8 h. Conversion and yield were determined by GC analysis.

**Table 5-3.** Effect of oxidants on the cross-dehydrogenative coupling of phenylacetylene (**1a**) and *N,N*-dimethylcyclohexylamine (**2a**).<sup>[a]</sup>



Entry	Oxidant	Conv. [%]		Yield of <b>3aa</b> [%]
		<b>1a</b>	<b>2a</b>	
1	OMS-2/O <sub>2</sub>	95	56	85
2	Activated MnO <sub>2</sub> <sup>[b]</sup> /O <sub>2</sub>	6	<1	1
3	β-MnO <sub>2</sub> /O <sub>2</sub>	48	26	38
4	TBHP <sup>[c]</sup> /O <sub>2</sub>	6	15	1

[a] Reaction conditions: ZnBr<sub>2</sub> (5 mol%), oxidant (100 mg), **1a** (1.0 mmol), **2a** (2.0 mmol), CPME (2 mL), 100 °C, O<sub>2</sub> (1 atm), 8 h. Conversion and yield were determined by GC analysis.

[b] Commercially available. [c] 1.0 mmol of 70 % TBHP in water was utilized.

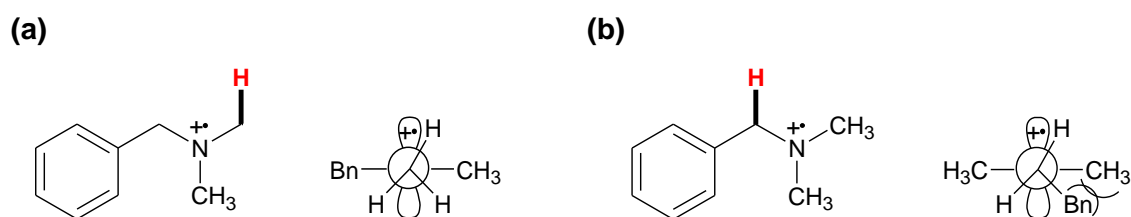
### 5.3.2. Substrate Scope

The substrate scope for the present  $\text{ZnBr}_2$  and OMS-2 co-catalyzed cross-dehydrogenative coupling of terminal alkynes and tertiary amines was investigated using molecular oxygen as the terminal oxidant. Various structurally diverse propargylamines could be synthesized from terminal alkynes and tertiary amines by employing the present catalyst system (Scheme 5-3). The isolation of the propargylamine products was very simple, and the isolated yields are summarized in Scheme 5-3.

Aromatic alkynes with electron-donating or -withdrawing substituents were all good coupling partners of **2a** to afford the corresponding propargylamines (Scheme 5-3, entries 1–10). The cross-couplings of 2-, 3-, and 4-ethynyltoluenes with **2a** were almost equally effective, which indicates that the steric effect of substituents on aromatic rings is negligible in the present system (Scheme 5-3, entries 2–4). Halo-substituted aromatic alkynes also reacted smoothly with **2a** without dehalogenation, which allows further derivatization of these propargylamines using halo-functionalities (Scheme 5-3, entries 6–8). Alkynes containing heterocycles, such as 3-ethynylthiophene and 3-ethynylpyridine, were also applicable to the present cross-coupling (Scheme 5-3, entries 11 and 12). In addition, an enyne could efficiently react with **2a** to give the corresponding propargylamines (Scheme 5-3, entry 13). Apart from aromatic alkynes, an aliphatic one could also act as the coupling partner, although the desired product was obtained in a low yield (Scheme 5-3, entry 14). With regard to amine coupling partners, various aliphatic tertiary amines could be utilized. In all these cases, the alkynylation occurred exclusively at the methyl positions without the methylene and the methine alkynylation (Scheme 5-3, entries 15–18). This selectivity can be attributed to a

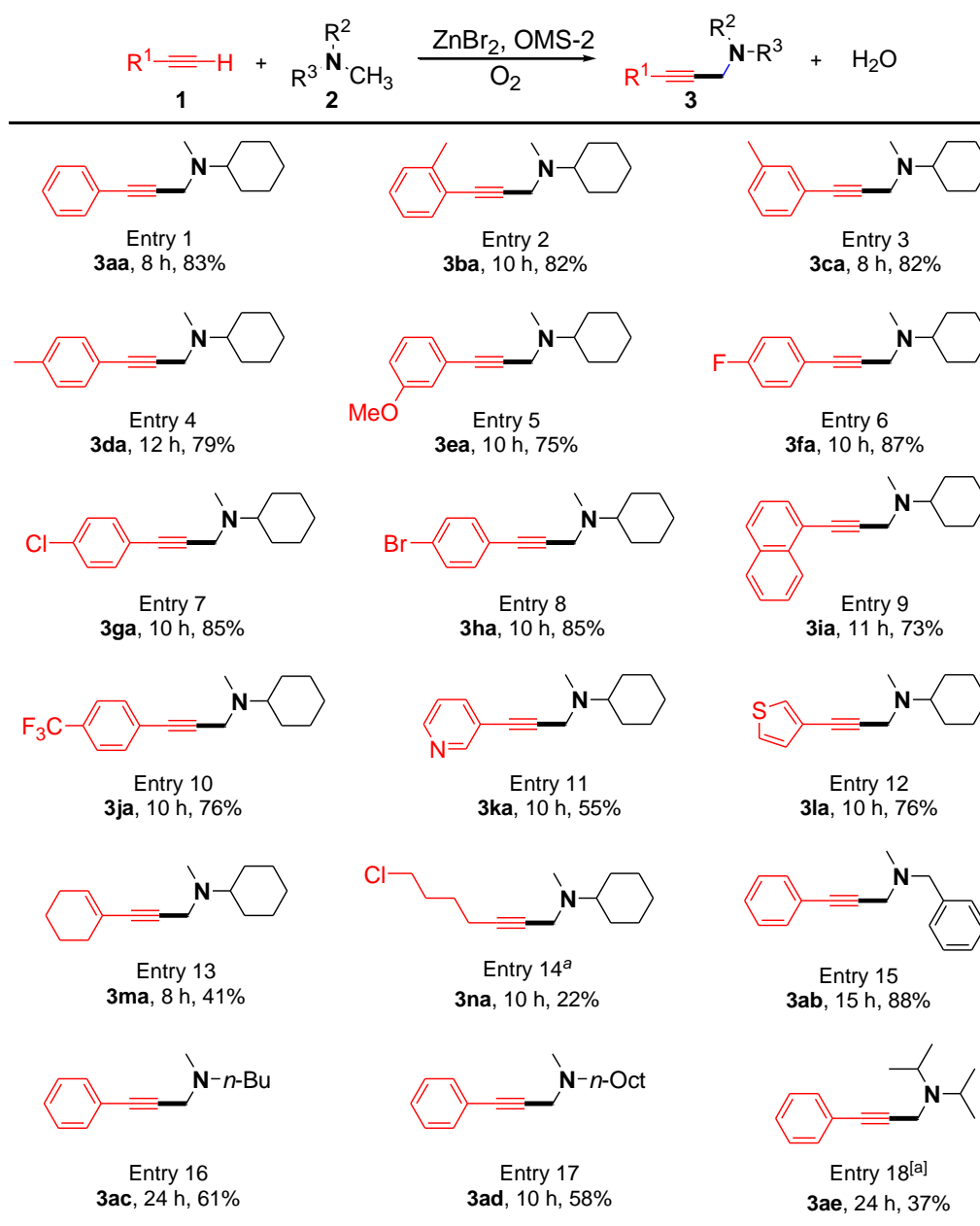


stereoelectronically controlled deprotonation of amine cation radicals (step 2 in Scheme 5-4).<sup>[12]</sup> For the stereoelectronically controlled deprotonation, the transition state requires overlap between the half-vacant nitrogen p orbital and the incipient carbon radical p orbital.<sup>[12]</sup> Lower energy of the conformation of the proposed transition state necessary for deprotonation of the methyl group (Figure 5-1), due to the steric repulsion, results in the kinetically favored deprotonation of the less substituted  $\alpha$ -C–H bond (methyl > methylene > methine).<sup>[12]</sup> It is, however, possible that a relatively small stereoelectronic effect results in the thermodynamically favored formation of the more substituted free radical.<sup>[12]</sup> In the present cross-coupling, the kinetic factor is likely dominant in the deprotonation step.



**Figure 5-1.** Conformations of the proposed transition states for the stereoelectronically controlled deprotonation of tertiary amine radicals.

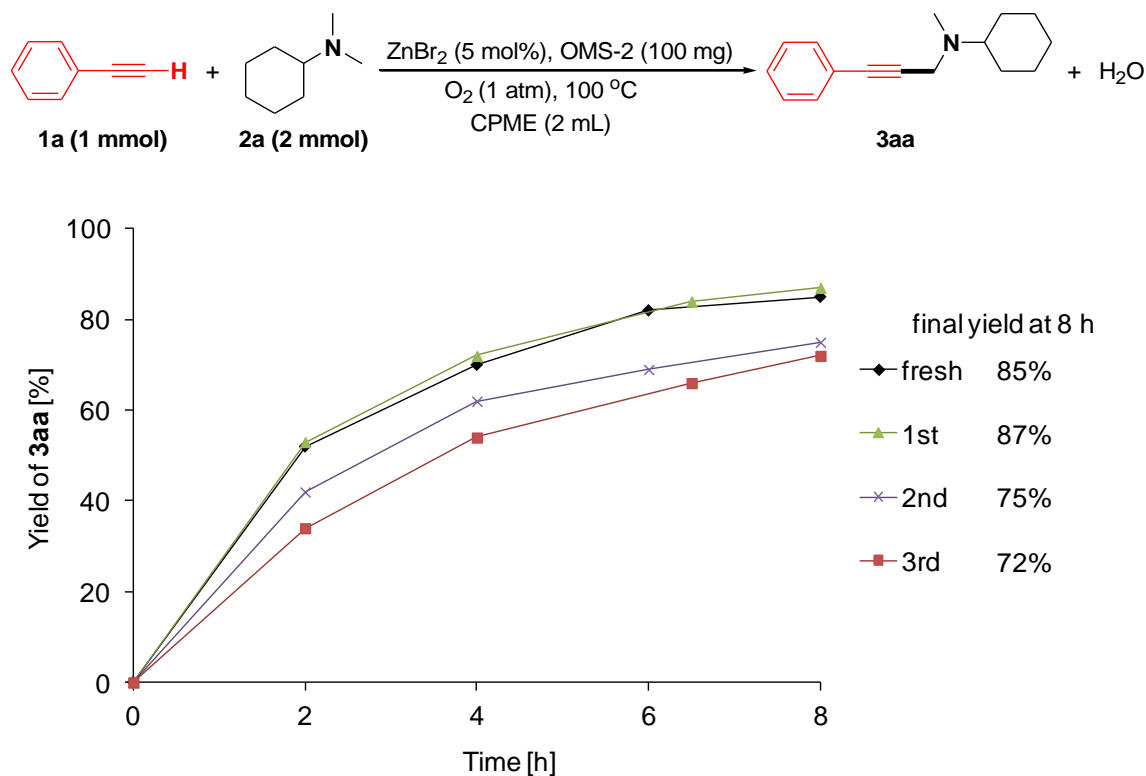
The cross-coupling of **1a** with an aniline derivative, *N,N*-dimethylaniline, did not proceed under the conditions described in Scheme 5-3. Upon the addition of a stoichiometric amount of triethylamine as a base, the corresponding propargylamine could be obtained in 6% yield for 24 h. In this case, the cross-coupling of triethylamine and **1a** did not proceed. These results suggest that the basicity of amines (for deprotonation of terminal alkynes) and the steric effect of substituents of amines (stereoelectronic effect) are two very significant factors for the present cross-dehydrogenative coupling reaction.



**Scheme 5-3.** Scope of the present cross-dehydrogenative coupling of terminal alkynes and tertiary amines. Reaction conditions: **1** (1.0 mmol), **2** (2.0 mmol), ZnBr<sub>2</sub> (5 mol%), OMS-2 (100 mg), CPME (2 mL), 100 °C, under O<sub>2</sub> (1 atm). Yields (based on **1**) of isolated products are shown. [a] ZnBr<sub>2</sub> (20 mol%).

### 5.3.3. Recyclability of OMS-2

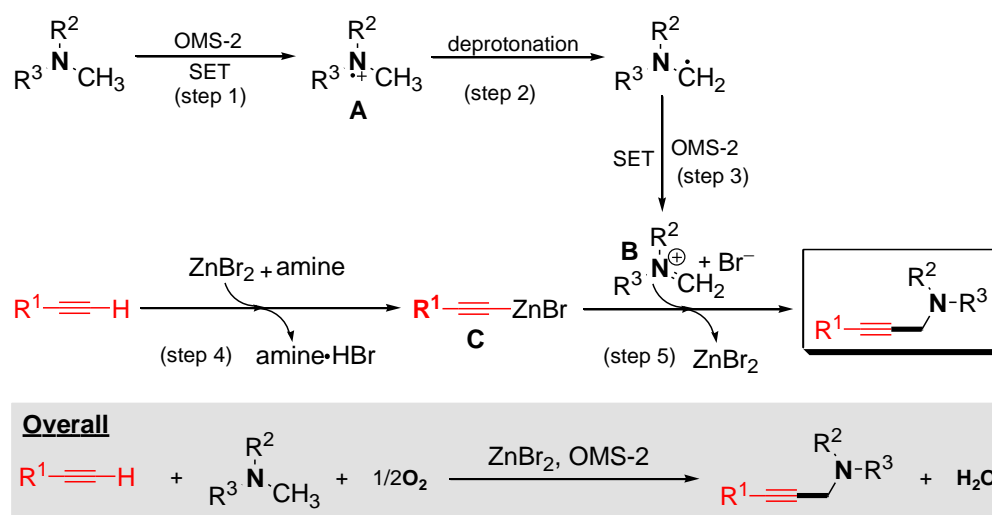
The recyclability of OMS-2 for the present cross-dehydrogenative coupling was examined (for the detailed experimental procedures, see section 5.2.3). After the cross-coupling of **1a** and **2a**, OMS-2 could easily be retrieved from the reaction mixture by simple filtration with >97 % recovery. The retrieved OMS-2 could be reused at least three times for the cross-coupling, although its performance gradually decreased (fresh: 85 % yield of **3aa** for 8 h, the 1st reuse: 87 %, the 2nd reuse: 75 %, and the 3rd reuse: 72 %, Figure 5-2).



**Figure 5-2.** The reaction profiles for the reuse experiments. The reaction conditions were the same as those described in Table 5-1.

### 5.3.4. Reaction Mechanism

The plausible reaction mechanism for the present  $\text{ZnBr}_2$  and OMS-2 co-catalyzed cross-dehydrogenative coupling of terminal alkynes and tertiary amines is shown in Scheme 5-4. The reaction likely proceeds through (1) single-electron transfer (SET) from a tertiary amine to OMS-2 to give an amine cation radical species **A** (step 1), (2) successive deprotonation of the cation radical species **A** (step 2) and second SET to generate an iminium intermediate **B** (step 3), and (3) nucleophilic attack of a zinc acetylide species **C** to the iminium intermediate **B** to give the corresponding propargylamines as the final product (step 5). As mentioned in 5.3.2, the stereoelectronic effect also supports this mechanism. The iminium species **B** has been detected during the reaction of the tertiary amine in the presence of OMS-2 and  $\text{LiBF}_4$  by NMR analysis.<sup>[10]</sup> The zinc acetylide species **C** can be formed from a terminal alkyne in the assistance of the tertiary amine as a base (step 4).<sup>[9]</sup> The reduced OMS-2 can be reoxidized by molecular oxygen.<sup>[13]</sup>



**Scheme 5-4.** A plausible reaction mechanism for the present cross-dehydrogenative coupling of terminal alkynes and tertiary amines.

## 5.4. Conclusion

In summary, the ZnBr<sub>2</sub> and OMS-2 co-catalyzed cross-dehydrogenative coupling of terminal alkynes and tertiary amines to propargylamines has successfully been developed. Various structurally diverse propargylamines can be synthesized by employing the present catalyst system. The present cross-coupling can utilize molecular oxygen as the terminal oxidant, providing a green synthetic procedure for propargylamines.

## 5.5. References

- [1] a) J. Louvel, J. F. S. Carvalho, Z. Yu, M. Soethoudt, E. B. Lenseink, E. Klaasse, J. Brussee, A. P. IJzerman, *J. Med. Chem.* **2013**, *56*, 9427; b) I. Bolea, A. Gella, M. Unzeta, *J. Neural Transm.* **2013**, *120*, 893; c) O. Bar-Am, T. Amit, O. Weinreb, M. B. H. Youdim, S. Mandel, *J. Alzheimers Dis.* **2010**, *21*, 361.
- [2] a) B. Alcaide, P. Almendros, J. M. Alonso, I. Fernández, G. G. Campillos, M. R. Torres, *Chem. Commun.* **2014**, *50*, 4567; b) H. V. Wachenfeldt, F. Paulsen, A. Sundin, D. Strand, *Eur. J. Org. Chem.* **2013**, 4578; c) Y.-L. Zhao, C.-H. Di, S.-D. Liu, J. Meng, Q. Liu, *Adv. Synth. Catal.* **2012**, *354*, 3545; d) X. Xu, P. Du, D. Cheng, H. Wang, X. Li, *Chem. Commun.* **2012**, *48*, 1811; e) T. Sugiishi, A. Kimura, H. Nakamura, *J. Am. Chem. Soc.* **2010**, *132*, 5332.
- [3] a) A. Chevalier, C. Massif, P.-Y. Renard, A. Romieu, *Chem. Eur. J.* **2013**, *19*, 1686; b) Y. Zhao, A. H. Hoveyda, R. R. Schrock, *Org. Lett.* **2011**, *13*, 784; c) K. T. Sylvester, P. J. Chirik, *J. Am. Chem. Soc.* **2009**, *131*, 8772.
- [4] T. Murai, Y. Mutoh, Y. Ohta, M. Murakami, *J. Am. Chem. Soc.* **2004**, *126*, 5968.

- [5] a) V. Srinivas, M. Koketsu, *Tetrahedron* **2013**, *69*, 8025; b) Y. He, M.-F. Lv, C. Cai, *Dalton Trans.* **2012**, *41*, 12428; c) C. Wei, C.-J. Li, *J. Am. Chem. Soc.* **2002**, *124*, 5638; d) C. Koradin, K. Polborn, P. Knockel, *Angew. Chem. Int. Ed.* **2002**, *41*, 2535.
- [6] a) S. A. Girard, T. Knauber, C.-J. Li, *Angew. Chem. Int. Ed.* **2014**, *53*, 74; b) C. J. Scheuermann, *Chem. Asian. J.* **2010**, *5*, 436; c) C.-J. Li, *Acc. Chem. Res.* **2009**, *42*, 335.
- [7] a) E. Boess, C. Schmitz, M. Klusmann, *J. Am. Chem. Soc.* **2012**, *134*, 5317; b) X. Xu, X. Li, *Org. Lett.* **2009**, *11*, 1027; c) M. Niu, Z. Yin, H. Fu, Y. Jiang, Y. Zhao, *J. Org. Chem.* **2008**, *73*, 3961; d) Z. Li, D. S. Bohle and C.-J. Li, *Proc. Natl. Acad. Sci.* **2006**, *103*, 8928; e) Z. Li, C.-J. Li, *Org. Lett.* **2004**, *6*, 4997; f) Z. Li and C.-J. Li, *J. Am. Chem. Soc.* **2004**, *126*, 11810; g) X. Xu, Z. Ge, D. Cheng, X. Li, *Arkivoc* **2012**, *107*; h) Q. Shen, L. Zhang, Y.-R. Zhou, J.-X. Li, *Tetrahedron Lett.* **2013**, *54*, 6725; i) Z. Xu, W. Yu, X. Feng, M. Bao, *J. Org. Chem.* **2011**, *76*, 6901; j) P. Liu, C.-Y. Zhou, S. Xiang, C.-M. Che, *Chem. Commun.* **2010**, *46*, 2739; k) C. M. R. Volla, P. Vogel, *Org. Lett.* **2009**, *11*, 1701; l) X. Chen, T. Chen, Y. Zhou, C.-T. Au, L.-B. Han, S.-F. Yin, *Org. Biomol. Chem.* **2014**, *12*, 247; m) M. Rueping, R. M. Koenigs, K. Poschorny, D. C. Fabry, D. Leonori, C. Vila, *Chem. Eur. J.* **2012**, *18*, 5170; n) J. W. Tucker, Y. Zhang, T. F. Jamison, C. R. J. Stephenson, *Angew. Chem. Int. Ed.* **2012**, *51*, 4144; o) D. B. Freeman, L. Furst, A. G. Condie, C. R. J. Stephenson, *Org. Lett.* **2012**, *14*, 94.
- [8] K. Yamaguchi, Y. Wang, N. Mizuno, *ChemCatChem* **2013**, *5*, 2835.
- [9] a) S. Enthaler, *ACS Catal.* **2013**, *3*, 150; b) P. Geoghegan, P. O'Leary, *ACS Catal.* **2012**, *2*, 573; c) X.-F. Wu, H. Neumann, *Adv. Synth. Catal.* **2012**, *354*, 3141; d)

- X.-F. Wu, *Chem. Asian. J.* **2012**, *7*, 2502; e) D. E. Frantz, R. Fässler, E. M. Carreira, *J. Am. Chem. Soc.* **1999**, *121*, 11245; f) D. E. Frantz, R. Fässler, E. M. Carreira, *J. Am. Chem. Soc.* **2000**, *122*, 1806; g) N. K. Anand, E. M. Carreira, *J. Am. Chem. Soc.* **2001**, *123*, 9687; h) D. E. Frantz, R. Fässler, C. S. Tomooka, E. M. Carreira, *Acc. Chem. Res.* **2000**, *33*, 373; i) R. Fässler, D. E. Frantz, J. Oetiker, E. M. Carreira, *Angew. Chem. Int. Ed.* **2002**, *41*, 3054; j) J. Kuang, S. Ma, *J. Am. Chem. Soc.* **2010**, *132*, 1786; k) T. Sugiishi, H. Nakamura, *J. Am. Chem. Soc.* **2012**, *134*, 2504.
- [10] R. N. DeGuzman, Y.-F. Shen, E. J. Neth, S. L. Suib, C.-L. O'Young, S. Levine, J. M. Newsam, *Chem. Mater.* **1994**, *6*, 815.
- [11] *Purification of Laboratory Chemicals*, 3rd ed. (Eds.: D. D. Perrin, W. L. F. Armarego), Pergamon Press, Oxford, **1988**.
- [12] a) F. D. Lewis, T.-I Ho, J. T. Simpson, *J. Org. Chem.* **1981**, *46*, 1077; b) F. D. Lewis, *Acc. Chem. Res.* **1986**, *19*, 401.
- [13] a) Y.-C. Son, V. D. Makwana, A. R. Howell, S. L. Suib, *Angew. Chem. Int. Ed.* **2001**, *40*, 4280; b) T. Oishi, K. Yamaguchi, N. Mizuno, *ACS Catal.* **2011**, *1*, 1351; c) K. Yamaguchi, H. Kobayashi, T. Oishi, N. Mizuno, *Angew. Chem. Int. Ed.* **2012**, *51*, 544.





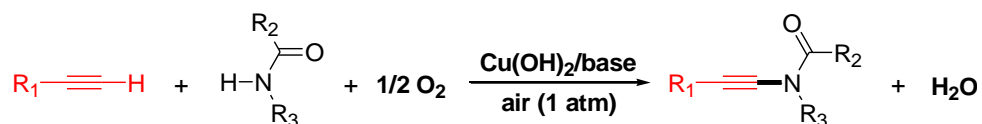
# **Chapter 6**

## **General Conclusions**

This thesis has demonstrated the successful developments in several late transition metal catalyzed novel aerobic cross-dehydrogenative coupling reactions between two nucleophiles or between nucleophiles and electrophiles by employing different strategies and metal catalysts depending on the coupling partners involved. Specifically, (1) copper catalysts have been found to be viable catalysts for the selective cross-coupling of two different nucleophiles which have acidic C–H or X–H bonds (Chapters 2 and 3); (2) supported gold nanoparticles have turned out to be effective for the  $\beta$ -amination of  $\alpha,\beta$ -unsaturated aldehydes (or ketones) due to their ability of the selective dehydrogenative oxidation of C–C single bonds to C=C double bonds even in the presence of aldehyde functionalities (Chapter 4); (3) OMS-2 has turned out to be a powerful oxidant for the oxidation of tertiary amines to iminium species, which are susceptible to nucleophilic attack by acetylide species generated by the cooperation of zinc catalysts with amine bases (Chapter 5).

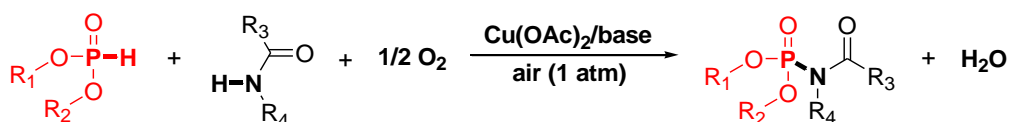
Chapter 2 describes the simple heterogeneous  $\text{Cu}(\text{OH})_2$  catalyst in combination with an appropriate base can efficiently promote the selective cross-dehydrogenative coupling of terminal alkynes and amides in 1 atm of air (Scheme 6-1). The cross-coupling shows high selectivity even without relying on the slow addition technique, which is often required to suppress the Glaser–Hay alkyne homo-coupling when using homogeneous copper catalysts. Such high selectivities to the desired cross-coupling are achieved for the first time when the two coupling partners are mixed in a single step. The scope of the present procedure is very broad with respect to both terminal alkynes and amides, and various kinds of structurally diverse ynamides can be synthesized in moderate to high yields (56–93% yields). A novel green synthetic route to imides via the combination of the oxidative cross-coupling and the hydration of

ynamides by the Sn–W mixed oxide catalyst has also been developed. The theoretical atom efficiency is 100% for the one-pot imide synthesis.



**Scheme 6-1.** Cu(OH)<sub>2</sub>-catalyzed selective cross-dehydrogenative coupling of terminal alkynes and amides using air as the terminal oxidant.

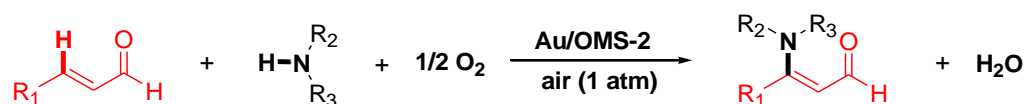
In Chapter 3, the novel Cu(OAc)<sub>2</sub>-catalyzed cross-dehydrogenative coupling of *H*-phosphonates and amides using air as the terminal oxidant has successfully been developed (Scheme 6-2). Cu(OAc)<sub>2</sub> in combination with an appropriate base has been turned out to be an efficient catalyst system for the cross-coupling. The substrate scope for the cross-coupling is broad, and various dialkyl *H*-phosphonates can efficiently react with nitrogen nucleophiles, such as oxazolidinone, lactam, pyrrolidinone, urea, indole, and sulfonamide derivatives, to give the corresponding *N*-acylphosphoramidates in moderate to high yields (52–99% yields). Overall, this cross-coupling procedure provides a straightforward route to synthesize the valuable *N*-acylphosphoramidates from readily available *H*-phosphonates and amides.



**Scheme 6-2.** Cu(OAc)<sub>2</sub>-catalyzed cross-dehydrogenative coupling of *H*-phosphonates and amides using air as the terminal oxidant.

In Chapter 4, gold nanoparticles supported on OMS-2 (Au/OMS-2, average particle

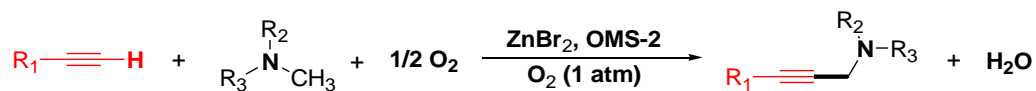
size of gold: 4.1 nm) has been found to efficiently catalyze the  $\beta$ -amination of  $\alpha,\beta$ -unsaturated aldehydes to enaminals (Scheme 6-3). Various kinds of  $\alpha,\beta$ -unsaturated aldehydes can smoothly react with a large variety of secondary amines to afford the corresponding enaminals in moderate to high yields using air as the terminal oxidant (50–97% yields). In addition, the catalysis is intrinsically heterogeneous, and the catalyst can be reused at least 5 times without a significant loss of its high catalytic performance. The reaction proceeds through the aza-Michael addition of amines to  $\alpha,\beta$ -unsaturated aldehydes to give  $\beta$ -aminoaldehydes followed by the oxidation of the  $\beta$ -aminoaldehydes to enaminals. In particular, the key step for the amination, that is, the selective dehydrogenative oxidation of a saturated C–C single bond to the corresponding C–C double bond even in the presence of an easily oxidizable aldehyde functionality using the supported gold nanoparticle catalyst, rather than palladium-based catalysts, has been achieved for the first time.



**Scheme 6-3.** Au/OMS-2-catalyzed selective  $\beta$ -amination of  $\alpha,\beta$ -unsaturated aldehydes using air as the terminal oxidant.

In Chapter 5, the  $\text{ZnBr}_2$  and OMS-2 co-catalyzed cross-dehydrogenative coupling of terminal alkynes and tertiary amines using molecular oxygen as the terminal oxidant has successfully been developed. Various kinds of terminal alkynes can efficiently react with tertiary methyl amines to give the corresponding propargylamines in moderate to high yields. The reaction proceeds through the OMS-2 promoted oxidation of tertiary amines to the corresponding iminium intermediates, to which zinc acetylide species

attack nucleophilically.



**Scheme 6-4.** ZnBr<sub>2</sub> and OMS-2 co-catalyzed cross-dehydrogenative coupling of terminal alkynes and tertiary amines using molecular oxygen as the terminal oxidant.

The aerobic cross-dehydrogenative coupling reactions developed in this thesis avoid using pre-functionalized substrates as well as hazardous reagents, providing simple and efficient alternatives to the existing synthetic procedures for several synthetically important compounds, such as ynamides, imides, *N*-acylphosphoramidates, enaminals, and propargylamines. In addition, these reactions can be regarded as green synthetic procedures due to their use of molecular oxygen as the terminal oxidant and generation of water as the sole by-product.

Aerobic cross-dehydrogenative coupling reactions are without doubt one of the most fascinating synthetic tools due to its high efficiency and environmentally benign nature. Theoretically, any complex compounds could be synthesized by simply connecting different C–H or X–H bonds, which is a long-chased dream for synthetic chemists. However many challenges still exist for further developments in this area. The outlooks of this rapidly expanding area will be briefly described as follows.

1. Homogeneous catalysts have been the main stream when developing new cross-dehydrogenative coupling reactions. The studies in this thesis have shown that heterogeneous catalysts such as metal oxides and nanoparticles can also be promising candidates considering their properties of easy separation and reuse,

most importantly, their rich oxidation chemistry. Especially, when a reaction involves strongly coordinating compounds which might be problematic in homogeneous systems, heterogeneous systems can be considered alternatively. In addition, the development of efficient heterogeneously catalyzed functional group transformations which show low selectivities in homogeneous systems is expected to be achieved by employing the potential of the heterogeneous catalysts.

2. For the copper-mediated cross-coupling reactions, their detailed reaction mechanisms are currently still unclear. Most of the current researches are based on the empirical evaluation in terms of metal source, ligands, and bases. Therefore, more knowledges about the insights of the reactions are urgently needed to break the bottleneck in this field. For example, in the  $\text{Cu}(\text{OH})_2$ -catalyzed cross-coupling reaction, why such a high selectivity can be achieved and how to explain the higher activity of bulky  $\text{Cu}(\text{OH})_2$  than highly dispersed supported copper hydroxide catalysts are two main unsolved problems. The solutions to these problems may be very important for the development of more efficient catalysts.
3. More sophisticated design of heterogeneous nanoparticle catalysts by fine control of their components (for multimetallic particles), sizes, morphologies, and/or supports, is needed to explore their full potential use in fine chemical synthesis. Multifunctional catalysts can be developed by integrating versatile acid-base and redox properties, which would allow the development of new organic transformations.

## **List of Publications**

## ■ Main Publications

1. “Heterogeneously Catalyzed Efficient Hydration of Alkynes by Tin-Tungsten Mixed Oxides”

Xiongjie Jin, Takamichi Oishi, Kazuya Yamaguchi, Noritaka Mizuno

*Chem. Eur. J.* **2011**, *17*, 1261–1267.

2. “Heterogeneously Catalyzed Selective Aerobic Oxidative Cross-Coupling of Terminal Alkynes and Amides with Simple Copper(II) Hydroxide”

Xiongjie Jin, Kazuya Yamaguchi, Noritaka Mizuno

*Chem. Commun.* **2012**, *48*, 4974–4976.

3. “A Green Synthetic Route to Imides from Terminal Alkynes and Amides by Simple Solid Catalysts”

Xiongjie Jin, Kazuya Yamaguchi, Noritaka Mizuno

*Chem. Lett.* **2012**, *41*, 866–867.

4. “Copper-Catalyzed Oxidative Cross-Coupling of *H*-Phosphonates and Amides to *N*-Acylphosphoramidates”

Xiongjie Jin, Kazuya Yamaguchi, Noritaka Mizuno

*Org. Lett.* **2013**, *15*, 418–421.

5. “Gold-Catalyzed Heterogeneous Aerobic Dehydrogenative Amination of  $\alpha,\beta$ -Unsaturated Aldehydes to Enaminals”

Xiongjie Jin, Kazuya Yamaguchi, Noritaka Mizuno

*Angew. Chem. Int. Ed.* **2014**, *53*, 455–458.



6. “Aerobic Cross-Dehydrogenative Coupling of Terminal Alkynes and Tertiary Amines by a Combined Catalyst of Zn<sup>2+</sup> and OMS-2”

Xiongjie Jin, Kazuya Yamaguchi, Noritaka Mizuno

*RSC Adv.* **2014**, *4*, 34712–34715.

### **Related Publications**

1. “Heterogeneously Catalyzed Self-Condensation of Primary Amines to Secondary Amines by Supported Copper Catalysts”

Insu Kim, Shintaro Itagaki, Xiongjie Jin, Kazuya Yamaguchi, Noritaka Mizuno

*Catal. Sci. Technol.* **2013**, *3*, 2397–2403.

2. “Oxidative Nucleophilic Strategy for Synthesis of Thiocyanates and Trifluoromethyl Sulfides from Thiols”

Kazuya Yamaguchi, Konomi Sakagami, Yumi Miyamoto, Xiongjie Jin, Noritaka Mizuno

*Org. Biomol. Chem.* **2014**, *12*, 9200–9206.



# **Acknowledgement**

I wish to express my deepest gratitude to Professor Noritaka Mizuno, my great supervisor, for his invaluable comments and suggestions throughout my doctoral study. Without his generous acceptance, my dream of studying in Japan would have never been fulfilled. His broad and profound knowledge in the research field deeply engraved in my mind.

Great thanks must go to the judging committee members of this thesis, Professor Kazuyuki Ishii, Professor Shū Kobayashi, Professor Kyoko Nozaki, Professor Makoto Yamashita, and Professor Kazuya Yamaguchi, for their valuable comments and suggestions to improve this thesis.

I would like to give hearty thanks to Professor Kazuya Yamaguchi whose comments and suggestions were innumerable throughout the course of my study. Without his kind guidance for every aspect in both research and daily life, my study in Japan would have never been so smooth.

Many thanks must go to Professor Sayaka Uchida, Professor Keigo Kamata, Dr. Kazuhiro Uehara, Dr. Kosuke Suzuki, Dr. Yoshiyuki Ogawawara, and Dr. Mitsuhiro Hibino, the staff members of the Mizuno laboratory, for their priceless discussion and suggestions.

I would like to thank Ms. Chizu Umezu for her support in daily life with kindness and warm heart.

Special thanks also go to the students in the laboratory. Their warm heart and kindness were, are, and will be a great motive for me to continue the study in Japan. Thanks for leaving me such a good impression on Japan-a lovely country. The friendship in the laboratory is always the greatest treasure for me. Especially, thanks to my dear classmate, Kosei Sugahara, for his encouragement and support.

I owe many thanks to The Okazaki Kaheita International Scholarship Foundation. I am grateful to Osamu Shimomura, Jun Okudaira, and Atsuko Mihashi for their thoughtful care and advice. Thanks to the students in the foundation, who are my brothers and sisters in Japan. Without their support, my life in Japan would never be so smooth.

I would like to express my special thanks to the Japanese Ministry of Education, Culture, Sports, Science and Technology, for the financial support during the last 3 years.

Finally, I would like to owe special thanks to my family. They are my heroes. I dedicate this thesis to my dear family.

JIN Xiongjie

February, 2015